AD NUMBER

AD859983

NEW LIMITATION CHANGE

TO

Approved for public release, distribution unlimited

FROM

Distribution authorized to U.S. Gov't. agencies and their contractors; Administrative/Operational Use; AUG 1969. Other requests shall be referred to Naval Undersea Research and Development Center, San Diego, CA 92132.

AUTHORITY

USNURDC ltr, 15 Sep 1971

NUC TP 156
(Part 2 of NWC TP 4442)

U.S. NAVAL UNDERSEA
RESEARCH AND DEVELOPMENT
CENTER
SAN DIEGO, CALIFORNIA

SAN CLEMENTE ISLAND ROCKSITE PROJECT: OFFSHORE GEOLOGY

PART 2. RECONNAISSANCE SURVEY AROUND THE ISLAND

By
J. B. Ridlon
Systems Technology Department

August 1969

NAVAL UNDERSEA RESEARCH AND DEVELOPMENT CENTER

An activity of the Naval Material Command

Charles B. Bishop, Capt., USN
Commander

Wm. B. McLean, Ph.D.
Technical Director

Two preliminary geological and geophysical marine investigations of the offshore region of San Clemente Island, California, were conducted during 1966 as part of the Rocksite Project. The second survey, a detailed, continuous seismic-reflection profiling and bottom-sampling operation off parts of the west side of the island, is covered in Part 1 of this report (San Clemente Island Rocksite Project--Offshore Geology, Part 1, by J. B. Ridlon. China Lake, Calif., U. S. Naval Weapons Center, 1968. NWC TP 4442). The first survey, a reconnaissance around the island by continuous seismic-reflection profiling only, is covered in this volume, which is actually Part 2 of the report mentioned above.

Considerable subject matter and terminology from Part 1 are referred to in Part 2. For this reason, it is recommended that the reader have some acquaintance with Part 1 before beginning this volume. However, the essence of the introduction to Part 1 is repeated here.

For details of survey methods as they relate to instrumentation, navigation, and field procedures, as well as the basic principles of profile interpretation and related geologic considerations, reference to Part 1 is essential.

This report was reviewed for technical accuracy by C. F. Austin and P. St. Amand, both of the Naval Weapons Center.

Released by
P. F. BACON, Head,
Guidance and Control Division
13 August 1969

Under authority of
A. J. TICKNER, Head,
Systems Technology
Department

PROBLEM

Interpret results of a nearshore geophysical and geological survey of the area off San Clemente Island, Calif., as part of the Rocksite Project.

RESULTS

Bathymetry of the island block is shown to differ from that of published charts. Extensive offshore faulting relates partially to that which occurs on the island. Differentiation of a major pre-orogenic surface from the post-orogenic sedimentation is established. A steep magnetic gradient off the east side is considered the consequence of (1) volcanic flow, (2) a possible deep basic mass related to a large positive anomaly off the northwest side of the island, and (3) major faulting. Anomalous magnetic trends also reflect some of the major structural and outcrop trends. Earthquake epicenter analyses suggest less seismic activity than the adjacent land area, a tendency to quiescence at present, and an association of recent fault activity with recent epicenters. The post-orogenic sediments, believed to have followed major transportation channels from the island block by means of turbidity currents, sand flows, and slides, have been deposited in basin lows developed by faulting and folding.

RECOMMENDATIONS

The most favorable area for tunneling appears to lie between Mail and China Points, at least in a generally seaward direction paralleling the major faults. However, faulting will still be a problem. The eastern side of the island appears dangerous. The southern end and northwest side offer some possibilities, but certain areas should be avoided entirely and highly detailed tests and investigations should be completed before any tunneling operation is attempted in any area of the island.

CONTENTS

INTRODUCTION

San Clemente Island (Fig. 1 and 2) was selected early in 1966 for consideration as a possible site for a permanent, manned, under-the-sea-floor installation with direct ocean access for marine environment studies (Project Rocksite). However, an almost complete lack of knowledge concerning the offshore geology of the area necessitated extensive marine geological and geophysical surveys.

These surveys revealed that the general bathymetry differs from that which is presently encountered on published charts of the area (Fig.3). Extensive offshore faulting was determined to be partially related to faulting that occurs on the island. Five rock and sediment units were acoustically determined and delineated, and two are recommended as favorable for tunneling. Earthquake epicenter analyses suggest less seismic activity than on the adjacent land area, a tendency to quiescence at present, and an association of recent fault activity with nearby epicenters.

The eastern side of the island was determined to be unfavorable for tunneling because of the considerable faulting, slumps, and slides that are known to be present.

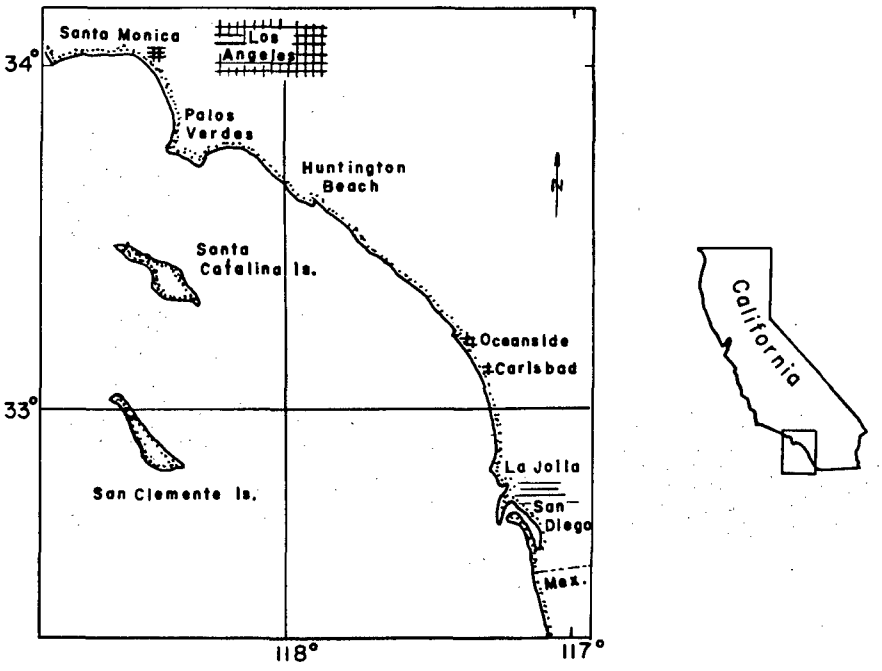

FIG. 1. Index Map of San Clemente Island.

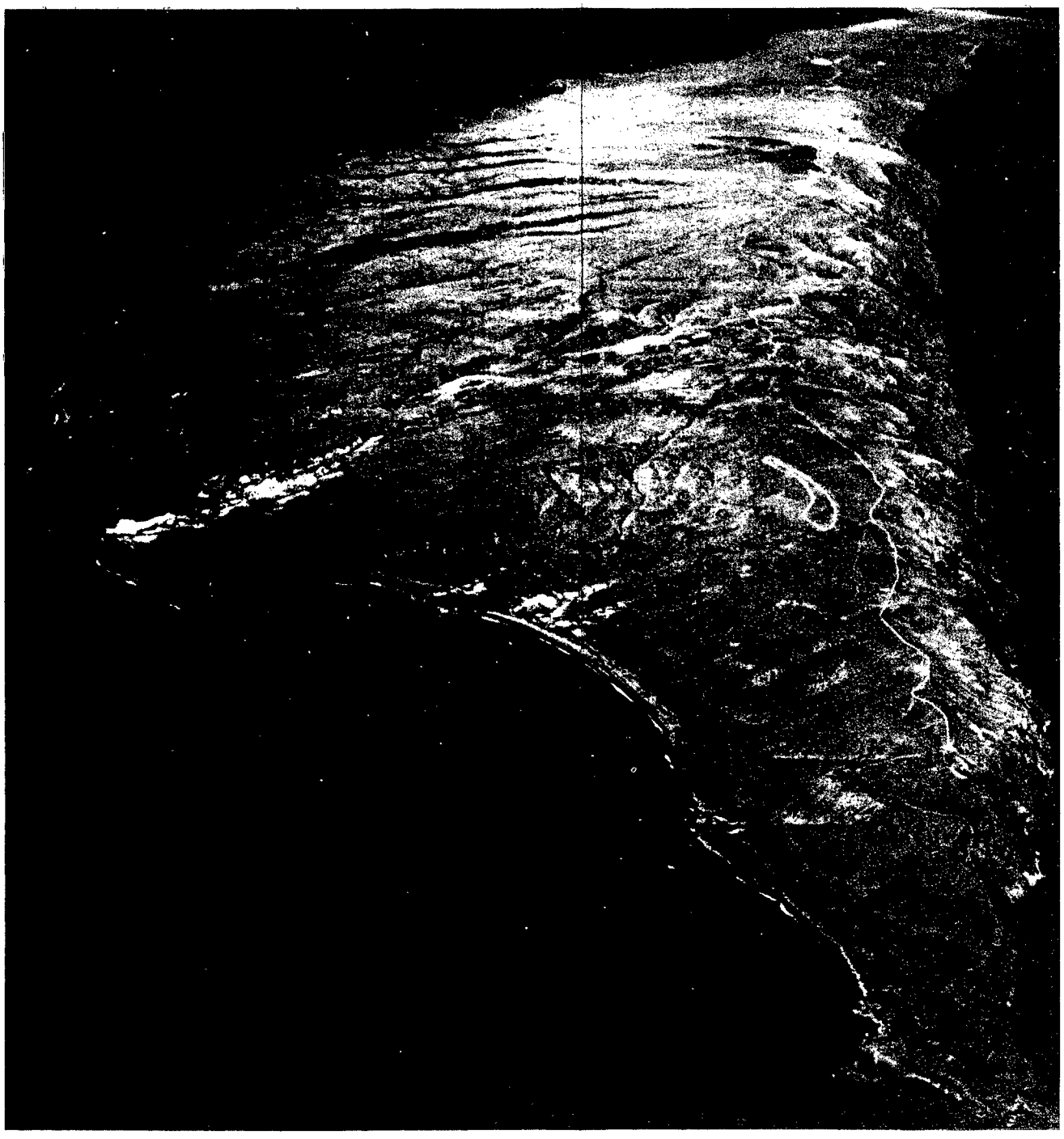

FIG. 2a. Aerial Photograph of San Clemente Island Looking Southwest.

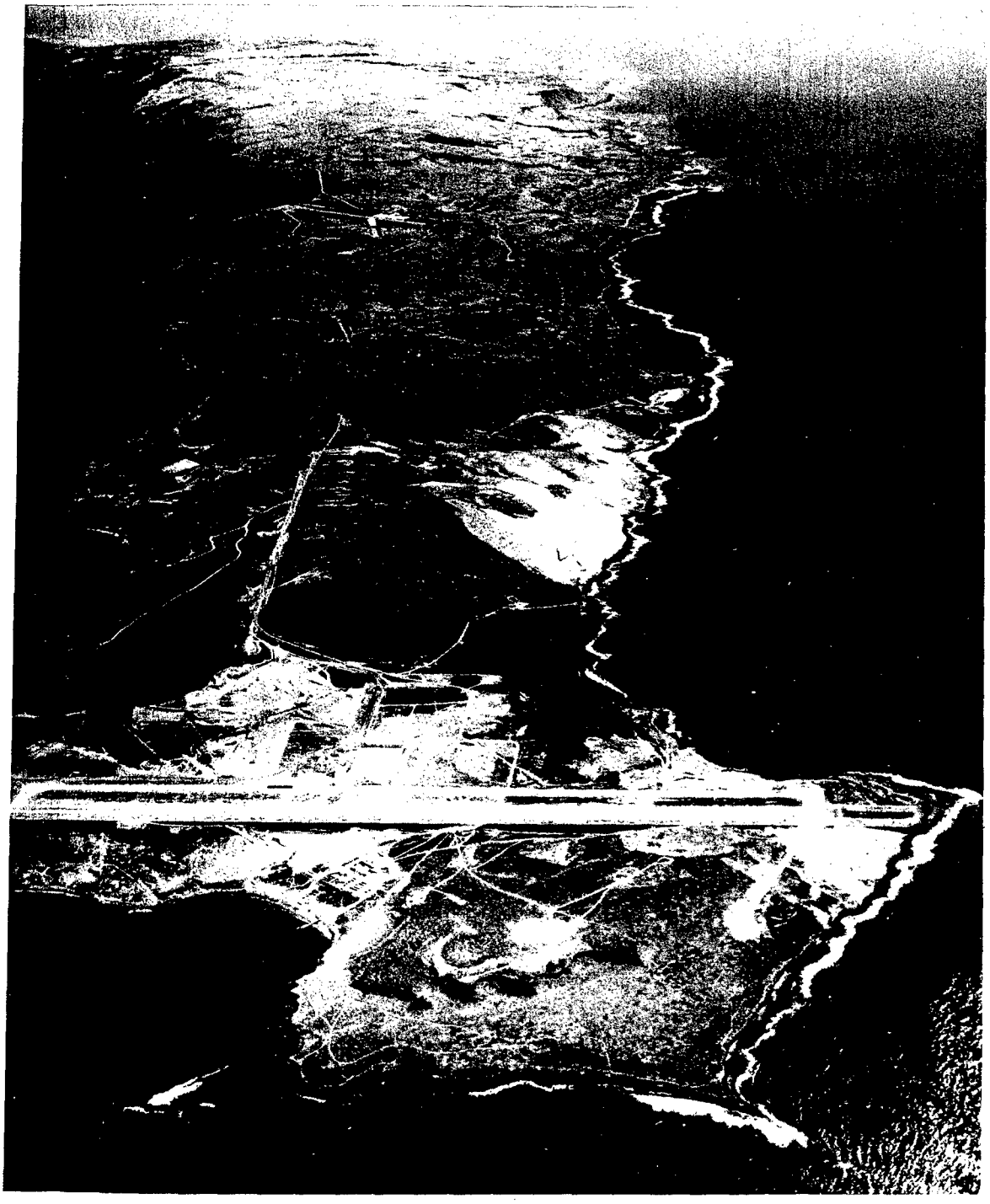

FIG. 2b. Aerial Photograph of San Clemente Island Looking Southeast.

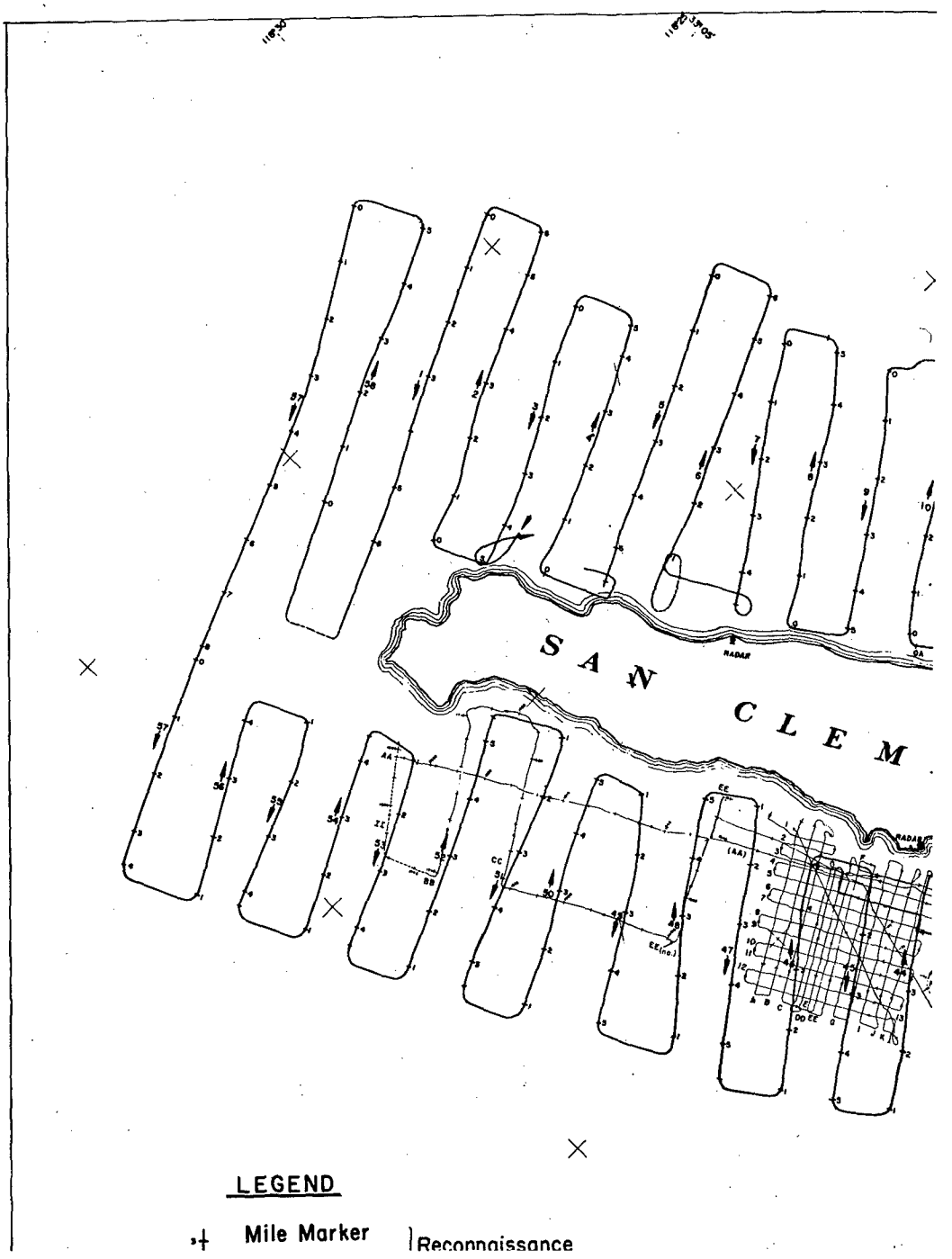
SAN CLEM
RADAR
LEGEND
Mile Marker
Reconnaissance

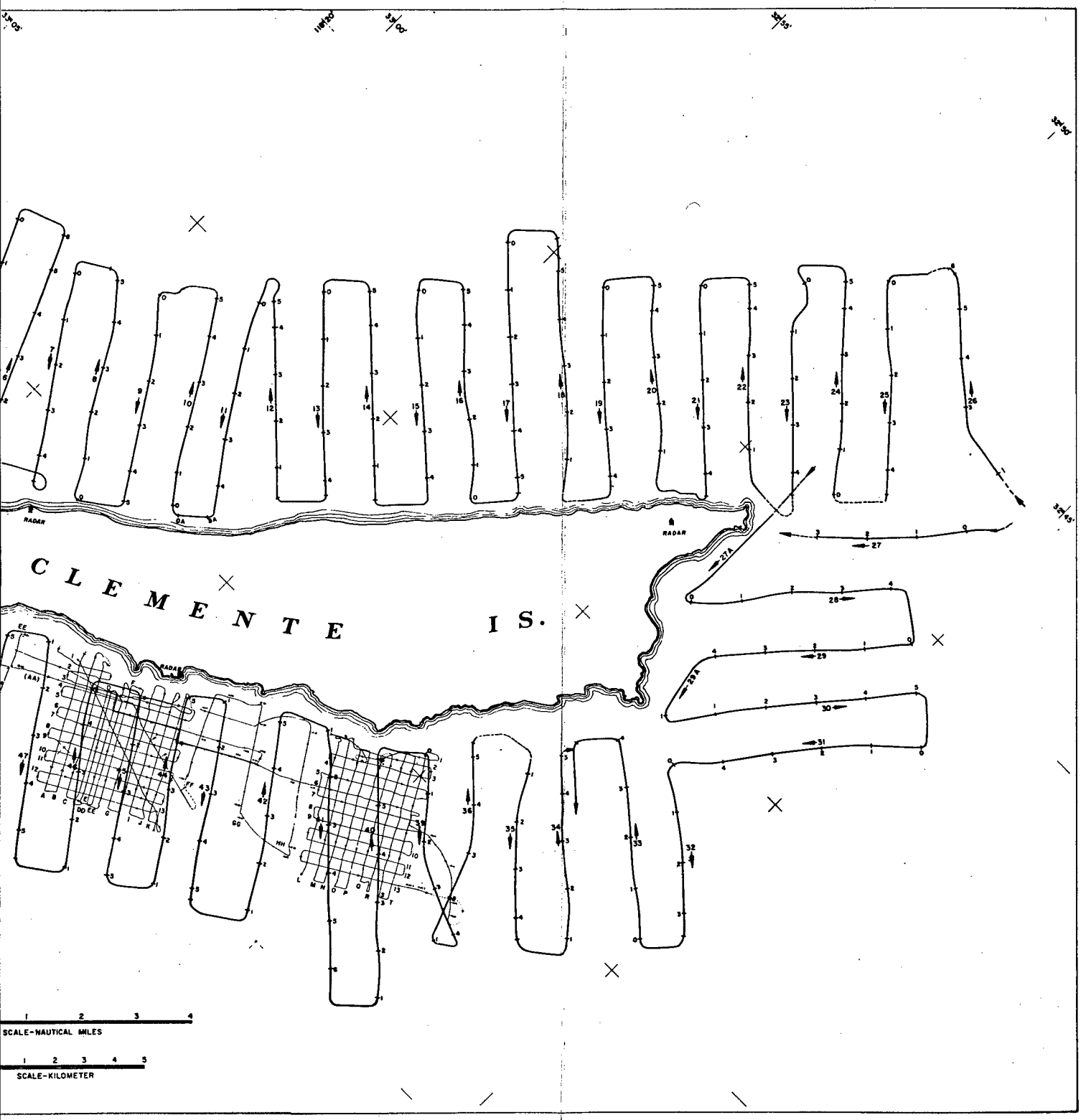

G. 3. Ship's Tracks for Acoustic-Reflection Profile Surveys, July and August 1966.

2

In fact, faulting can hardly be avoided in any attempt to tunnel into the studied area. However, major volcanic rock outcrops seaward of the submerged terrace along the west side of the island are recommended as possible areas for tunneling. In addition, some thick sections of the Miocene (Unit C) sedimentary rocks in this area might provide a safe tunneling medium. Highly detailed offshore seismic profiling, visual studies, and test-core holes to ascertain rock structures are recommended before a selection of any tunnel-site area is made.

PREVIOUS INVESTIGATIONS

The geology of San Clemente Island is known mainly from reconnaissance studies. Smith (Ref. 1) describes the general geologic features in considerable detail. Olmsted (Ref. 2) refines the areal geology of Smith and furnishes additional data on the age and lithology of the rocks and deposits described in Ref. 1. Mitchell and Lipps (Ref. 3) report on vertebrate fossil collecting and the general depositional environment of the sedimentary rocks scattered over the island. Merifield and Lamar (Ref. 4) made a detailed structural survey of two areas, each of about 6 square kilometers, around Eel and Lost Points. The author of this report has made a general foot reconnaissance of parts of the island to further ascertain structural relationships.

In 1964, offshore structural and sedimentation information was taken by means of continuous seismic profiles made by personnel of the U. S. Naval Ordnance Test Station (now Naval Weapons Center), China Lake, Calif., aboard the U. S. N. S. Gear (Fig. 4). Depth and thickness data, as interpreted from the seismic-profile survey, are listed in Appendix A.

In 1966, both reconnaissance and detailed surveys of the offshore areas surrounding the island were made aboard two smaller vessels. The principal objective of the reconnaissance survey was to delineate the general seafloor topography, subseafloor structures, and rock types that would influence site selection. The detailed survey provided offshore geologic information for potential sites at Eel and Lost Points. The nature and structure of the shallow rock units were also resolved by the detailed survey.

General bathymetric data for the nearshore area around the island are available from U. S. Coast and Geodetic Survey soundings, as well as from the publications of Shepard and Emery (Ref. 5), Emery (Ref. 6), and Gaal (Ref. 7).

TIDES AND CURRENTS

Little information is available on current velocities in the immediate vicinity of San Clemente Island. In 1959, current measurements were made near Wilson Cove at depths of 36 and 72 feet by Marine Advisers of La Jolla, Calif. Considerable daily variations of current azimuth and magnitude were encountered during the measuring period, which ran from January through August. Velocities ranged from less than 0.1 to 1.5 ft/sec. It is

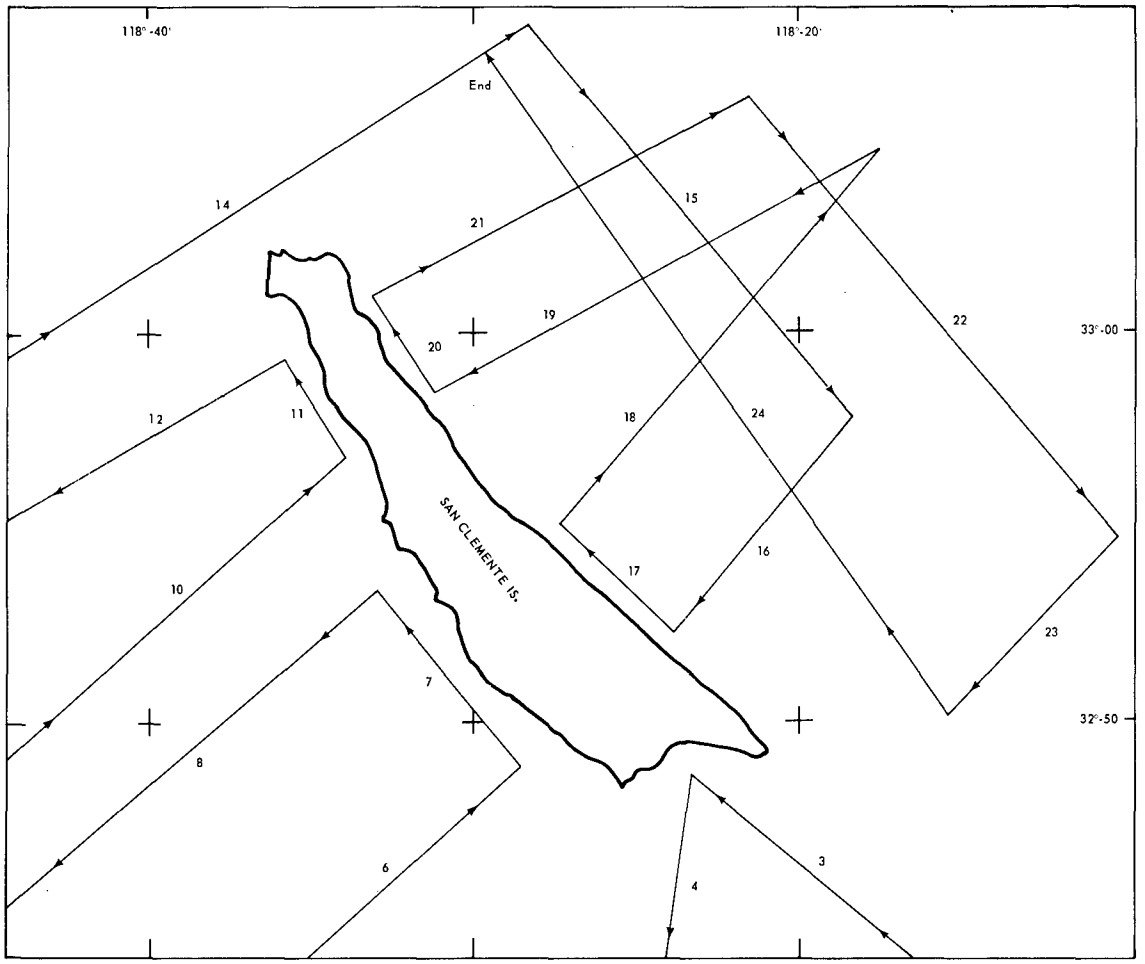

FIG. 4. Ship's Tracks of 1964 U. S. N. S. Gear Continuous Seismic Profile Exercise in Area of Interest.

probable that considerable eddying occurs in this area, as a result of boundary conditions along the island. In a more recent survey, current measurements in the same general area ranged from zero to about 1.5 knots, with rotary direction vectors (Ref. 8). Tidal forces are believed to exert an influence over the entire regime to the greatest depth measured (1,829 meters).

TEMPERATURE, SOUND VELOCITY, AND SALINITY

Nine stations around San Clemente Island were established in November 1964, during a cruise of the U. S. N. S. Davis (AGOR-5), for the continuous recording of sound velocity, temperature, and pressure data. Three stations are located immediately off the northeast side of the island; a fourth lies off the central southwest side (Fig. 5). These stations were used for velocity-depth corrections for the reconnaissance survey profile (Appendix B). Along the northeast side, the ocean temperature ranges from about 18°C at the surface to a minimum of between 4 and 5°C at depths greater than 800 meters. The gradient is

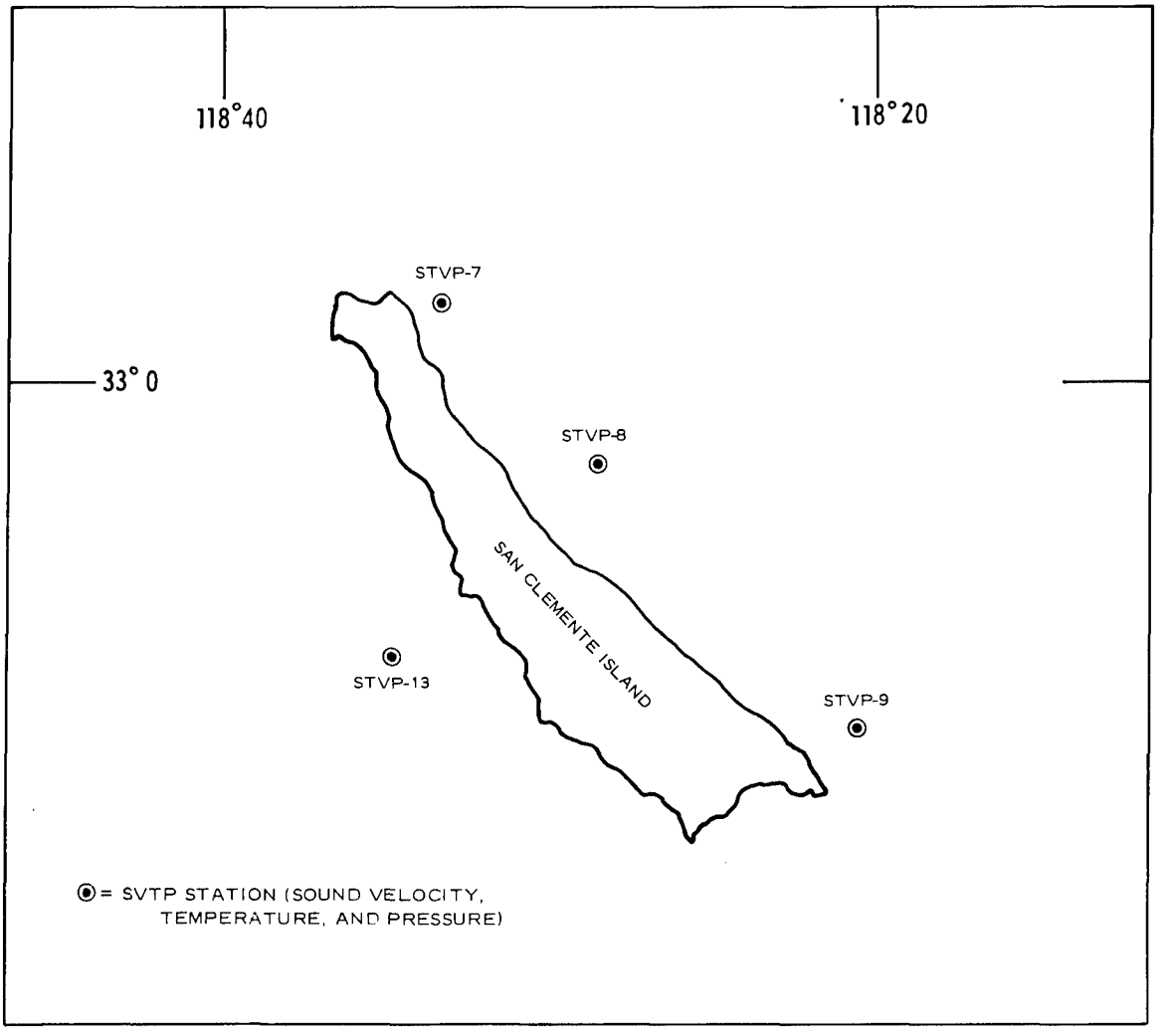

FIG. 5. SVPT Stations Around San Clemente Island.

rapid to approximately 70 meters, which represents the main thermocline. Below this depth, the gradient is gradual and broadens. Data from the station off the southwest side indicate that a slightly shallower thermocline is present. However, the general gradient is very similar to those of the east side. Off the southeast end, and along the San Clemente rift valley and basin (Ref. 5), temperatures range from 18°C at the surface to slightly less than 2°C at depths below 1,500 meters. The mean surface water temperature around San Clemente Island ranges from 14.4°C during the winter to 18.3°C in the summer (Ref. 9). The more recent survey off Wilson Cove (Ref. 8) yielded temperature values ranging from 18.5°C at the surface to 2.85°C at a depth of 1,483 meters.

Few salinity data are available for the immediate area of study. The average salinity for the Santa Catalina Basin is 34.43 0/00 (Ref. 10). Data from one of the stations of the November 1964 cruise, taken off the southeast end of the island, show an average of 34.12 0/00 (measured to 1,855 meters).

Sound-velocity data from the stations of the 1964 cruise (Ref. 7) show a slight increase in velocity within the first 10 meters of depth, from northwest to southeast along the east side of the island. A minimum velocity zone lies roughly between 600 and 1,000 meters of depth. The velocity range in this area is from 1,479 to 1,513 meters/second. The minimum sound-velocity values off Wilson Cove occur between depths of 700 and 800 meters (Ref. 8).

BATHYMETRY

The dominant topographic and bathymetric trend in the Continental Borderland is northwest-southeast; bathymetrically, there is a semblance of an equally important east-west trend [Shepard and Emery (Ref. 5); Emery (Ref. 6); Gaal (Ref. 7); Krause (Ref. 10); Moore (Ref. 11)]. The San Clemente Island block generally follows the strong northwest-southeast bathymetric trend, but also demonstrates a subtle northeast-southwest bathymetric trend across the central part of the island block. The bottom waters surrounding San Clemente Island can be divided into three distinct regions:

1. Western. This region is characterized by a relatively wide shelf. The 100-meter contour is located between 2 and 4 kilometers from shore. Depths in excess of 500 meters are found beyond 6 kilometers from shore.
2. Eastern. The eastern region is fronted by a steep submarine slope. Depths in excess of 1,200 meters are found within 4 kilometers from shore.
3. Southern. An area with depths in excess of 1,800 meters is present within 25 kilometers of the southeast end of the island.

The proximity of deep water emphasizes the relief of this island block above the surrounding basins.

Gaal (Ref. 7) roughly outlined the physiographic provinces of the Santa Catalina Basin. The San Clemente Island block and ridge form the southwest border of the basin. In this report, a classification of the bathymetric regions adjacent to the island is compiled from three distinct geomorphic areas. These areas (Fig. 6) are based on the following:

1. Irregular topography generally representing the San Clemente Slope of Gaal but divided by a shallow marine shelf
2. A prominent marine shelf, averaging slightly more than 100 meters below sea level and broader off the west side and ends of the island
3. The ridge–trough area, mostly equivalent to the San Clemente apron and south Catalina Basin Plain of Ref. 7, including perched troughs within the slope province

The Emery Seaknoll and Southern Plateau are placed within the irregular topography area, as are smaller high areas within the ridge–trough area. The term "apron" may be fitting for certain areas, since gentle sloping and fanning of some Pleistocene(?)–Recent sediments is evident in some of the seismic profiles around the island.

Figure 7 is presented for comparison with other published bathymetric charts (for example, the Coast & Geodetic Survey Charts 5111 and 1206N-15).

PROMINENT FEATURES AND TRENDS

Several prominent submarine geomorphic features are distinguished in the area of study. Of primary importance is the San Clemente Escarpment along the east side of the island block. At sea level, the island equivalent of the escarpment levels out to form a 1/2- to 3/4-kilometer-wide shelf at an approximate depth of 100 meters.

From the seaward end of the shelf, the seafloor slopes steeply to a depth slightly more than 1,000 meters. Reconnaissance Profile 4 (Fig. 8) is taken as a representative example of this slope at the northern part of the island; the average slope at this location is about 21 degrees. The average of the seismic profile slopes along the east side of the island is 18 degrees. However, calculations made by the writer in 1962, for the slope immediately south of Wilson Cove and based on sound-velocity, pressure, and temperature (SVPT) data, indicated slopes up to 27 degrees. Local slopes have been measured as steep as 35 degrees by deep-submersible vehicle survey.[1] The entire slope is marked by an average dip variance ranging from 12 to 21 degrees (Fig. 9). The general strike of this major feature is N40°W. In a broad sense, the escarpment forms a very linear feature. However, a slight northeast concavity is evident along the central to northern end of the island (Fig. 2).

At the seaward declivity of the terrace along the western side of the island, the slope steepens sharply to about 15 to 17 degrees and continues to a depth of roughly 500 meters, at which it assumes a more moderate incline of 4 to 5 degrees. Bathymetric data from around the island indicate that numerous gullies cut into the seaward slope off the terrace and sometimes into the terrace proper.

A less outstanding yet important bathymetric feature of the western slope area is a volcanic high approximately 7 km southwest of Lost Point. This feature is revealed in U.S.C.&G.S. Chart 5111 as two separate highs aligned approximately N70°W. This alignment is maintained in Fig. 7, but is interpreted as a single, elongated high.

For roughly the same distance offshore, there is a general tendency for shoaling of the island block's slope region southeastward along the western side of the island. This change is sharply defined across the area to the northwest of Eel Point, which is also more uniform in slope than the area to the south. Major re-entrants, protuberances, and depressions are also more prominent to the south of Eel Point.

Shoreward, the major submarine terrace is terminated by a steeper and more irregular surface related to the volcanic topography on the island. Marked differences (from previous charts) are also obvious for the basin areas off the slope. On the east side of the island block, the slope grades abruptly into a submarine ridge–trough zone composed of discontinuous linear segments of crustal blocks. The basin–trough zone is a second major feature; its surface reflects distinctive geometric patterns of highs and depressions (Fig. 7) developed by faulting and folding of crustal rocks. The alignment of these patterns is often apparent by

[1] Personal communication from R. E. von Huene, U. S. Geological Survey, Menlo Park, Calif. (1967).

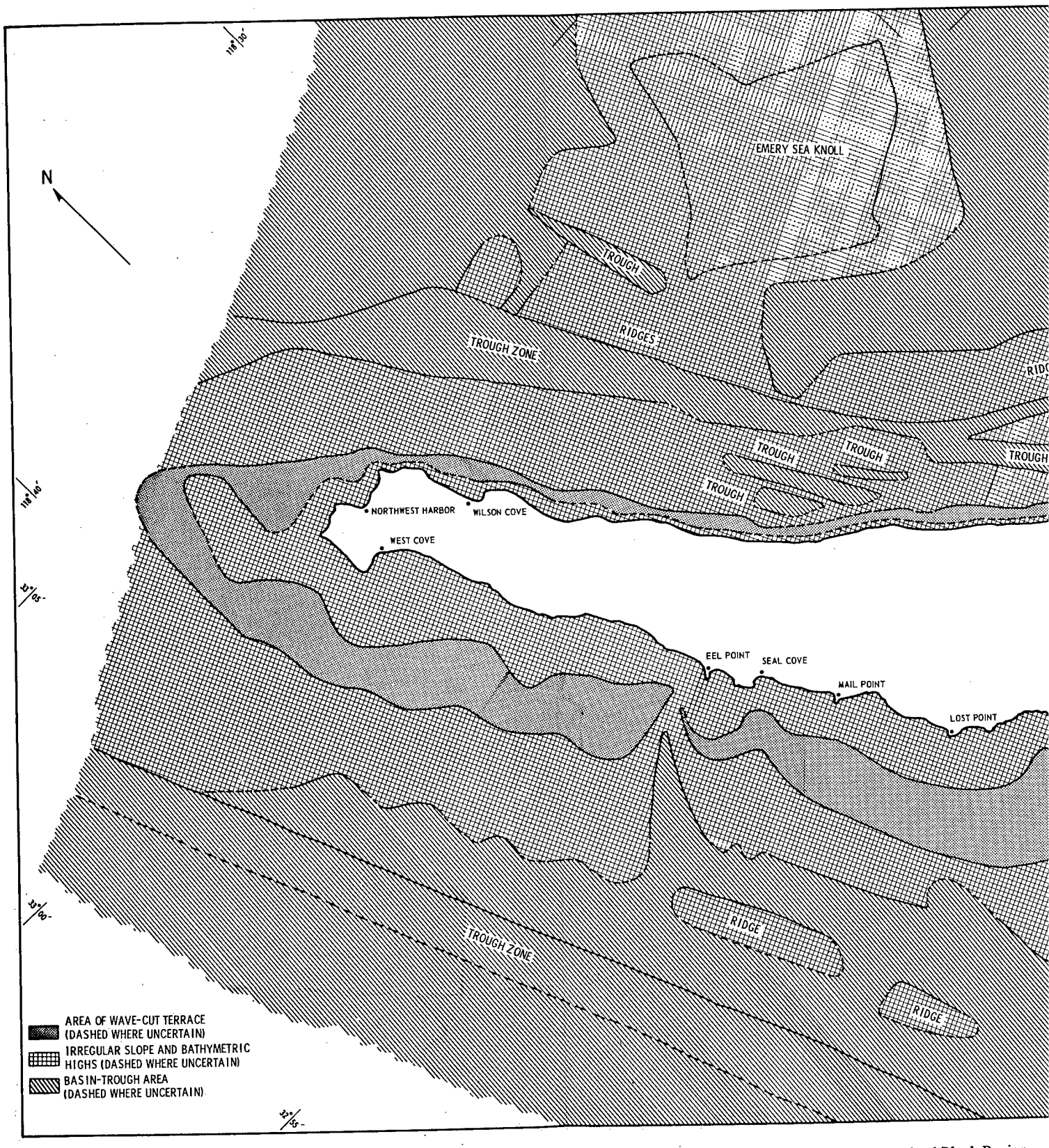

FIG. 6. Physiography of San Clemente Island Block Region.

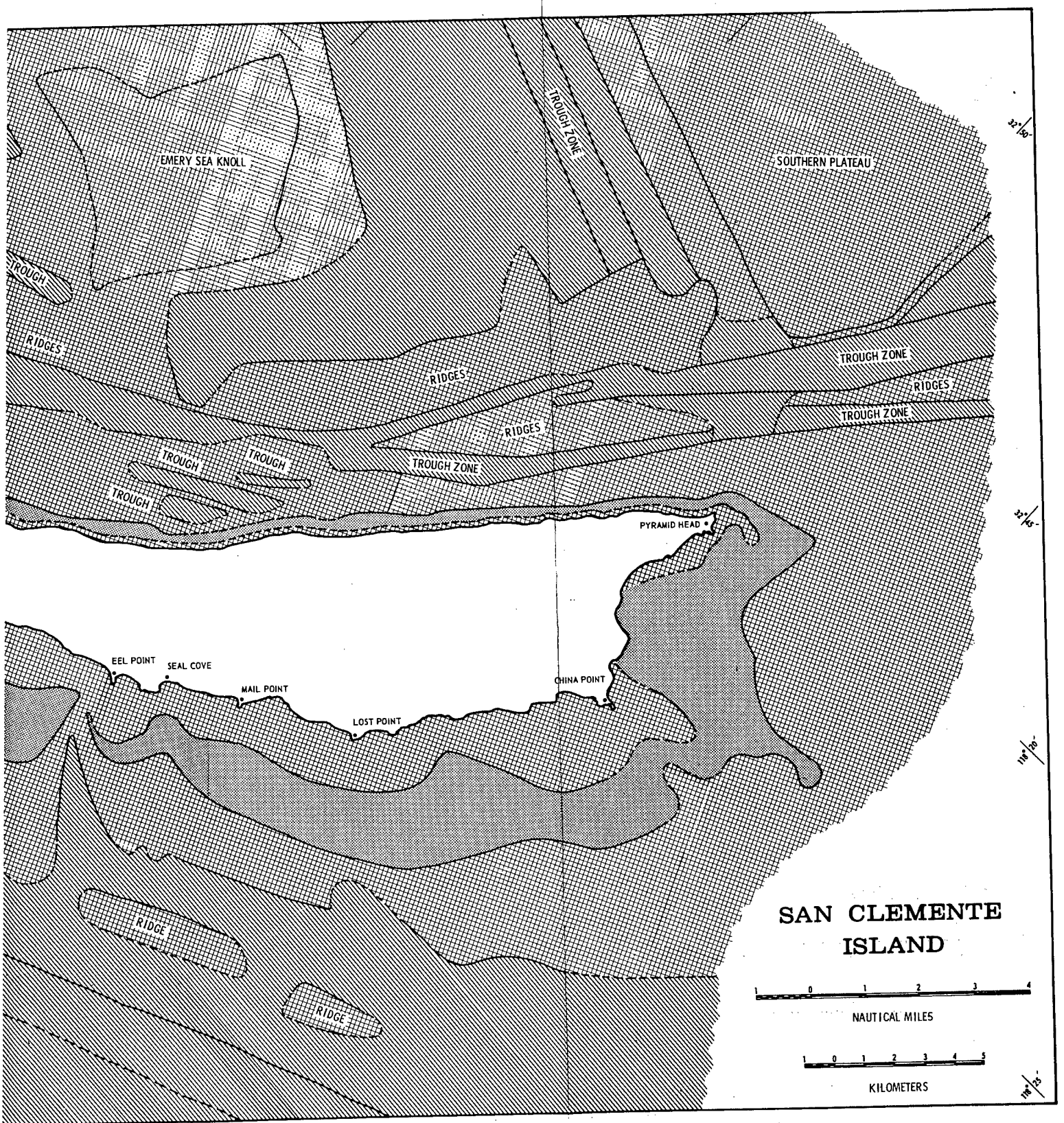

FIG. 6. Physiography of San Clemente Island Block Region.

2

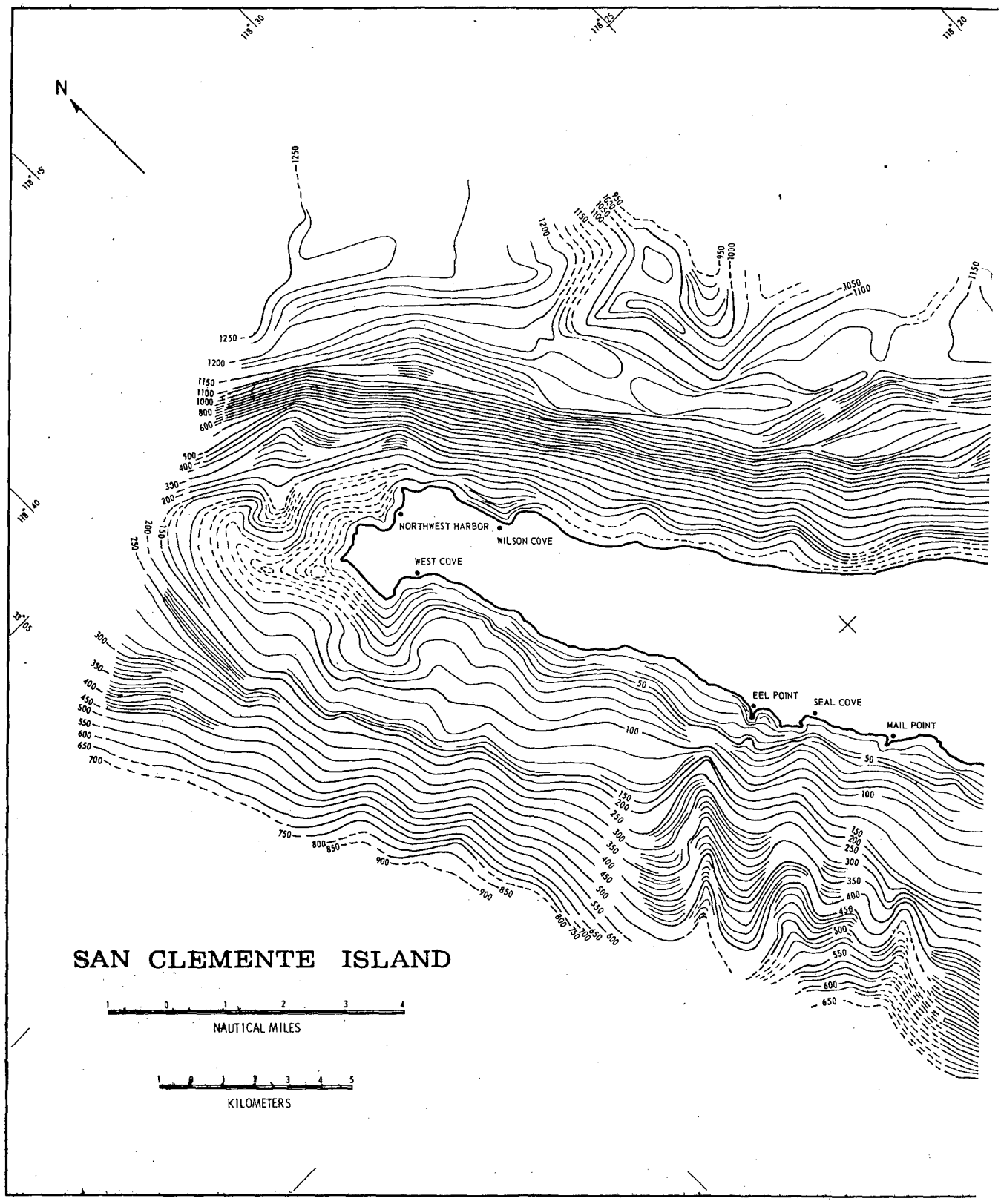

FIG. 7. Bathymetry of San Clemente Island Region Based on Reconnaissance Seism is taken from U. S. Coast and Geodetic Survey Chart 5111.

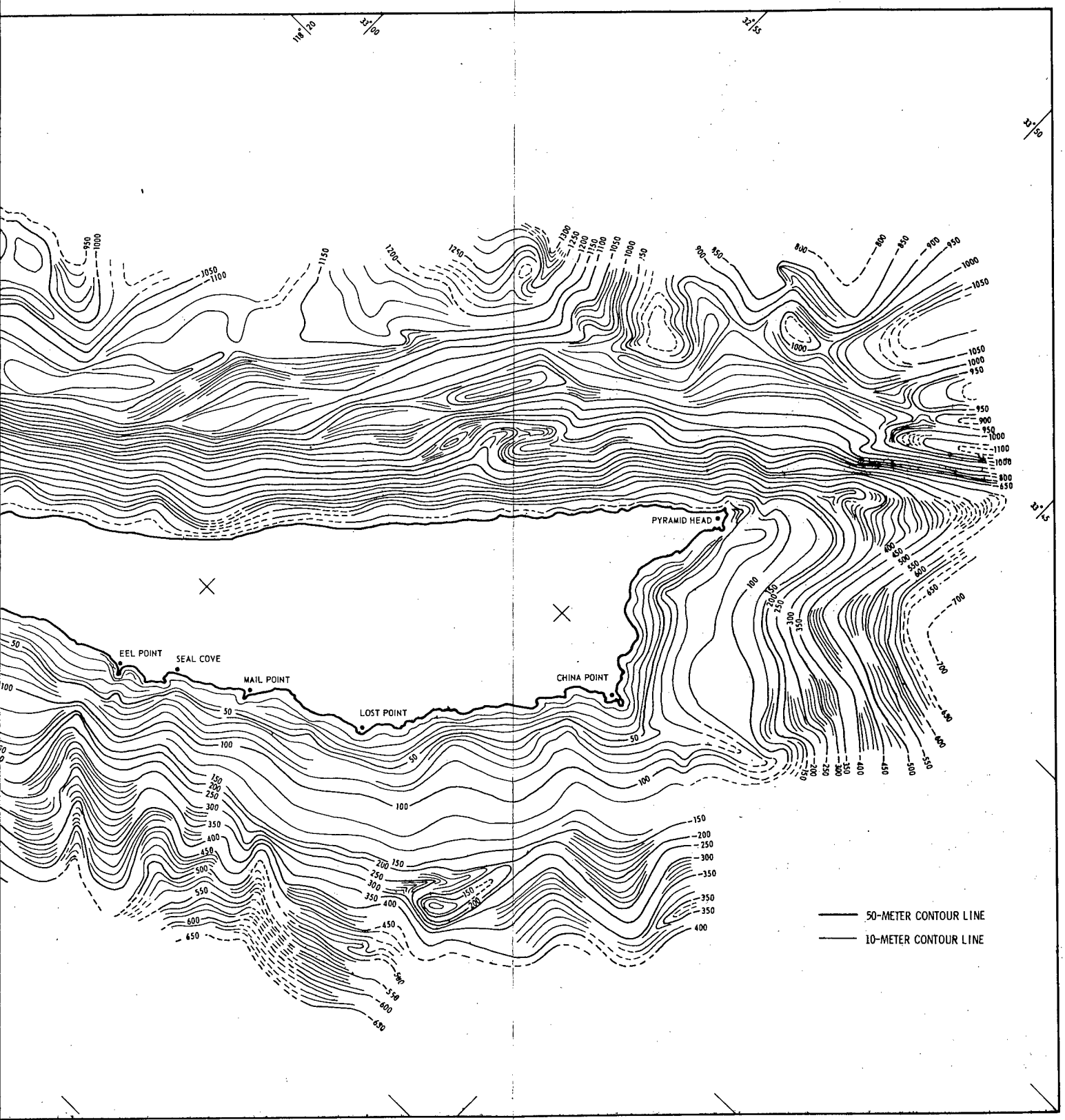

ente Island Region Based on Reconnaissance Seismic Profile Data. Much of near-shore control for this figure
odetic Survey Chart 5111.

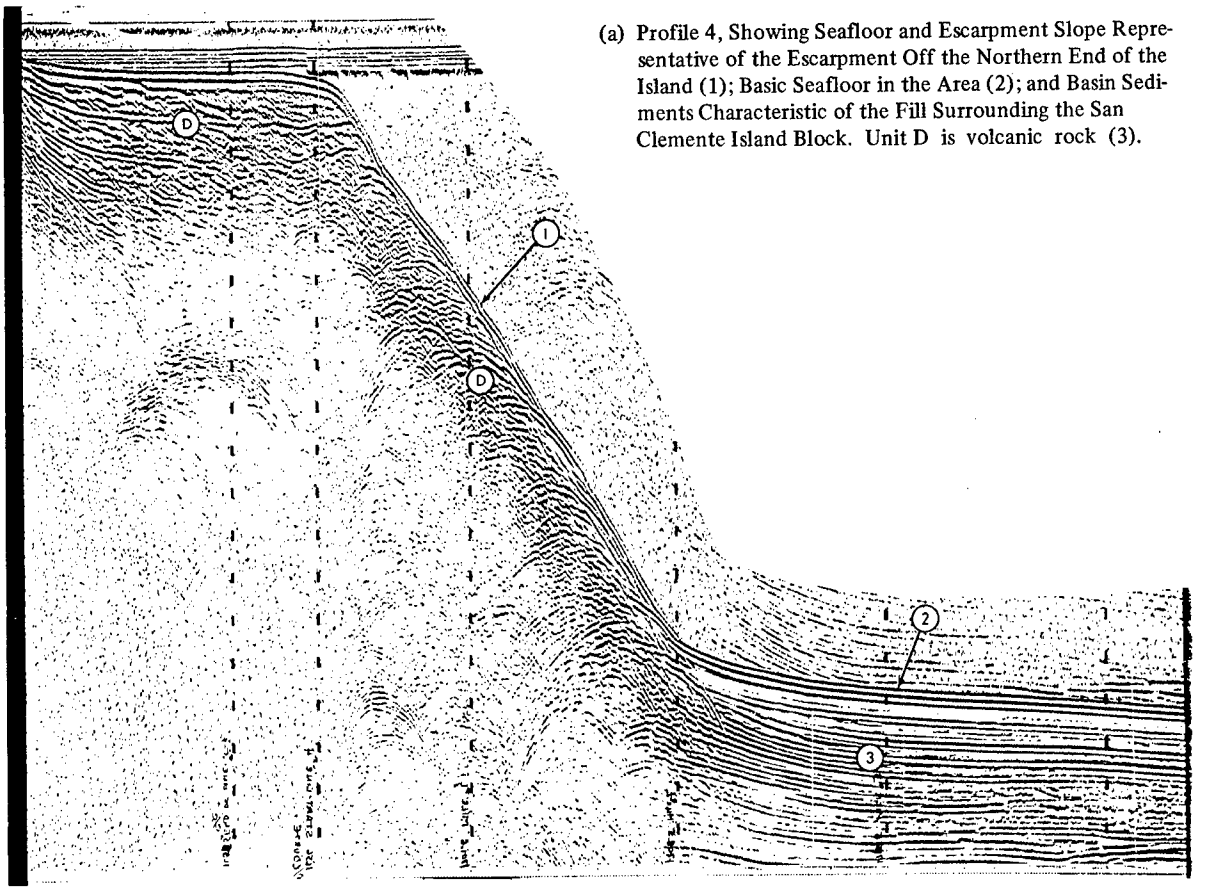

(a) Profile 4, Showing Seafloor and Escarpment Slope Representative of the Escarpment Off the Northern End of the Island (1); Basic Seafloor in the Area (2); and Basin Sediments Characteristic of the Fill Surrounding the San Clemente Island Block. Unit D is volcanic rock (3).

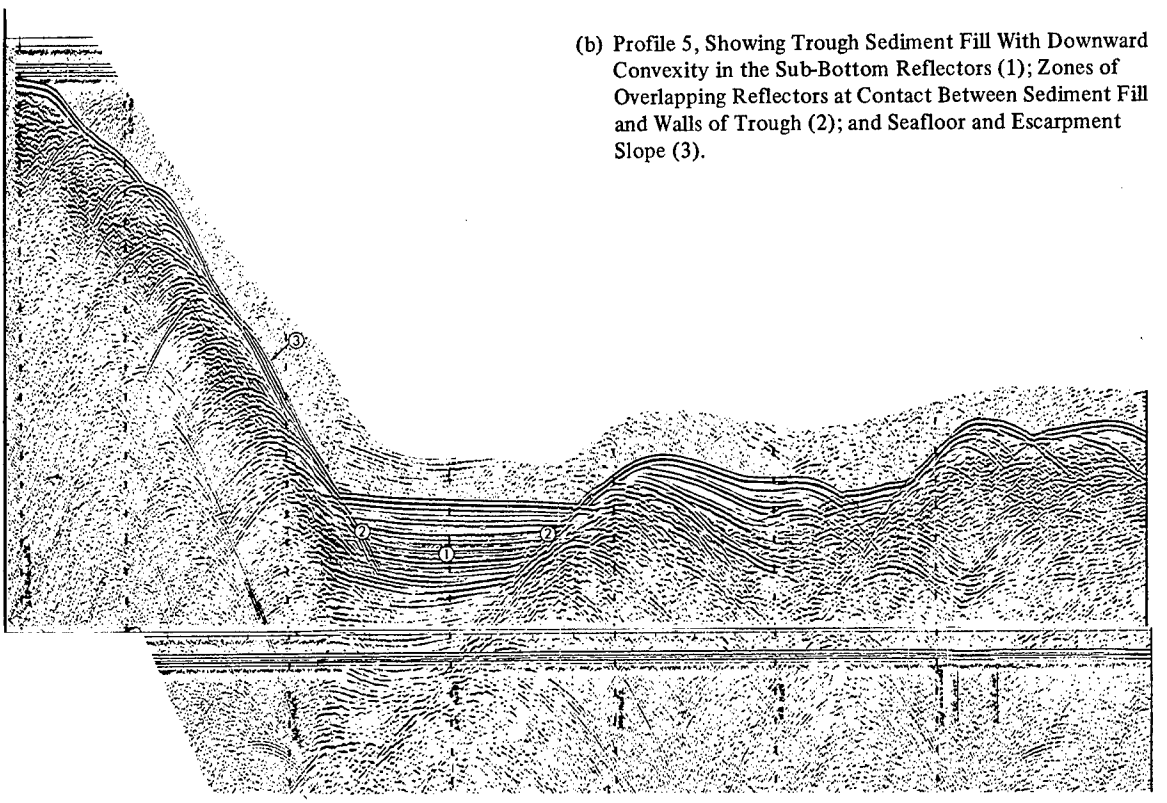

(b) Profile 5, Showing Trough Sediment Fill With Downward Convexity in the Sub-Bottom Reflectors (1); Zones of Overlapping Reflectors at Contact Between Sediment Fill and Walls of Trough (2); and Seafloor and Escarpment Slope (3).

FIG. 8. Reconnaissance Profiles.

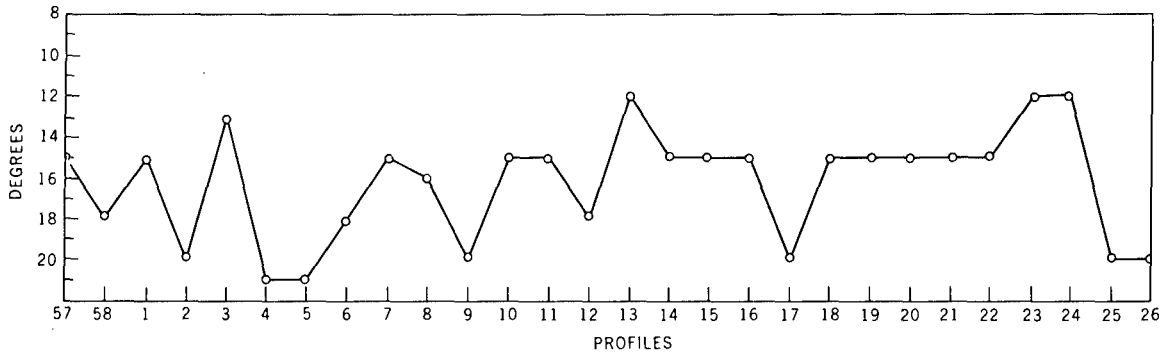

FIG. 9. Variation of San Clemente Escarpment Slope. Measurements based on slope-corrected average of each seismic-profile slope.

the appropriate positioning of the seismic profiles of the area. The linear bathymetric trends of this zone are mostly aligned in either a northerly or a northwesterly direction. These trends are more striking along the northeastern edge of the surveyed area, where the geometric pattern of highs and depressions is pronounced in the vicinity of the Emery Seaknoll and the Southern Plateau (Fig. 6). The topography that lies generally between the island and the Emery Seaknoll, and along the ridge–trough area, tends to slope downward in a northwest and southeast direction.

The western outline of the Emery Seaknoll appears more irregular than shown heretofore on bathymetric maps. Gaal (Ref. 7) describes this sea-basin high as sub-rounded, conical, and with relatively steep slopes, all of which suggest a volcanic structure. However, Gaal does report that the southwestern slope suggests a breached or faulted portion of the structure because of its more irregular topography. A fan-shaped configuration of three ridges is apparent to the southeast of Pyramid Head, at the edge of the mapped area. A trough, bordering the southwest side of the westernmost ridge, is the only linear depression of the ridge–trough zone that lacks a flat bottom. According to profile records, this trough appears to be relatively devoid of sedimentary fill.

A third major feature is the offshore shelf, which broadens around the ends of the island and is prominent along the southwest side. It is similar to the elevated benches cut into the southwest flank of the island. The terrace is generally smooth, is nearly flat, and averages a nearly 1-degree slope. The terrace ranges from about 0.2 to 2.0 nautical miles in width along the western side of the island, with an average width of nearly 1 nautical mile.

The alignment of the Emery Seaknoll with the more shallow central part of the ridge–trough zone, the shoaling of the southwestern slope area, the inferred upward bowing of the island (Olmsted, Ref. 2), and the bathymetric high southwest of Lost Point, are all related to an east-west regional bathymetric trend. However, the secondary trend of the study area is northeast-southwest.

The re-entrant caused by Eel Ridge Canyon on the west side of the island forms a complete break in the shelf; the canyon and shelf break are considered important features of the island block's structural genesis (see Part 1).

GENESIS OF BATHYMETRIC FEATURES

Bathymetric features, especially those of the deep seafloor, are presumed to be relatively little modified by weathering and erosion, compared with those on land. As a consequence, bathymetric features may be considered reasonably reliable representations of tectonic structure. Such features are most commonly modified by rock and sediment mass movement and sedimentation. Thus the configurations of what are considered fault-controlled features, such as ridges, troughs (grabens), crustal blocks, and folding, are interpreted as essentially linear and sharply defined features. These considerations have strongly influenced the interpretation of Fig. 7.

Profile interpretation indicates that faulting is the major factor controlling the bathymetry in the area of study. Many of the elevations and depressions appear to be offsets of formerly more extensive linear features, a phenomenon that becomes more apparent when the structure and sedimentation trends along this zone are studied. These structural-morphological features are a consequence of depression-sediment fills and ridges formed by faulted and folded crustal blocks.

The dissection of the southwestern slope area is seemingly the consequence of both faulting and erosion. The erosional pattern appears to follow the fault trends, at least partially, and may have developed largely during the Late Pleistocene lowering of the sea level. Erosional development along the northeastern slope may have resulted largely from slumping, sand flows, and turbidity currents, which have partly followed fault zones.

According to the theory of Bradley (Ref. 12), the major San Clemente Island terrace was probably cut during slow submergence (considered a sea level rise in this case); thus it is probably a wave-cut terrace of Late Pleistocene age (Ref. 13, 14, and 15). Higher terraces, representing sea-level stands of the recent transgression (Ref. 14 through 20), may be present along the nearshore submarine volcanic outcrop area. Emery (Ref. 6 and 21) has postulated two higher submerged terraces for San Clemente Island; however, these are not readily apparent, primarily because many of the profiles do not reach close enough to shore. Nevertheless, two horizontal sequences noted on a few of the profiles may be related to higher sea-level stands. These are located at depths of about 28 to 30 meters and 55 to 64 meters. The lower level approximates the lower one noted by Emery (Ref. 6), the upper corresponds to Curray's upper Holocene regression (Ref. 13 and 14), and Emery's diagram (Ref. 6, p. 35) shows the two upper terrace levels as being very discontinuous. Data from the present study suggest that some of the discontinuous sections are related to oblique faulting, which has elevated sections of the main terrace.

STRATIGRAPHY

Certain geologic and geomorphic features of the San Clemente Island offshore region are defined in Part 1 of this report. These features are used as a basis for further discussion and integration of the broader geologic aspects revealed by the reconnaissance survey.

Moore's classification of the borderland stratified rocks and sediments (Ref. 11) is used in this part of the study. The strata are divided into pre-orogenic and post-orogenic units. This division is based on the internal structures and their relationships to adjoining faults and basement or volcanic rock masses; the division relates highly faulted and folded strata and volcanic rocks, mainly of Miocene age, to that of the subsequent basin and trough fill.

In most areas, differentiation of post- and pre-orogenic strata was not difficult. However, definition of Unit B was only possible for parts of the 1966 reconnaissance survey through the use of special filtering on a rerun of tapes made on that survey. The rerun filter setting (118 to 245 Hz) resulted in better resolution on the profile records.

Unit A is not defined, but is included in the definition of major fan, apron, and trough deposits referred to as Unit X. Unit B is defined only for the west side and ends of the island; this unit is not detectable on the profile records for the narrow shelf on the east side. Furthermore, a division of Units C and D on the east side was too difficult for definitive analysis because of the complex nature of the structure, side echoes, and overlap by multiples. As a consequence, only post-orogenic sediments (Unit X) and the post-orogenic surface are used in the study of this area. Distinction of the post-orogenic surface is shown in line drawings of selected opposing profiles along the length of the island (Fig. 10).

The limits of profile resolution, profile density, and error for interval-velocity correction factors are the bases for the isopach map intervals used for the various geologic units in the reconnaissance survey.

Figure 11 shows the geometric relationship of the lithologic units described in Part 1.

Unit B. The acoustic and geologic nature of this unit is described in Part 1 of this report. Figure 12 is a composite of the detailed and reconnaissance survey data. A difference in the outlining of the geomorphic depressions on the post-orogenic surface should be noted between the surveys. Closer control in the area outside of the detailed survey undoubtedly would reveal much more irregularity in the configuration of the isopach intervals; it is suspected that the unconformity is highly irregular over the entire area studied.

Some profiles along the east side of the island disclose a complete lack of this unit; however, other profiles did not reach the wave-cut terrace. Presumably, some small sections of the unit are present along this side of the island.

Unit C. The acoustic properties of this unit are described in Part 1. Figure 13, a composite of the detailed and the reconnaissance survey data, shows seven major thick areas:

1. The first and second areas, which are located immediately southwest of West Cove, and are the thickest (Fig. 14a)
2. A third area, which is an elongated and almost rectangular accumulation immediately to the southeast of the first two
3. The fourth and fifth areas, off Mail and Lost Points, that trend northeast-southwest
4. The sixth and seventh areas, located off the south end of the island

The first and second areas are essentially a composite of one northwest-trending part that appears to have been dissected by both erosion (Fig. 14b) and faulting with an apparent offset. This composite part of Unit C lies between two slightly exposed (bathymetric) volcanic highs and constitutes a major depression fill in this area. The third area represents a dissected graben (see Part 1, Fig. 37a). The fourth and fifth areas can also be considered a composite of one part of the unit, which has been dissected by erosion and faulting with a possible offset. The configuration of the sixth and seventh areas strongly suggests preservation by faulting, as do the terrestrial equivalents of Unit C in this area.

Figure 13 more clearly defines the major exposure of volcanic rock seaward of the wave-cut terrace in the detailed survey area. In addition, the irregular configuration of this exposure more strongly illustrates the structural control described in Part 1.

There is little more that can be shown about the lithologic nature of this unit beyond the information provided by the detailed survey. Island field work, however, provides some evidence for the portion of Unit C off the West Cove area. Unit C is preserved close to shore in this area (Fig. 13). Along the shore, and mixed with a predominance of volcanic cobbles and boulders, are cobbles of thinly stratified, buff to greenish-grey (5GB8/1 to 5Y-5GY6/1), finely crystalline, dense, well indurated carbonate rock. The rock has been identified as dolomite by X-ray analysis. This part of Unit C may be related to the Miocene section at Wilson Cove (Ref. 2), where a shale unit contains a cementing material of dolomite.[2] Apparently, the more resistant strata of Unit C are carbonate or well indurated carbonate-cemented clastic rocks; these are presumably of minor importance in the unit because of the paucity of outcrops observed along the wave-cut terrace and in the scattered erosional remnants along the shore.

Profile interpretation suggests that blocks and ridges of Unit C are preserved along the entire San Clemente fault zone; these are shown as exposed upthrown as well as buried crustal blocks that are presumed to be underlain by volcanic rock. Some profiles indicate that the thickness of Unit C in this zone corresponds to a sound velocity of roughly 0.6 second one-way travel time (approximately 400 meters).

Unit D. This unit is the most widespread of all the described units. As a bathymetric outcrop, however, it is exceeded by Unit C in the studied area. Bathymetrically, it comprises all of the irregular topographic area shoreward of the wave-cut terrace, and most of the San Clemente Escarpment. The exposures at the near-shore area are believed to be

---

[2]Personal communication from J. C. Vedder, U. S. Geological Survey, Menlo Park, Calif.

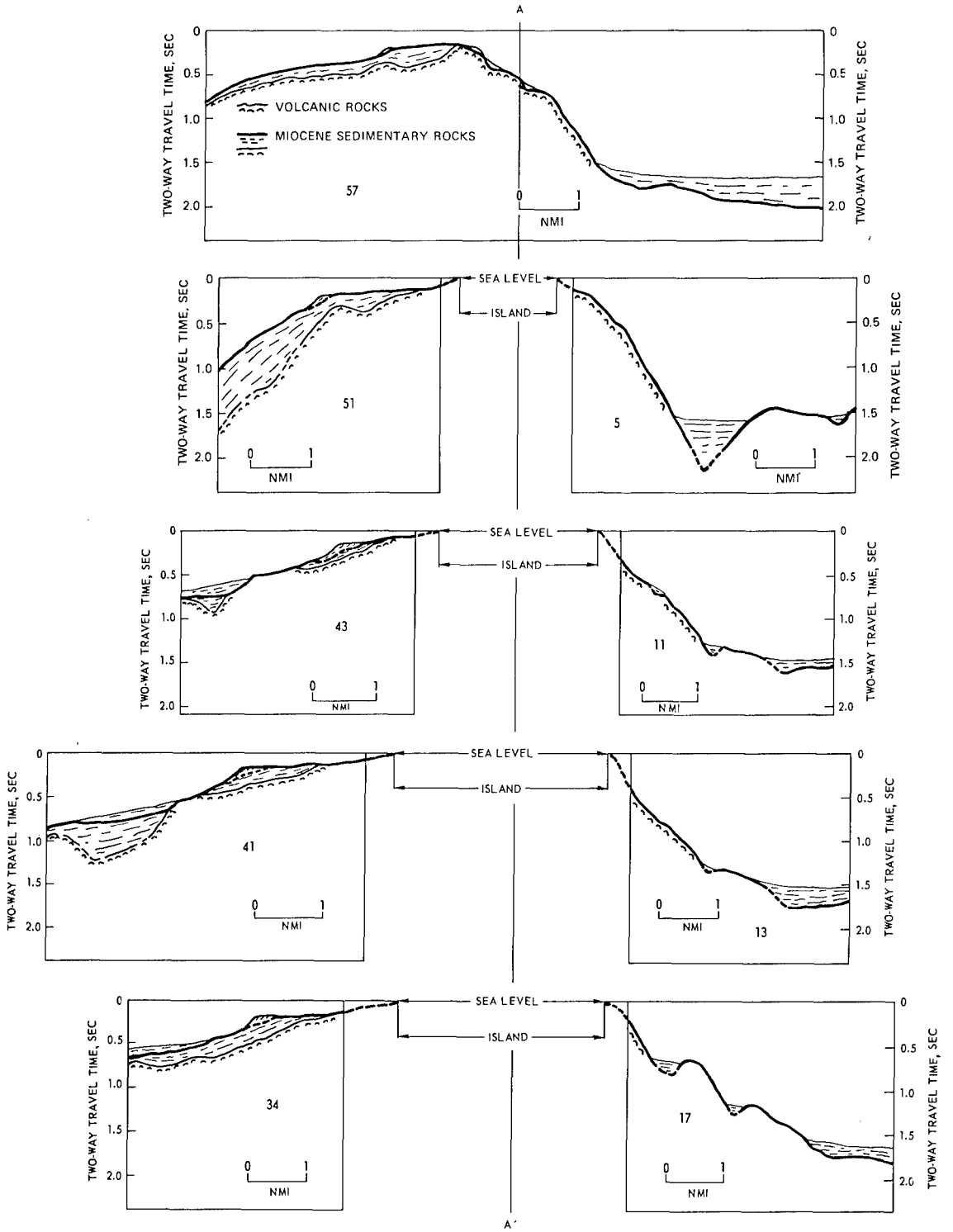

FIG. 10. Line Drawings Based on Selected Reconnaissance-Survey Seismic-Reflection Profiles. Lines on map show position of profile relative to Line A-A′, and are not representative of actual length and position of profile relative to the island. The heavy line denotes a post-orogenic surface (with Unit A removed).

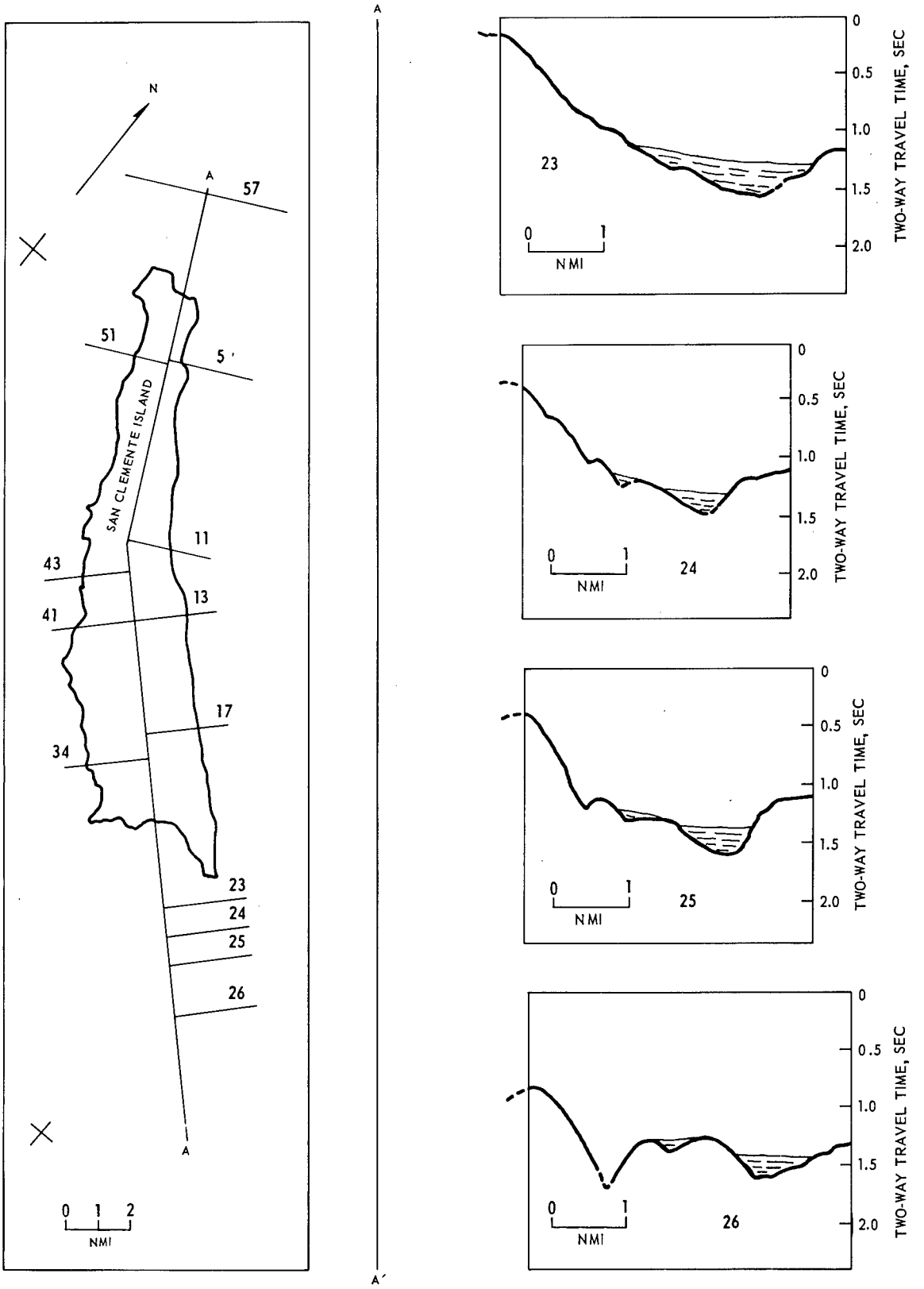
N
A
57
51
5'
SAN CLEMENTE ISLAND
11
43
13
41
17
34
23
24
25
26
A
0 1 2
NMI
A'
23
0 1
NMI
0
0.5
1.0
1.5
2.0
TWO-WAY TRAVEL TIME, SEC
24
25
26

FIG. 10. (Contd.)

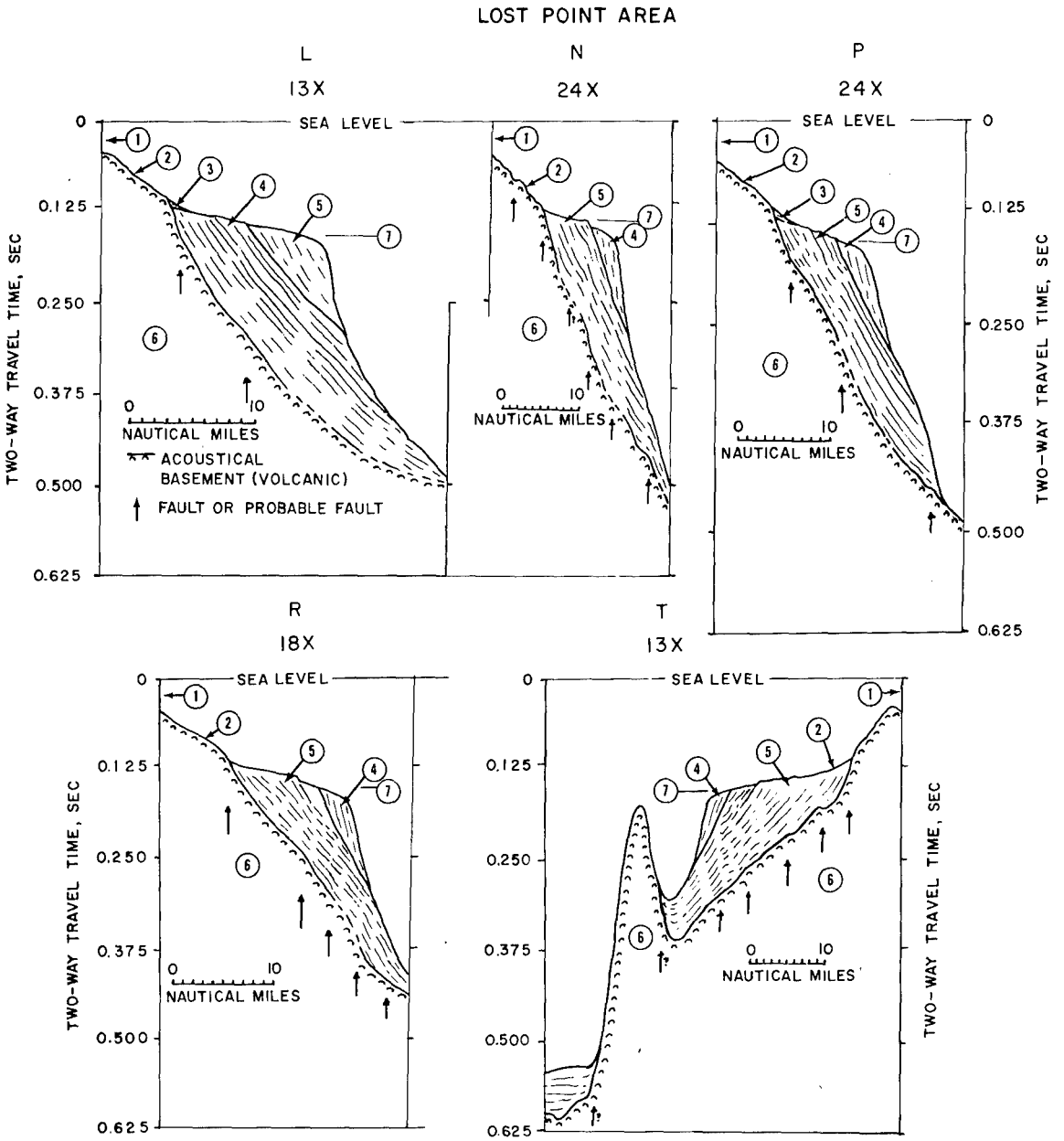

FIG. 11. Line Drawings of Profiles L, N, P, R, and T, Lost-Point Area. Key: (1) shoreward; (2) seafloor; (3) Unit A; (4) Unit B; (5) Unit C; (6) Unit D; and (7) wave-cut terrace. Note offsets of terrace related to faulting. In one case (Profile N), the offset appears to be at the contact of Units B and C. (See Fig. 2 for location of profiles.)

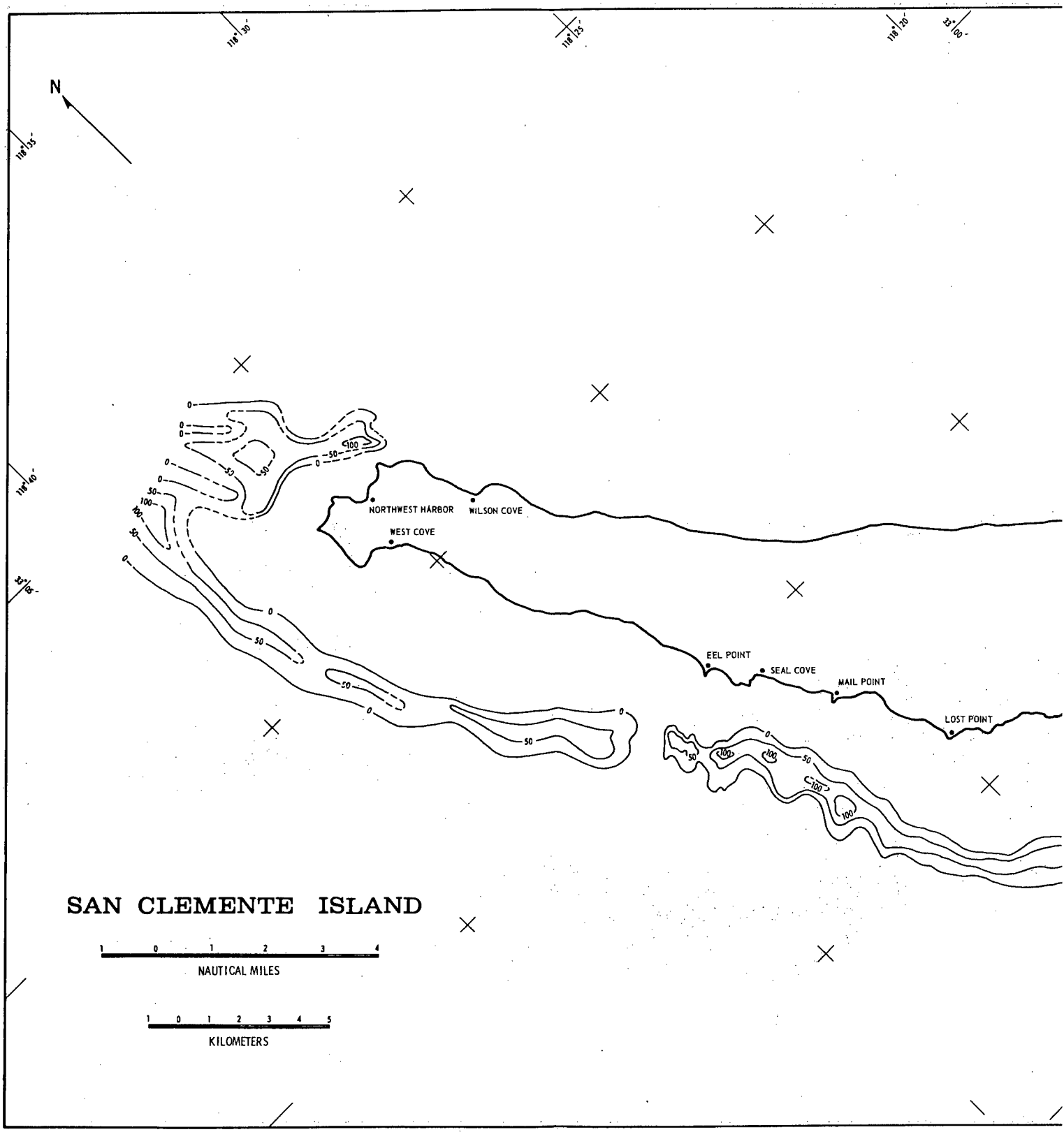

FIG. 12. Isopach Map of Unit B, Reconnaissance Survey. Irregular nature of contours off Eel a
of composite control from detailed and reconnaissance survey data.

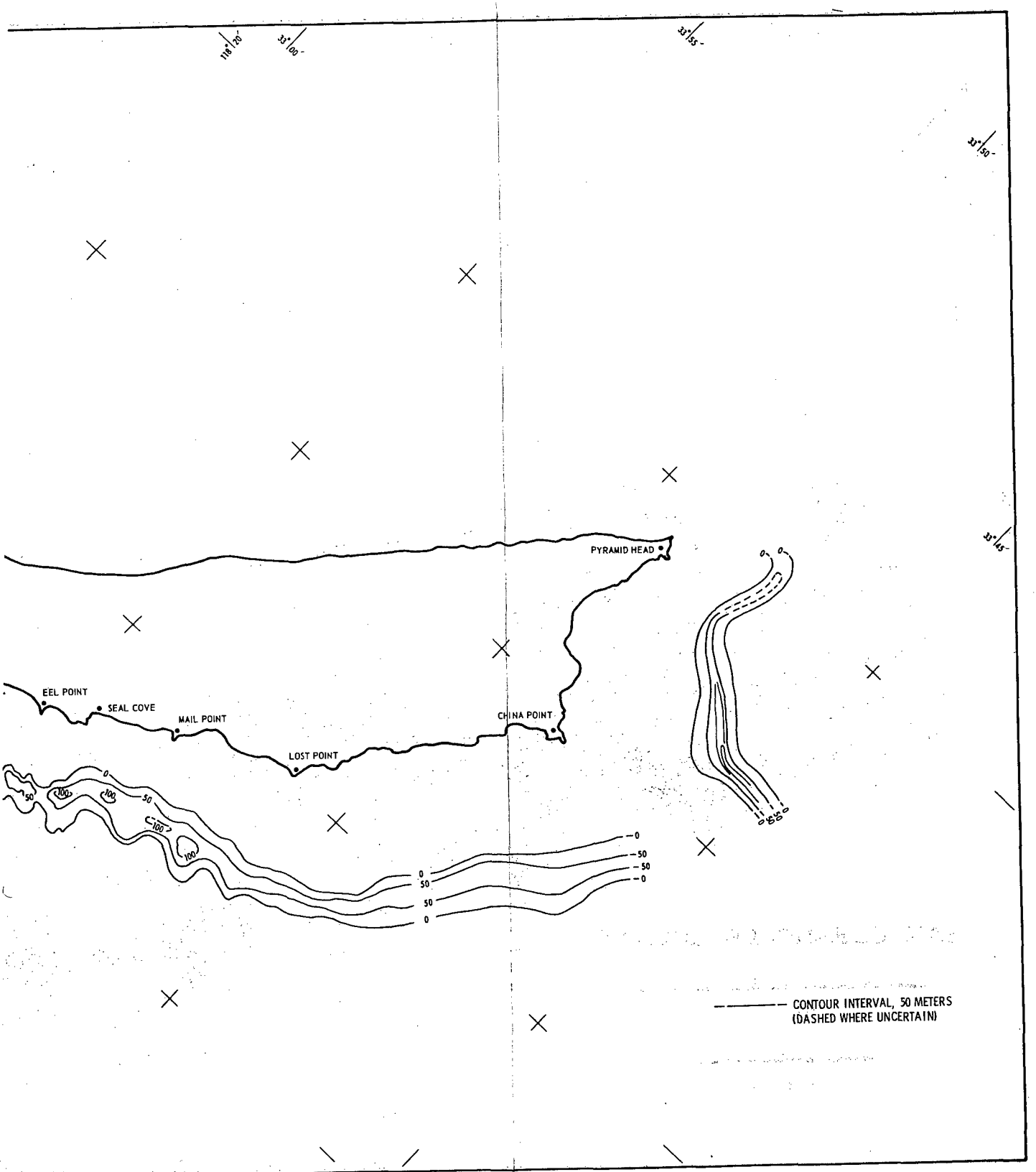

, Reconnaissance Survey. Irregular nature of contours off Eel and Lost Points is result
ed and reconnaissance survey data.

2

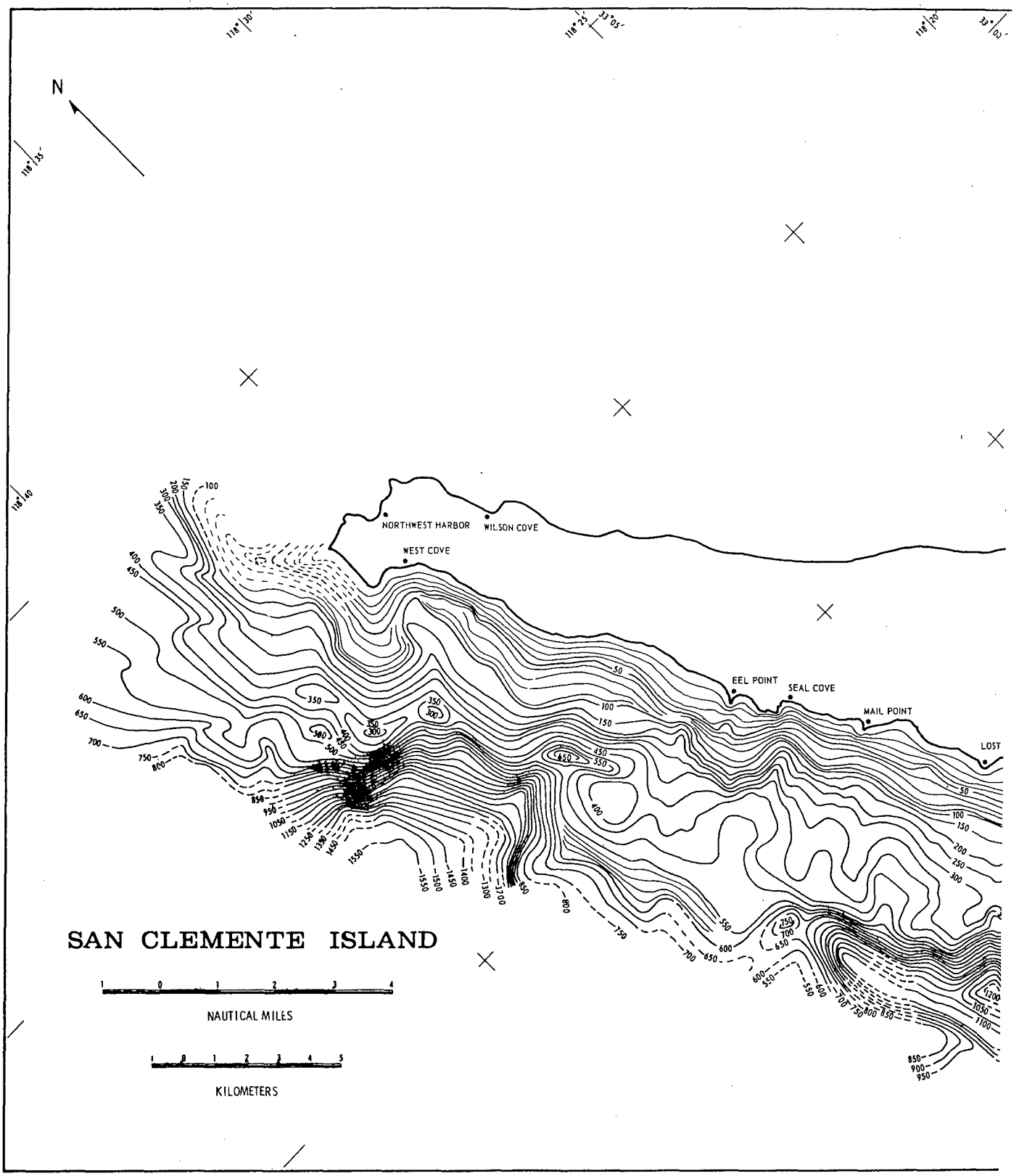

FIG. 13. Isopach Map of Unit C.

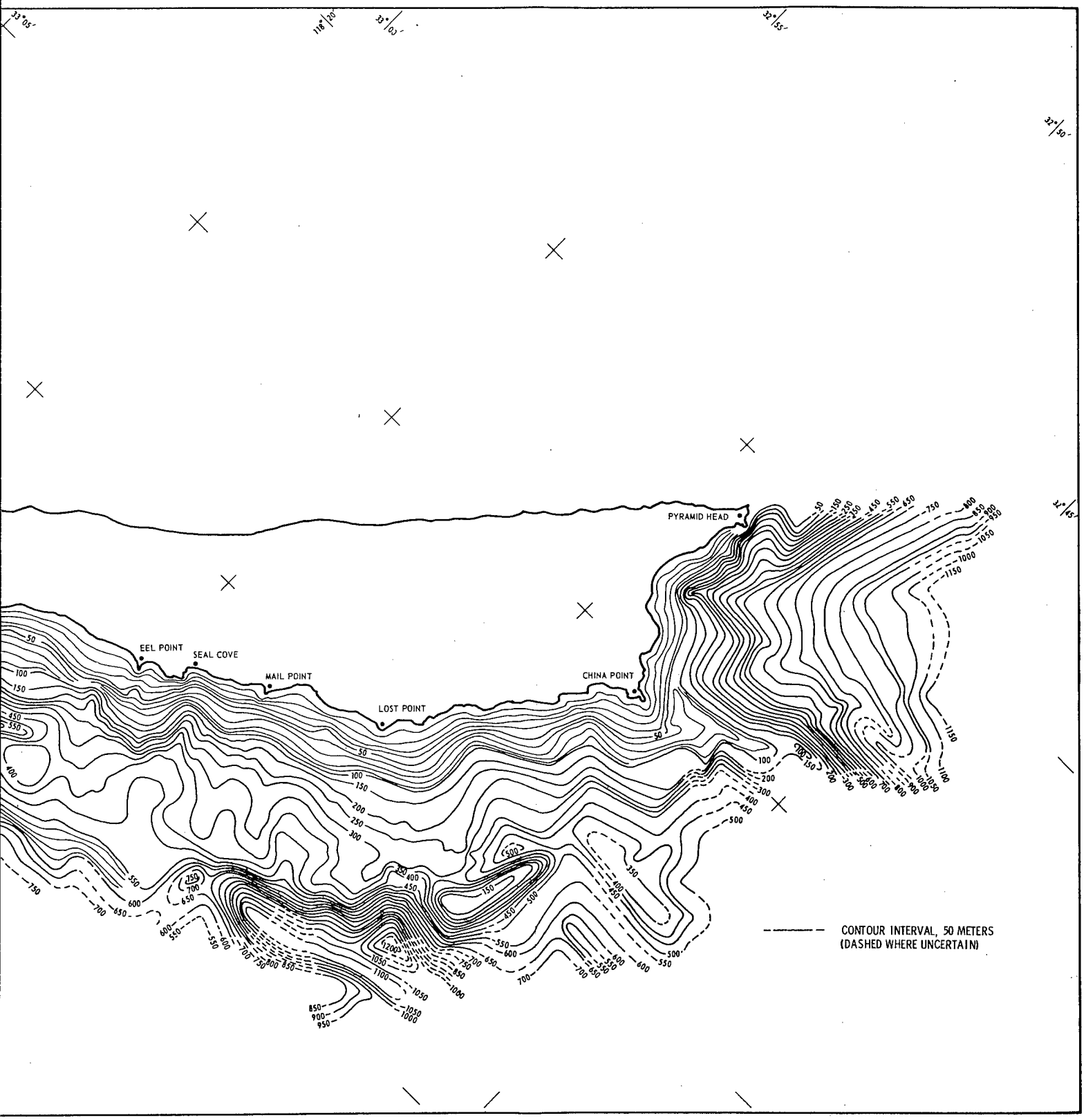

FIG. 13. Isopach Map of Unit C.

2

similar to those around the island in which depressions are filled to various degrees by the very coarse bioclastic debris of Unit A (see Part 1). Ridges of this unit form breaks in the escarpment that are considered of fault origin. The ridges act as natural dams for sediment transported downslope.

The Emery Seaknoll is interpreted from dredge hauls as volcanic rock (Ref. 7). Profile interpretation corroborates this interpretation and indicates that much of the northern part of the Southern Plateau is also volcanic rock.

Unit X. This unit comprises the post-orogenic strata. Only the major sections are isopached (Fig. 15), so that the aerial configuration of these sediments might be shown. The zero isopach line represents (as for Unit A of Part 1) the approximate pinch-out of the main sections of the unit. Unit X actually extends beyond this line as a thin veneer that mostly comprises hemipelagic sediment overlying bathymetric highs.

A surficial part of Unit X corresponds to Unit A of the detailed survey. Part of the subjacent section undoubtedly correlates with Unit B, although profile correlation was too tenuous to relate the two units specifically. However, Unit X is subdivided into two and possibly three significant unconformities in the basin areas off the east side of the island. These subdivisions are believed to correspond to Units A and B and a possible third period of deposition (possibly Pliocene). Gaal (Ref. 7) reports two post-orogenic sediment unconformities near the margins of the Santa Catalina Basin that he believes are Pliocene to Recent in age. Moore (Ref. 11) contends that all of the post-orogenic sediments are Pleistocene or younger.

A maximum thickness of slightly greater than 550 meters is recorded in the triangular basin pattern off the Wilson Cove area. Most other areas along the San Clemente fault zone have thicknesses of less than 300 meters. Unit X outlines geometric patterns that are generally linear, abruptly terminated, and often triangular to rectangular in shape (Fig. 7). Some are also elongated and oval in outline. The planar sediments of this unit are clearly outlined in the perched troughs along the escarpment. Much of the upper part of the elongated section of the shelf off Northwest Harbor, which is interpreted as Unit B (Fig. 12), could be the equivalent to Unit X.

With a maximum thickness of 100 meters off the west side of the island, Unit X is interpreted here as a combination of apron and minor fan deposits (Ref. 22). Isopach configurations along this side of the island suggest trends of sediment trajectories that follow the geomorphic pattern; for further discussion, see the section entitled Sediment Transport and Deposition below.

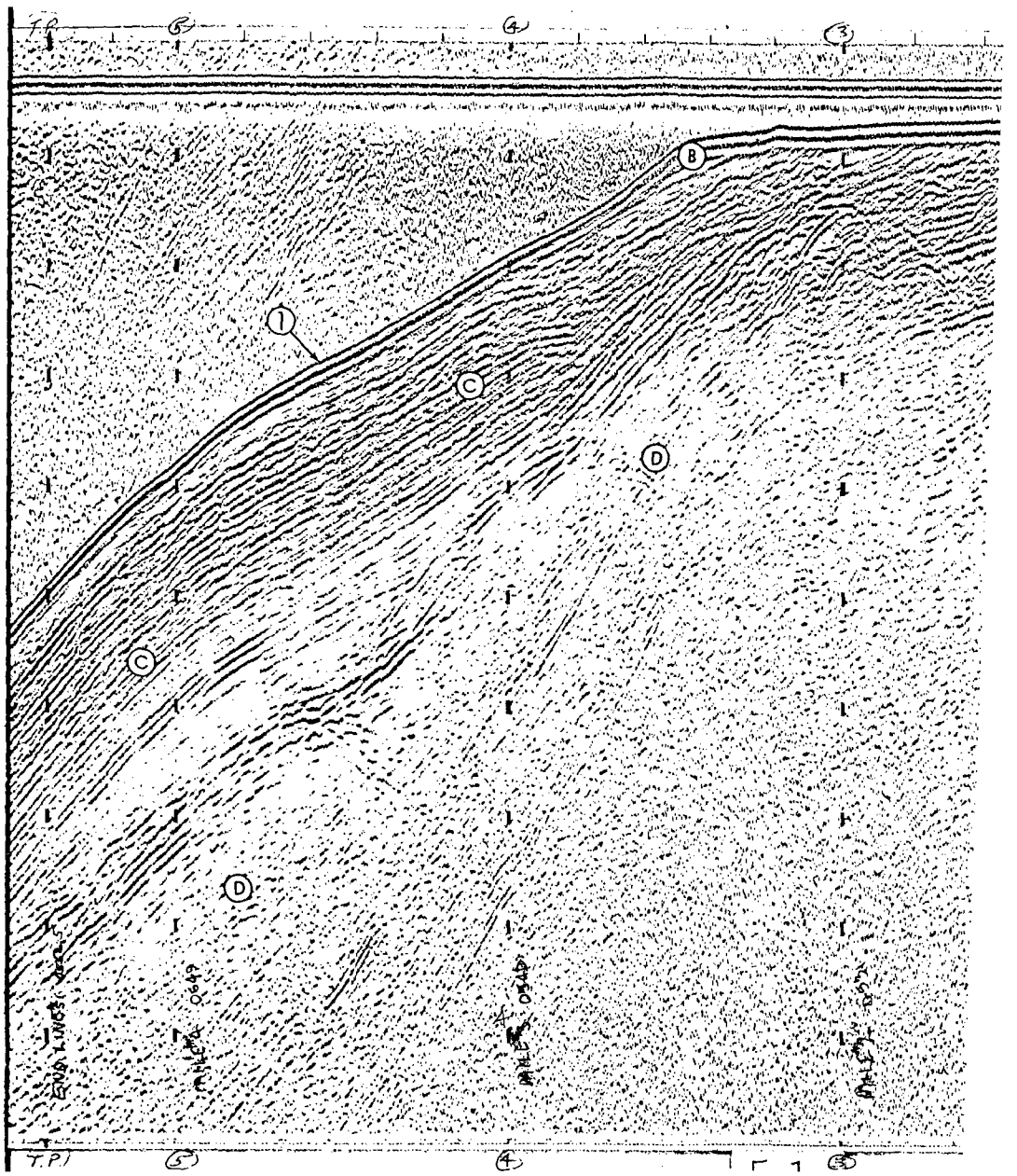

(a)

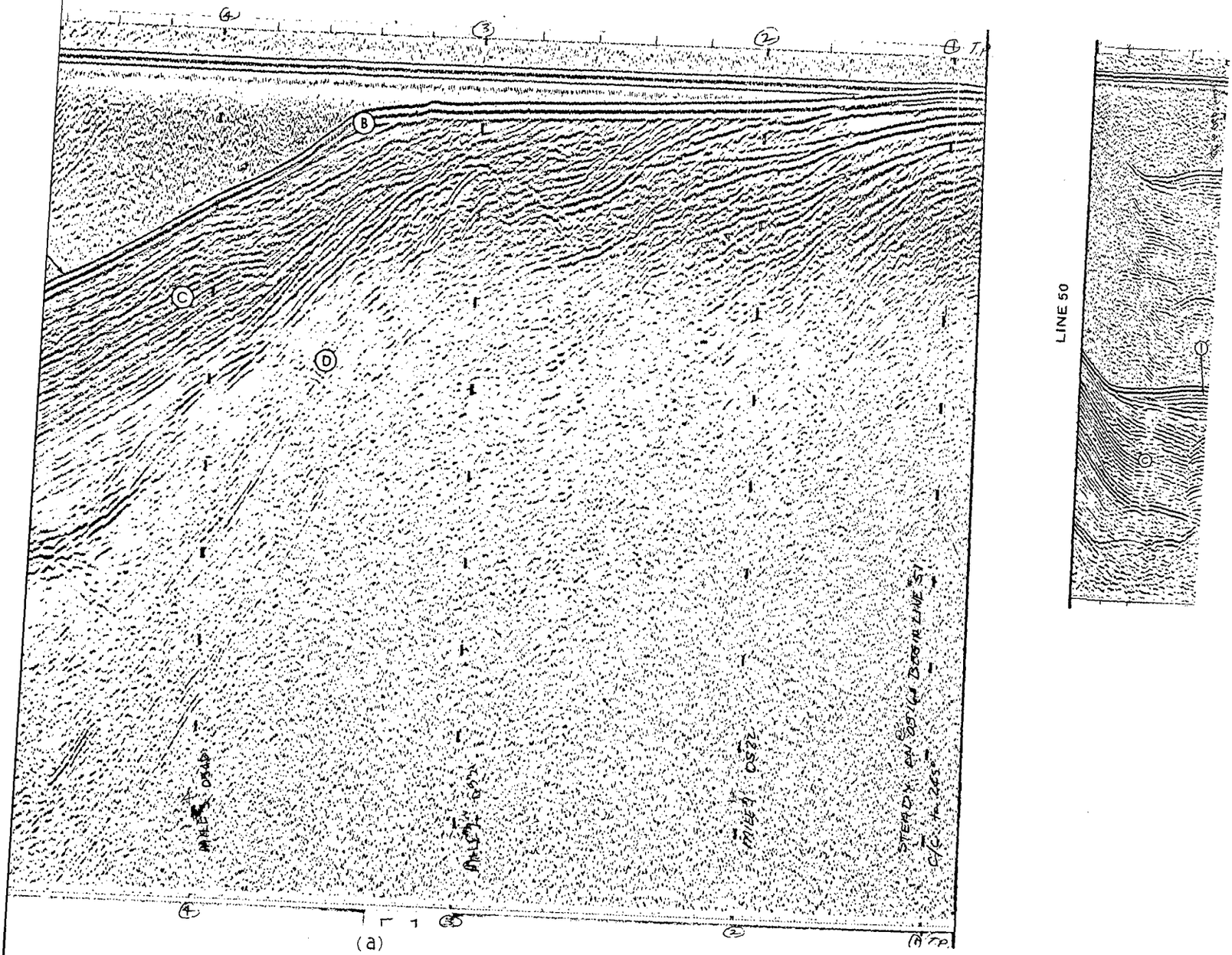

FIG. 14. Reconnaissance Survey Seismic Profiles.
(a) Profile 51, Showing Unit B, Unit C, Unit D, Seafloor (1).
(b) Profile 50, Showing Unit B, Unit C, Unit D, and Post-Orogenic Fill in Zone Dissected by Faulting and Erosion (1).

2

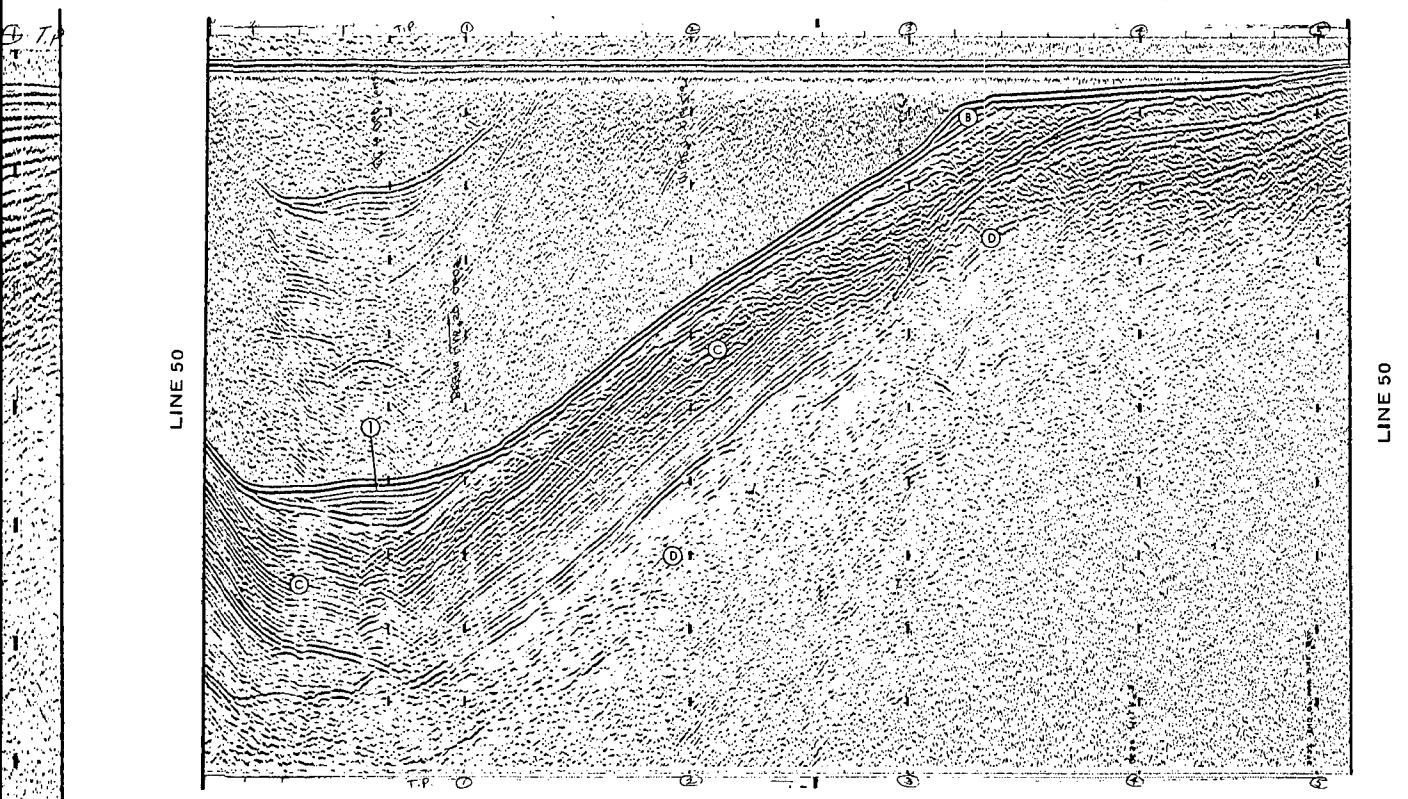

ofiles.
nit D, Seafloor (1).
nit D, and Post-Orogenic Fill
sion (1).

3

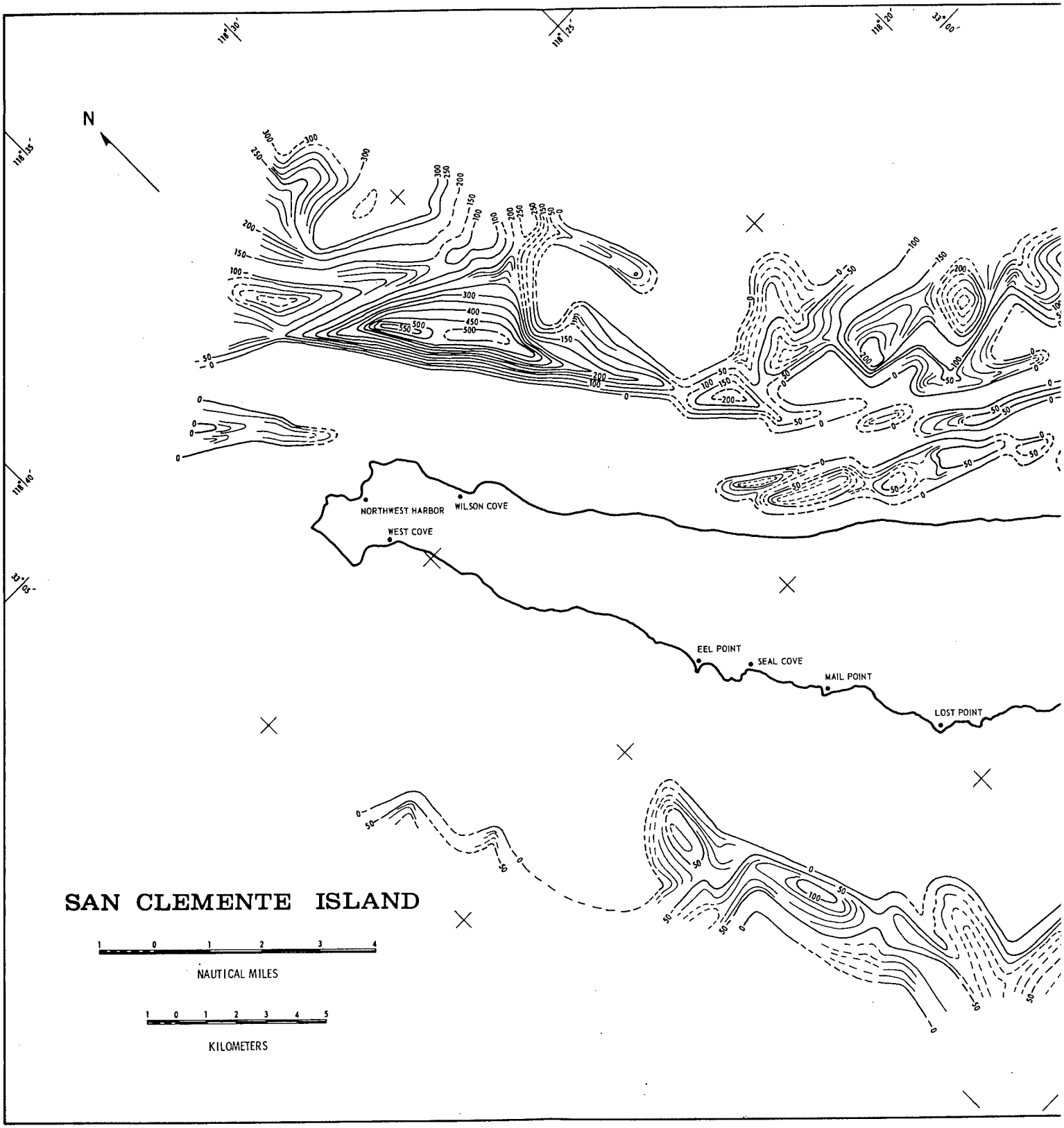

FIG. 15. Isopach Map of Unit X. Note outlining of apron and fan deposits off west side of island, trough fil

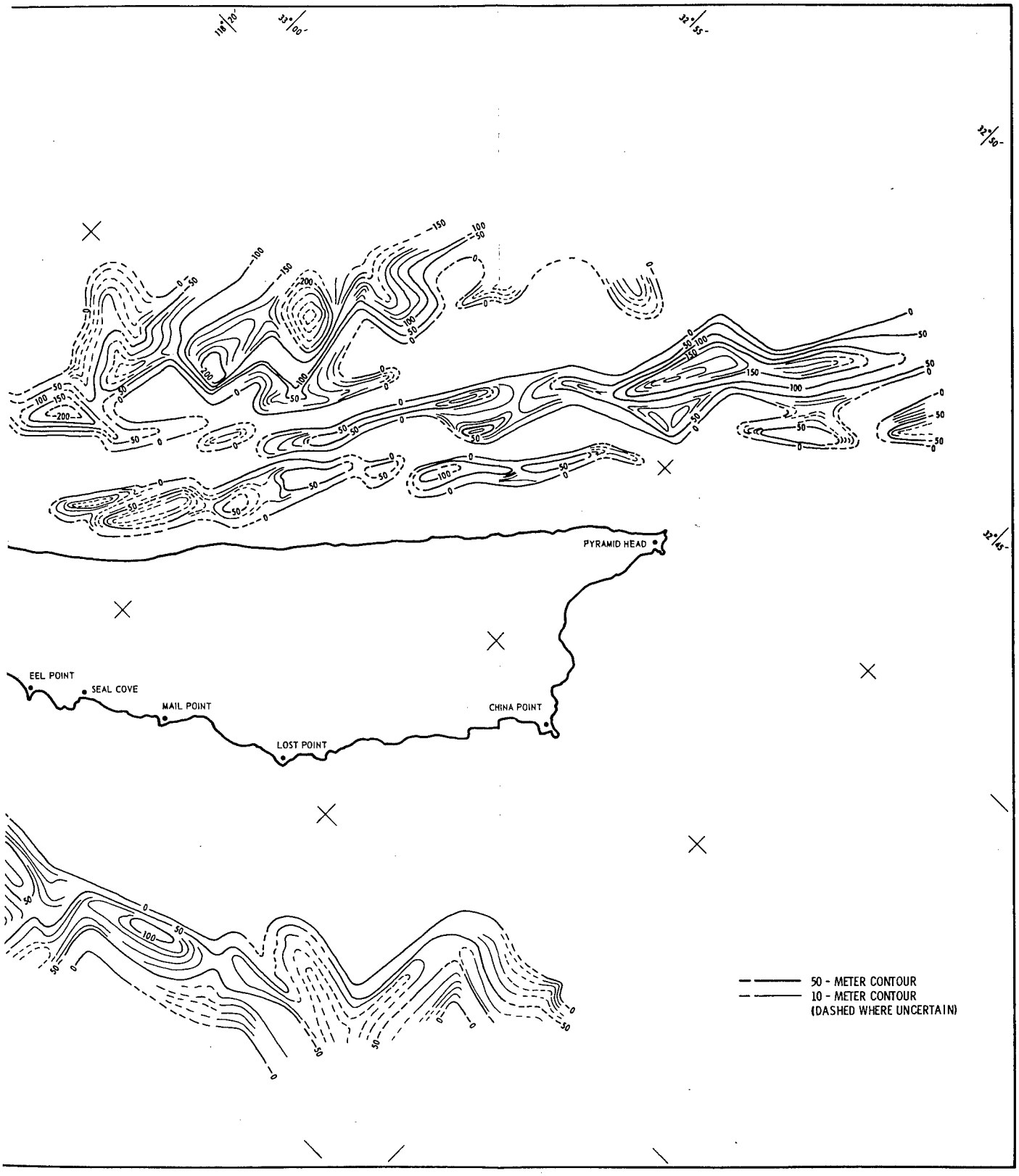

g of apron and fan deposits off west side of island, trough fills and structural lining off east side.

2

TECTONISM AND RELATED GEOLOGY

FAULT EVIDENCE IN AREA OF STUDY

Certain geologic and geomorphic features of the San Clemente Island offshore region are defined above and are used as a basis for further discussion and integration of the structure revealed by the seismic profile surveys.

The present study uses the results of previous investigations, coupled with continuous seismic profiling, as the bases for structural interpretations. Integration of internal structure and topography is used to differentiate fault scarps from flanks of folded sedimentary structures (see Part 1).

Anomalous Fault Trends. Major faulting, which is apparent from all offshore survey data, is generally related to faulting on the island. Anomalous trends in the isopach intervals of the geologic units are attributed primarily to faulting.

A tectonic map of the San Clemente Island block region (Fig. 16) was made with the objective of showing small, as well as large, faults or probable faults to indicate stress trends. Ridges, linear depressions, and anticlinal-synclinal folds are depicted by the same symbol; it is often difficult to differentiate small features of this type on the profiles because of the "velocity effect." Where faults could be confidently projected to those identified on the island, they are tied together by dashed lines. Island faulting is mainly taken from Olmsted (Ref. 2), with modifications resulting from the work of Merifield and Lamar (Ref. 4) and the author's field and aerial photographic interpretation.

A major fault-strike trend to the northwest is particularly evident along the east side of the island, and represents the San Clemente fault zone. The main fault of the zone is defined as the break (and trough) at the base of the San Clemente Escarpment (Fig. 10, Profiles 5, 11, and 13, and Fig. 16). A second, more northerly, major fault trend cuts obliquely across the island block; it is pronounced immediately off the northern one-third and the south end of the island. A third fault trend is strongly evident to the east of the San Clemente fault zone, and cuts the central and south parts of the island block.

Statistical Analysis of Faulting. The use of faults and other displacements to reconstruct stress fields is often a tenuous and far from simple procedure. Statistical treatment of the data is one method that allows elimination of local anomaly deviations. Rose diagrams of various sections of the region of study (Fig. 17a-e, Table 1) indicate that a basic three-directional fault trend exists. Together, these trends appear to be the result of horizontal compressional stress, with the principal axis oriented roughly 30 degrees to the long axis of the island in a northerly direction. Specifically, the rose diagram of Fig. 17a shows a major fault-strike trend averaging N40°W, which is considered a principal shear direction. This trend is very close to that of the San Clemente Escarpment (Ref. 5, Chart 1) and the San Clemente fault as defined by Moore (Ref. 11, Fig. 13). A second average trend is at N13°E. The rose diagram of Fig. 17b has an average trend of N10°W. That of Fig. 17c

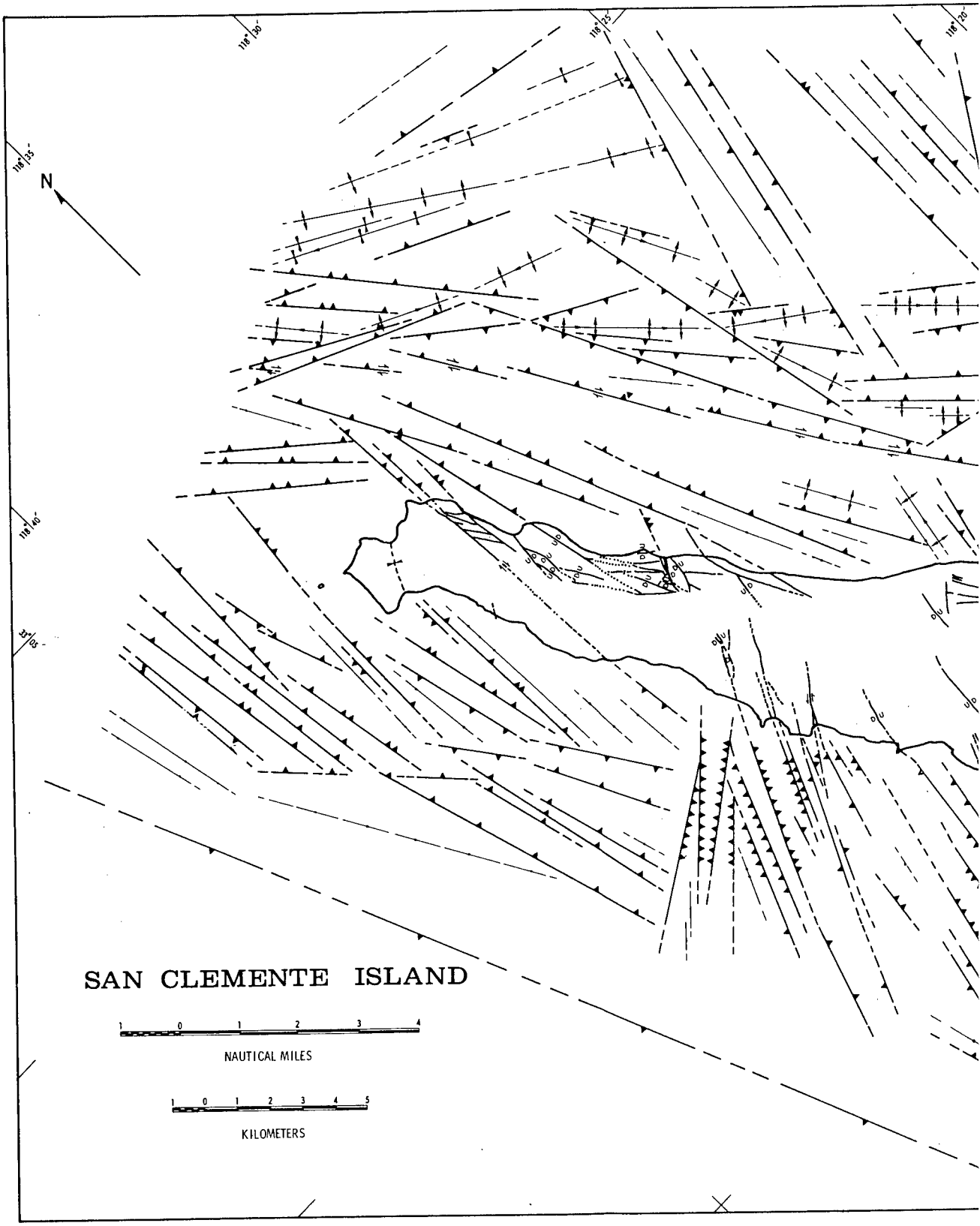

FIG. 16. Tectonic Map of San Clemente

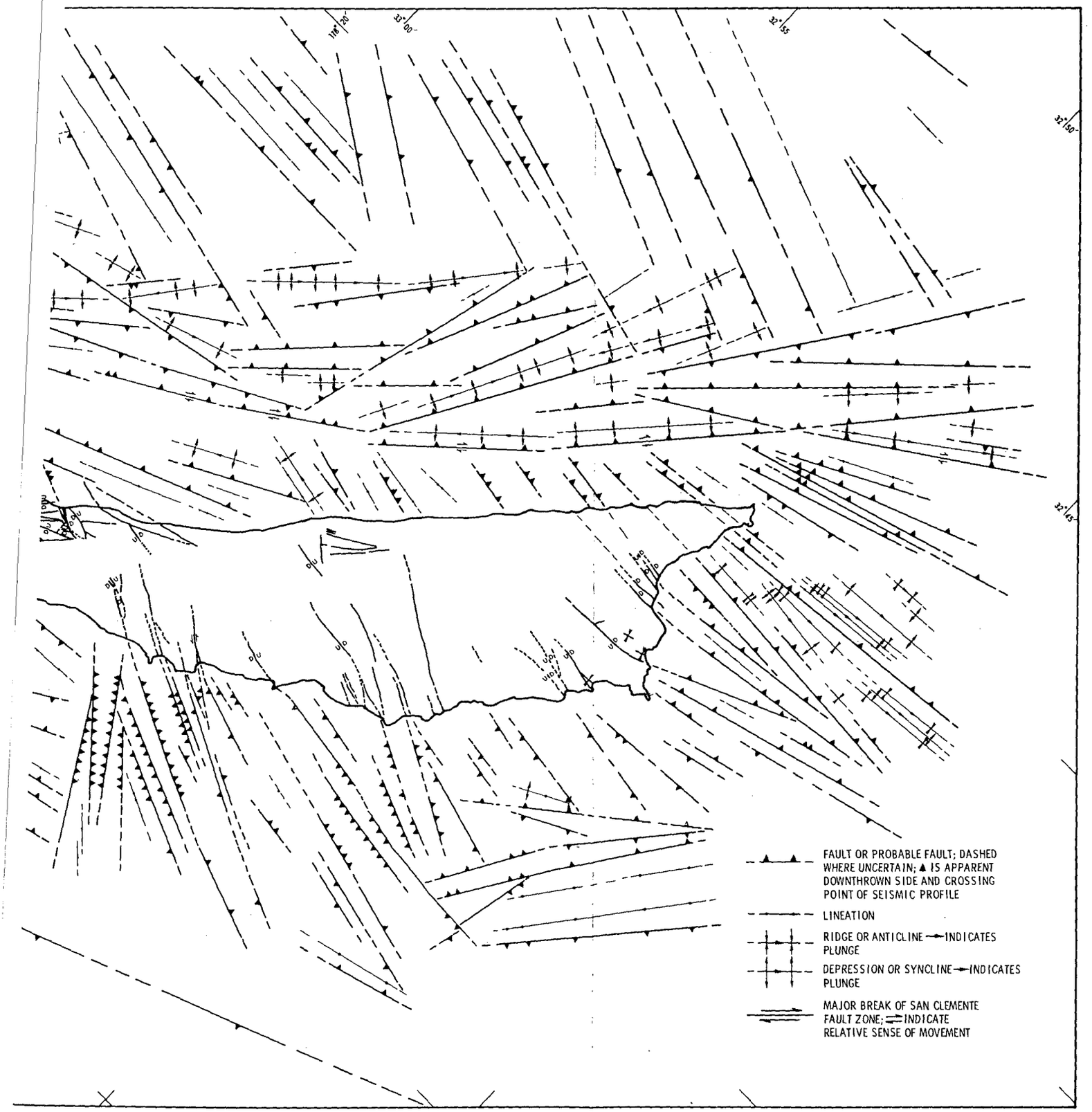

FIG. 16. Tectonic Map of San Clemente Island Block Area.

2

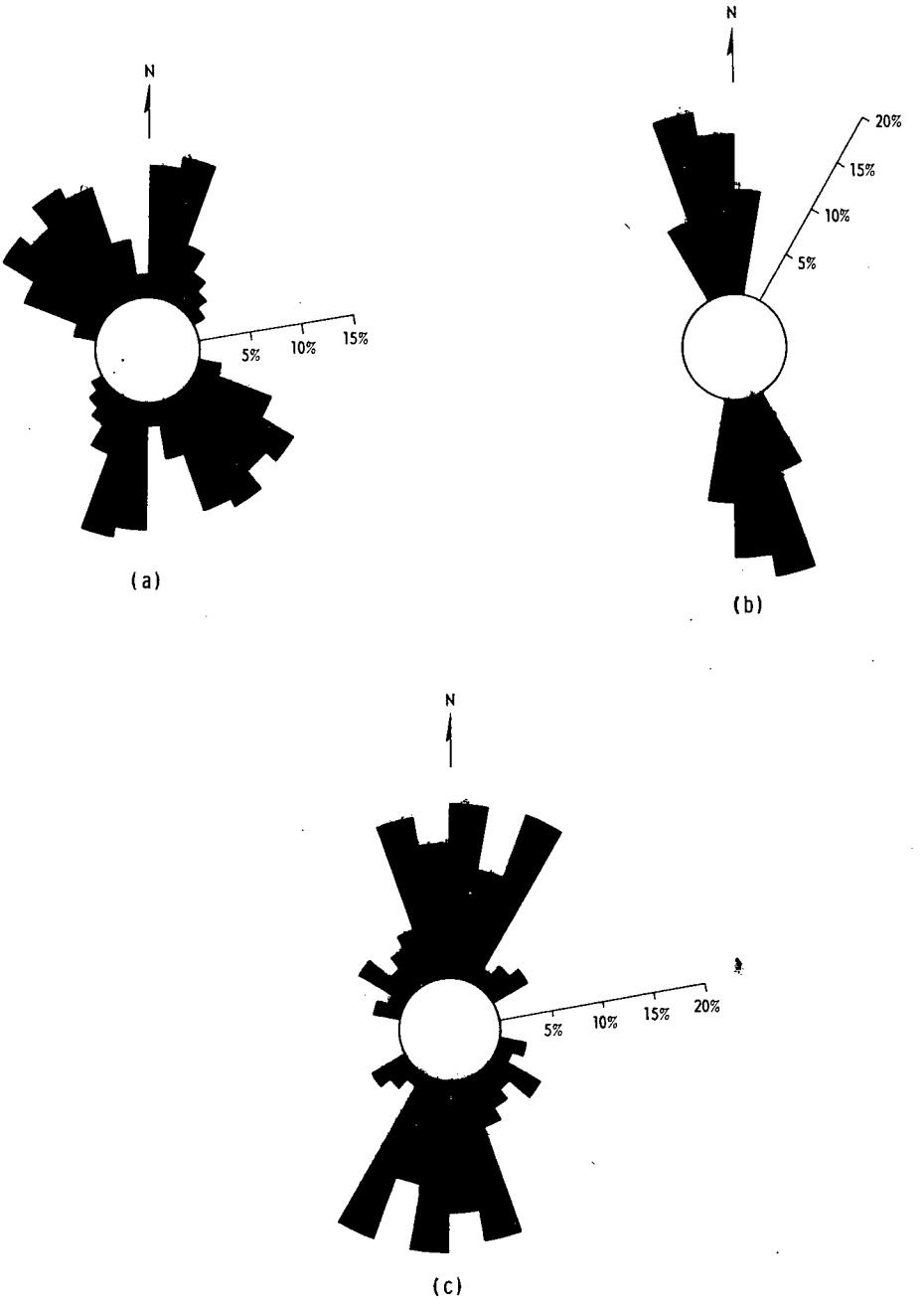

FIG. 17. Rose Diagrams of Fault Strikes in San Clemente Island Block Area (10-Degree Increments).
(a) Northeast Side.
(b) South End.
(c) Southwest Side.

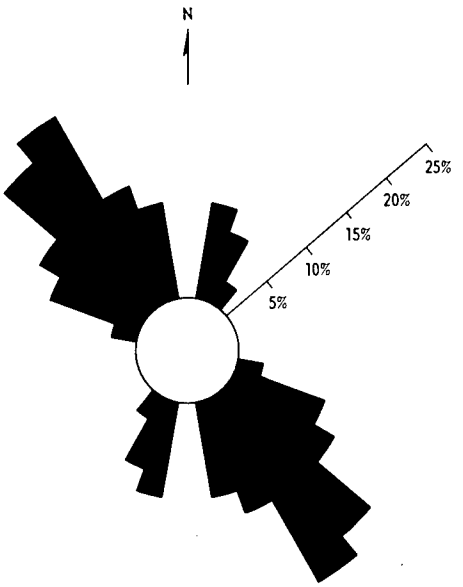

(d)

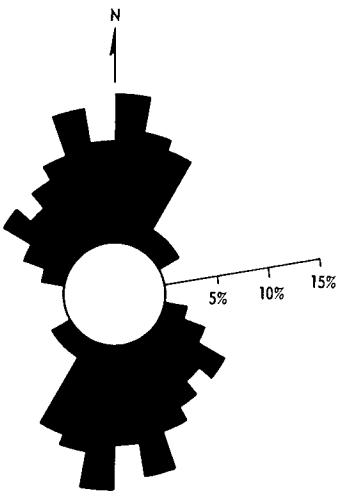

(e)

FIG. 17. (Contd.)
(d) Recent Fault Activity.
(e) Total Faults in Studied Area.

TABLE 1. Frequency of Fault Occurrence

Azimuth	NE side of island		SW side of island		South end of island		Reactivated fault		Total faults	
	No. of occurrences	Percent of occurrences	No. of occurrences	Percent of occurrences	No. of occurrences	Percent of occurrences	No. of occurrences	Percent of occurrences	No. of occurrences	Percent of occurrences
N70-80W	2	2.22	2	2.56	...	...	1	2.27	4	2.13
N60-70W	7	7.78	1	1.28	...	...	4	9.10	8	4.25
N50-60W	10	11.12	4	5.13	...	...	5	11.36	14	7.45
N40-50W	9	10.00	2	2.56	...	...	8	18.18	11	5.85
N30-40W	11	12.22	3	3.84	...	...	9	20.45	14	7.45
N20-30W	10	11.11	4	5.12	3	15.00	5	11.36	17	9.04
N10-20W	5	5.55	12	15.39	7	35.00	4	9.09	24	12.77
N -10W	2	2.22	10	12.82	6	30.00	...	...	18	9.57
N -10E	11	12.23	13	16.67	4	20.00	...	...	28	14.89
N10-20E	12	13.33	8	10.25	...	...	4	9.10	20	10.64
N20-30E	5	5.56	13	16.66	...	...	3	6.82	18	9.57
N30-40E	3	3.33	1	1.28	...	...	1	2.27	4	2.13
N40-50E	2	2.22	2	2.56	...	...	...	...	4	2.12
N50-60E	1	1.11	3	3.84	...	...	...	...	4	2.12
Total	90		78		20		44		188	

has three trends that average N18°W, N7°E, and N24°E. Figure 17d, based on what are believed to be recent offsets of the seafloor at basin and trough fills, has an average trend of N42°W with a secondary trend at N20°E. All of these trends shown in Fig.17a-e have an anomalous grouping pattern (Fig. 18). The averages of these groups (Fig. 19) result in a pattern whose included angles very closely coincide with the theoretical angle (taking frictional effects into consideration) between primary shear faults (e.g., Ref. 23 and 24), but modified by tensile fracturing between the directions of primary shear.

Anomalous Lithologic Trends. Figure 12 depicts the broad offshore structural fabric along the west side and ends of the island. However, from evidence presented under the detailed survey, the structural outlining is primarily the result of deposition on the unconformity at the post-orogenic surface. Closer spacing of the data would better define any isolated depressions, such as those revealed by the detailed survey.

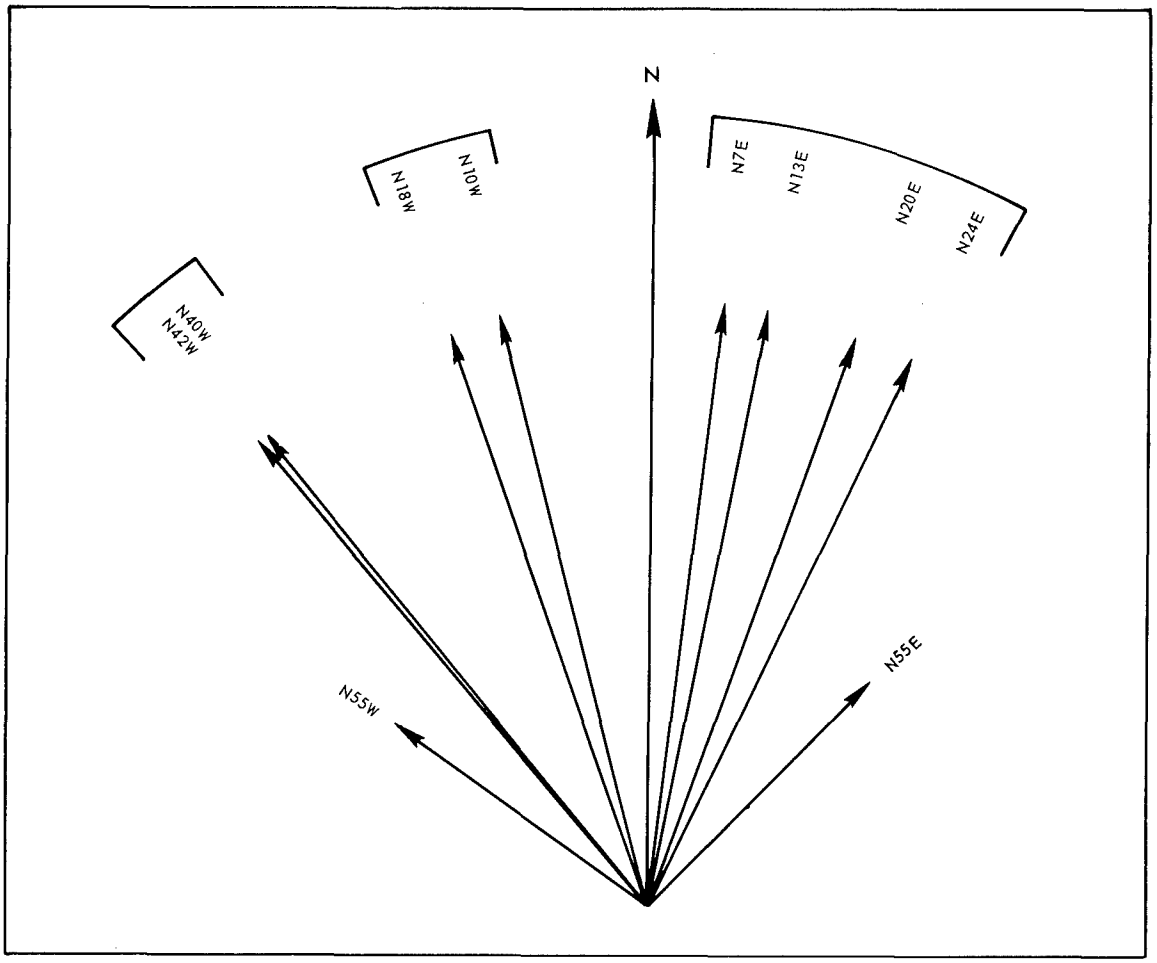

FIG. 18. Clustering of Fault-Strike Averages in Rose Diagrams of Fig. 17.

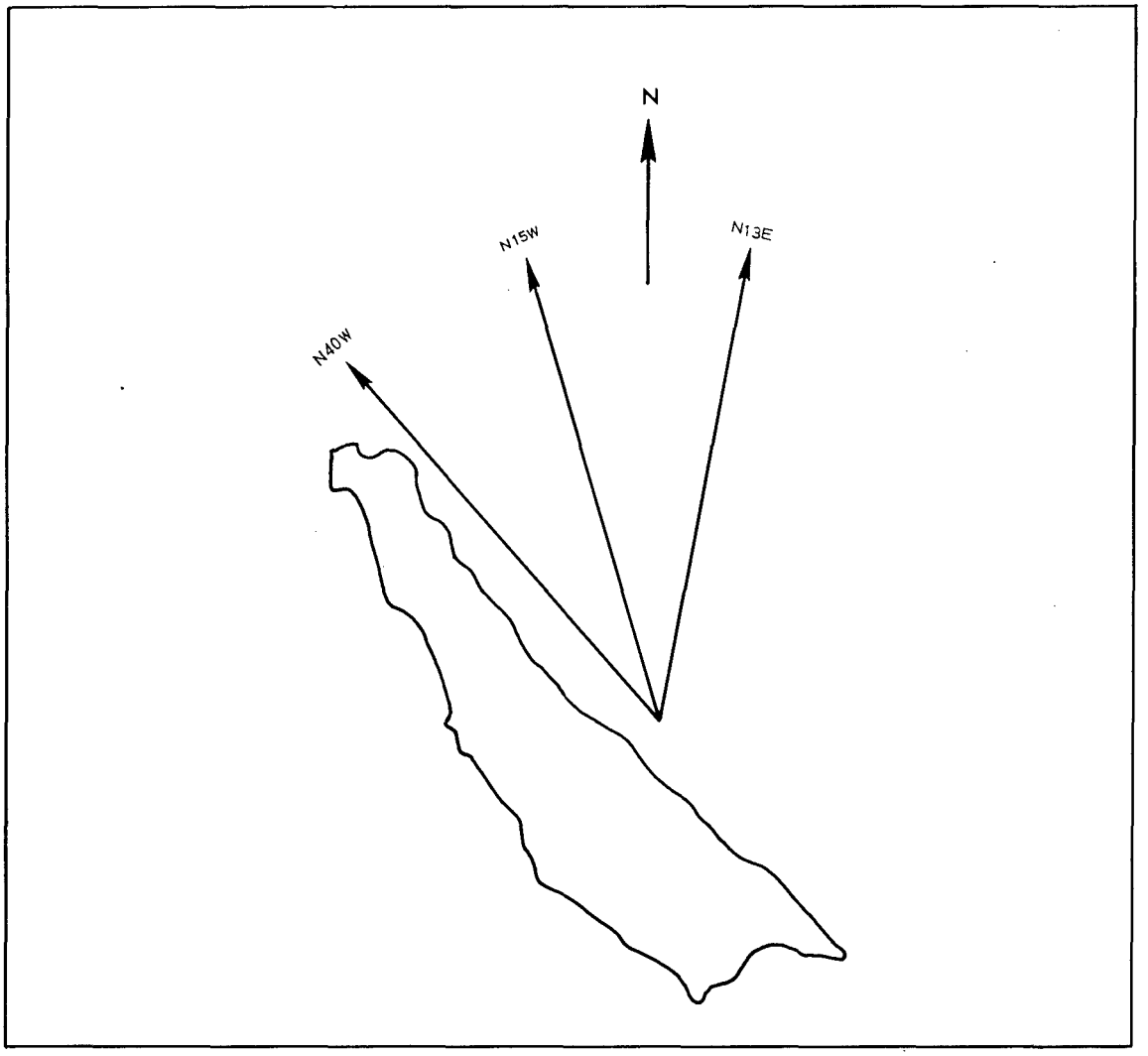

FIG. 19. Average of Fault Strikes, Giving Three Major Azimuths (see Fig. 17).

The lower part of the northwest-trending deposit off the north end of the island may be remnants of pre-orogenic strata preserved by faulting; a clear-cut definition of Unit B was difficult and tenuous, as based on the profiles of this area.

The only separation of Unit B along the west side of the island is at Eel Ridge Canyon. This break further emphasizes the contrast in the physiological and structural nature of these areas to the north and south along this side.

The structural trend illustrated in Fig. 13 tends to substantiate the one shown on the tectonic map. A pronounced change in this trend is noted to the north and south of the Eel Point-Lost Point area. The areas to the north and south are similar by virtue of having northwesterly and northerly trends, respectively. The area between Eel and Lost Points has northerly to northeasterly trends.

Figure 13 more clearly defines the major exposure of volcanic rock seaward of the wave-cut terrace in the detailed survey area. In addition, the irregular configuration of this exposure more strongly illustrates the structural control disclosed by the detailed survey.

The adjacent major thick sections southwest of West Cove appear to have right-lateral offset. The thick graben section immediately north of Eel Ridge Canyon has been severed by the northerly and northwesterly striking faults. A possible section of the graben immediately to the north has been offset by one of the north-striking faults. The two thick sections off Mail and Lost Points are dissected by a right-lateral offset (if these sections are considered to have been together before faulting). An apparent offset is present near the center of the thick section off Lost Point.

Presumably, the two thick sections off the south end of the island have been dissected and preserved by faulting, as their island complements have been. Some normal faulting is suggested by a predominance of blocks downthrown to the southeast. Normal faulting in this area is especially fitting for the cluster of faults immediately off Pyramid Head. The horsts to the south of China Point and off Pyramid Head are probably the result of tensional stress followed by normal faulting.

Profile interpretation suggests that blocks and ridges of Unit C are preserved along the entire San Clemente fault zone; these are shown as exposed upthrown as well as buried crustal blocks that are presumed to be underlain by volcanic rock. Some profiles indicate a Unit C thickness in this zone that corresponds to a sound velocity of roughly 0.6 second one-way travel time (approximately 400 meters).

Some of the broader structural trends of the island block are well delineated in Fig. 20. Normally, faulting should be better preserved by the cover of Unit C, provided that the surface separating Units C and D does not represent too great a hiatus. An interesting feature that suggests a hiatus between these units is the tendency for the sloping volcanic rock surface to "flatten" beneath and slightly seaward of the present submerged terrace. This may represent the remnant of a pre-Unit C wave-cut terrace.

The volcanic topographic highs off West Cove are emphasized in Fig. 20, which clearly shows the major depression that has preserved the thick parts of Unit C in this area.

Other major features described in Part 1 but reviewed here are (1) an elongated, north-trending topographic high immediately west of the detailed survey area with an adjacent trough to the east; (2) the pronounced southeast-trending topographic high off Lost Point; and (3) a complementary high to the west of (2) and (3). These topographic highs show trends, cutoffs, and offsets that strongly suggest structural control aligned with the inferred faulting in this area. Conceivably, these may also be vents for the volcanic flows that comprise the upper part of the island block. This is suggested especially for the high off West Cove that is believed responsible for a major magnetic high in this area (Ref. 6, 7, and 25).

In sum, structural trends of some areas in Fig. 20 do not correspond very well to the equivalent areas in Fig. 13; this reflects, in part, the extent of erosion on the surface of Unit C.

Because of the difficulties encountered in profile interpretation for the east side of the island, only post-orogenic sediments (Unit X) and the post-orogenic surface (Fig. 10) are used in the structural analysis of this area.

Figure 21 best illustrates the general over-all tectonic pattern for the east side of the island. Intersections of faults at various angles are outlined clearly by the linear trends and sharp discontinuities of the topographic highs and lows along the San Clemente fault zone. Furthermore, some of the geometric patterns suggest that more extensive faulting is present, featuring either completely separate faults or extensions of those defined in Fig. 16. Some northeast-striking faults suggest that left-lateral offsets have affected (crossed) the main fault zone to a much greater extent than shown by Fig. 16. This suggestion is enforced by Fig. 7.

The deepest part of the post-orogenic surface in the studied area is at the base of the San Clemente Escarpment off Wilson Cove. Depths to slightly greater than 1,700 meters are recorded in the triangular-shaped depression. The general shallowing nature of the main fault zone off the central part of the island is also evident.

Most of the pre-orogenic surface along the San Clemente Escarpment is considered volcanic rock and is, therefore, the equivalent of Unit D. Ridges of this surface form breaks in the escarpment that are considered of fault origin. These ridges act as natural dams to sediment transport. The contour patterns in Fig. 21 along the submerged part of the San Clemente Escarpment subtly reflect the interpreted fault pattern; the patterns are marked by a change of trend midway along the island. However, the area along the escarpment across from Eel and Mail Points may be affected more by the northeast-trending faults than is indicated by Fig. 21; the fill by Unit X sediments (Fig. 15) further suggests this because of offsets in these deposits.

Figure 15 further substantiates the structural fabric along the San Clemente fault zone. Offsets stand out very clearly. Pivotal, normal, or thrust faults resulting in minor crustal blocks are considered responsible for some of the trends along the fault zone and adjacent basin areas.

Specifically, the effect of intersections by lateral faulting is indicated by right- and left-lateral offsets around the southwest flank of the Emery Seaknoll (Fig. 16 and 21). In addition, the upthrust of crustal blocks and the development of depressions are strongly suggested. The effect of fault intersection across the entire San Clemente fault zone by the northeast-striking faults is also more readily seen that is apparent in Fig. 16. Note the right-lateral offsets in the perched troughs prevalent along the San Clemente Escarpment. The troughs, elongated northwest-southeast, are conceivably the consequence of slump blocks resulting from weak zones developed by the northeast and north-northwest-striking faults.

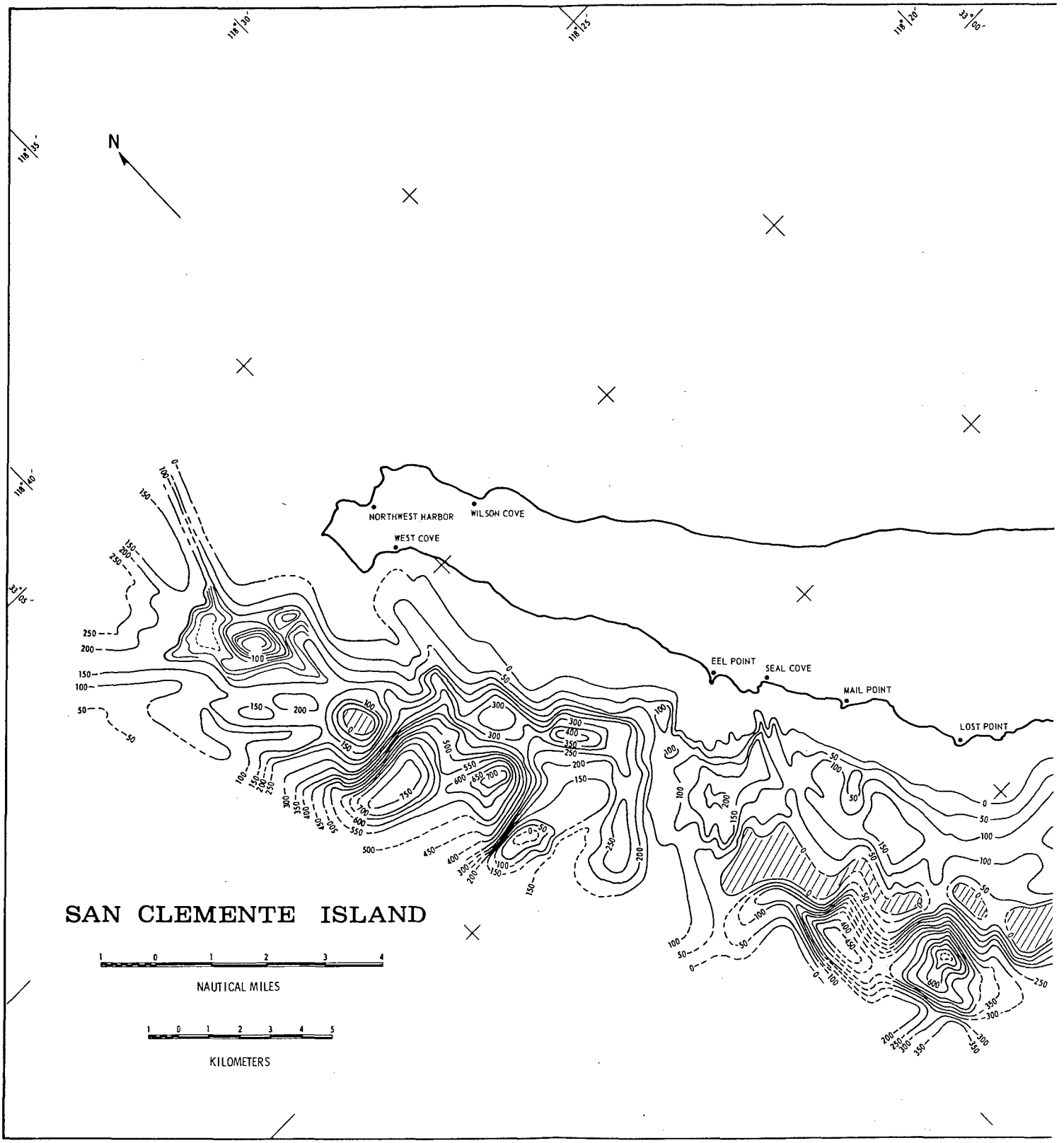

FIG. 20. Map of Structure Contours on Surface of Unit D.

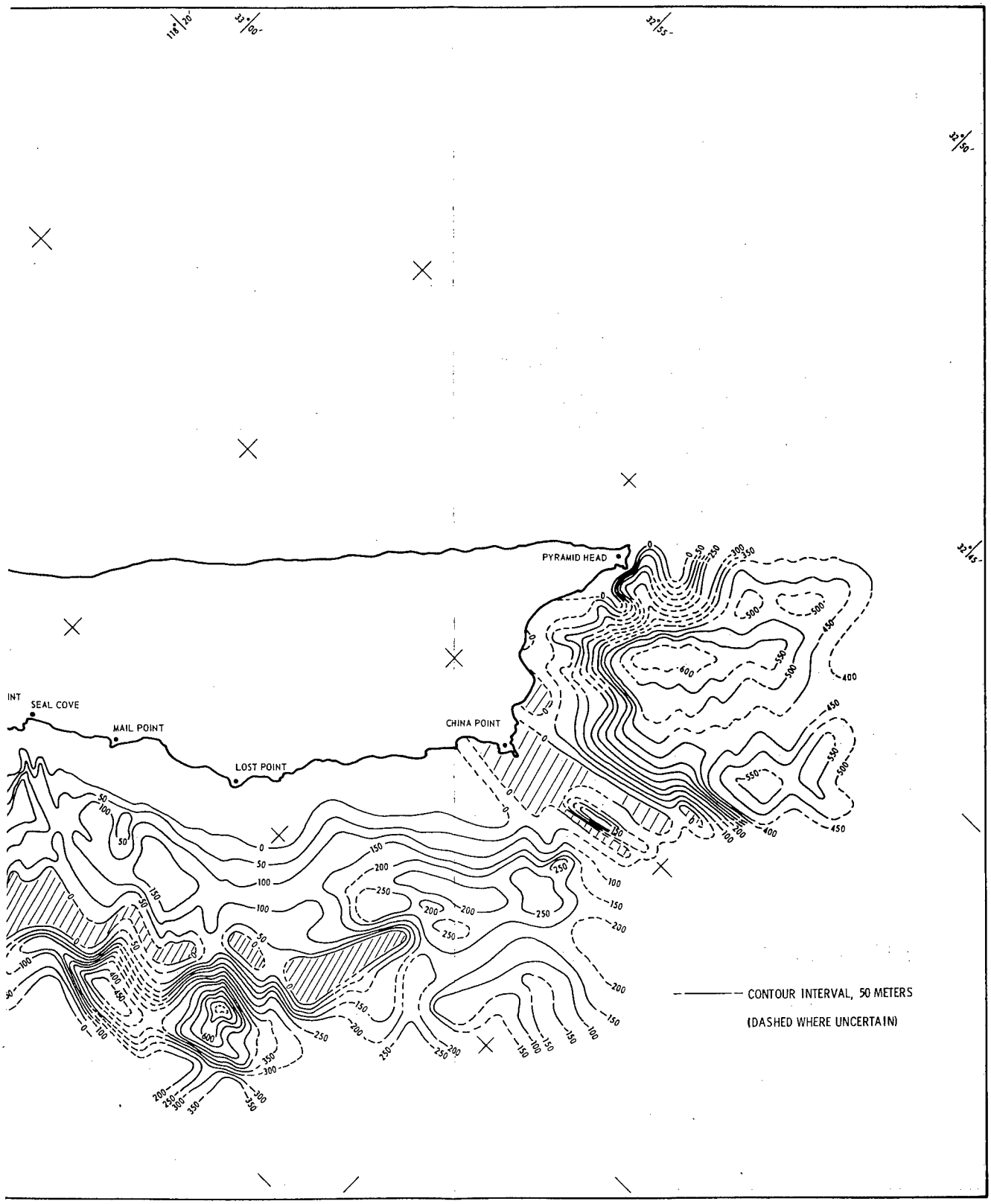

of Structure Contours on Surface of Unit D.

2

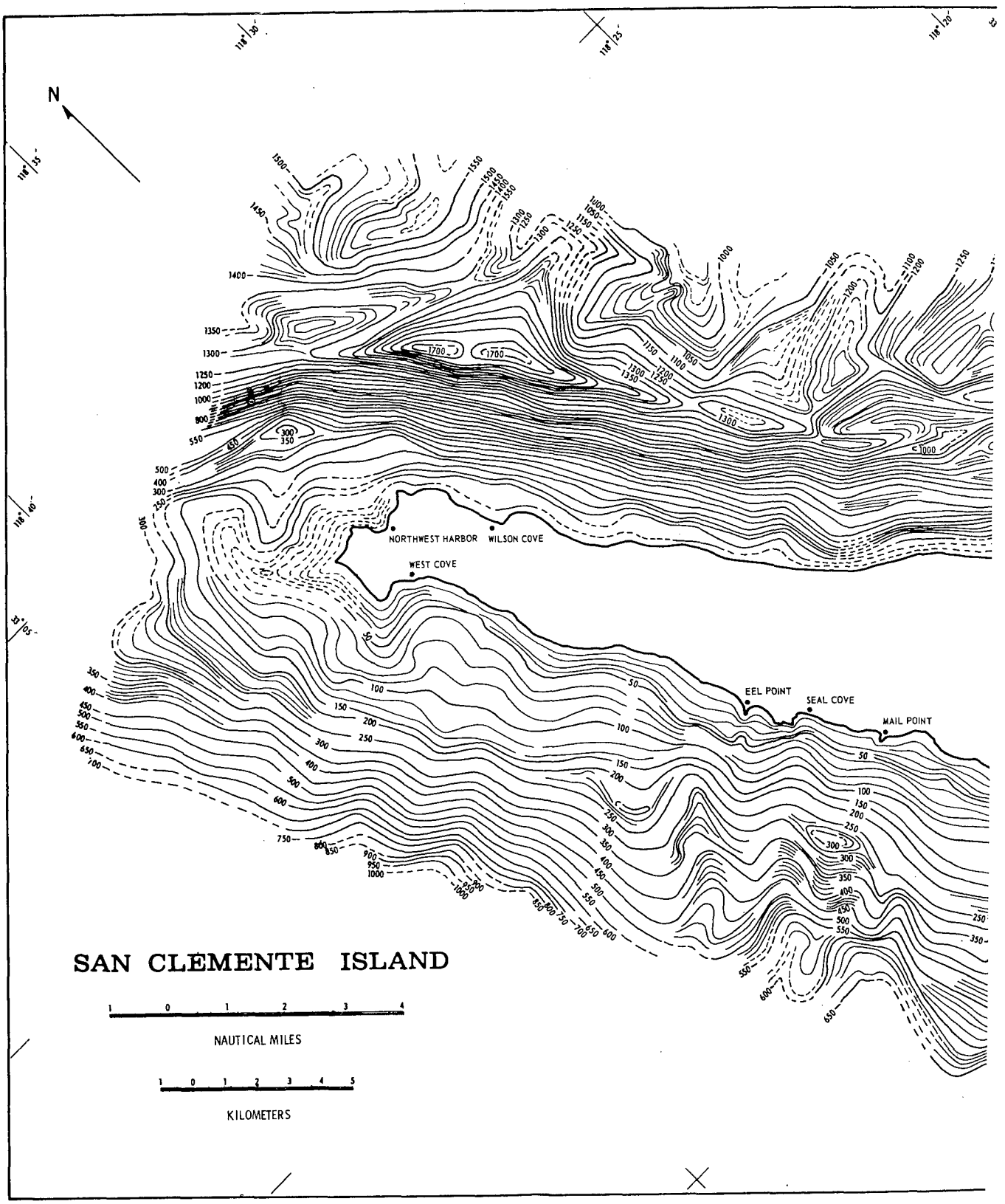

FIG. 21. Map of Structure Contours on Post-O

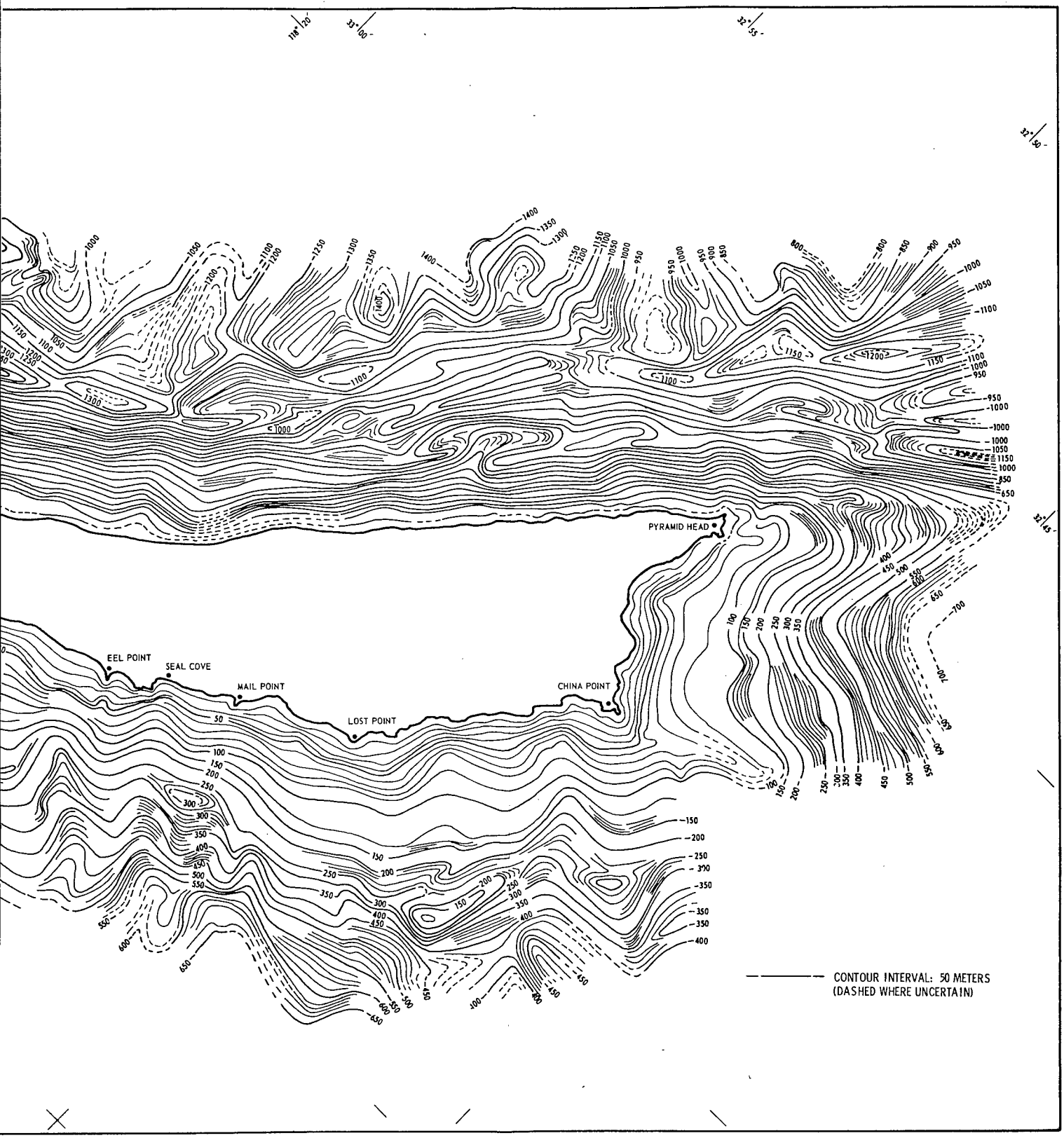

FIG. 21. Map of Structure Contours on Post-Orogenic Surface.

2

NATURE OF STUDY AREA FAULTING

The main purpose of this section is to analyze the structure of the San Clemente Island crustal block by a study of faulting, folding, and uplift in light of the lateral faulting.

Many authors disagree on the types of tectonic movement in the earth's crust and the interpretations applied to areas of study (see, for example, Ref. 25, 26, 27, and 28).

Moody and Hill (Ref. 29) have evaluated newer concepts of fault dynamics by a re-evaluation of published data, mechanics of faulting, and field observations. These authors develop the hypothesis that anticlinal folds, thrust faults, and wrench faults[3] can be generated from movement on a large wrench fault. They conclude that, for any given tectonic area, at least eight directions of wrench faulting and four directions of anticlinal folding, thrusting, or both, should accommodate the structural elements of that region (Fig. 22). These authors base some of their concepts on those developed by Anderson (Ref. 24) and McKinstry (Ref. 27).

San Clemente Fault Zone. Shepard and Emery (Ref. 5) show a bathymetric reversal in the direction of the scarp slope along the strike of the San Clemente fault. These authors tend to favor a horizontal shift of about 40 kilometers to explain this phenomenon, and give several reasons for this concept over that of pivotal faulting. Allen, et al. (Ref. 30), believe that the San Clemente fault is a continuation of the Agua Blanca fault, with a presumed lateral displacement of up to at least 11 kilometers. This displacement is similar to that of the San Andreas and San Jacinto faults of the coastal area.

Although the inferred fault scarps are of high relief in many areas of the Continental Borderland, this relief is considered relatively small compared with the postulated lateral movement along such features as the San Clemente-Agua Blanca faults, as well as those in the Southern California-Baja California region. Furthermore, Moody and Hill (Ref. 29) believe that the last increment of wrench-fault movement in many cases is essentially vertical and simulates a high-angle normal fault or high-angle thrust fault. This is illustrated by Anderson (Ref. 24, p. 170) for the San Andreas fault.

Referring specifically to the San Clemente Island block relief, local relief may also result from lateral faulting if a high area is brought into juxtaposition to a low area, accompanied by buckling of the moving block (Ref. 31) or thrust faulting (Ref. 32). Kingma (Ref. 33) suggests that a block may be squeezed up if caught between two strike-slip faults.

Moody (Ref. 34) postulates that shape change and shifting of crustal blocks may result from the stresses involved in wrench faulting. This could cause certain blocks to collapse (forming present basins) as a result of the dominant vertical movement along the pre-existing shear pattern. The San Clemente Escarpment could have been developed by such a shifting of crustal blocks.

---

[3] Synonomous with strike-slip, transcurrent, and, in the broad sense, lateral faults. The particular terminology is used here whenever it relates to a certain author's usage.

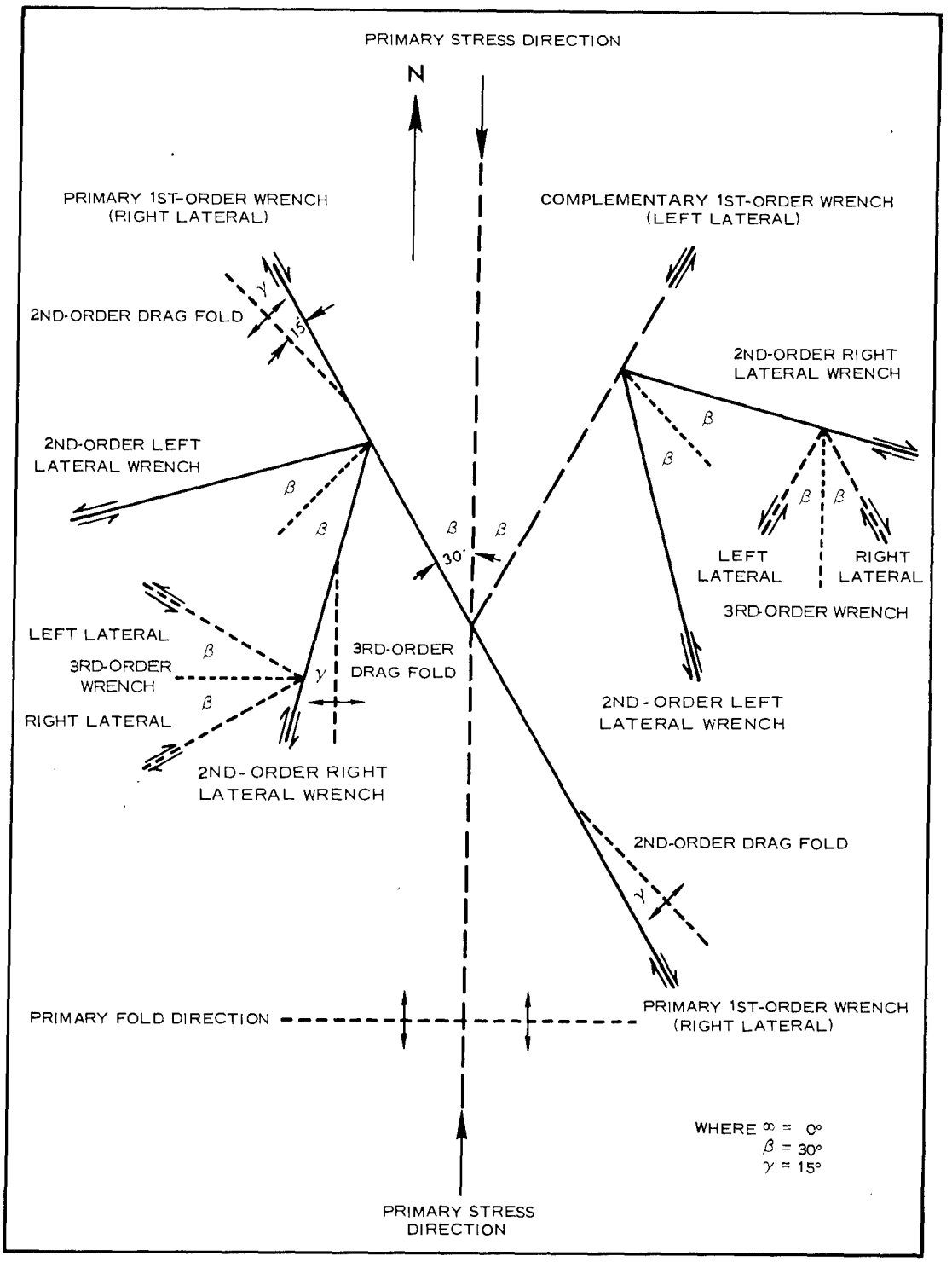

FIG. 22. Plan of Wrench Fault System Under North-South Compression (From Ref. 29).

Wrench faults are generally characterized by steeply dipping fault planes. However, Moody and Hill (Ref. 29) state that wrench faults with a dip much less than 70 degrees have been described in the literature. The fact that the San Clemente Escarpment has a maximum slope of only slightly more than 30 degrees is not considered a major obstacle to the wrench-fault hypothesis. Slumps and slump scars indicate that the slope has been modified since its inception. Erosion has undoubtedly had some modifying effect. Seismic profile records suggest that the fault tends to steepen slightly with depth, although this is not conclusive because of the hyperbolic nature of the acoustic response from bathymetric troughs.

St. Amand (Ref. 35) proposes that the most striking property of large lateral faults is the consistent straightness, or at least the smooth and gradual curvature, of the fault strike. This is sometimes supplemented by the occurrence of a trough, usually sediment-filled, along the strike of the fault. St. Amand also states that small-scale features attributable to smaller scale faulting are often found in the trough. Examples of these features are given, such as the thrusting of minor fault slices or the formation of small grabens. The trough itself may be developed by the formation of a graben through normal faulting on both sides of the main fault, or along the sides of thrust faults associated with the lateral faulting. St. Amand concludes that any fault having a straight trace more than a few miles in length has undergone lateral movement. All of the above properties are evident along the San Clemente fault zone.

Seismic epicenter evidence (Ref. 7) indicates that the zone representing the San Clemente fault has been relatively active since 1934, the first year that epicenter data were recorded. The earthquake foci are believed to be several kilometers in depth (Ref. 36). If these foci are associated with the San Clemente fault, as suggested, this fault must extend to several kilometers in depth. Normally, lateral faults are believed to be deep-seated, in particular those that are large primary lateral faults (Ref. 24 and 29).

From these considerations, lateral faulting (Fig. 22 and 23) is inferred to be the primary mechanism for the development of the San Clemente fault. Arguments in favor of this inference are sufficiently important to justify the basic assumption that this fault represents the primary shear direction of the essentially horizontal compressional stress pattern, such as the one postulated by Moody and Hill (Ref. 29).

Until detailed knowledge of the entire San Clemente fault zone and its associated fault blocks has been gained, so as to permit a precise definition of the fault mechanism, the assumption above seems to be the most realistic so far.

Assessment of Structural Model. The rose diagrams (Fig. 17) provide a reasonable statistical basis for the stress pattern postulated above because of the assumption that the San Clemente fault is the primary horizontal shear direction. The diagrams provide a close analogy between the average of the fault strikes and the theoretical application. According to Moody and Hill's theoretical wrench-fault system (Ref. 29), the N40°W trend is considered the primary first-order right-lateral wrench and the N13°E is the complementary first-order left-lateral wrench. The N15°W trend corresponds to the primary stress direction,

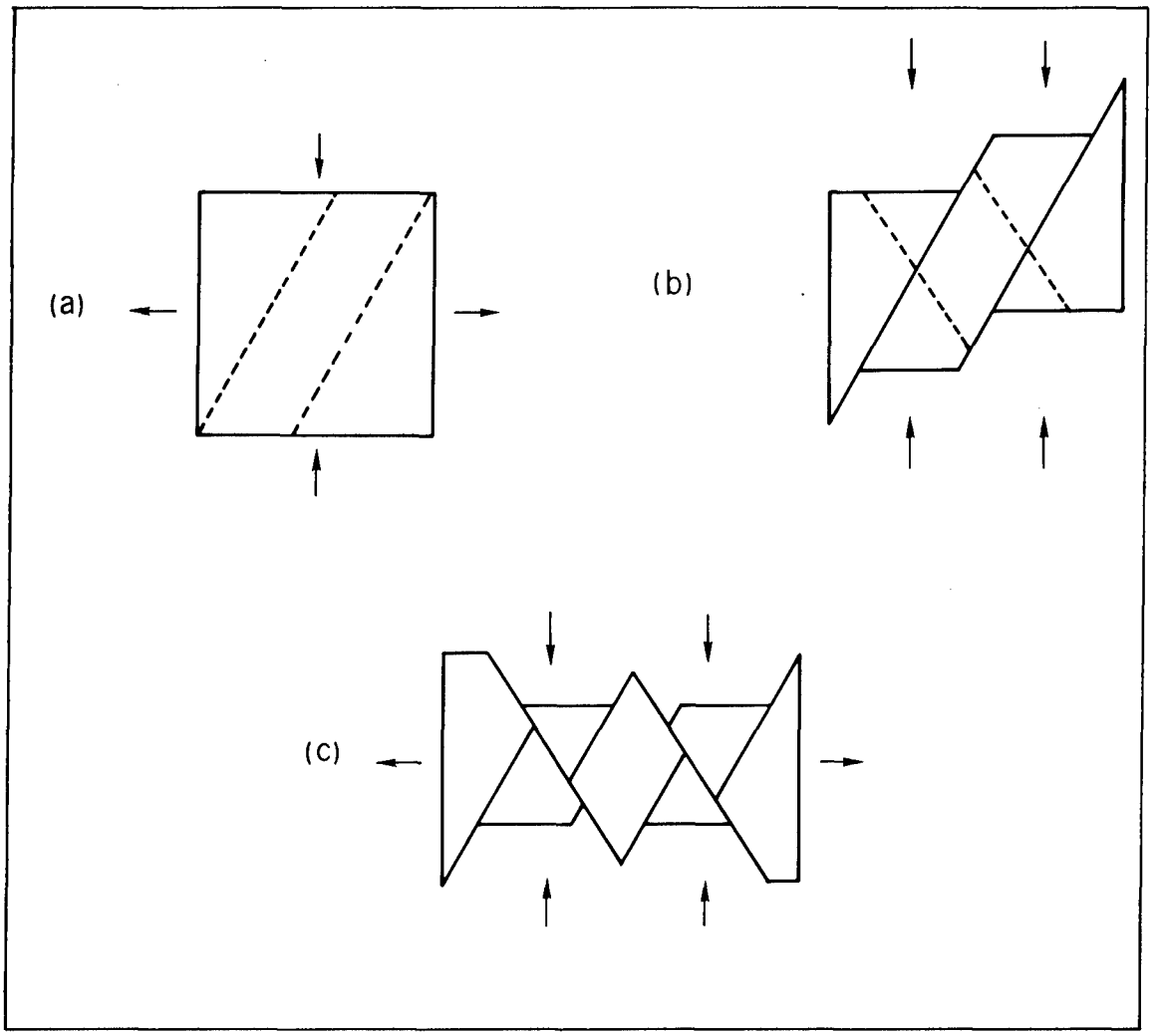

FIG. 23. Deformation Caused by Wrench Faults (From Ref. 24). Arrows denote general compression and extension.
(a) Initial State.
(b) Left-Lateral Shearing.
(c) Combined Left-Lateral and Right-Lateral Fracturing, Resulting in Block Division of General Region.

which in turn relates to tensile fractures, as defined by Beloussov (Ref. 26) and shown in Fig. 24a. The shear pattern closely corresponds to the definition of the basic San Andreas fault shear-stress pattern by Moody and Hill.

If the statistical model is valid, a positive empirical assessment of the pattern of faulting in various parts of the study area would tend to justify it. Using N15°W as the principal compressional stress direction, much of the offshore and island faulting is readily associated with the tensile-component-modified version of Moody and Hill's wrench-fault system.

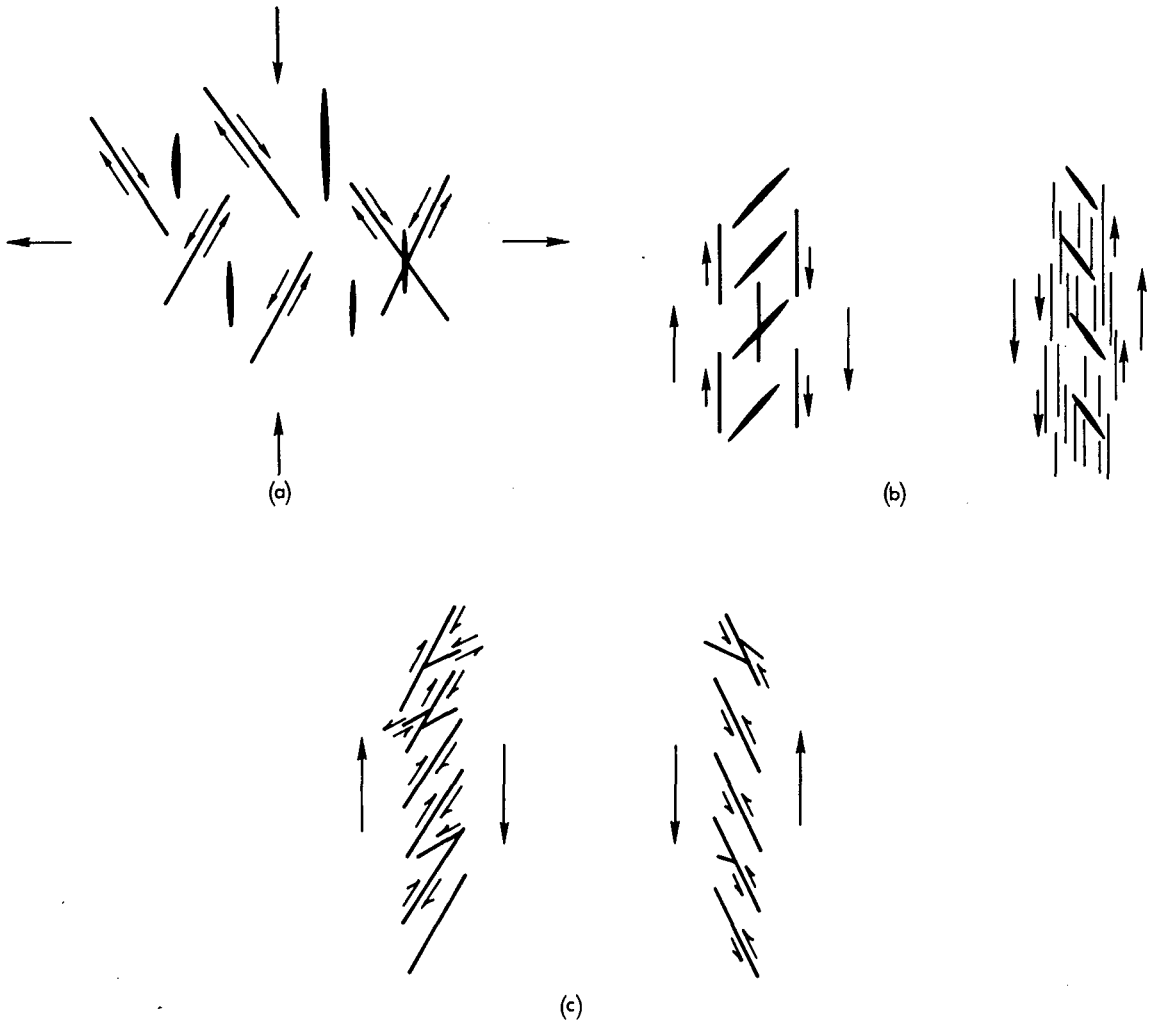

FIG. 24. Tectonic Stress Patterns (After Ref. 26). Fine lines are shear fractures; heavy lines are tension fractures; arrows show direction of displacement.

(a) Tension-Compression.
(b) Shear Deformation Produced by Couple With Formation of en Echelon System of Joints.
(c) Same as (b), but With Formation of en Echelon System of Shear Fractures.

An example of offshore tensile faulting is the existence of many faults off the south end of the island, where normal or pivotal faulting has developed and resulted in crustal block rotation with the downthrown side to the east. In addition, the many north to northwest-striking groups of faults north of Eel Ridge Canyon are considered of tensile-strain origin. This area contains a graben and horst assemblage that provides a criterion for this interpretation. Some offsets by north-northwest-trending faults along the northwestern part of the San Clemente fault zone may be attributable to east-west tension resulting in slight dilation (Fig. 24b and c) and perhaps related to a shear couple. This aspect of the problem will be discussed below. Some of the faulting within the offshore area between Pyramid Head and Eel Ridge Canyon may also have developed from a shear couple.

The major fault across the northern end of the island that shows right-lateral displacement is related to second-order right-lateral wrench faulting.

A second fault, intersecting Seal Cove and showing a left-lateral displacement, closely aligns with the second-order left-lateral wrench-fault direction.

According to Olmsted (Ref. 2), movement on the island faults appears to have been chiefly vertical, but on many the movement has been of the strike-slip variety. This implies a combination of lateral and normal (or thrust) faulting. However, Merifield and Lamar (Ref. 4) state that the faults studied in the central part of the island dip steeply, and that the rake of striations on slickensided gouge zones show a dominance of oblique movement more in the horizontal than the vertical direction. The steepness of dip and the more horizontal movement correspond more to a near-horizontal compression related to wrench faulting (Ref. 24 and 29). Merifield and Lamar (Ref. 4) state the following in their description of faulting at the central part of the island: "In the cases where the sense of movement could be demonstrated, the north-northeast to northeast-trending faults have moved in a left-lateral sense and the north-northwest-trending faults have moved in the right-lateral sense." These movement senses are consistent with the stress model proposed for the study area.

The complex series of faults along the eastern side of the island is considered mostly a combination of lateral shear and tensile faulting that results in the slide or slump blocks so prevalent along that side.

Olmsted (Ref. 2) has related the sympathetic faults between the two main northward-trending faults near Wilson Cove to tensional stress. In this sense, the two main faults would then be essentially shear-derived and related to second-order right-lateral wrench faulting.

Lineations across the island at N75°-85°W (Fig. 25) may be second-order right-lateral wrench faults. This interpretation is strengthened by some apparent right-lateral offsets along the shorelines of the island.

An example of offshore horizontal movement is the series of en echelon offsets of the main San Clemente fault that are mostly consistent with left-lateral faulting. The faults that apparently cause these offsets are not shown. The offsets are presumed to be related, at least in part, to the northeast-striking faults along the northwest and southeast sides of the Emery Seaknoll, as well as to those that cut the escarpment. These fault series readily correspond to the complementary first-order shear direction.

The area between the Emery Seaknoll and the island contains several examples of varied, apparent offsets. This area illustrates the complexity that could result from lateral shear between two opposing topographic highs. In plan view, the fault pattern tends to "rotate" around the west side of the Emery Seaknoll, the smaller of the highs. Apparently, the effects of both tension and shear are felt in this area.

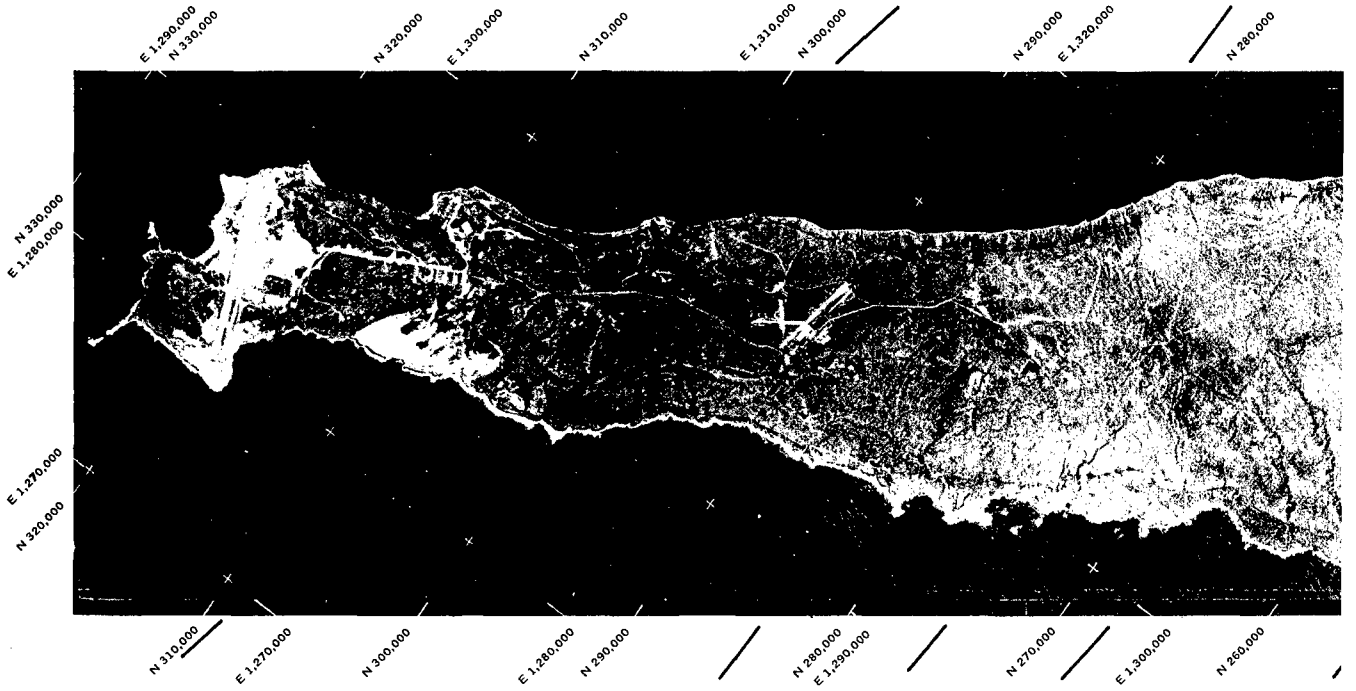

FIG. 25. Photomosaic of San Clemente Island. Heavy solid lines outside of border indicate app

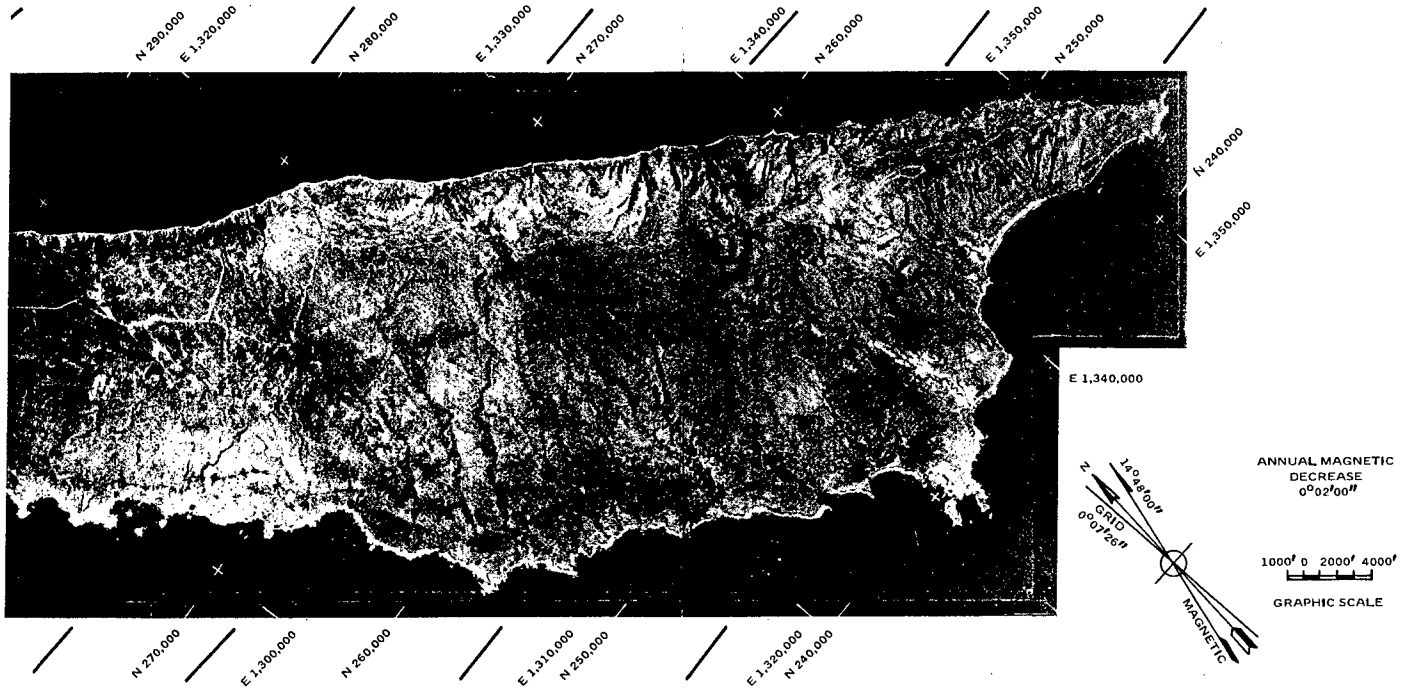

l. Heavy solid lines outside of border indicate approximate trend of WNW lineations on island.

2

Extrapolation of the several northwest and northeast-striking faults at the northwestern end of the study area will lead to intersections that well illustrate the pattern of primary and complementary shear directions.

A further analogy to the postulated stress pattern is shown by an analysis of the ridges and folding off the east side of the island. Most of these features have northwesterly strikes. Under the Moody and Hill system, these features are considered second-order drag folds or ruptures (reverse or thrust-fault ridges). A few additional northerly-trending features close to the Emery Seaknoll are presumed to be compression ridges (Ref. 29 and 37) related to the primary wrench fault.

The gentle folding off the southern end of the island (Fig. 26) is mostly parallel to sub-parallel with the associated faulting. This feature presumably resulted from either drag folding (third-order) or drag by the series of fault blocks that appear to have rotated eastward in a counterclockwise direction.

The syncline between Northwest Harbor and West Cove is related to the second-order drag fold of the complementary left-lateral shear faulting.

The drag-fold interpretation is strongly supported by statistical analysis. According to Ref. 29, the value of the critical angle γ (Fig. 22) has not been determined satisfactorily; however, it generally varies between 5 and 30 degrees, with an average of 15 degrees. Figure 27a and Table 2 show that the majority, i.e., 80%, of these tectonic features have formed between 30 and 60 degrees (γ = 0 to 30 degrees) from the postulated primary-stress direction. The remainder, being within 30 degrees northwest-southeast of the primary-stress direction, may be the previously mentioned compression ridges. Table 3 and Fig. 27b show that 75% of the folds, ridges, or both, are aligned within 10 degrees northeast-southwest of the primary-stress direction. These features are readily assigned to the third-order drag-fold phenomenon, as noted in Fig. 22. They correspond to the correct side of the primary first-order wrench fault and the position of the second-order right-lateral wrench fault.

The main bases for the tectonic interpretation in this section are the plan view of fault strikes plus the inferred relationship of these faults to the segmentation of crustal blocks, folds, and ridges, as interpreted from the seismic profiles. These bases have been supplemented by the work of other authors. A dynamic approach to the problem is very difficult, so that geometric relations have been used for a qualitative, general solution to the problem. Considering the degree of uncertainty attending this indirect method, substantial agreement with the theoretical application results from both statistical and geometric model analyses. Different interpretations may be applied, but the evidence strongly suggests that the lateral-fault tectonic system is the most applicable for the area studied.

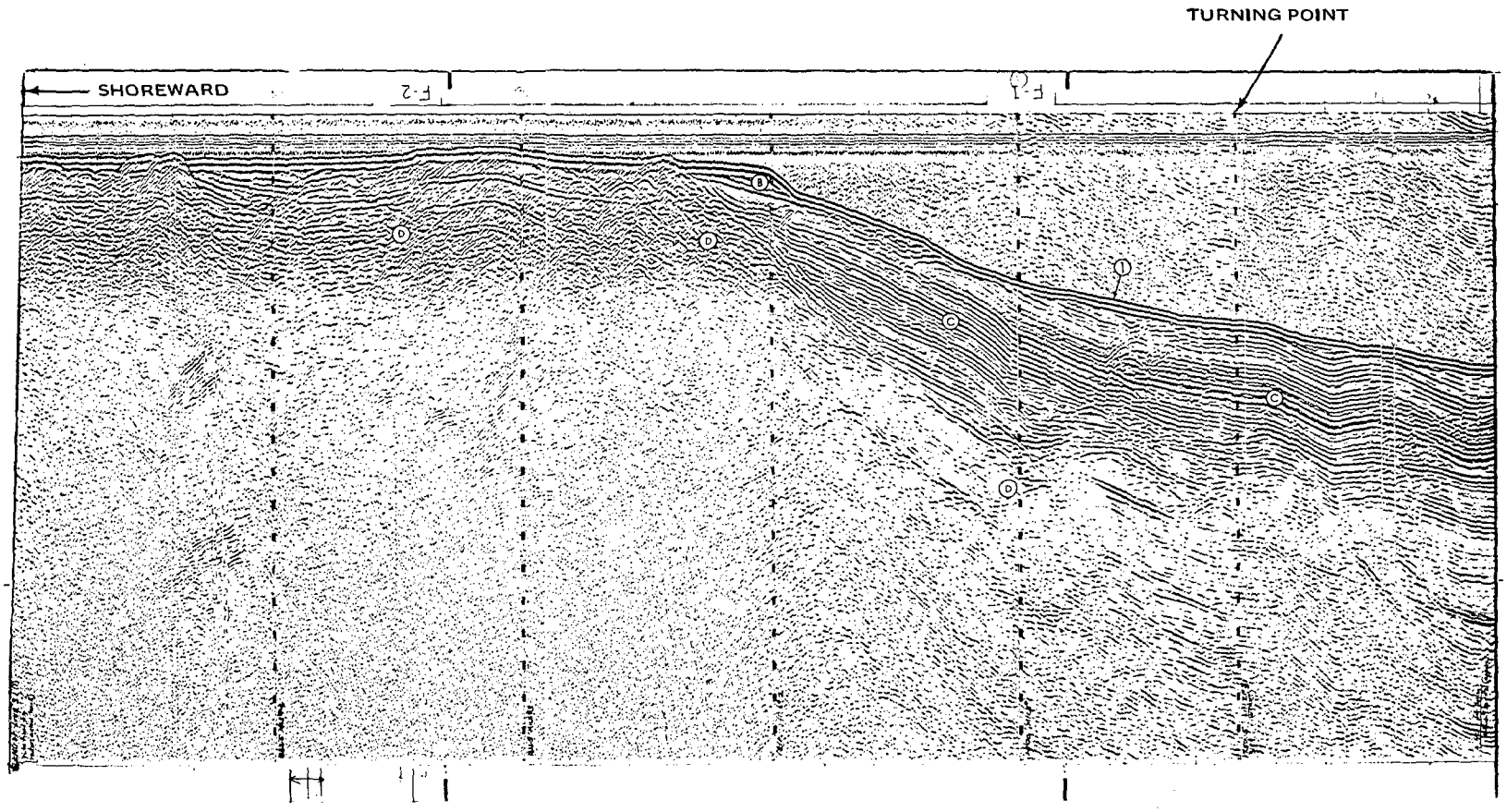

FIG. 26. Reconnaissance Survey Profile 31, Showing Unit B, Unit C, Unit D, and Seafloor (1). Note gentle folding and breaks of reflectors (faulting?) in right-hand position of Unit C.

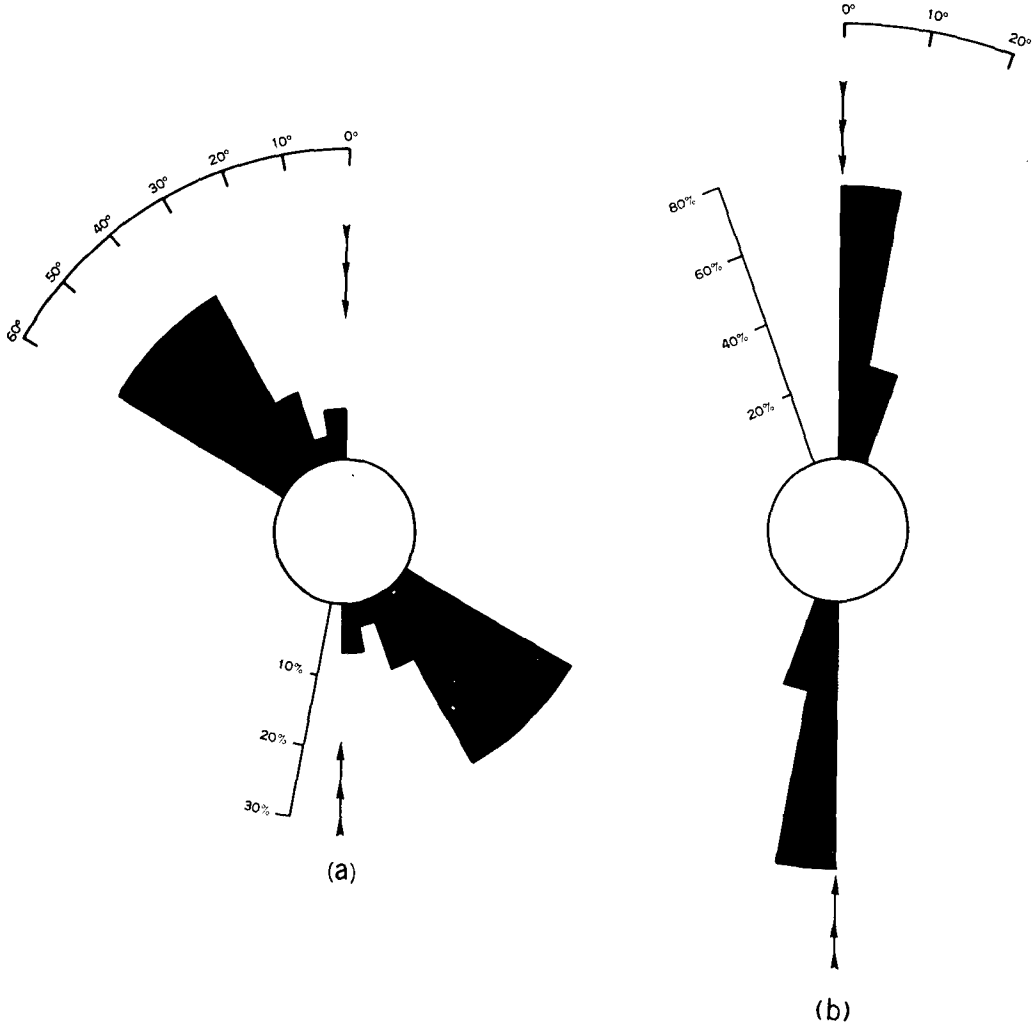

FIG. 27. Rose Diagrams of Fold Axes, Ridge Axes, or Both, Presumed To Have Resulted From Drag Folds. Triple arrows denote primary stress direction.

(a) Along San Clemente Fault Zone.

(b) Along Southern End of Island.

TABLE 2. Occurrence of Secondary Structures (Folds, Ridges, or Both) Along San Clemente Fault Zone

Degrees from γ	No. of occurrences	Occurrence percentage
0-10	2	6.67
10-20	1	3.33
20-30	3	10.00
30-40	8	26.67
40-50	8	26.67
50-60	8	26.67
	30	100.01

TABLE 3. Occurrence of Secondary Structures (Folds, Ridges, or Both) off Southern End of Island

Degrees from γ	Occurrence	Occurrence percentage
0-10	9	75.00
10-20	3	25.00
	12	100.00

ADDITIONAL TECTONIC CONDITIONS AND FEATURES

Uplift, Doming, and Tilting. There is no evidence of primary folding on the island block. As a consequence, the upthrow of the entire block, complemented by doming and tilting, must represent some release from the primary compressional force. Various authors have suggested reasons for relating crustal-block relief to lateral faulting. Buckling, thrust faulting, squeezing between strike-slip faults, and shape change and shifting are given as examples.

Bowing of the surficial dacite flows that cap the central part of the island is noted by Merifield and Lamar (Ref. 4). These authors suggest a 0-to-15-degree westerly to southwesterly dip on the west flank of the island and, from limited observation, a 10-to-30-degree northeasterly dip on the steep east flank. The latter dip is the possible result of drag by the San Clemente fault.

The rotation of the northeast fault-strike pattern offshore in the detailed survey area, which culminates at Eel Ridge Canyon, may have been caused partly by the upbowing of the island block (Fig. 28a-b). The Eel Point-Lost Point area lies across the island from the San Clemente fault-zone high next to the Emery Seaknoll (Fig. 28a). According to Beloussov (Ref. 26), both shear and tension fractures may be formed by bending and upwarping. Both of these processes may give rise to stretching that varies widely in intensity, depending on the shape of the uplifts. Under these conditions, the northwest-striking faults and lineations off China Point could be related to tension, as shown in Fig. 28b. A graben and in-facing scarp are the criteria for this conclusion. In some instances, one of the fracture systems predominates, most frequently the radial (shear) system. Accordingly, this could be the case for some of the northeast-trending fractures southeast of Eel Ridge Canyon. The north to northwest-striking faults associated with horsts and grabens northwest of the canyon may have been developed partly by uplift, as well as by tension from horizontal compression. If the direction of horizontal primary stress is accepted, and if upbowing is assumed to have occurred, then the fracturing of the island block can be assumed to be complex.

Shear Couple Condition. The major fault zone along the west base of the island block is interpreted from the 1964 survey profiles (Fig. 4). This fault zone is also shown by Moore (Ref. 11). The strike of this feature is N22°W and may be interpreted as a tensile feature associated with uplift of the island block. On the other hand, certain criteria strongly suggest that it is a second primary wrench fault that complements the San Clemente fault. The seismic profiles across this zone show a wide trough, which is relatively straight for several kilometers (Fig. 16) and appears to contain small segments of crustal blocks associated with faulting.

It is suggested that the San Clemente fault zone and the complementary zone comprise the main primary shear fractures of a shear couple encompassing the island block (assuming that the stress-field direction is correct). This may be the reason for a strong expression of inferred northerly striking tensile faults, as well as the spread of azimuth in the complementary first-order shear fracturing (Fig. 18). Kingma's and Lensen's interesting models pertaining to the development of horsts and grabens (Ref. 33 and 37, respectively) are particularly adaptable to this study. The San Clemente Island block has been upthrown

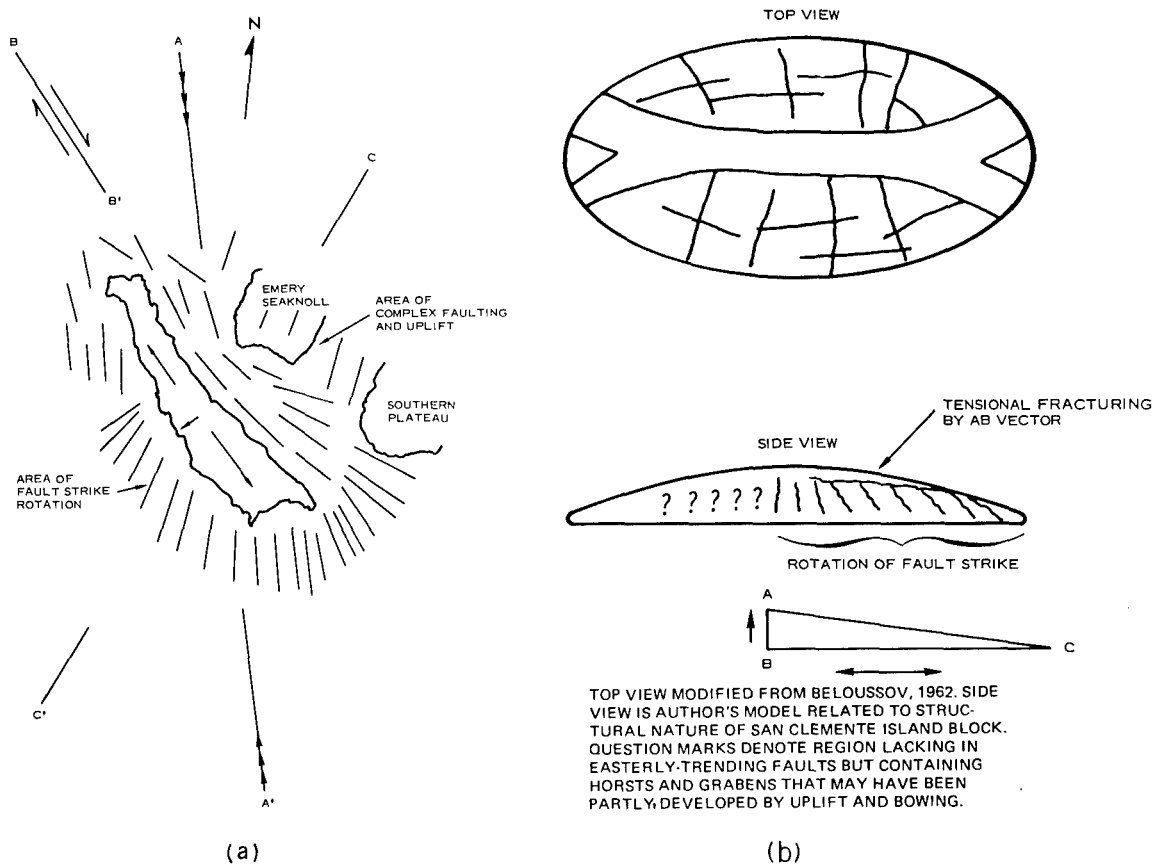

FIG. 28. Sketch of Proposed Upbowing and Subsequent Fracturing of San Clemente Island Block.
(a) Plan View, Showing Principal Horizontal Compressional Direction (A-A′) and Main Trends of Offshore Faulting. B-B′ is primary first-order wrench fault direction. C-C′ is trend of bathymetric high.
(b) Model Showing Relationship of Tension Stress by Upbowing of Island to Compressional Stress. AB vector is component of upbowing; BC is component of compression representing principal compression direction.

and tilted in a direction that may be in line with that postulated for a right-lateral sense of movement by these authors (see the section below). However, for this shear mechanism to be valid, the subparallel primary shear zones must intersect at some depth, and this is purely speculative at this time.

Wave-Cut Terrace. To ensure clear understanding of this section, the reader should refer to Fig. 6 of this volume, as well as to Fig. 8 and 18 of Part 1. The shoreward limit of the terrace is defined as the contact of Units C and D. The outer limit is defined as the point of declivity. This permits a better structural analysis of the prominent insular terrace.

Figure 29a-b strongly suggests the effects of post-terrace faulting. Fault evidence is indicated by the grouping of two to three adjacent measurements having the same or nearly the

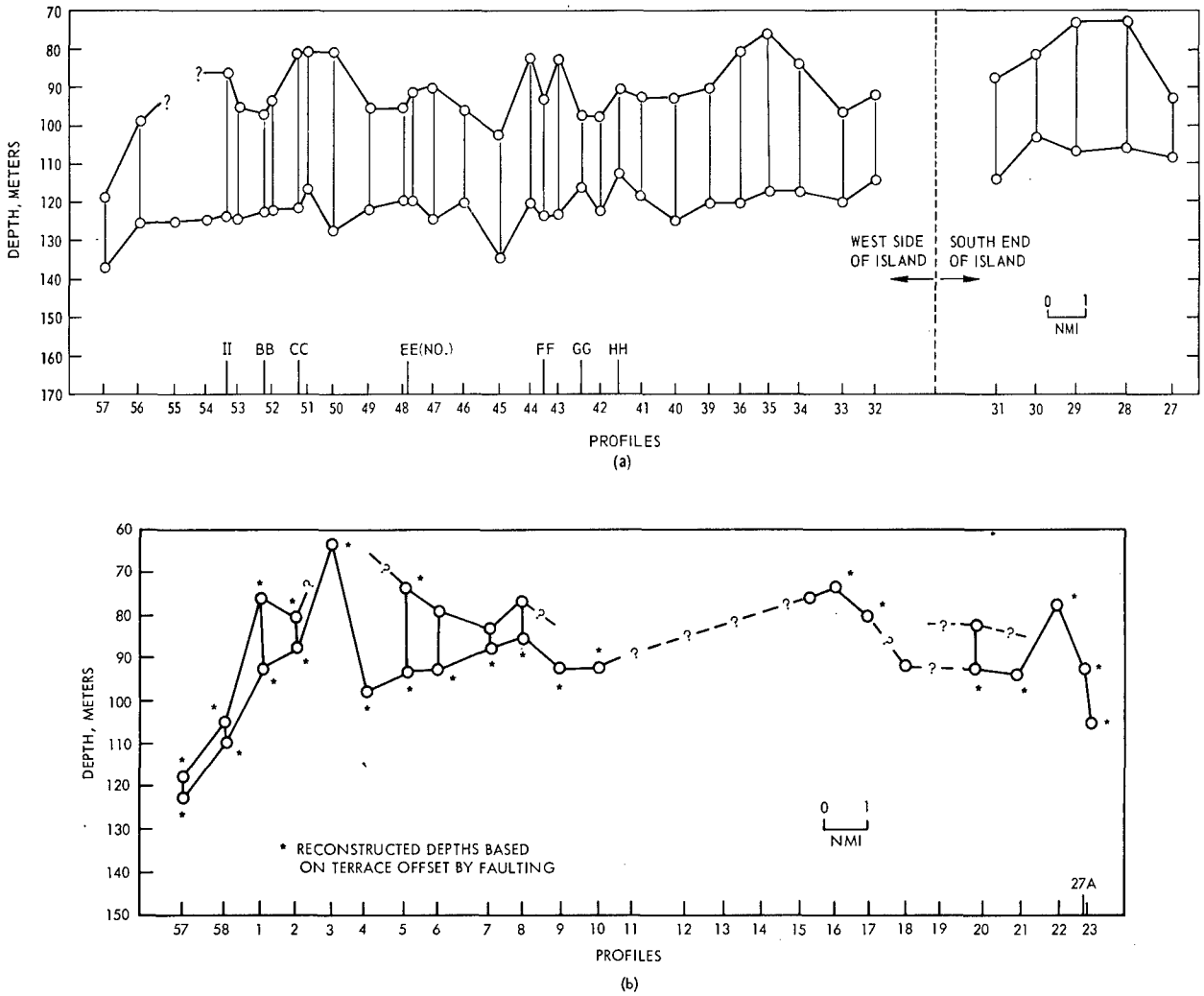

FIG. 29. Wave-Cut Terrace Diagrams.

(a) Profiles Along West Side and South End of Island. West-side profiles combine data from both detailed and reconnaissance surveys.

(b) East Side of Island. Lack of data along middle of island results from profiles missing terrace close to island.

same depths, which suggest minor horsts and grabens. This grouping is more prevalent on the west side of the island; however, a greater magnitude of depth difference occurs on the east side of the island.

The shallow depth at the outer end of the terrace off Wilson Cove, shown by Profile 3, corroborates the sense of throw for the major fault (Ref. 2) projecting from the island to form part of this cove. The effect of the northwest-striking fault pattern is indicated by the rapidly increasing depths across Profiles 2, 1, and 58, and the east part of 57. The faults have apparently developed a major offset in the terrace of this area (see, for example, Profile 57 in Fig. 10). The effects of northeast-striking faults is perceptible at the west end of

Profile 57. The sharp break in the southerly shoaling of the terrace between Profiles 8 and 11 is probably related to slump-block activity and a northwest-striking fault (Fig. 16). The sudden deepening of the terrace in the area of Profiles 23, 27, and 27A is related to the cluster of northerly striking faults off Pyramid Head that have downthrown blocks to the southeast.

No mention is made in either Ref. 2 or 4 of offset marine terraces on the island. The fact that offshore faulting (west side) has apparently offset the terrace suggests (1) that the faulting is more lateral and is disguised more readily on the island or (2) that the faulting is pivotal and has little effect on the island.

General northwesterly downward tilting is apparent in Fig. 29a. The northwesterly tilt is approximately 50 meters in 100 nautical miles, and is in very close agreement to Emery's estimate for regional warping of the Pleistocene Epoch terraces (Ref.28), although it is not in the same direction. Evidently, a post-Pleistocene component of tilting to the northwest has been peculiar to the San Clemente Island block. However, it is conceivable that a detailed analysis of other island terraces will show similar tilt. Tilting to the northwest is not so apparent in Fig. 29b, although this may be noted from Profiles 4 through 17 by means of an average alignment of the outer-terrace depths.

For the west side of the island, the average of the outer-terrace depths is 121.9 meters; the average for the inner depths is 91.1 meters (Table 4). The average terrace slope is very nearly 1 degree. It is noteworthy that 68% of the outer depths along the west side of the island have an average of 122.6 meters. The 121.9- and 122.6-meter averages imply that a close approximation of the pre-fault (post-tilt) outer-terrace depth is 122 meters.

Only the outer edge of the terrace along the east side of the island has yielded sufficient data for analysis. The average of 21 outer-depth measurements is 90.3 meters. The 19 measurements made with confidence average 91.1 meters. It is concluded that 90 meters is a close approximation of the original (post-tilt) outer depth of this part of the terrace.

The average outer depths of the terrace for both sides of the island indicate that the island block displays a slight northeasterly upward component of tilting. Although data are insufficient, a northeastward upward tilting is also suggested by the profile terrace data off the southern end of the island.

Based on the average of 0°07′ for continental slopes (Ref. 15), the near-1-degree average for the west side of the island also suggests westward tilting subsequent to the inception of the terrace.

The northeasterly component of tilt is calculated as 1/4 degree, based on the average horizontal distance across the island from outer terrace to outer terrace (4.8 nautical miles). Calculations based on the terrace data above show that the fulcrum of the northeast-southwest tilt is close to the northwesterly axis of the island, and that the net tilt is roughly westward.

TABLE 4. Depths to Wave-Cut Terrace

Profile No.	Present depth, m		Outer terrace depths			
	Inner	Outer	Range of difference, m	Frequency of occurrence	Percent of occurrence	Cumulative percent
			a. West Side			
57	118.6	137.3	0-2	13	42.0	42.0
56	99.6	125.8	2-4	9	29.0	71.0
55	?	124.4	4-6	4	12.9	83.9
54	?	124.4	6-8	2	6.4	90.3
II	85.4	123.0	>6-8	3	9.7	100.0
53	95.2	124.4	...	...	...	...
BB	96.4	122.0	...	...	...	...
52	93.7	121.4	...	...	...	...
CC	80.8	121.5	...	...	...	...
51	80.6	117.0	...	...	...	...
50	80.6	127.5	...	...	...	...
49	95.2	121.4	...	...	...	...
48	95.2	120.0	...	...	...	...
EE	90.8	119.0	...	...	...	...
47	89.3	124.4	...	...	...	...
46	?	120.0	...	...	...	...
45	102.5	134.6	...	...	...	...
44	82.0	120.0	...	...	...	...
FF	93.3	124.3	...	...	...	...
43	82.0	122.9	...	...	...	...
GG	97.6	115.9	...	...	...	...
42	97.9	122.9	...	...	...	...
HH	90.8	112.8	...	...	...	...
41	92.4	118.6	...	...	...	...
40	92.4	124.4	...	...	...	...
39	90.7	120.0	...	...	...	...
36	80.6	120.0	...	...	...	...
35	76.1	117.1	...	...	...	...
34	83.5	117.1	...	...	...	...
33	96.7	120.0	...	...	...	...
32	92.2	114.2	...	...	...	...
Avg.	91.1	121.9				
			b. East Side			
57	118.6[a]	122.9[a]	0-2	6	28.6	28.6
58	105.3[a]	109.7[a]	2-4	5	23.8	52.4
1	76.0[a]	92.2[a]	4-6	1	4.8	57.2
2	80.4[a]	87.7[a]	6-8	1	4.8	62.0
3	?	62.9[a]	>6-8	8	38.1	100.1
4	?	98.0[a]	...	...	...	...
5	73.2[a]	93.6[a]	...	...	...	...
6	79.0	92.2[a]	...	...	...	...
7	82.4	87.7[a]	...	...	...	...
8	76.0	85.0[a]	...	...	...	...
9	?	92.2[a]	...	...	...	...
10	?	90.7[a]	...	...	...	...
11	?	?	...	...	...	...
12	?	?	...	...	...	...

TABLE 4. (Contd.)

Profile No.	Present depth, m		Outer terrace depths			
	Inner	Outer	Range of difference, m	Frequency of occurrence	Percent of occurrence	Cumulative percent
b. East Side (Contd.)						
13	?	?	...	...	...	...
14	?	?	...	...	...	...
15	?	76.0	...	...	...	...
16	?	73.2[a]	...	...	...	...
17	?	80.4[a]	...	...	...	...
18	?	90.7	...	...	...	...
19	?	?	...	...	...	...
20	81.9	92.2[a]	...	...	...	...
21	?	93.6[a]	...	...	...	...
22	?	77.6[a]	...	...	...	...
27A	?	93.6[a]	...	...	...	...
23	?	105.3[a]	...	...	...	...
Avg.		90.3				
c. South End						
27	93.6	108.3	...	...	...	...
28	~73.2	105.3	...	...	...	...
29	~73.2	106.8	...	...	...	...
30	81.9	102.4	...	...	...	...
31	87.7	114.1	...	...	...	...

[a] Reconstructed depths based on terrace offset by faulting (Fig. 29b).

Gaal (Ref. 7) concluded from bathymetry studies that the submarine terraces of some of the Continental Borderland islands have a deeper western margin. Emery (Ref. 21) notes that tilting may have caused the difference in terrace depths on either side of San Clemente Island. In both Ref. 6 and 21, Emery postulates a regional west-to-south tilting of the borderland, based on submerged-terrace measurements. However, the tilting of the San Clemente Island block only partly conforms to these authors' data. It is conceivable that crustal-block segmentation, as well as the resulting shape change and block shifting, have imposed different structural histories on various crustal blocks, or groups of blocks, in the Continental Borderland area (Ref. 34); thus the block tilting of San Clemente Island need not conform entirely to that of other islands.

The average depth of the outer end of the terrace on the east side of the island is the same as the average for the inner depth at the western margin. This suggests that Smith (Ref. 1) and Olmsted (Ref. 2) are correct in their interpretation of upward bowing in the island volcanic rocks, and attests to a conclusion by this author that tilting (and possibly some upbowing) postdates the cutting of the major submarine terrace. A contradiction to the latter postulation is indicated by data from a few of the seismic profile terrace slopes off the east side of the island. The average of these is slightly more than 1/2 degree, which tends to support a predominantly westward post-terrace tilting.

A tilt of the island block of 5 degrees (the minimum cited in Ref. 2) would make the uppermost island terrace slope slightly greater than 5 degrees. If upbowing is considered, on the other hand, the return to a more gentle slope is possible. Not only are there no known precise measurements for the slopes of the island terraces, but the variable alluvial and colluvial fill, as well as post-terrace erosion and faulting, would tend to complicate efforts toward precise measurements of the true terrace slopes. The writer has made a Brunton compass measurement of the first major terrace above sealevel on the west-central side of the island. The slope angle is nearly 2 degrees, which is an order of magnitude greater than the slope of the submarine terrace and suggests considerable tilt, upbowing, or both, between the development stages of these terraces.

The narrowness of the terrace along the east side of the island may be attributed to either (1) differential erosion of the more resistant volcanic rocks, as compared with the softer Miocene sedimentary rocks, or (2) the terrace being a remnant resulting from faulting. The writer concurs with the first explanation because, according to the orogenic history of the borderland (Ref. 6 and 11), the San Clemente fault break at this level of the island had already taken place before the end of Wisconsin time. However, some loss of the terrace has probably resulted from slide or slump-block activity.

On the basis of the evidence presented here, much of the present structure of the San Clemente Island block developed during Pleistocene time. At the very least, Pleistocene orogeny has been important in developing the present structure. However, the relationship of the net downward and westward tilting to the primary compressional stress forces proposed in this paper is not fully understood. It is conceivable that the tilt is associated with both upward bowing in response to lateral compression and, possibly, a shear couple encompassing the island block.

Rift Valley. The San Clemente fault tends to bifurcate at the southern end of the island. This is the northern end of what is termed the Rift Valley by Shepard and Emery (Ref. 5). For unknown reasons, perhaps the result of initial conditions, dislocation, and nonelastic behavior (Ref. 24), the strike of the San Clemente fault has taken a smooth and gradual curvature from the south end of the Rift Valley to the north end of the island. As a consequence, it is logical to assume that, because of tensional stress, a "cross-strike separation" (or "pull-apart" feature) has developed to form the Rift Valley (Fig. 30). The 10-to-15-degree bifurcation of faults off Pyramid Head may have resulted from first-order right-lateral wrench faulting and breaks (thrusting) from second-order drag fold. Compression was (and is) probably greatest along the zone between the Emery Seaknoll and the island, and developed the upbowing and complex fracturing previously described for this area.

The Rift Valley is not apparent from bathymetry to the northwest of the island, bordering the Santa Catalina Basin. This lack might be explained as a structural modification by more northwesterly striking faults, heavy sedimentation in the area, and the additional tendency of the fault to become more linear. Bathymetry along this portion of the escarpment indicates a series of left-lateral offsets (Ref. 5, Chart 1) that could be related to second-order left-lateral wrench faulting. These faults, along with the main fault and others associated with the development of the Santa Catalina Basin, have possibly modified a rift-zone valley.

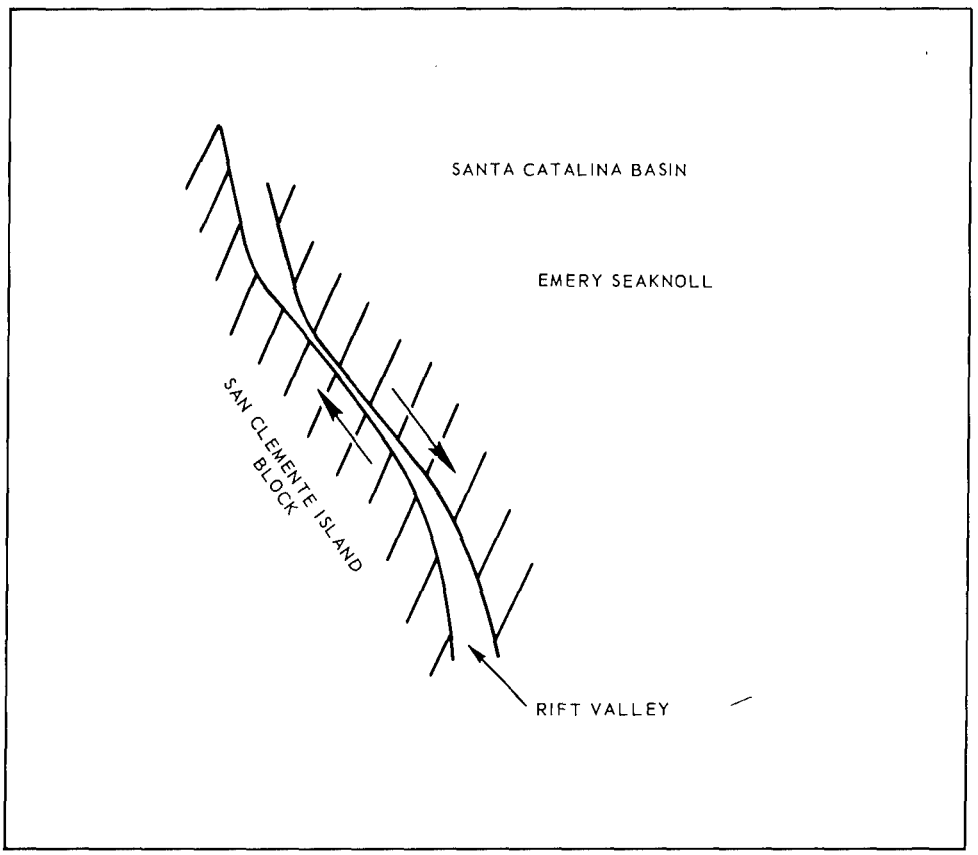

FIG. 30. Hypothesis for Tectonic Development of San Clemente Rift Valley.

GEOPHYSICAL CONSIDERATIONS

Magnetism. The first published, detailed magnetic studies of the northern Continental Borderland were made by Harrison and von Huene (Ref. 38), von Huene and Ridlon (Ref.39), and Harrison, et al. (Ref. 25); in the southern Continental Borderland, the first studies were made by Krause (Ref. 10).

The aeromagnetic survey in this study (Fig.31) is considered the most detailed of any made of an insular feature in the borderland region.

The principal features in Fig. 32 are a northeast-trending high of 1,000-gamma maximum off West Cove, and a northwest-trending low of −125 gamma off the northeast side of the island. Removal of the earth's regional gradient leaves a high of 1,100 and a low of nearly 25 gamma for these features (Fig. 33). The low in both maps closely conforms to the major pre-orogenic triangular depression filled with 550 meters of post-orogenic sediments. These high and low anomalies are present in the residual anomaly map (Fig. 34), but have a slight shift in position and trend. The major high becomes elongated east-west, with a maximum 100-gamma "bulge" centered over the large volcanic high defined by Seismic Profile 52

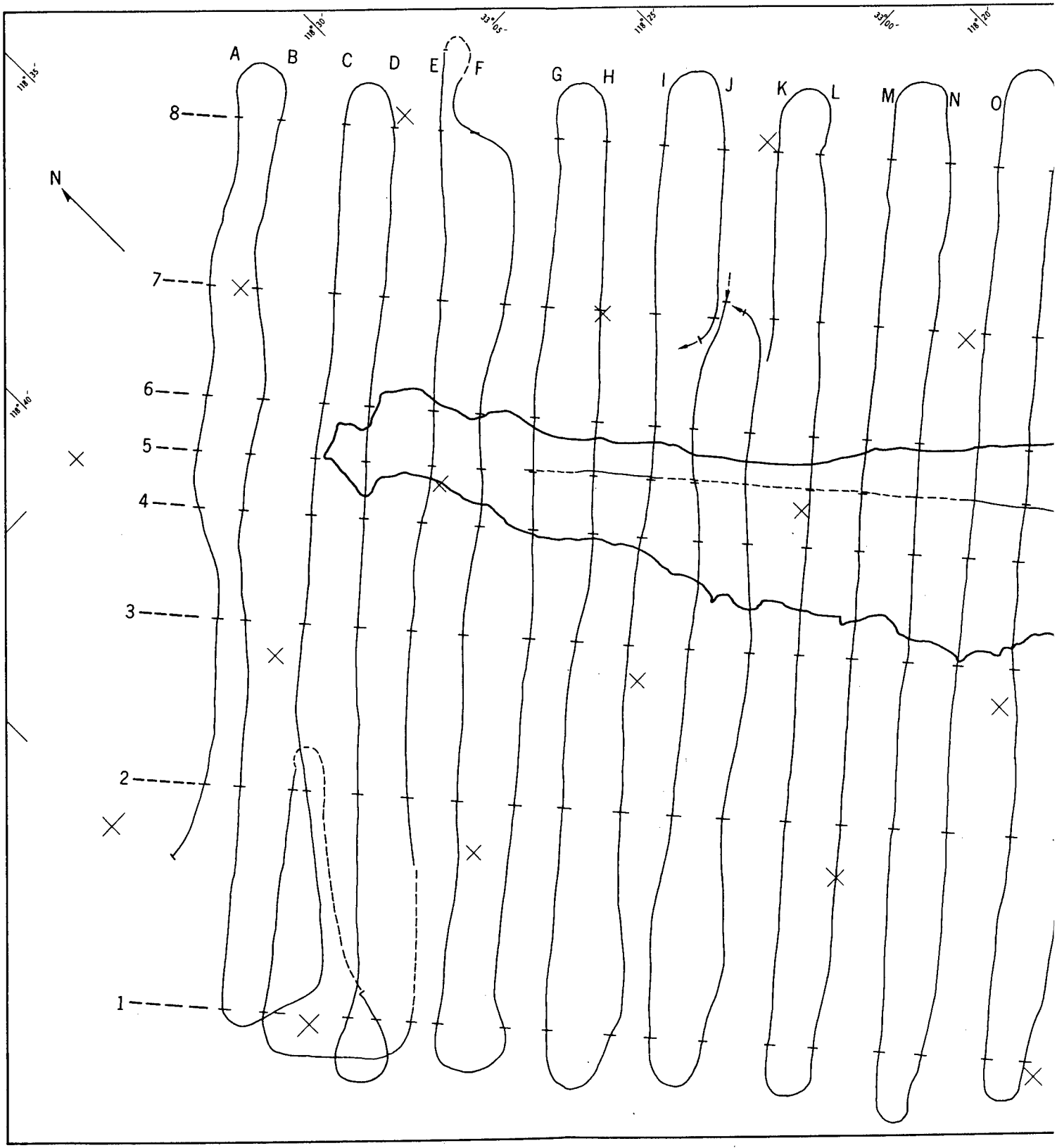

FIG. 31. Aeromagnetic Survey Flight Lines. Dashed lines indicate approximate flight line during

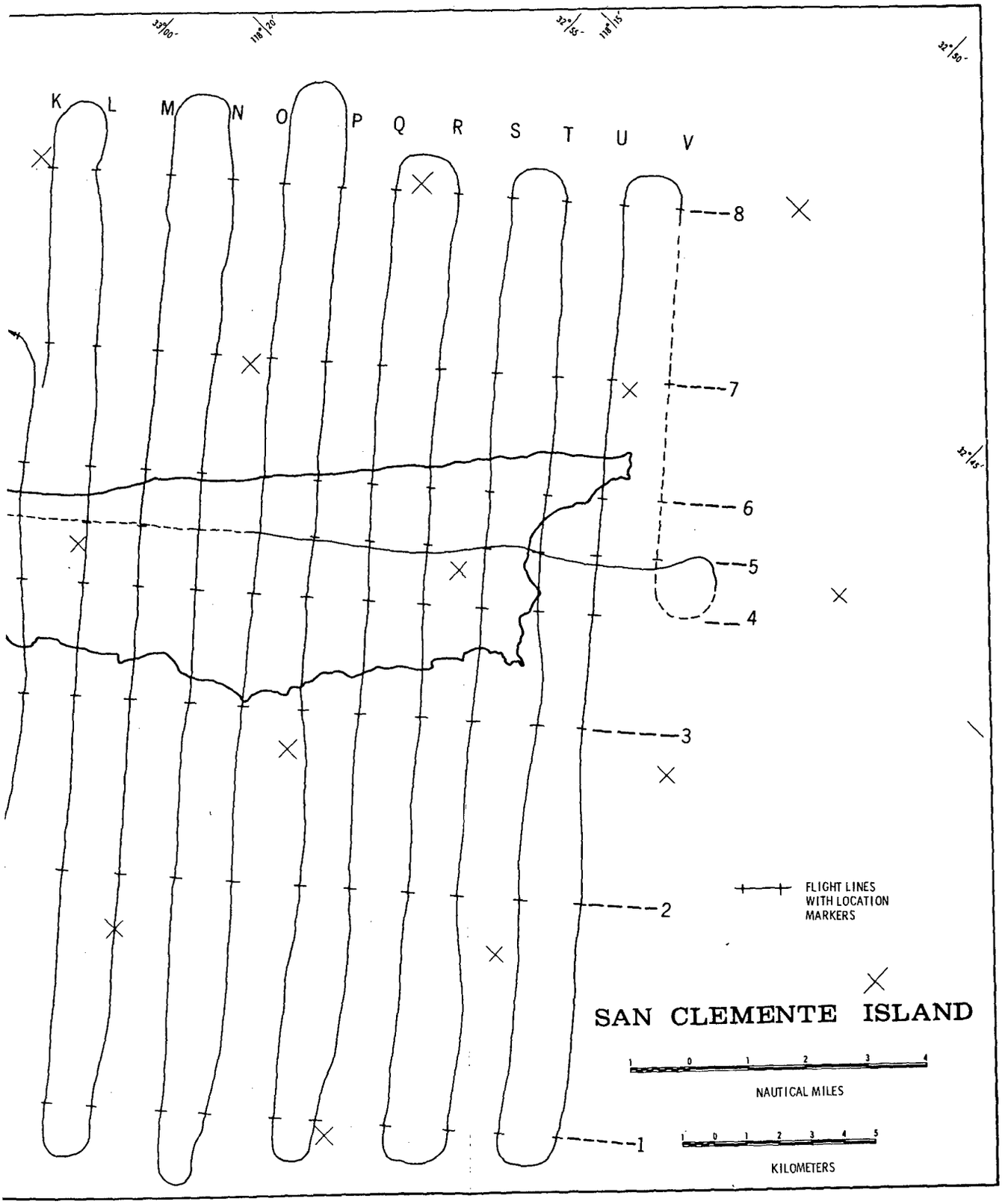

ashed lines indicate approximate flight line during loss of radar control from island.

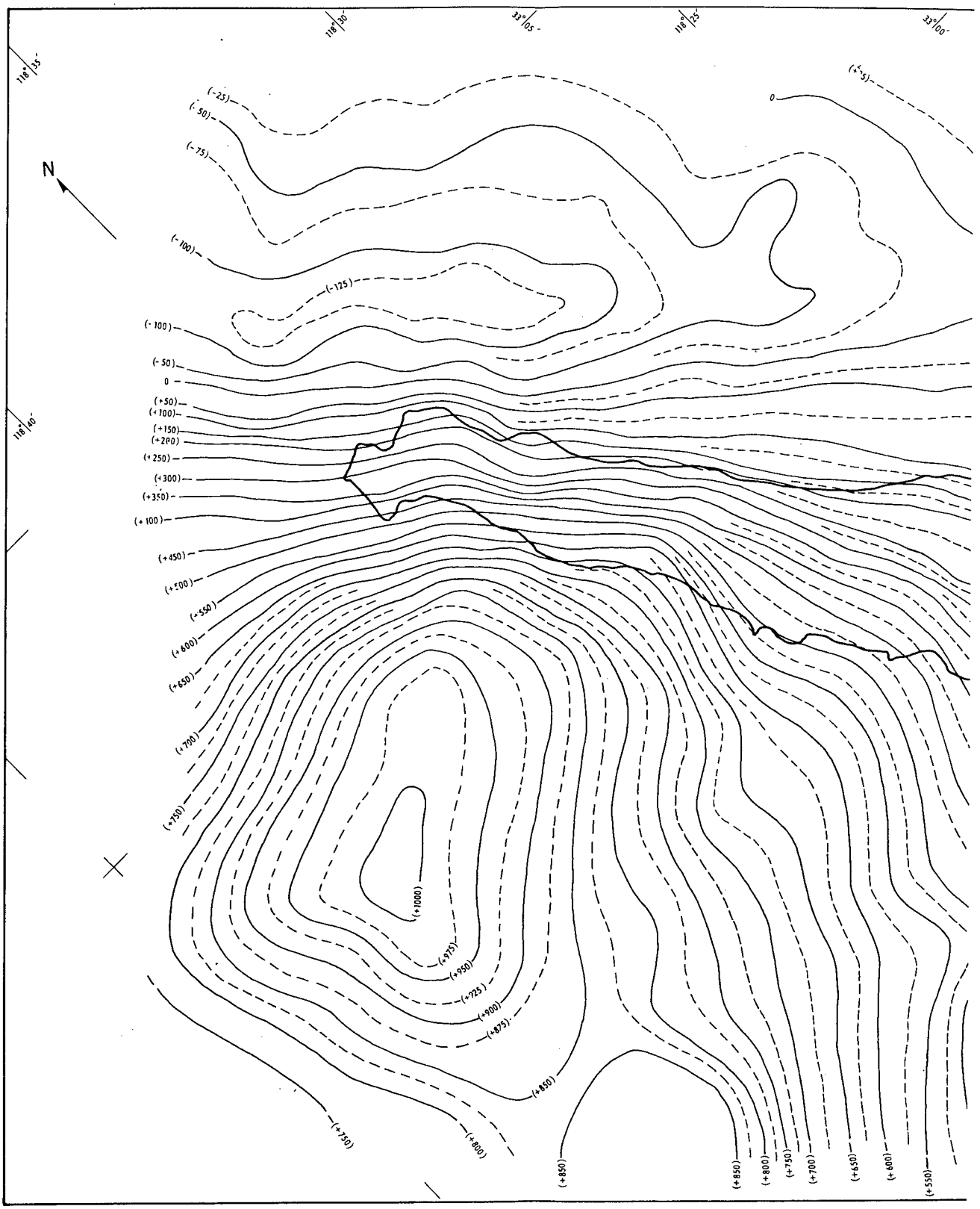

FIG. 32. Total Magnetic Intensity Map of San Cle

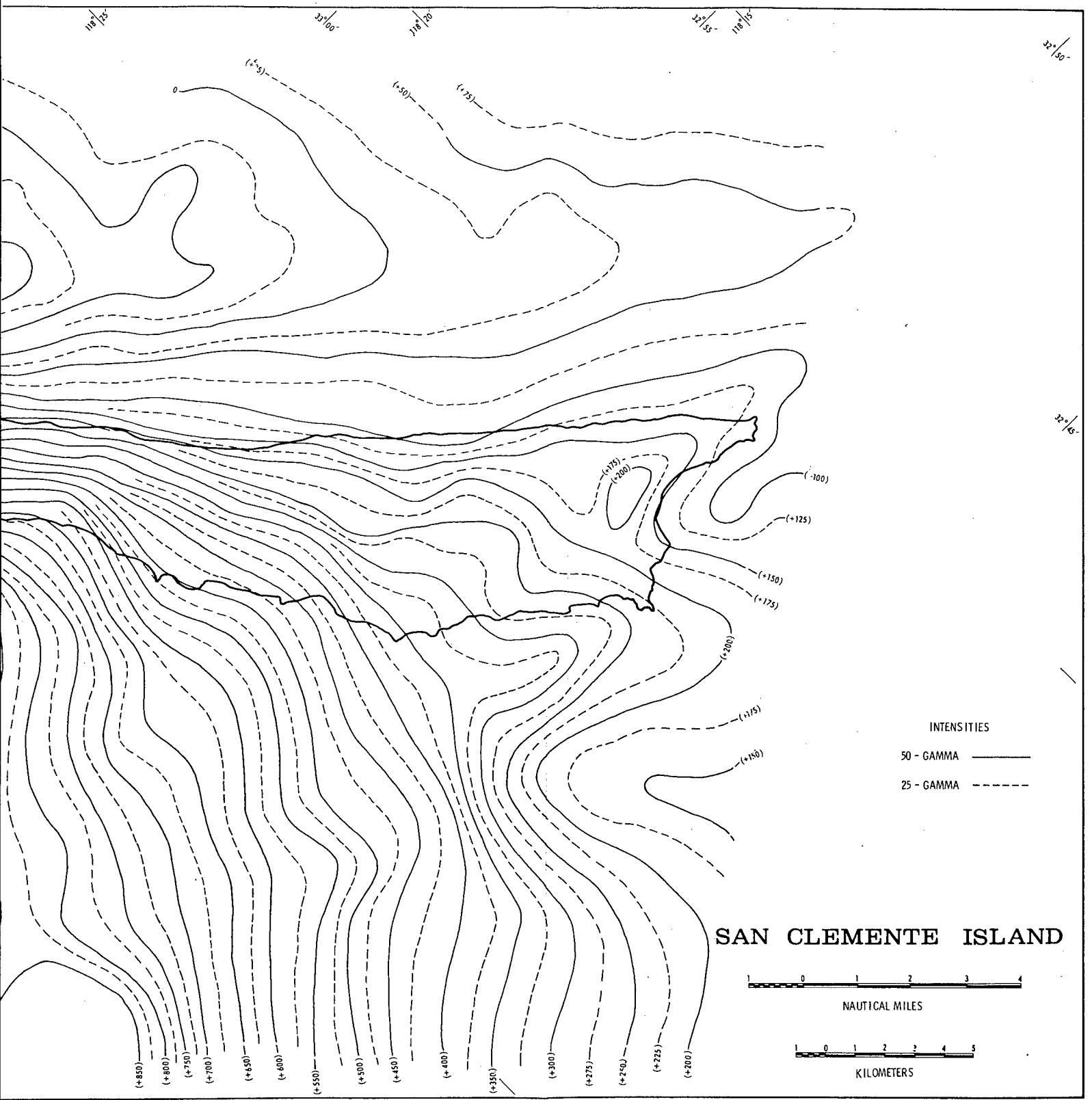

FIG. 32. Total Magnetic Intensity Map of San Clemente Island Block Region.

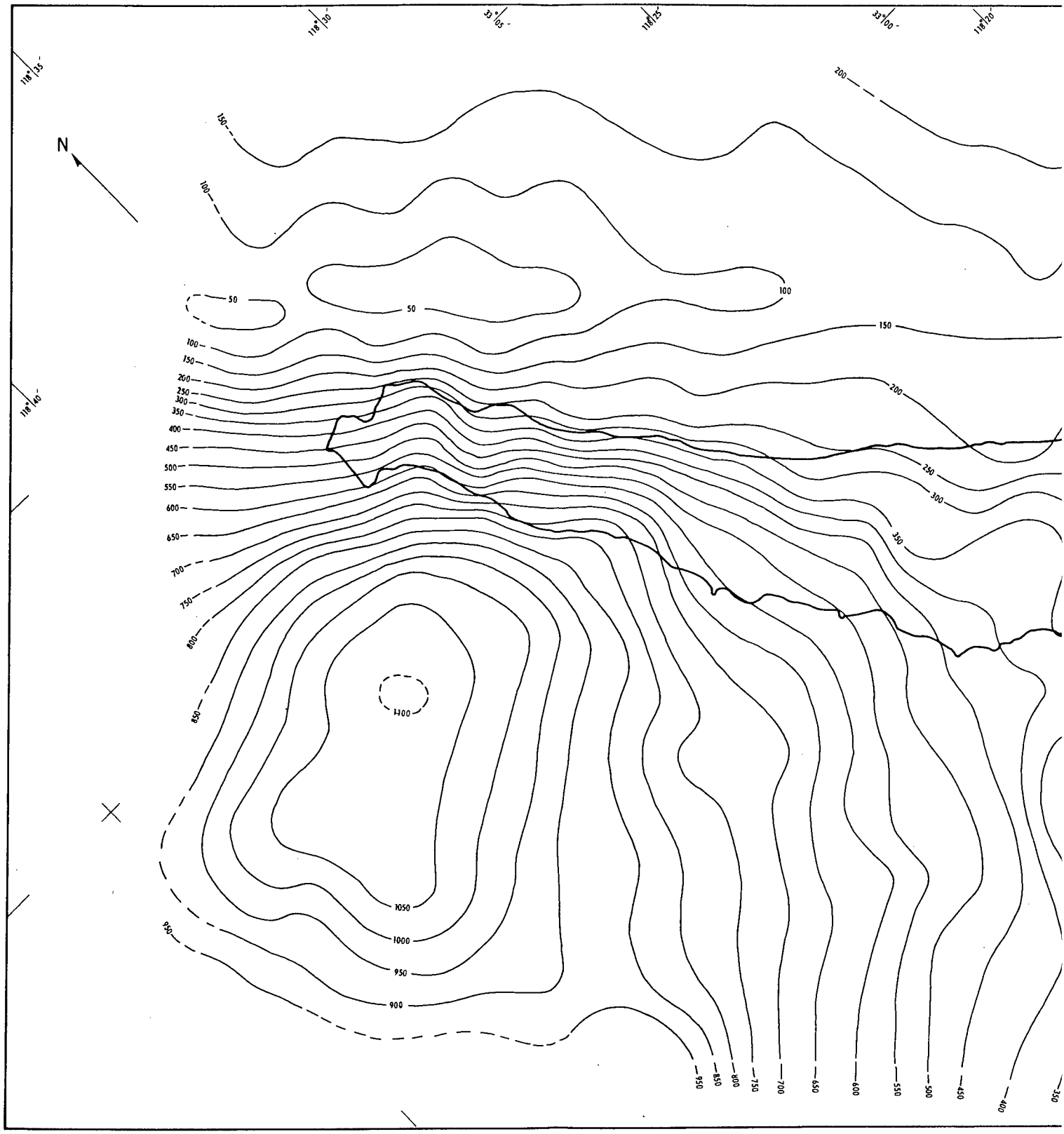

FIG. 33. Magnetic Anomaly Map of the San Clemente Island Block Area

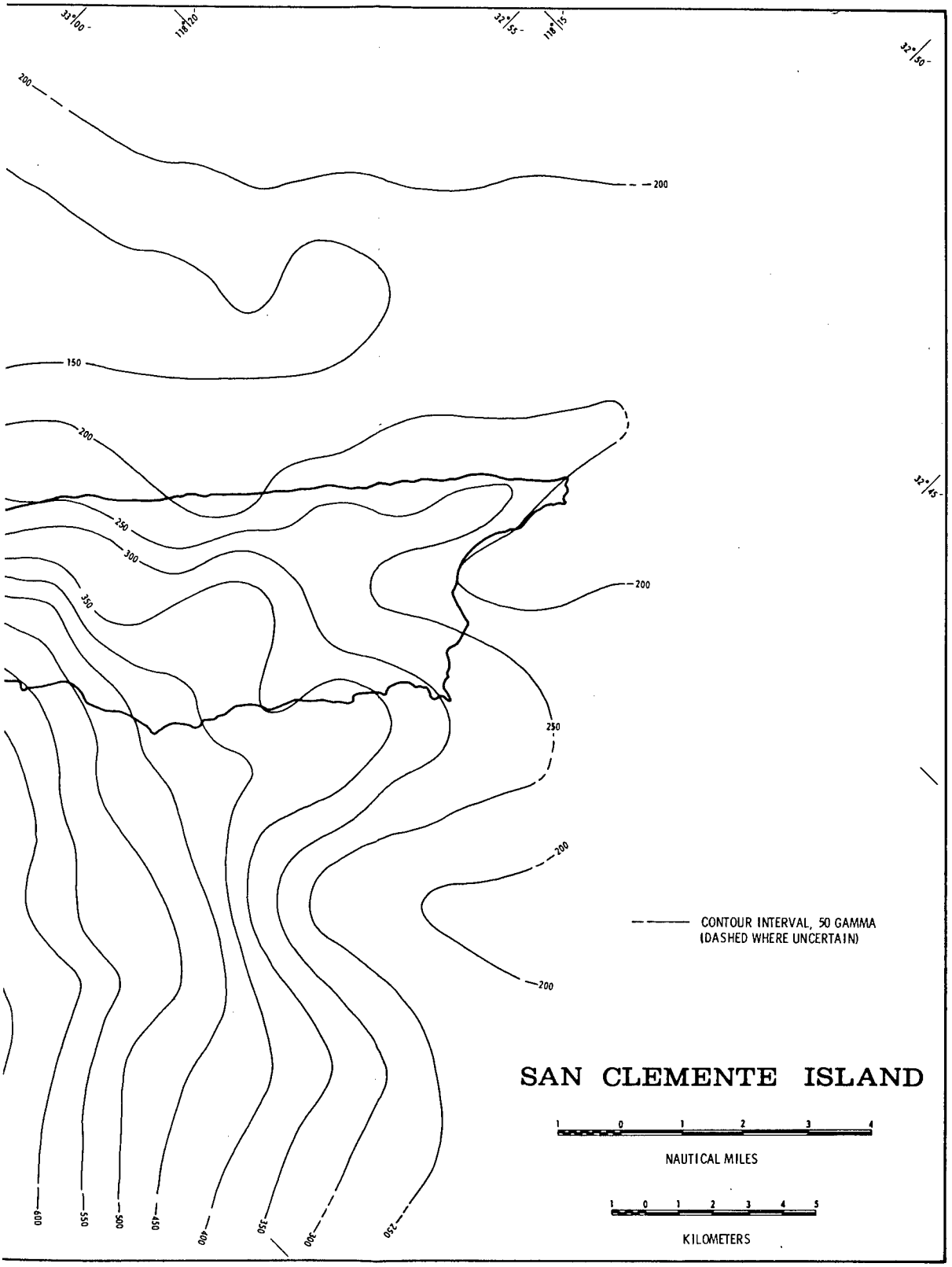

f the San Clemente Island Block Area. 2

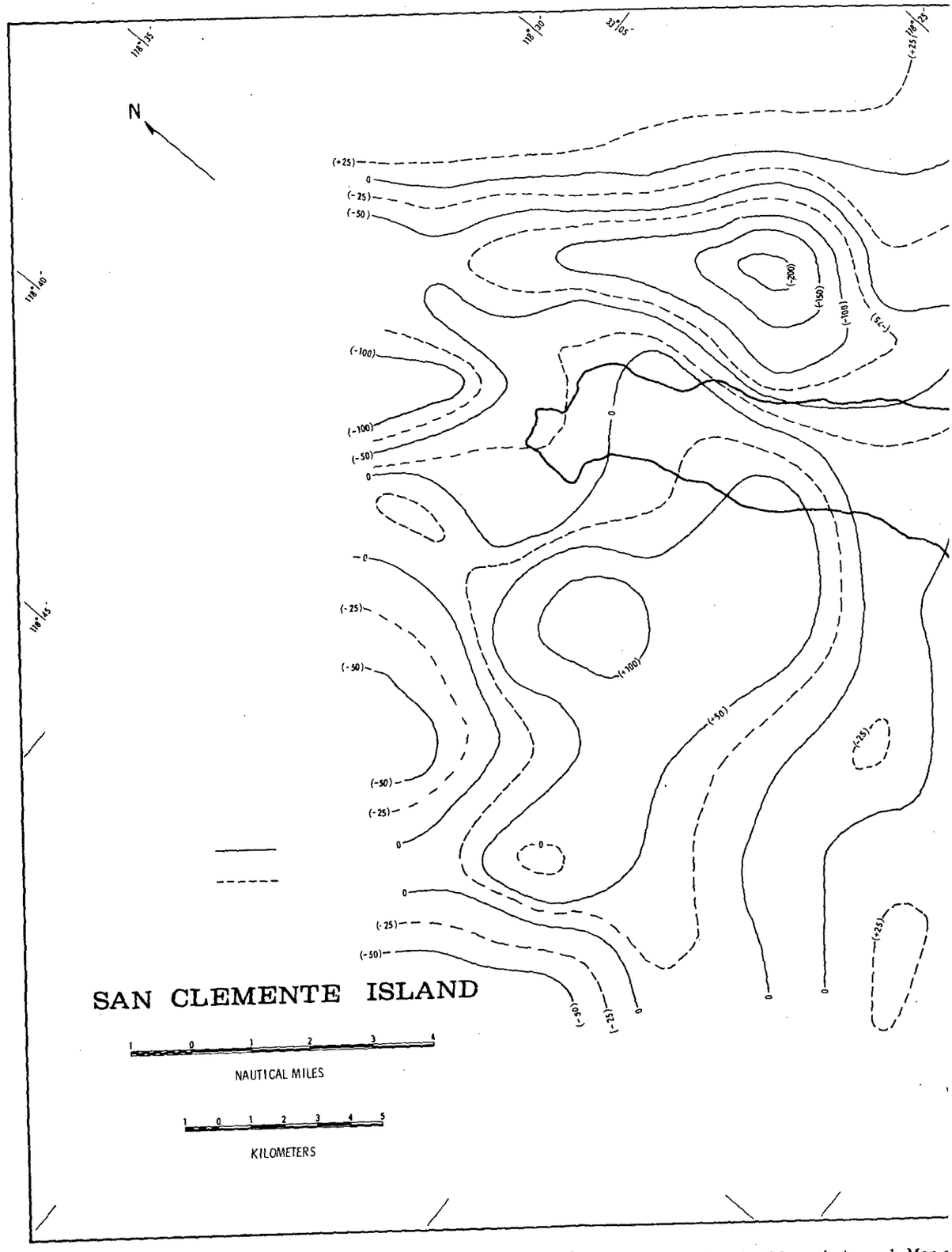

FIG. 34. Residual Magnetic Anomaly Map c

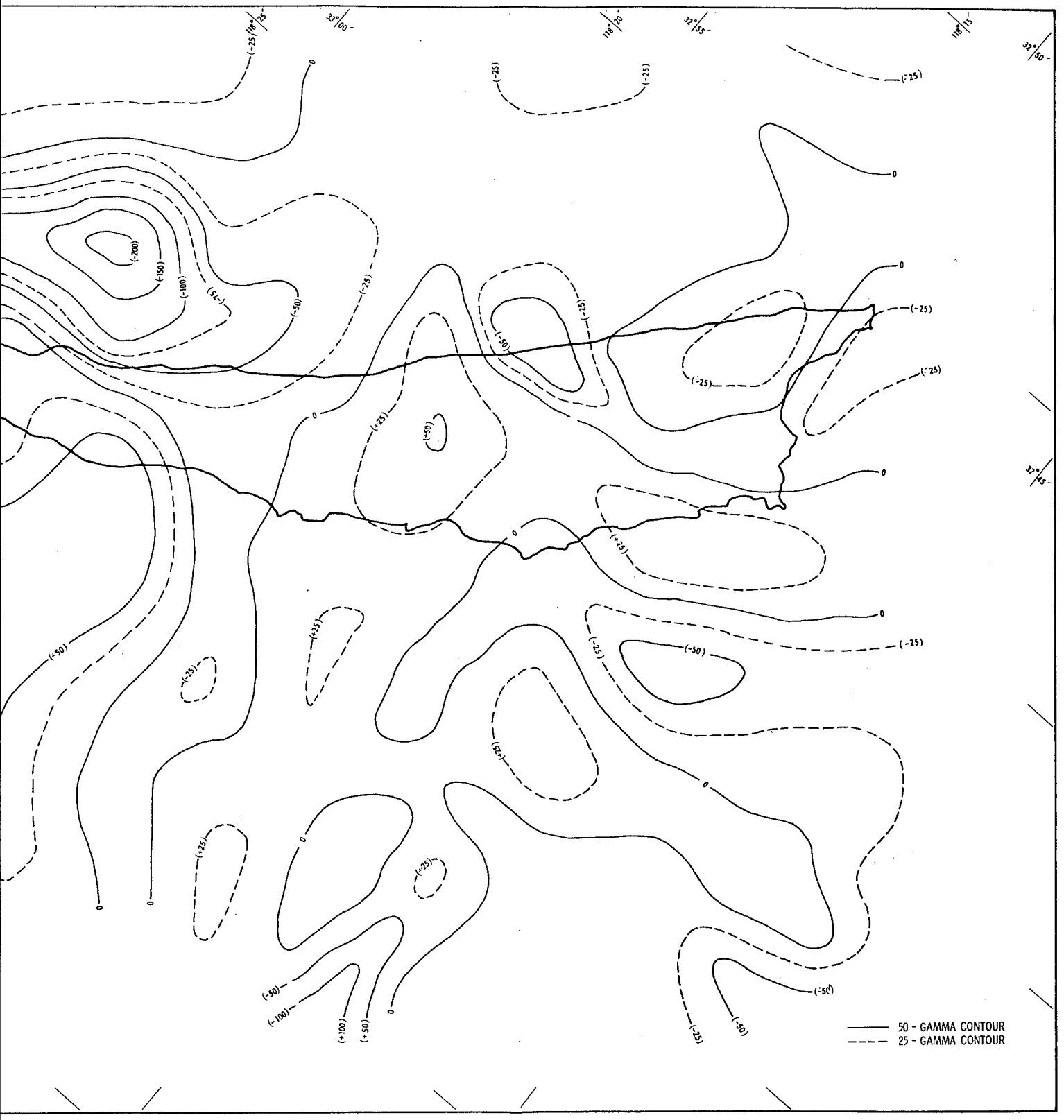

34. Residual Magnetic Anomaly Map of the San Clemente Island Block Area.

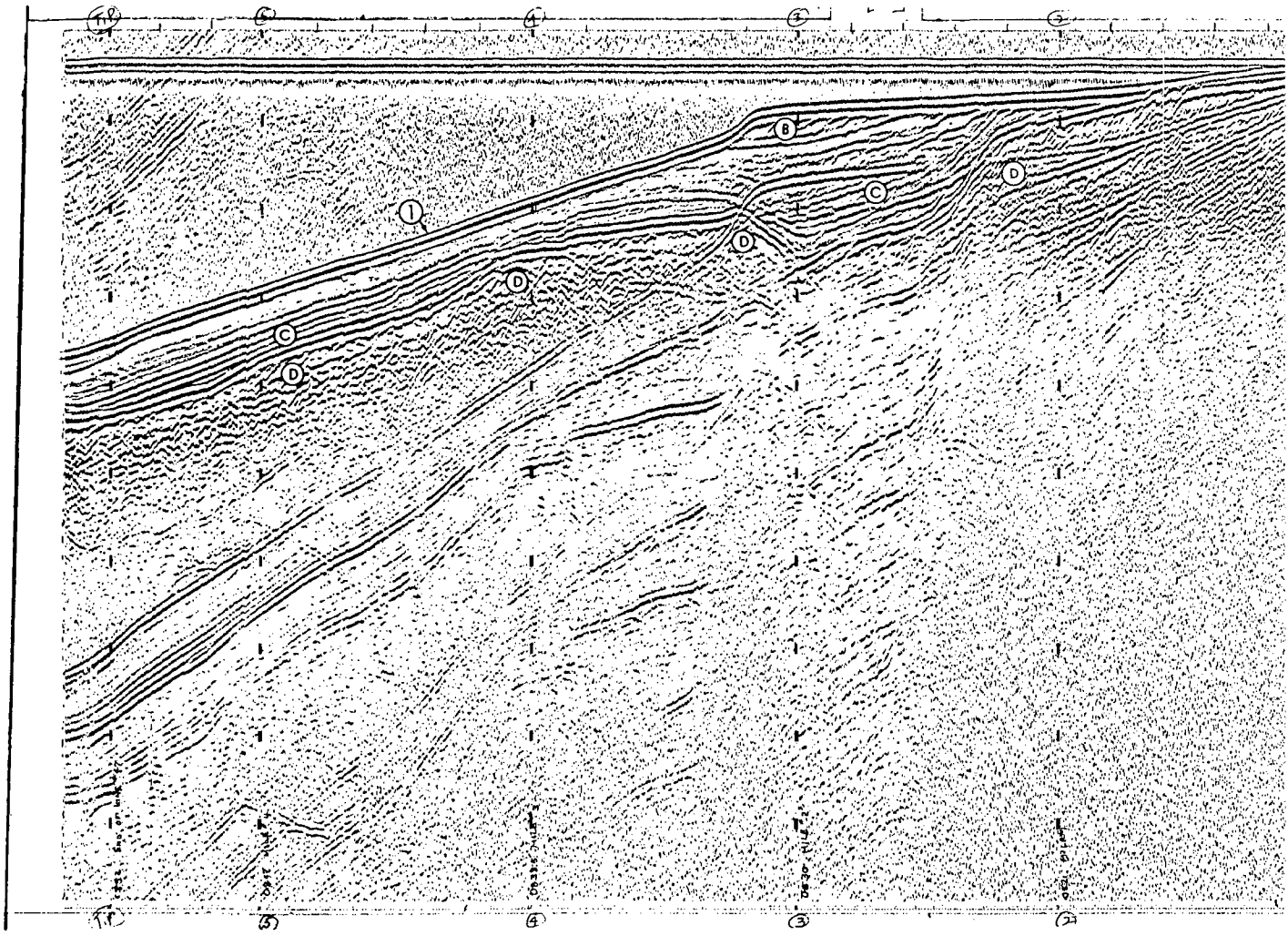

(a)

(a) Profile 47, Showing Seafloor (1) ar
representing graben and area of cha
(b) Profile 52, Showing Seafloor (1) ar
Plus Unit B, Unit C, and Unit D.

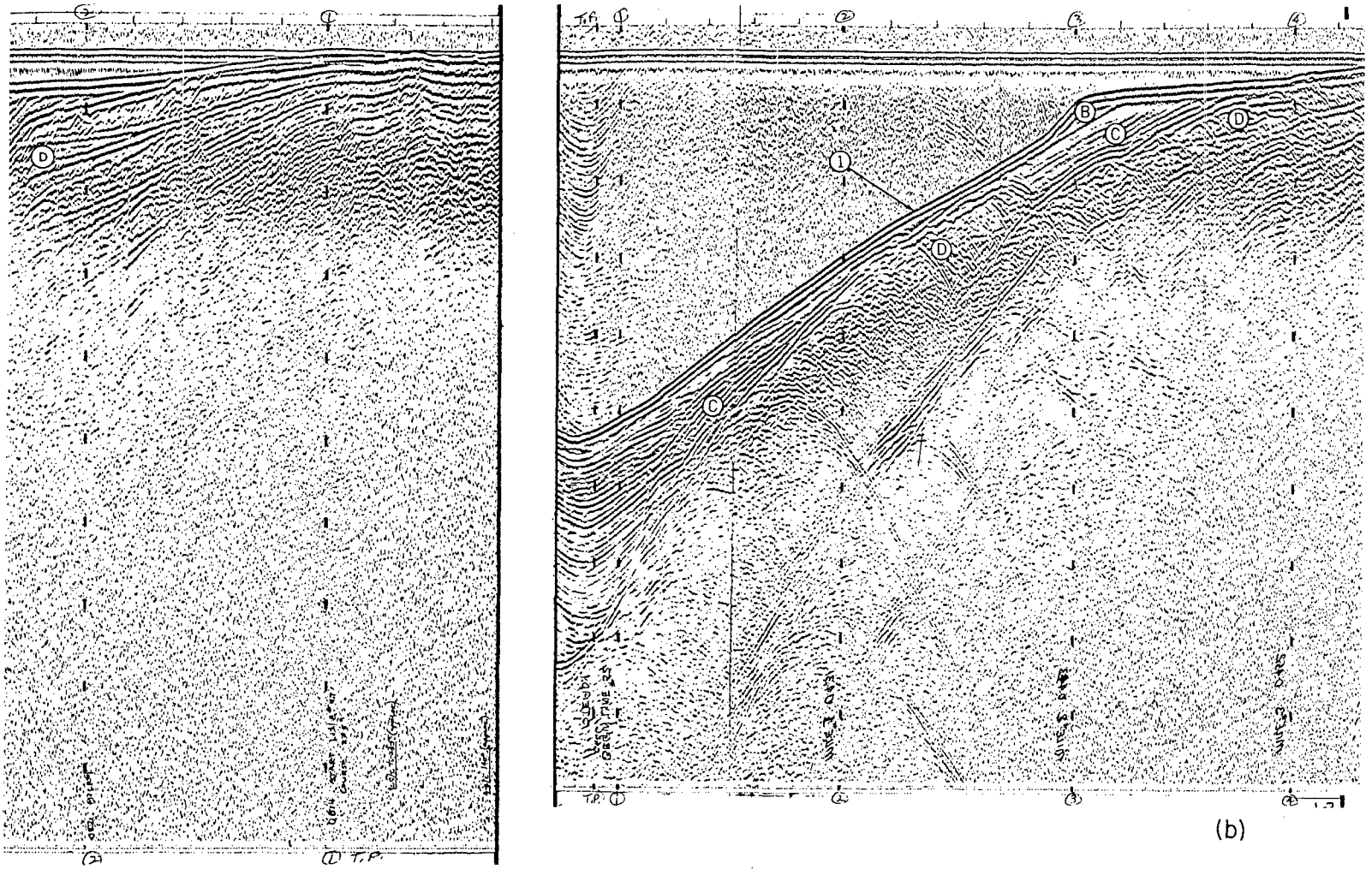

FIG. 35. Reconnaissance Survey Profiles.

2

i) Profile 47, Showing Seafloor (1) and Comparatively Gentle Slope in This Area, Unit B, Unit C, and Unit D. Note area at D-C-D, representing graben and area of change from northeasterly striking faults that intersect with northwesterly striking faults.

ii) Profile 52, Showing Seafloor (1) and General Area of Volcanic High That Also Represents a Major Magnetic High in This Region, Plus Unit B, Unit C, and Unit D.

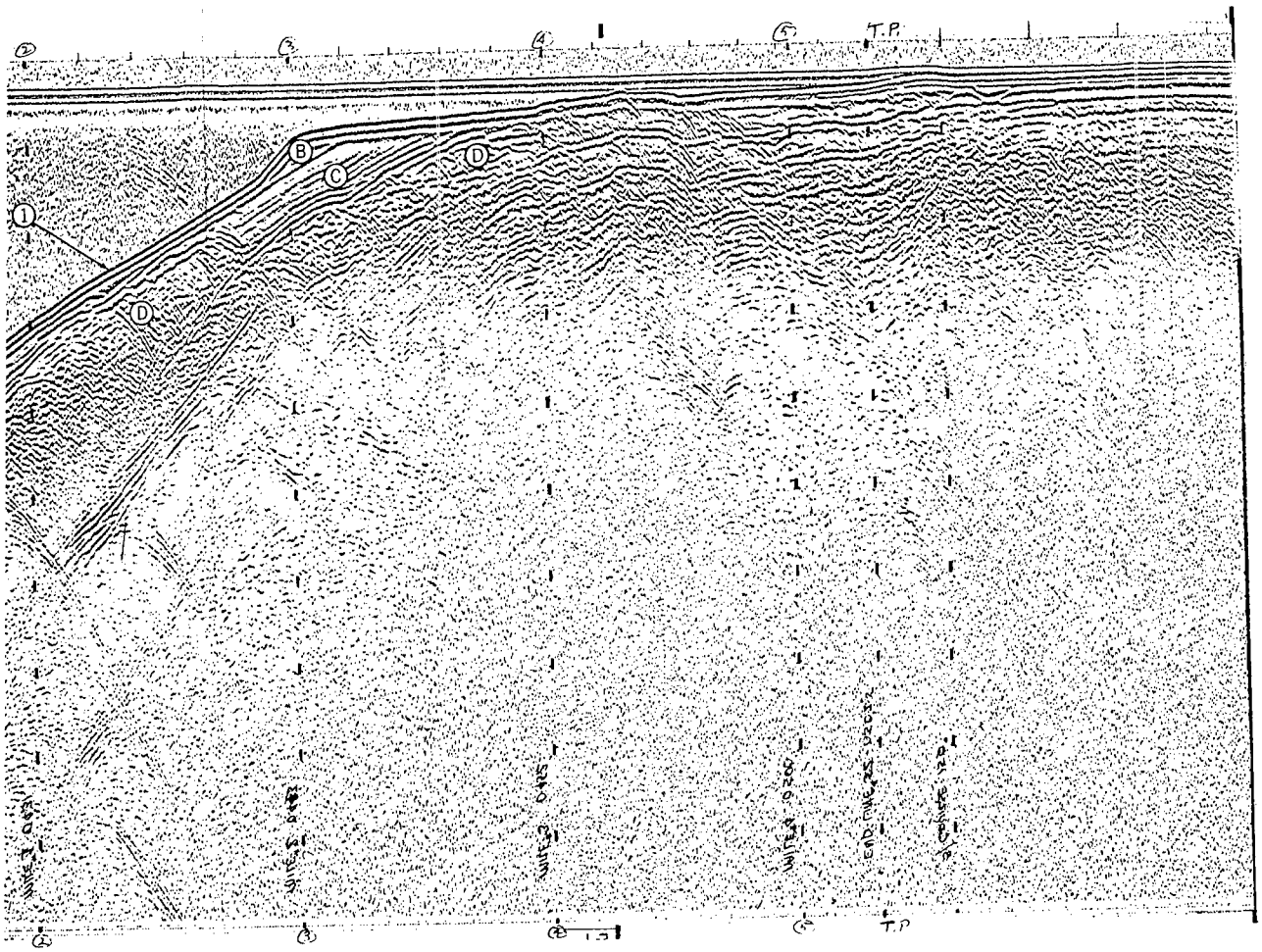

(b)

3

d Unit D. Note area at D-C-D,
westerly striking faults.
r Magnetic High in This Region,

(Fig. 35a-b) and by Fig. 20. The low is shifted slightly to the south of the major pre-orogenic surface depression.

The principal high off West Cove was recognized by Emery (Ref. 6), Harrison and von Huene (Ref. 38), and Harrison, et al. (Ref. 25). According to the latter reference, the maximum positive anomaly should occur off the southwest corner of the block if a large proportion of the volcanic rocks comprising the San Clemente Island block is responsible for the magnetic anomaly in the first place. In this connection, note that the maximum of the residual-map high is positioned at the bathymetric exposure of the volcanic high off West Cove and has a relatively steep magnetic gradient along the north slope. The east-west "wings" of the residual high may, however, correspond to a deeper source (Ref. 25). This deeper source is presumed even though the near-surface rocks undoubtedly contribute something toward an anomaly; these authors postulate a depth of 6 kilometers to the top of such a positive anomaly, but admit that an infinite number of shallower magnetic bodies could be developed to fit equally well. According to Emery (Ref. 6), the magnetic intensity of this high is greater than that encountered over outcrops of granodiorite and must therefore represent rock of more basic composition.

The flexures in the contours to the southeast of the major positive anomaly (Fig. 32 and 33) correspond to the general northeast-trending fault pattern along this part of the west side of the island. A noticeable flexure near Eel Point Canyon is presumably related to canyon faulting and the marked change in the fault pattern across this area. A change in the regional anomaly pattern along the west side is also evident across the canyon area on the residual map.

The compression of northeast-trending contours southeast of Lost Point closely corresponds to the northwest-trending volcanic rock high noted in the bathymetry and seismic profiles for this area. Figure 34 has a positive anomaly closely allied with this high. The negative anomaly immediately to the southeast aligns with a northwest structural trend (Fig. 13 and 16) southwest of China Point. The negative anomaly is closely identified with the northwest-striking faults and structural lineations interpreted for this area, but the anomaly possibly relates to the change from thin to thick parts of Unit C and the corresponding volcanic rock highs and depressions shown by the seismic profiles.

The origin of the small, positive residual anomalies at the central and southern parts of the island (Fig. 34) is not known. It is possible that deeper (thicker) masses within the volcanic rock sequence, or in zones of higher magnetic susceptibility, are responsible. Curiously, the positive anomaly in the central area corresponds to a compression of the contours (Fig. 1 of Ref. 39). This, in turn, coincides with the dacite flow on the island. Since the magnetic properties of the island's volcanic rocks have not been measured, it is not known whether this anomaly is related to the dacite flows.

The pronounced, elongated negative anomaly along the eastern margin of the island tends to conform to the post-orogenic surface and sediment fill trends (Fig. 21 and 15). Major flexures in the contours are present where the complex zone of faulting and crustal blocking occurs between the Emery Seaknoll and the island. The general tendency for a more positive

magnetic trend southeastward is probably related to a gradual surfacing of the magnetic source, as well as to the presence of the Emery Seaknoll and Southern Plateau volcanic rock highs. A slight negative anomaly (Fig. 34) marks the elongated sediment basin between the highs.

The author suggests that the steep magnetic gradient off the San Clemente Escarpment is the product of (1) the margin of the mass of volcanic flows; (2) the postulated deep basic mass related to the large positive anomaly off West Cove; and (3) major faulting that has cut both the mass of volcanic rocks and the deeper and probably more basic rock type.

Gravity. There were very few published data on gravity measurements for the southern California region until 1957 (Ref. 6). Since that time, and particularly in recent years (Ref. 25, 38, and 40), considerable surface-ship gravity work has been done for much of the northern Continental Borderland.

Gravity data combined with those of seismic refraction aid in the solution of the gravity profile (Ref. 15 and 18). Harrison and von Huene (Ref. 38) and Harrison, et al. (Ref. 25), have based much of their gravity interpretations for the Continental Borderland on the seismic refraction data of Shor and Raitt (Ref. 36).

The San Clemente Island block is interpreted as an igneous feature, specifically a thick mass of volcanic rocks with sharp boundaries possibly caused by faulting (Ref. 38). Shor and Raitt's northeast-southwest cross section (Fig. 2 of Ref. 36) shows a cutoff of their 4.6-km/sec velocity layer along the northeast side of the block. The 4.6-km/sec layer is considered normal for either volcanics or consolidated sediments by these authors. The interpreted thickness for this layer is roughly 1.5 kilometers.

San Clemente Island is the only topographic high in the region that is not associated with a major Bouguer anomaly. This lack is attributed to the vesicular texture or low density of the andesitic rocks postulated for the upper part of the island block (Ref. 38).

Seismicity. The Pacific Coast region of North America, a part of the circum-Pacific orogenic belt, is considered one of the major seismic areas of the world. Richter (Ref. 41) has sectioned this region into several seismic provinces. San Clemente Island is located within the offshore province south of the Channel Islands.

Most earthquake epicenters of the southern California region are concentrated in the land areas. The greatest seismic activity in the northern Continental Borderland has been in the San Pedro Basin area (Fig. 36) next to a similar concentration on land. The curves of Fig. 37a-b show that the frequency of shock occurrence increases moderately from San Clemente Island out to roughly 60 kilometers, and then markedly from 60 to 90 kilometers from the island center. This phenomenon results mostly from a marked increase in activity within the San Pedro Basin. The shoreward concentration tends to give a misleading aspect to any analysis of epicenter occurrence versus distance from the island. The greatest concentration of epicenters within 40 kilometers occurs near and off the southeastern part of the island. The relatively high activity in this area is noted in the southern California region

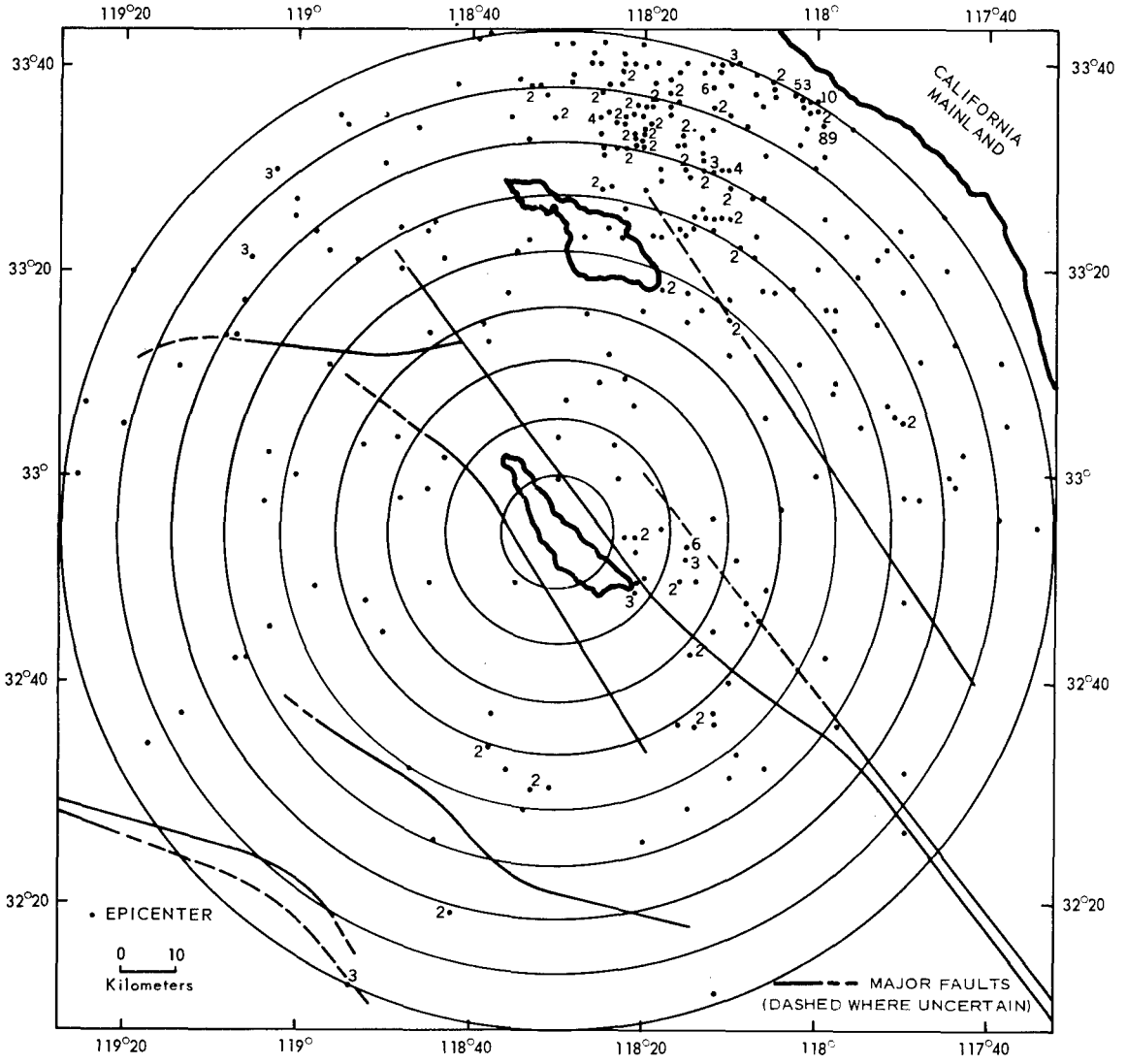

FIG. 36. Epicenter Map of Earthquake Shocks Within 90-Kilometer Radius of San Clemente Island. More than one shock indicated by number at location. Map center taken to be 32°55'N, 118°30'W. Circles represent 10-km intervals.

strain-release map of Allen, et al. (Ref. 42). Note that the two shocks of magnitude greater than 5.0 (Richter scale) in the entire compiled data occurred close to the island, one at Pyramid Head and the second at a point 37 kilometers southwest of China Point.

A period of relatively low seismic activity has been observed in the northern Continental Borderland since the latter 1930's (Fig. 37a). An increase in such activity has been noted recently, but may be only momentary. By way of comparison, the curve of Fig. 37b shows that seismic activity in the area closer to the island is more cyclical in nature, but still suggests a possible upswing at the present. The 40-kilometer range in Fig. 36 was selected to cover only the area of major faults believed to be closely related to the San Clemente Island block structure.

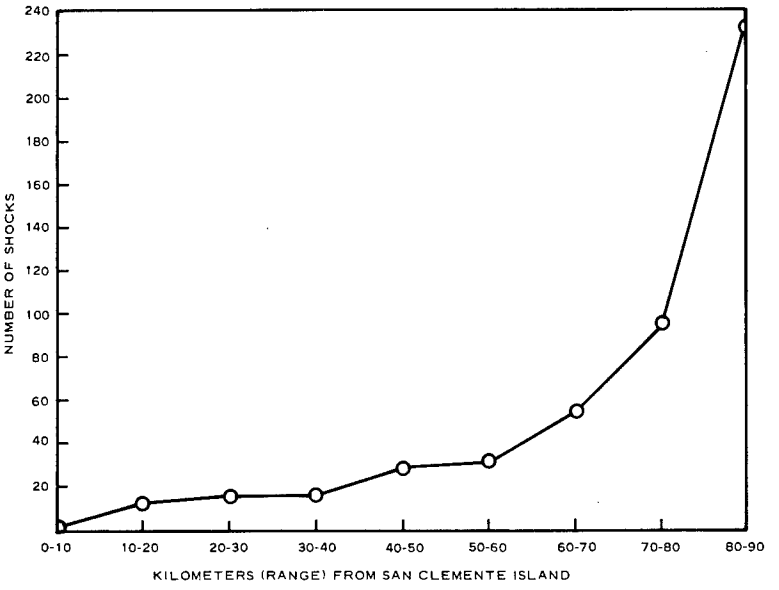

(a)

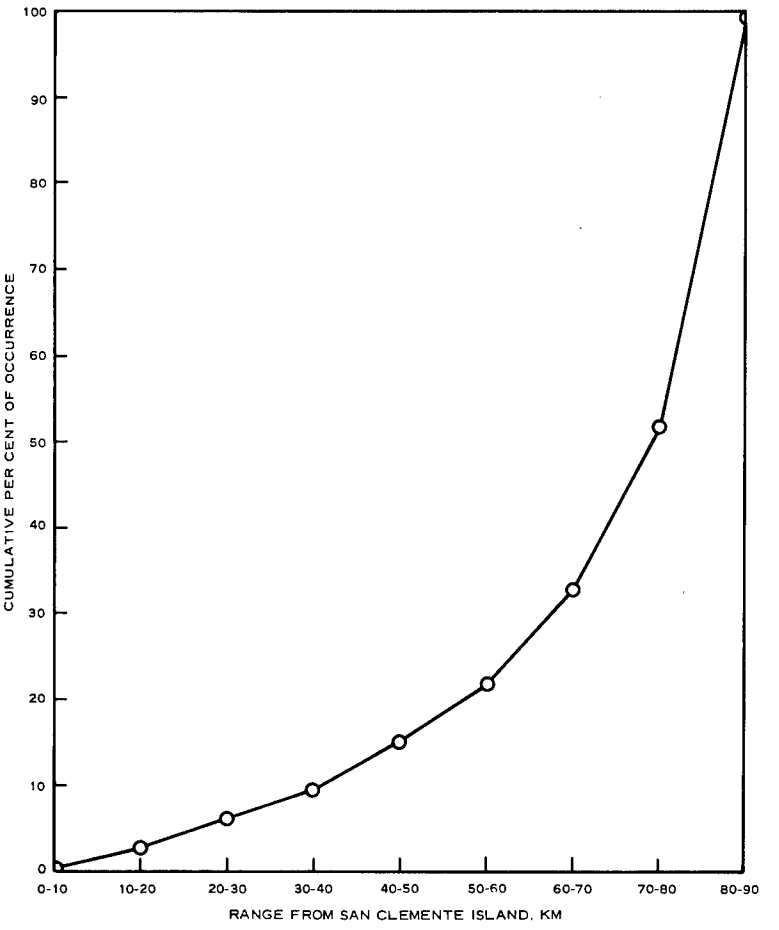

(b)

FIG. 37. Frequency of Shock Occurrence With Distance From San Clemente Island.

(a) Number of Shocks Versus Distance.

(b) Cumulative Percent of the Occurrences in (a).

Figure 38 shows the cyclical nature of the number of shocks versus time. Figure 39 is similar, but suggests that the study area may be in a period of momentary quiescence.

Earthquake shocks of lower magnitude occur less frequently per unit area in the northern Continental Borderland than in adjacent land areas (Fig. 40). A slightly higher tendency is noted for those shocks in the 5-to-6 magnitude range.

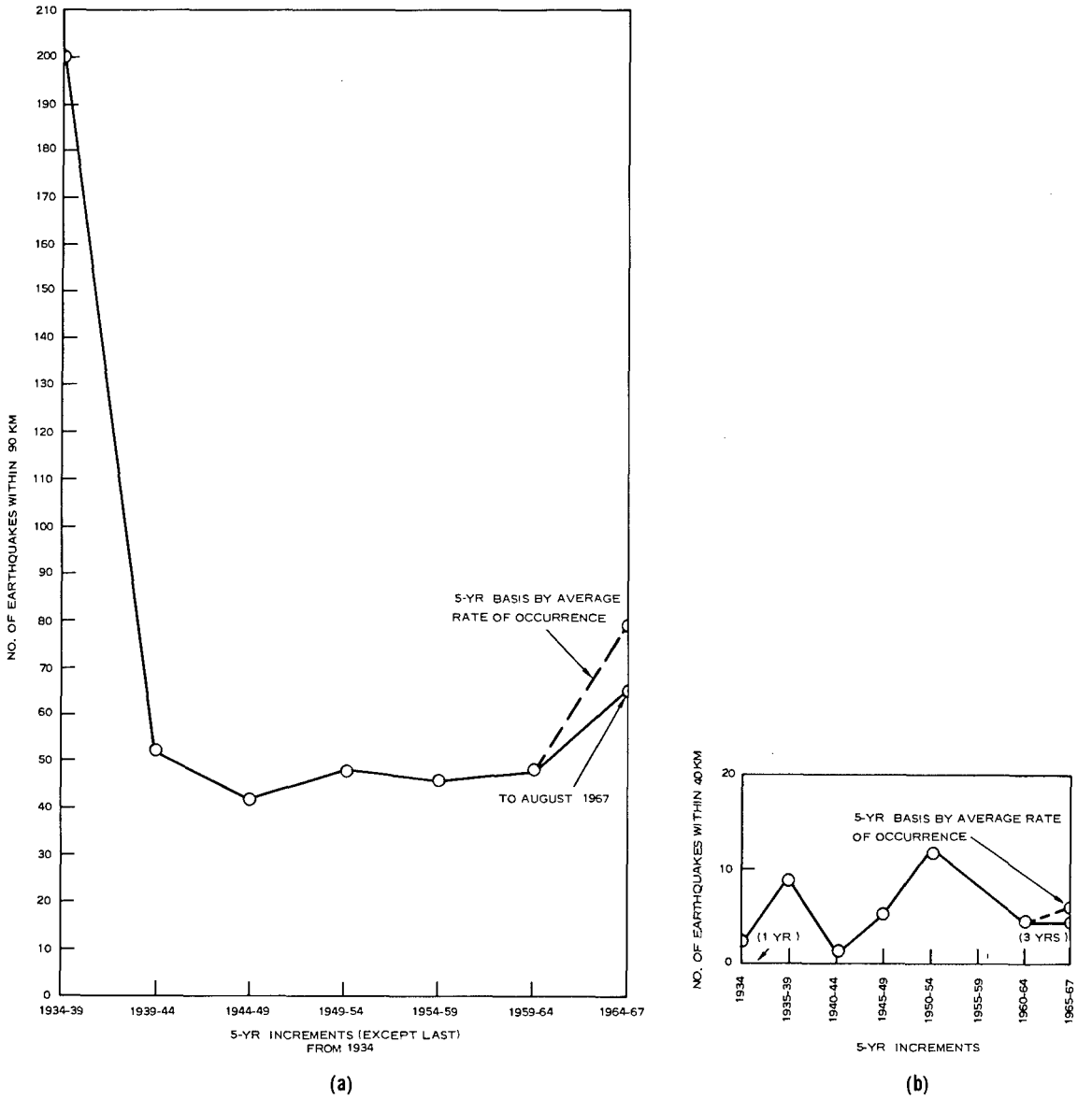

FIG. 38. Frequency of Earthquake Shock Occurrence Versus Time in Increments of 5 Years.
(a) 90-km Range From San Clemente Island.
(b) 40-km Range From San Clemente Island.

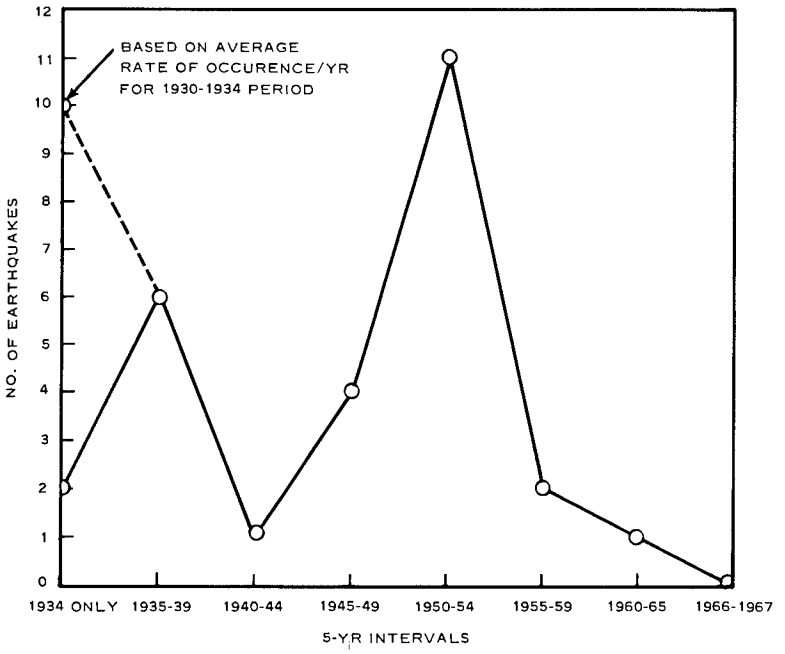

(a)

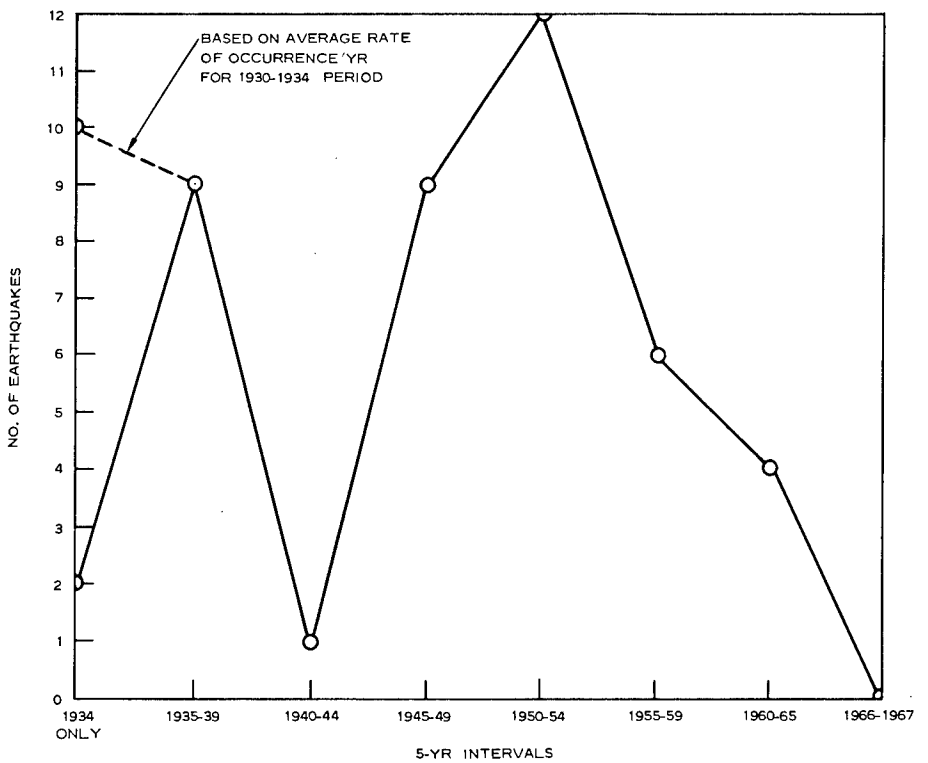

(b)

FIG. 39. Frequency of Earthquake Shocks in Vicinity of San Clemente Island.
(a) Shocks in Immediate Vicinity.
(b) Immediate Vicinity Plus Shocks in Nearby Area That Are Possibly Related to Active Faults Associated With the San Clemente Island Block. (See Fig.36.)

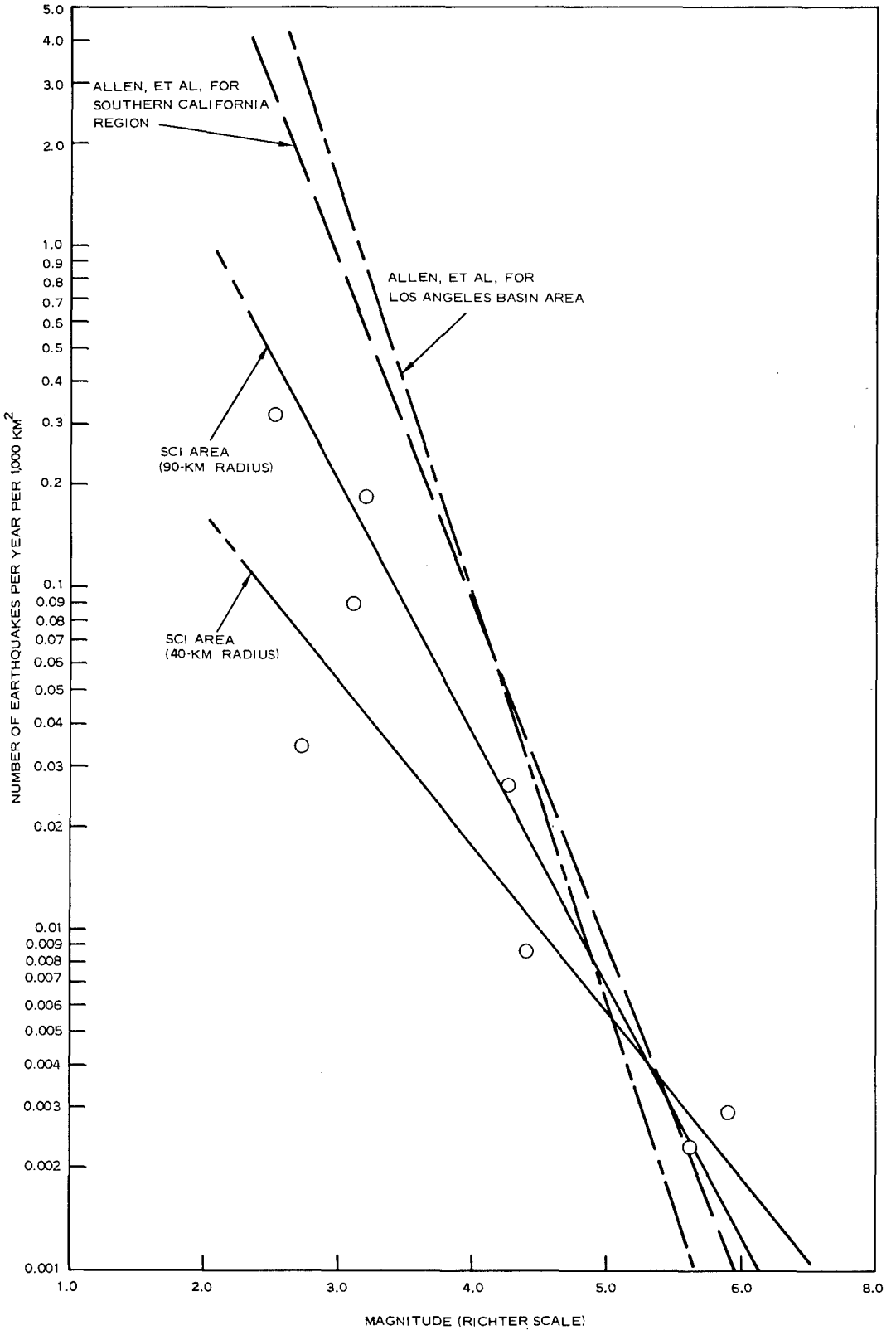

FIG. 40. Frequency of Earthquake Shocks per Unit Area Versus Magnitude for Areas Within 40 and 90 km of San Clemente Island to 1967, Compared to Similar Data for Other Areas of Southern California (Ref. 42).

Attempts to correlate earthquake epicenters with known and inferred geologic structures in the southern California region have been made by many authors (e.g., Ref. 6, 30, 43, and 44). Earthquakes associated with the San Clemente fault, the Agua Blanca fault, and the San Andreas-Gulf of California rift zone are frequent and large. Extensive deformations are probably occurring along these zones (Ref. 10).

Evidence of very recent fault activity has been noted on several of the seismic profiles along the eastern side of the island. Certain offsets, as well as a change of dip in the post-orogenic sediments at the seafloor (Fig. 41), are readily aligned with inferred faulting in the area. Some of these features may have resulted from sedimentation processes (for example, channeling, onlap, and compaction), but fault alignment, apparent lack of levees, and the equivalent elevation of some features across the profiles, tend to favor the fault interpretation. Some offsets at the bases of slopes suggest fault rejuvenation, with the shoreward slope representing a resurgence of sedimentation. Periodic fault rejuvenation is also suggested on the profiles (Fig. 9b) by a downward convexity in the reflectors at depths below the seafloor in the San Clemente fault zone. However, differential compaction could also account for at least part of this downwarping. The close relationship between the inferred recent fault activity and the epicenter locations in the area of study is illustrated in Fig. 42. The greatest concentration of these features is obviously along the San Clemente fault zone (Fig. 17d). The only epicenter in the study area west of the island is close to the major complementary fault outlining the western margin of the island block. Recent fault activity is not apparent in the basin sediments northwest of the Emery Seaknoll.

The evidence above suggests that the area from the Rift Valley to the Emery Seaknoll along the main fault zone is presently adjusting to local stress inequalities related to movement along the San Clemente fault.

SEDIMENT TRANSPORT AND DEPOSITION

SEDIMENTARY STRUCTURE

Structural ramifications of various sedimentary processes are averaged by the limitations of resolution in the reflection-profile method, so that the predominant process causing stratification emerges as the basis of the recorded internal structure (Ref. 11). A fundamental assumption is that the reflections from strata of turbidity-current deposits will characterize low bathymetric areas and show apparent truncation of the sediments against bathymetric highs or even gentle slopes. Sediments of hemipelagic origin will not uniformly blanket sharp or irregular highs, particularly in areas of pronounced currents. These sediments will drape over the more gentle highs, with no sharp truncation of the sediments in areas of mostly low current velocities. Turbidity-current sediments that show curvature by compaction may be differentiated from the hemipelagic type by the direction and magnitude of curvature and the retention of truncation against the bathymetric highs. These seismic-profile properties of hemipelagic and turbidity-current deposits are illustrated clearly by Hamilton (Ref. 45).

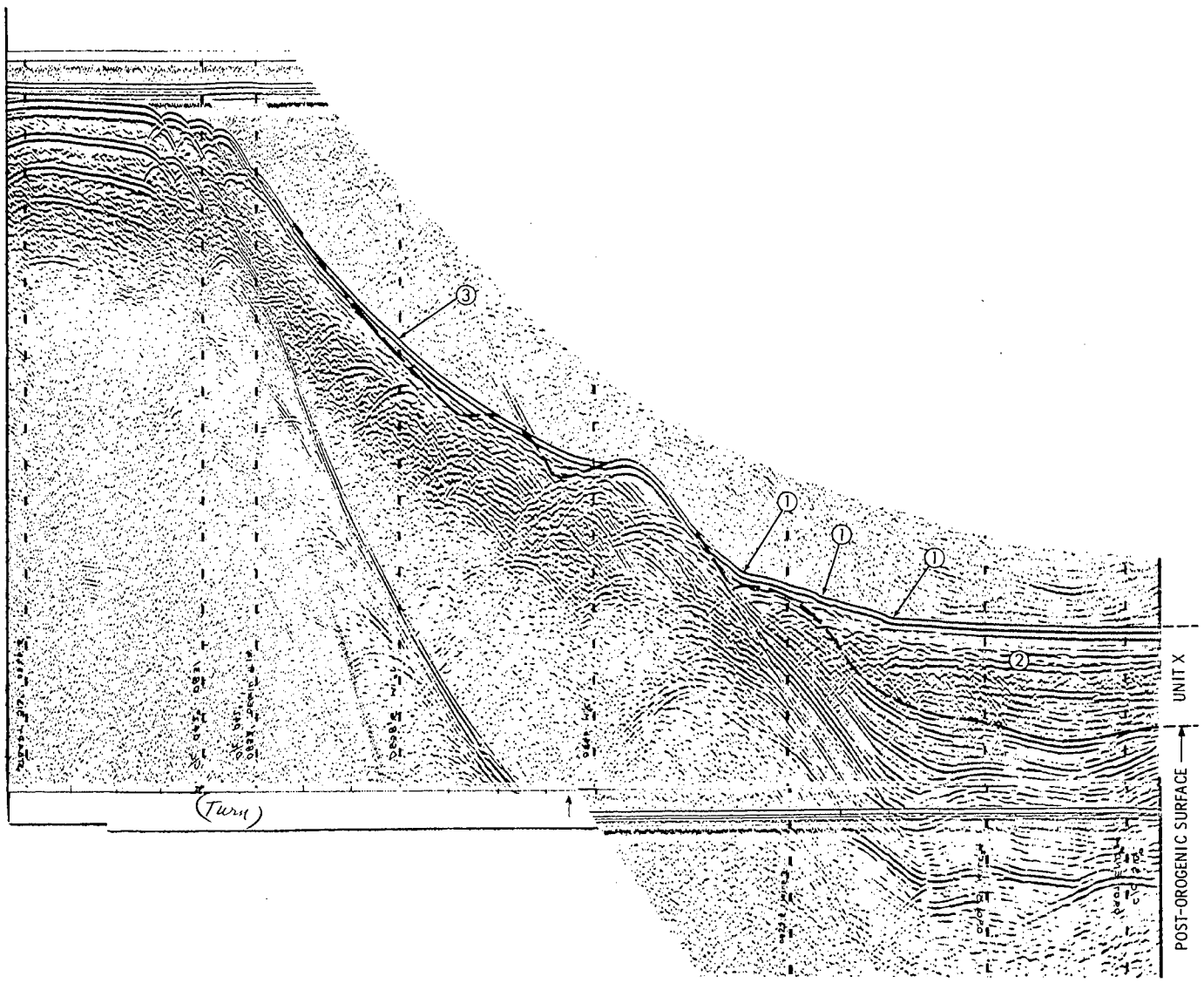

FIG. 41. Reconnaissance Survey Profiles 14 and 15. Offsets along seafloor
Unit X (2) is shown to lie in a major graben (or trough) zone; note seafloor
(a) Profile 14.
(b) Profile 15.

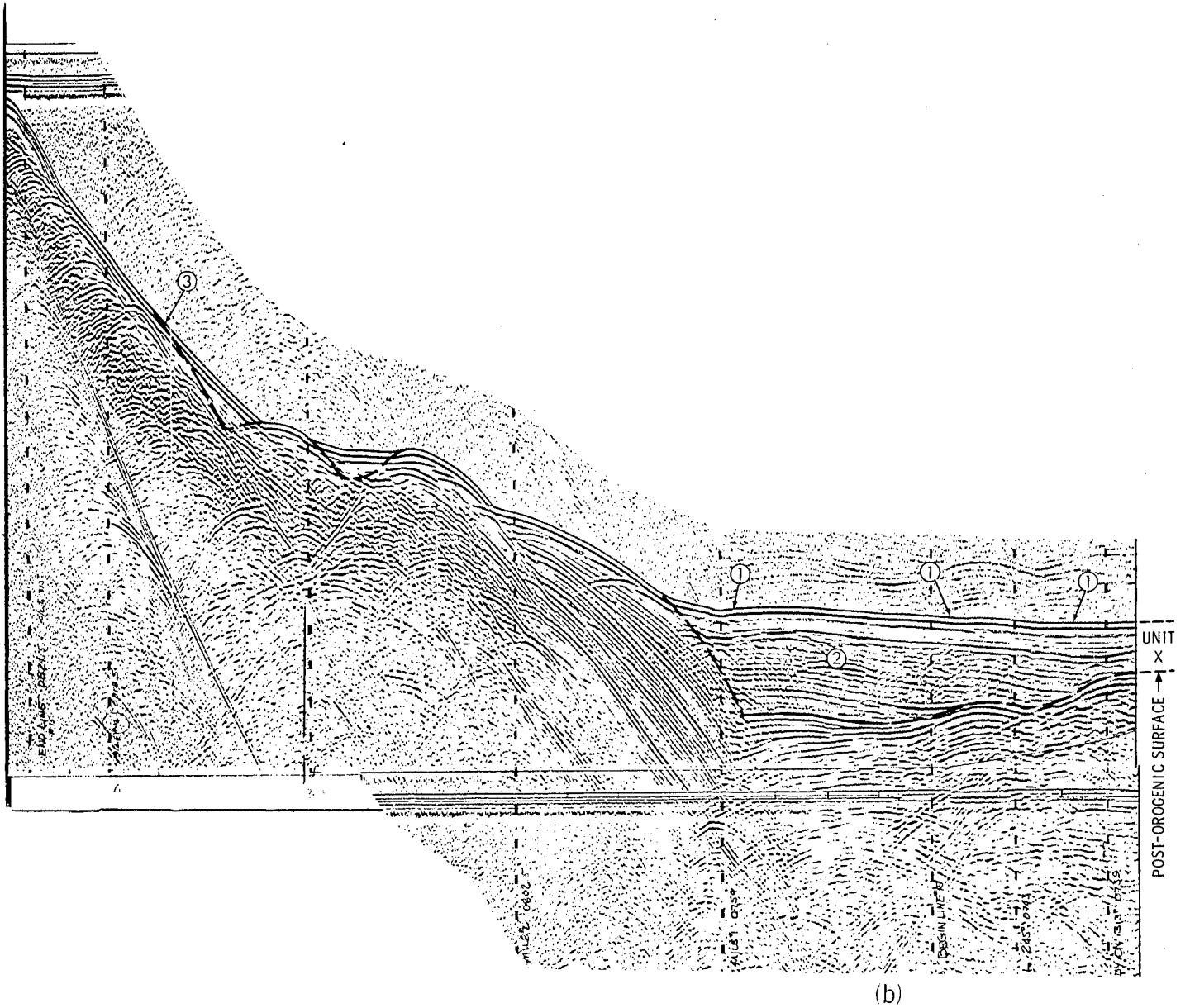

(b)

ɜ seafloor (1) suggest recent fault activity affecting Unit X sediments;
seafloor and veneer of Unit X sediments (3).
rofile 14.
rofile 15.

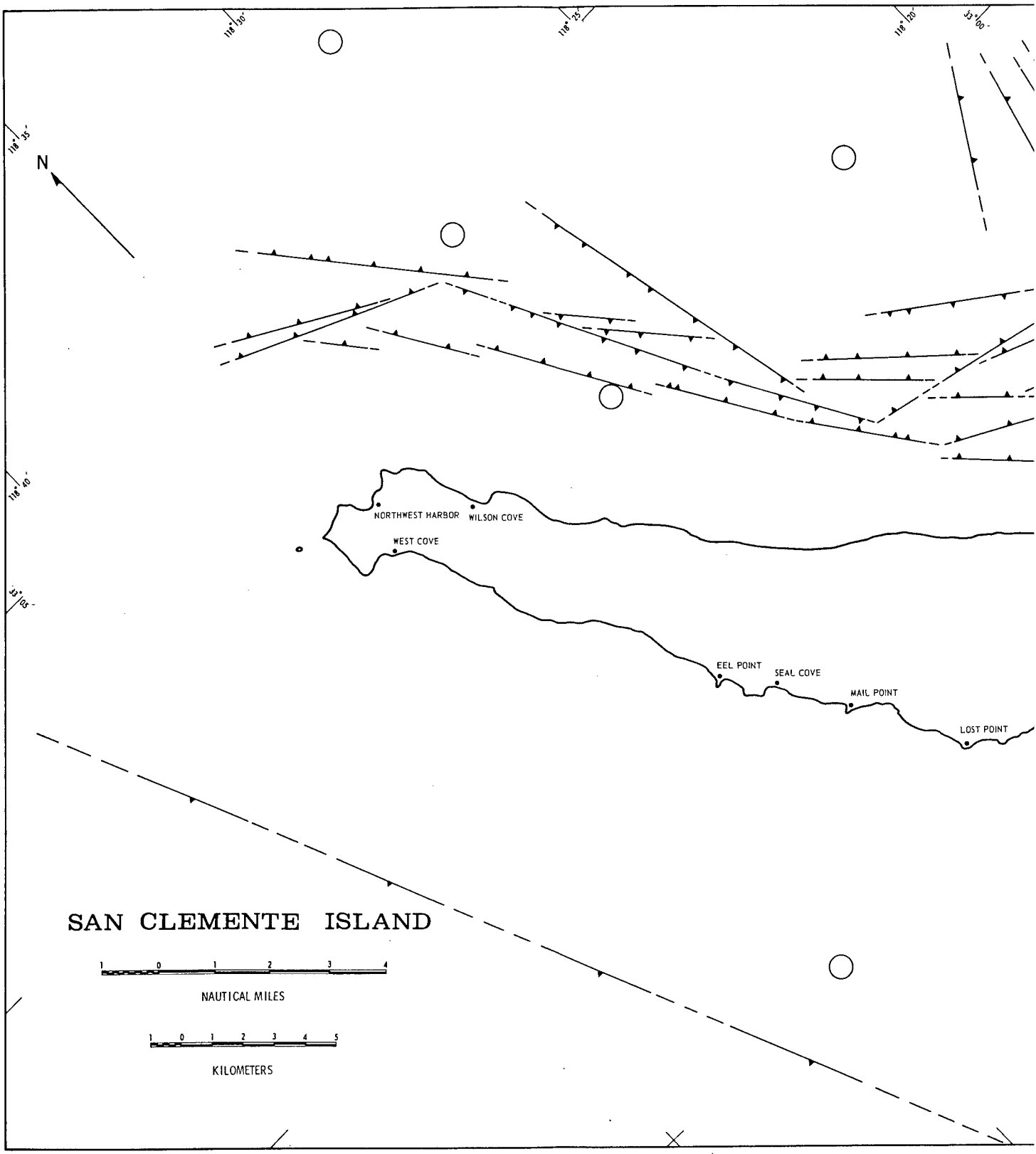

FIG. 42. Recent Fault Activity and Epicenter Locations in San Clemente Island Block Area. More than

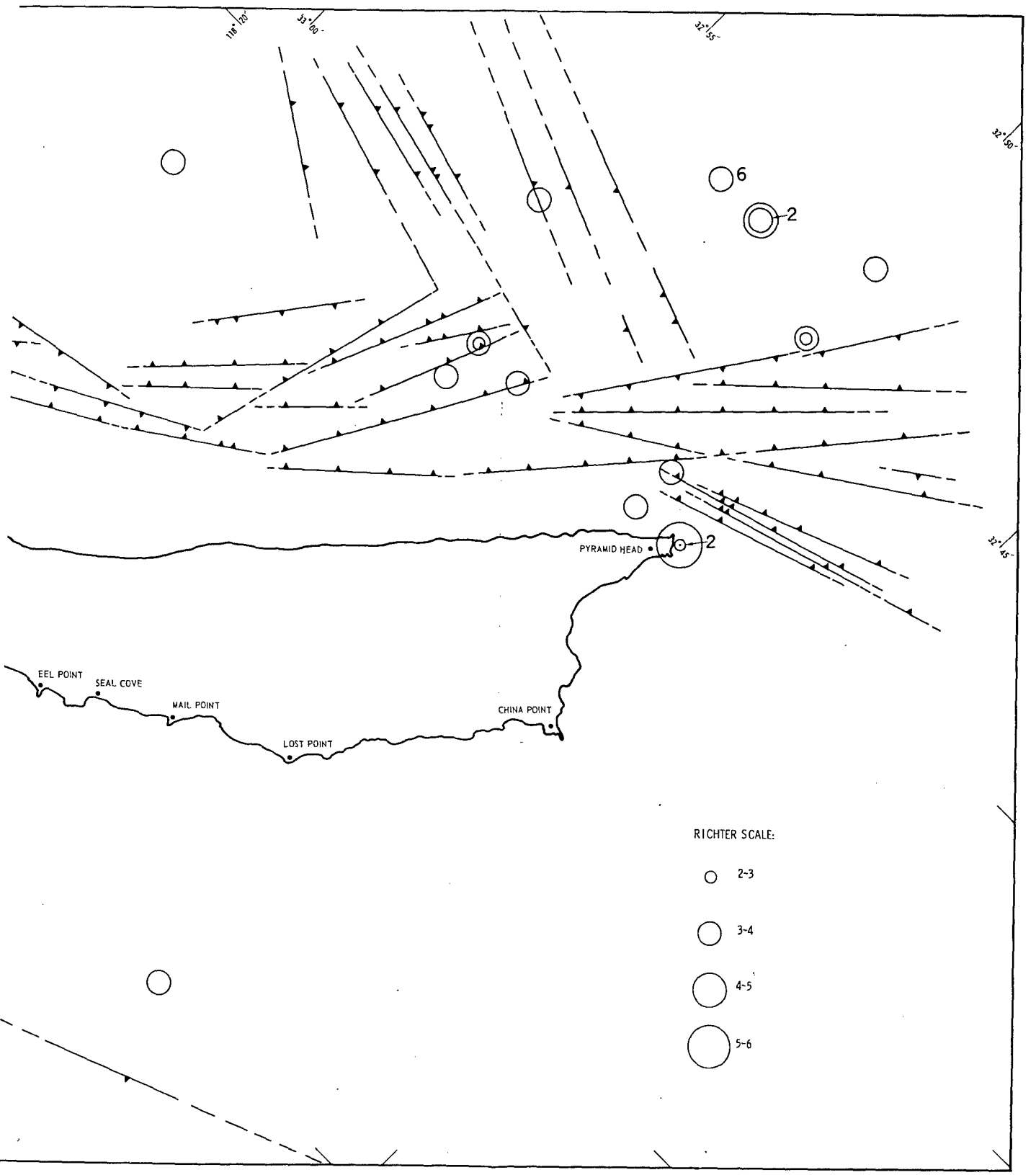

ıtions in San Clemente Island Block Area. More than one shock indicated by number next to location. 2

Moore (Ref. 11) postulates a relatively insignificant contribution of sediment of hemipelagic origin, as compared to that deposited by turbidity currents. Probably no more than 15% of the total thickness of Continental Borderland post-orogenic basin sediments is of hemipelagic origin.

SAN CLEMENTE ISLAND BLOCK

The major post-orogenic sediment fill forming the valley floor adjacent to the San Clemente Escarpment is mostly well defined on the seismic profiles, and appears to be continuously bedded within units defined by the two and possibly three unconformities (Fig. 43a-b). Some trough zones have been partially to completely filled by sediment (Fig. 10); some have overflowed to form a continuation with the broader basin areas. An exception is the apparently bare trough formed by a N35°W-striking fault immediately off the escarpment to the southeast of Pyramid Head (Profile 26, Fig. 10). Differences in elevation of some of the troughs are also noted in the figure. The trough areas apparently act as sediment traps and often as dispersal paths for terrigenous material derived from the slopes of the island block.

Near-horizontal deposits in the basin and trough areas off the east side of the island are considered partly of turbidity-current origin. Interpretation of the study-area seismic profiles, unpublished data on cores taken by the U. S. Naval Civil Engineering Laboratory (NCEL), Port Hueneme, Calif., and analysis of other cores of the area by Gaal (Ref. 7), are the bases for this conclusion. Five-foot cores, taken along the San Clemente fault zone and analyzed by NCEL, contain horizontal layers of sand and silt graded upward into clay and containing sharply defined lower contacts. Other coarse to very coarse sand layers contain shell debris, mineral grains, and small rock fragments, which suggest other than a hemipelagic or pelagic origin of deposition for these layers. Foraminifera in some of the better-defined, coarser sand layers are a mixture of both shallow- and deep-water species.[3] One core (AHF 8320, Fig. 44, and Appendix C) contained graded bedding of sand and silt layers with very abundunt mica, which is suggestive of displaced shallow-water sediments. Some of the coarse, shelly sand layers taken at the base of the escarpment undoubtedly resulted from submarine slides. However, the sand and silt layers with sharply defined bases in cores taken at the base of the escarpment may have resulted from submarine slides; the sand and silt layers that have sharply defined bases and grade upward into clay suggest deposition by turbidity currents.

By contrast, evidence for leveed channels at the seafloor (Ref. 22 and 45) is not apparent in any of the reflection profiles to suggest that turbidity currents have been recently active. Some channel-like seafloor depressions contained in the profiles are presumed to have been caused by recent fault activity. It is conceivable that some of these features may have been maintained by turbidity-current flows, and that a lack of profile resolution has masked any evidence of levees.

---

[3] Personal communication from J. Warme, Rice University, Houston, Tex.

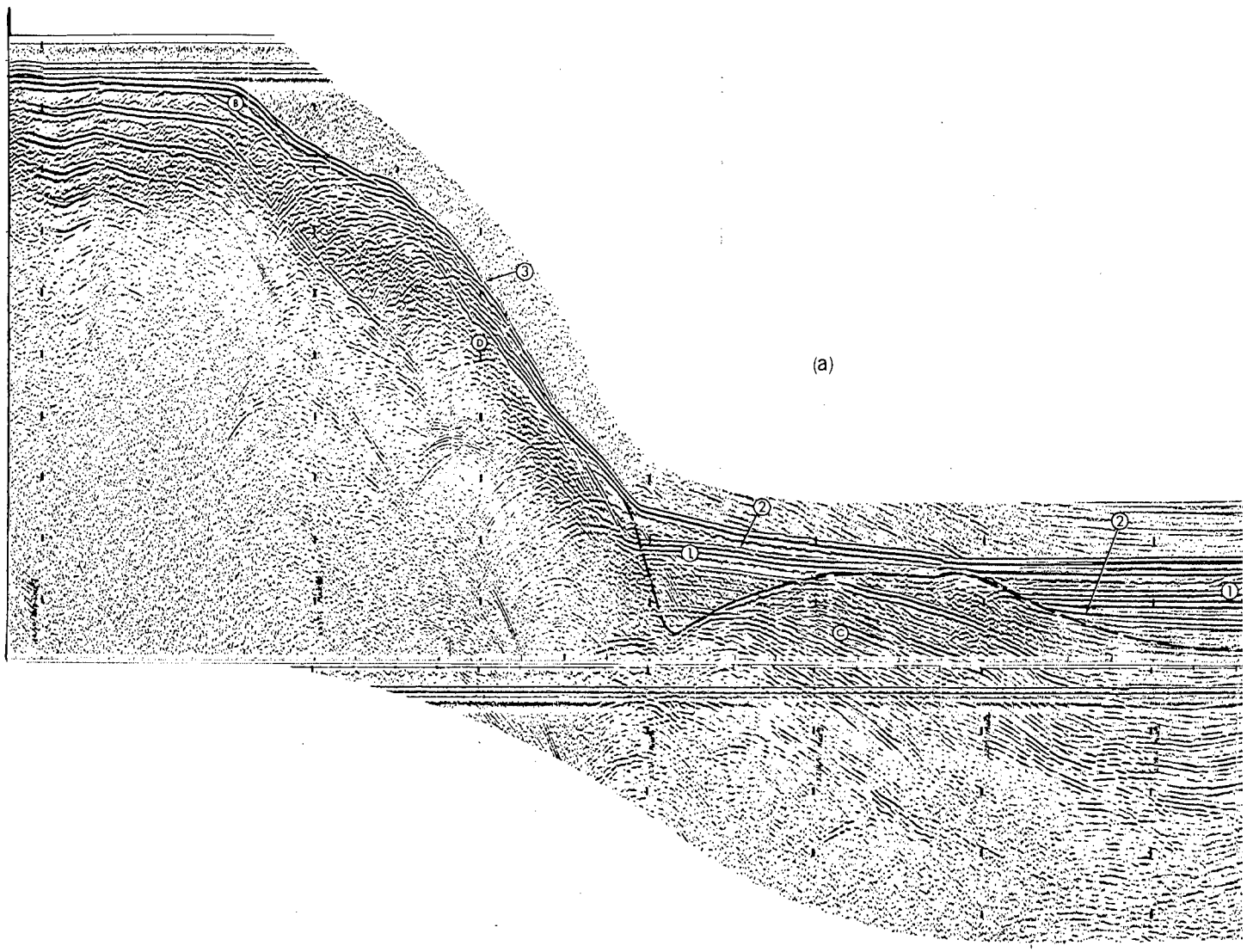

FIG. 43. Reconnaissance Survey Profiles. Da
(a) Profile 1, Showing Unit B, Un
(b) Profile 2, Showing Units B, C,
ment (3), Plus the Slope of th
shown is a fan or apron, poss
that presumably act as channe

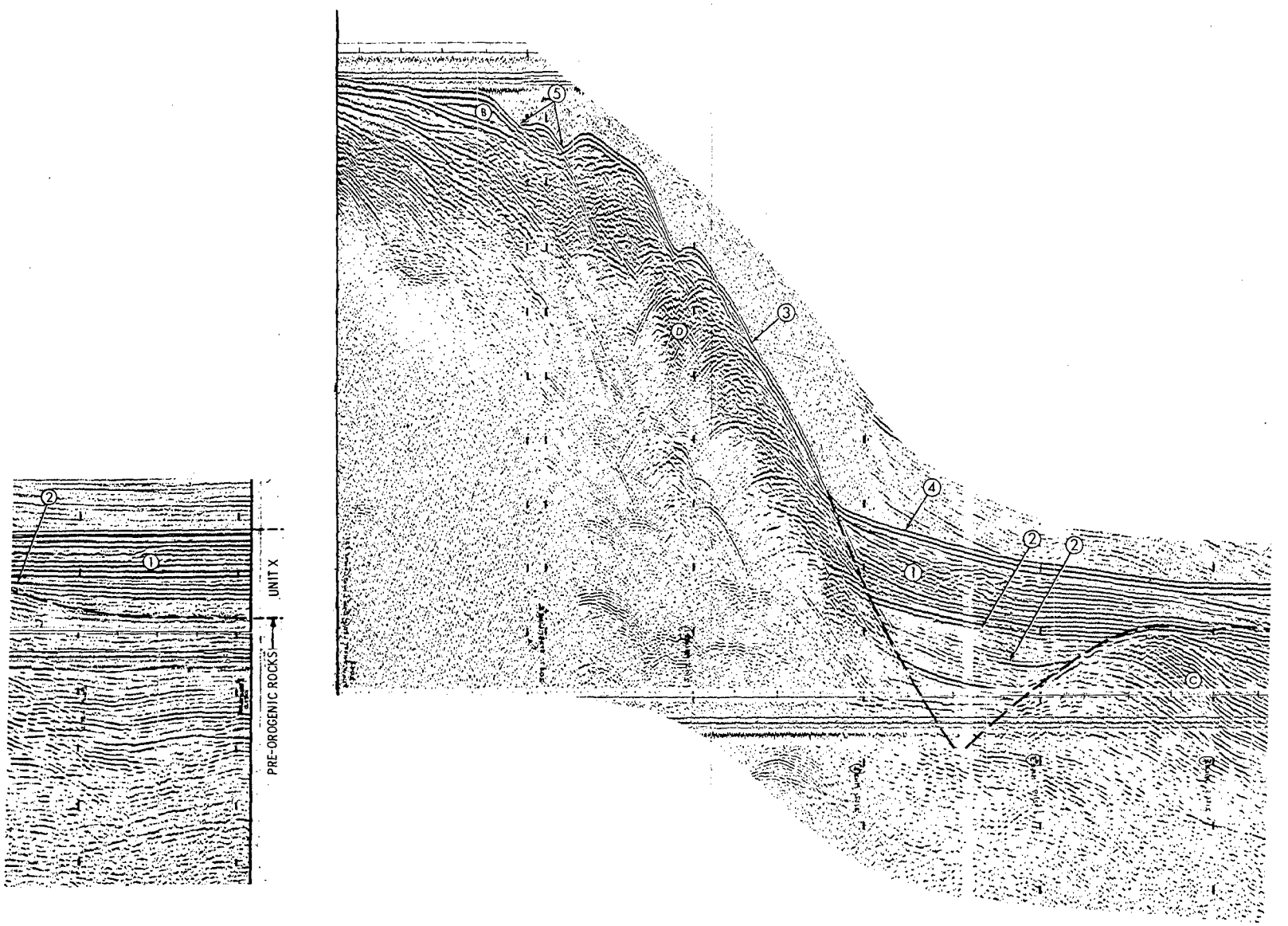

ce Survey Profiles. Dashed line is approximate boundary between Unit X (1) and pre-orogenic rocks.
1, Showing Unit B, Unit C, Unit D, Seafloor at Basin (2), and Seafloor at Escarpment (3).
2, Showing Units B, C, and D, Discontinuities in Unit X (2), the Seafloor of the Escarp-
·), Plus the Slope of the Unit X Surface (Seafloor) Next to the Escarpment (4). Also
is a fan or apron, possibly associated with fault rejuvenation, as well as gully-fault zones
esumably act as channels for submarine flows and slides of Unit X sediments (5).

2

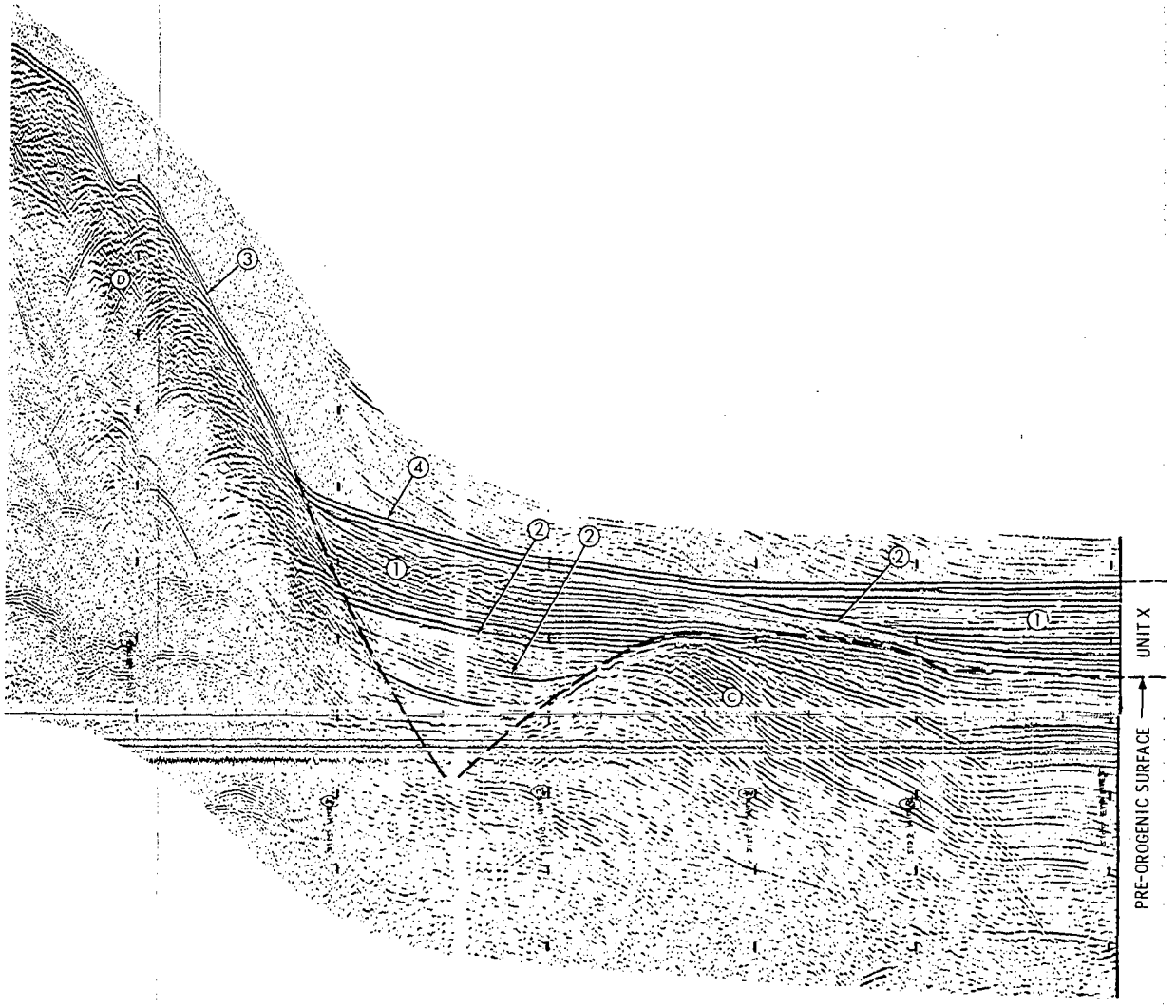

(b)

and pre-orogenic rocks.
rpment (3).
e Escarp-
. Also
ault zones
5).

3

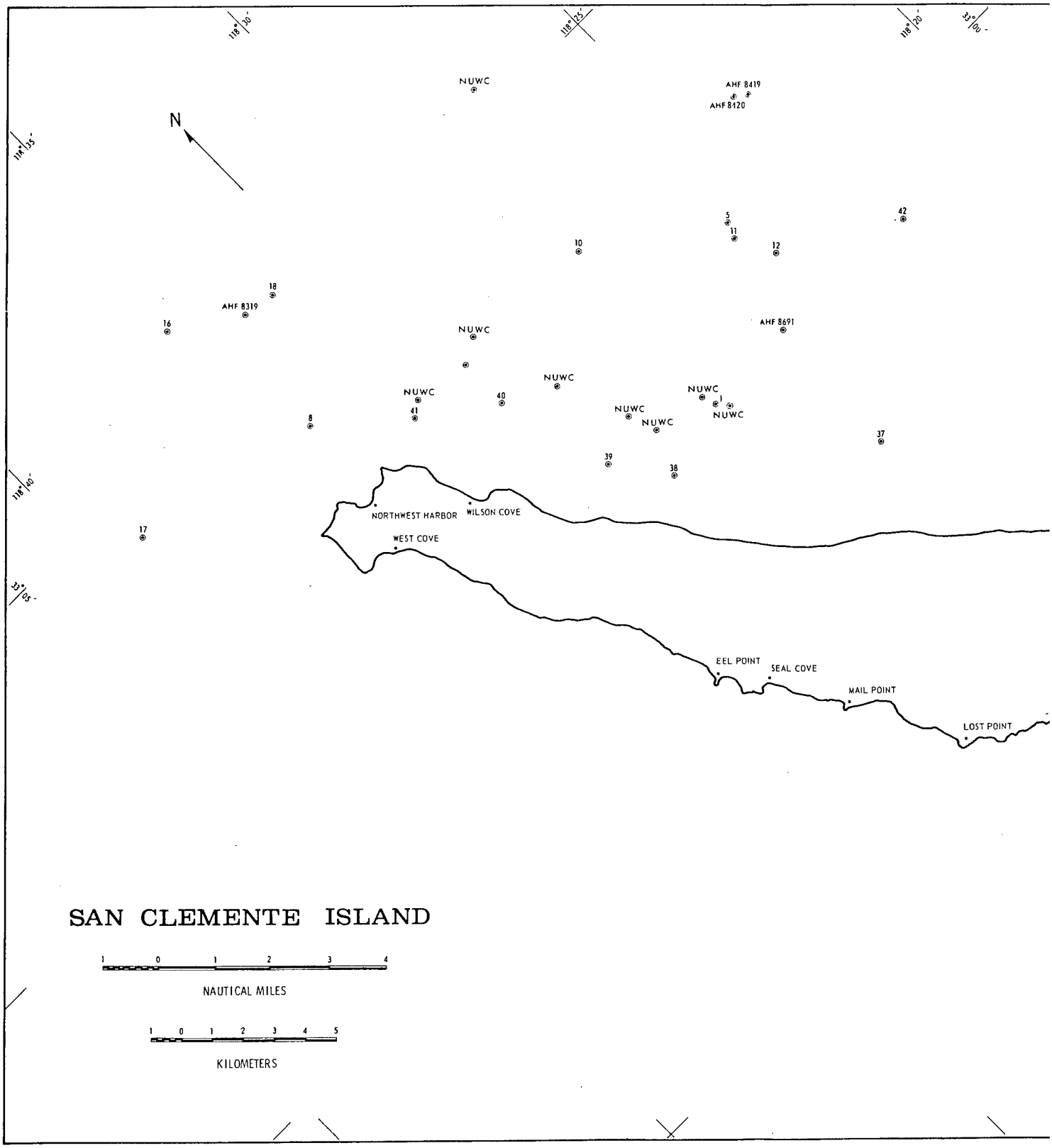

FIG. 44. Core Location Map.

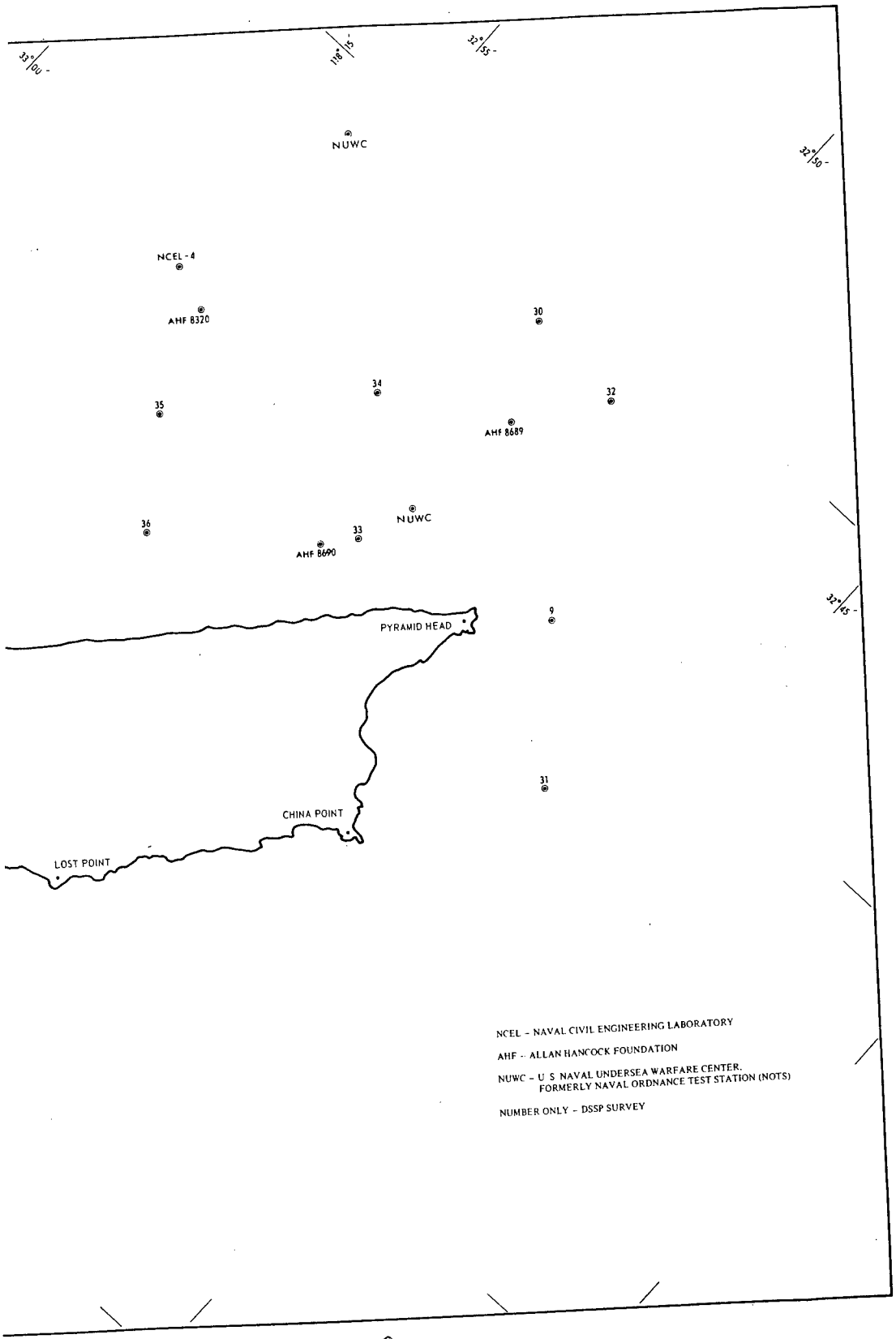
33°/00'
118°/15'
32°/55'
32°/50'
32°/45'
NUWC
NCEL - 4
AHF 8320
30
34
35
32
AHF 8689
NUWC
36
33
AHF 8690
9
PYRAMID HEAD
31
CHINA POINT
LOST POINT
NCEL - NAVAL CIVIL ENGINEERING LABORATORY
AHF - ALLAN HANCOCK FOUNDATION
NUWC - U S NAVAL UNDERSEA WARFARE CENTER.
FORMERLY NAVAL ORDNANCE TEST STATION (NOTS)
NUMBER ONLY - DSSP SURVEY

2

Map.

Disproportional sediment-layer thicknesses adjacent to the escarpment suggest fan or apron deposits that result from recurrent faulting along the island block followed by sand or turbidity-current flows.

SEDIMENT TRANSPORT AND DEPOSITIONAL DISTRIBUTION

Some conclusions as to the probable evolution of post-orogenic deposition can be drawn from bathymetry and from an examination of the surface distribution of Unit X. The following sediment transport and depositional distribution is proposed to satisfy the structure and the bathymetric conditions inferred by the seismic-reflection profile data.

The northeasterly structural and bathymetric trend across the island and Emery Seaknoll is apparent in Fig. 45 by the general northwest-to-southeast change of transport direction between the Emery Seaknoll and the island. A greater volume of post-orogenic sediments is present off the northeastern two-thirds of the island (Fig. 15). The elevation in the area of the intersection of Profiles I, J, and K (Fig. 46), and that of most of the profiles to the southeast, is shown to be considerably higher than along Profiles B, C, D, and E. Much of the sediment derived from the slopes off the southeastern (Pyramid Head) end of the island block has been carried to the southeast, as indicated by the southeastern plunge of Profiles G, H, and L. A later structural cutoff of transport to the south is suggested by the elevation difference between the northern ends of Profiles H and L and the intersection of Profiles I, J, and K.

A change of sediment transport direction from northwest to north-northeast is noted along the main San Clemente fault zone at the intersection of Seismic Profile 2 and Elevation Profile B (Fig. 3 and 45). For structural reasons, much of the present sediment transport in this area is to the northeast of the basin area off Wilson Cove, where it terminates in the Santa Catalina Basin.

At present, it is unlikely that any sediment from the island block is carried to the Santa Catalina Basin through the area between the Emery Seaknoll and the Southern Plateau. Some sediment transport may be directed off the west side of the Southern Plateau and southward into the Rift Valley, but elevation differences suggest that major sediment transport from the island source must be to the structural depression between the Emery Seaknoll and the Southern Plateau.

The lack of sediment in the trough southeast of Pyramid Head is attributed either to fault control that cut off the main supply from the island, or to very recent faulting that has not yet led to the development of an appreciable volume of sediment. The latter explanation appears more likely, since some smaller depressed areas containing fill are now cut off (relatively) and elevated above surrounding low areas.

Slope conditions and deposit shapes indicate that most of Unit X along the west side of the island block is a series of fan-apron deposits (Fig. 14b, 15, 45, and 47a-b) that are, for the most part, structurally controlled. These deposits appear to terminate mainly at the principal fault-zone trough paralleling the west side of the island block.

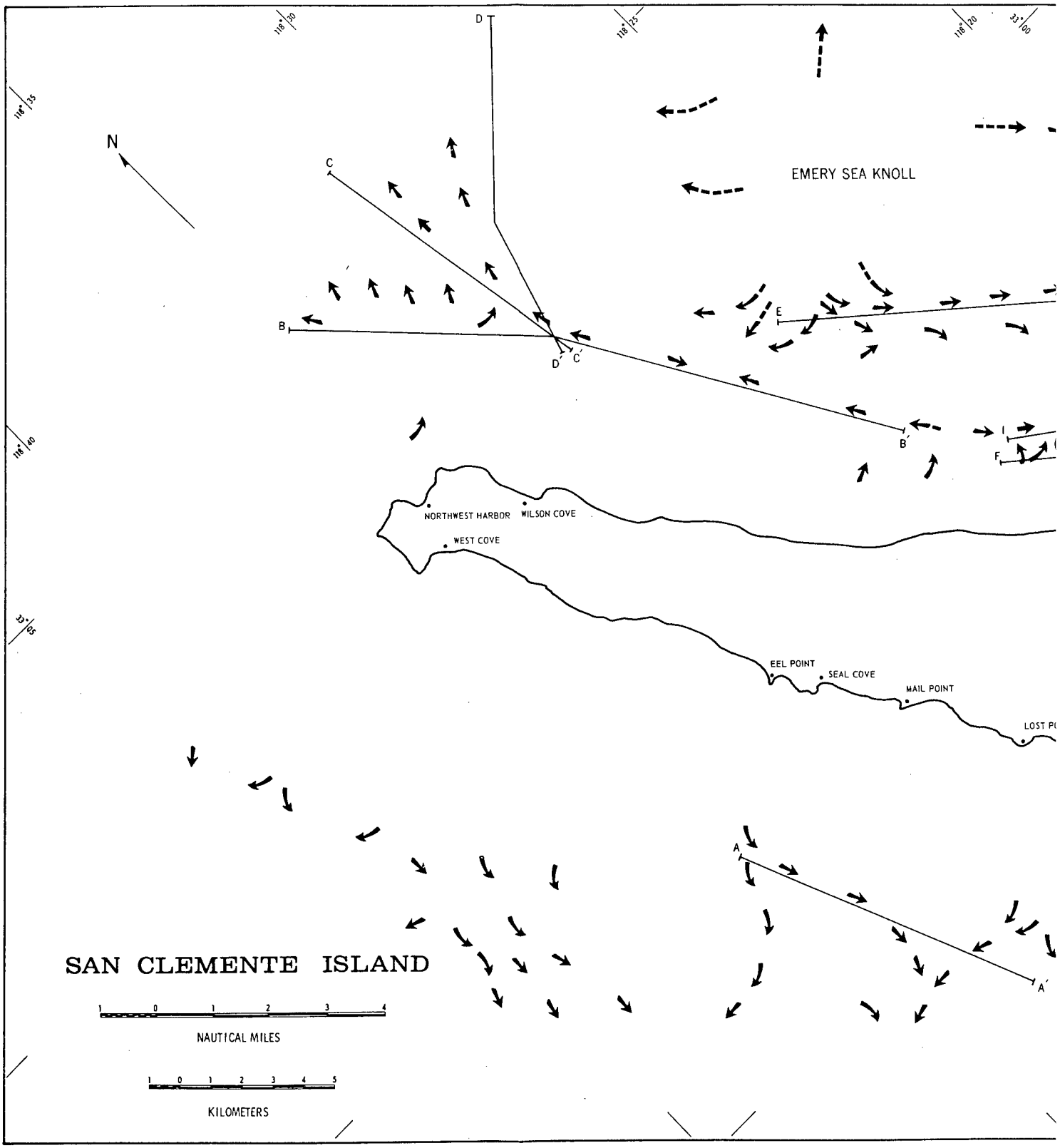

FIG. 45. Postulated Trajectories of Sediment Flow and Deposition (Arrows) Based on Bathymetric Elevation
L-L lie principally along trough zones. Dashed arrows show downslope trend off bathymetric highs. Sedimer
in some profiles, particularly on the steeper slopes and over the northwestern part of the San Clemente fault z

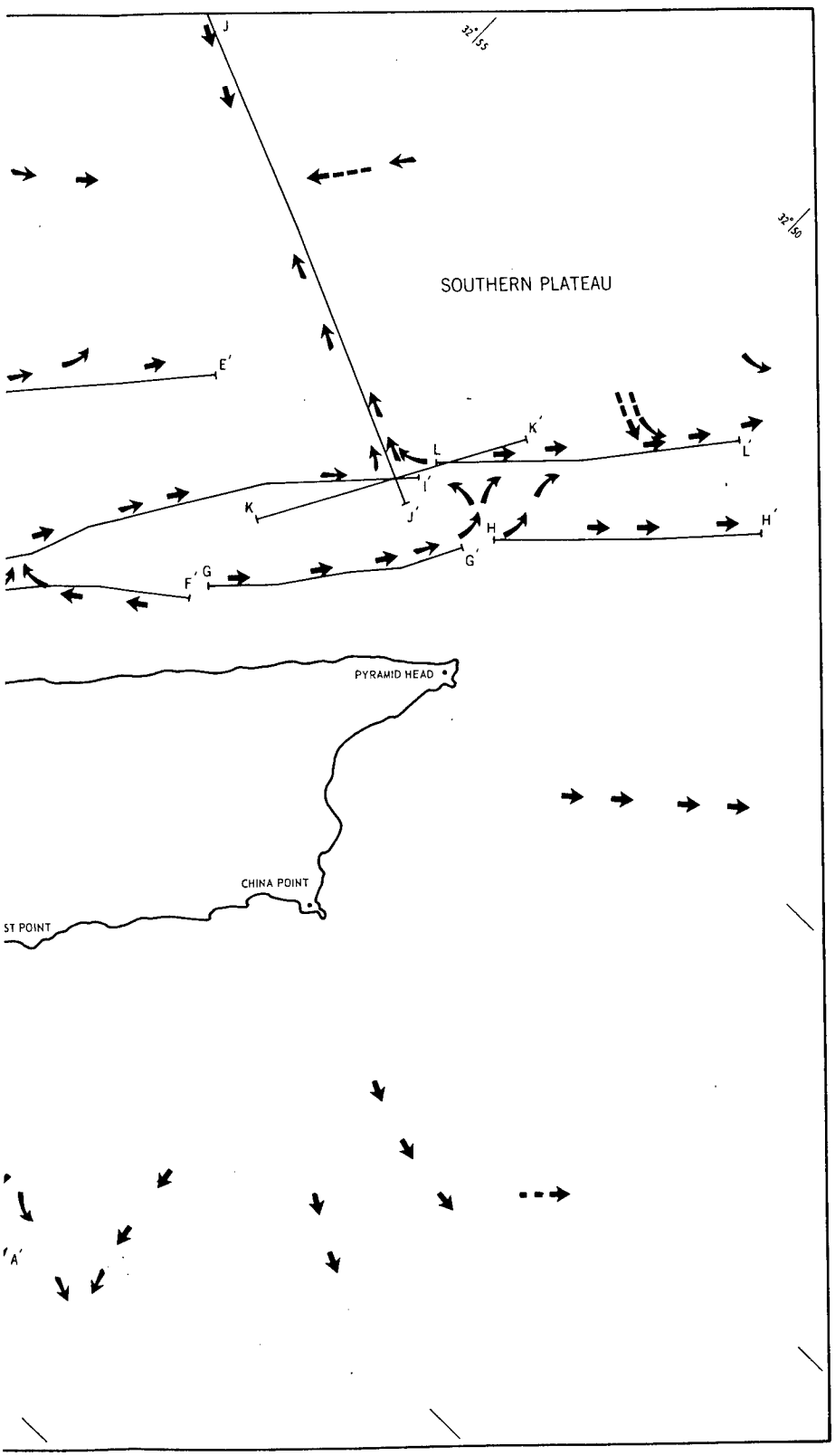

tion Differences. Cross-section lines A-A through iment overflow from relatively low areas is noted ult zone.

2

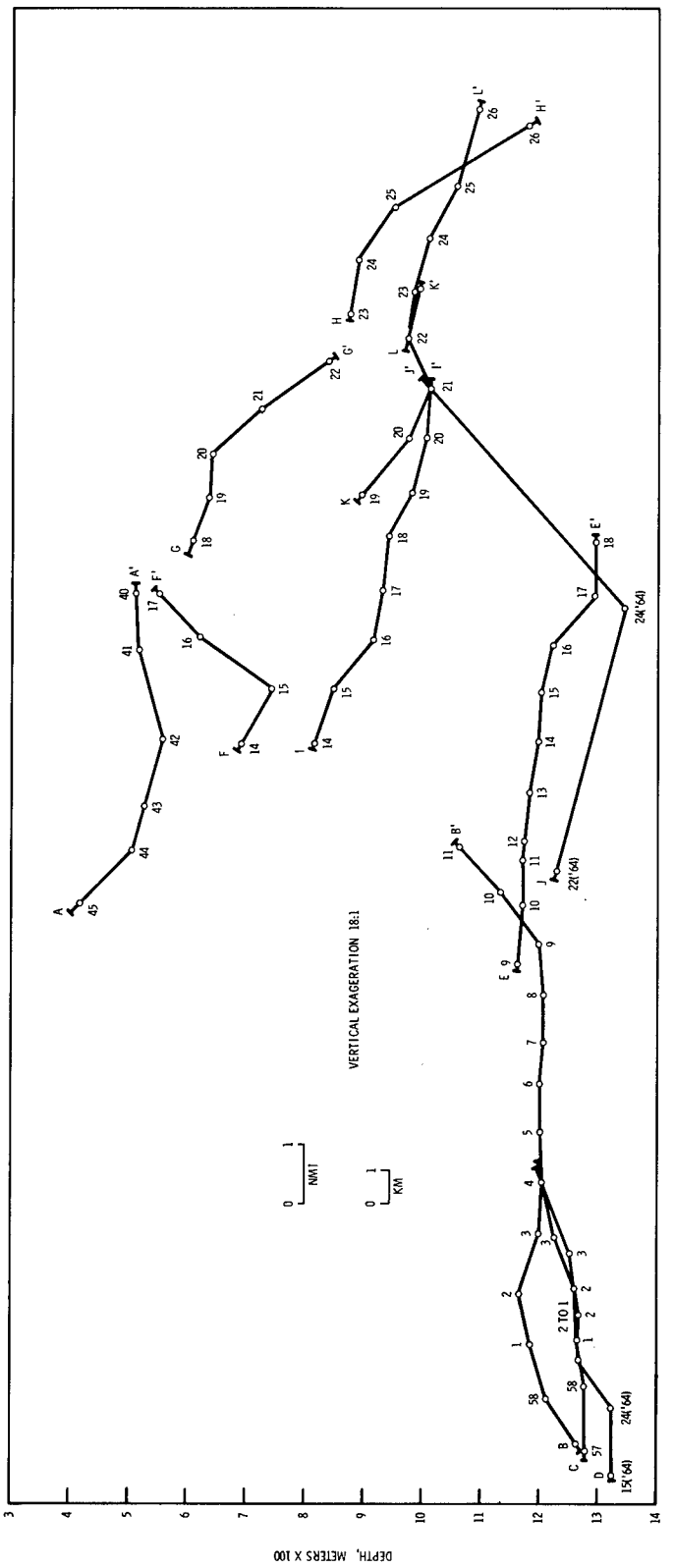

FIG. 46. Bathymetric Elevation Differences Along Cross-Section Lines Shown in Fig. 45. The number '64 refers to profiles made on the 1964 cruise (Fig. 4). All other numbers refer to reconnaissance survey profiles.

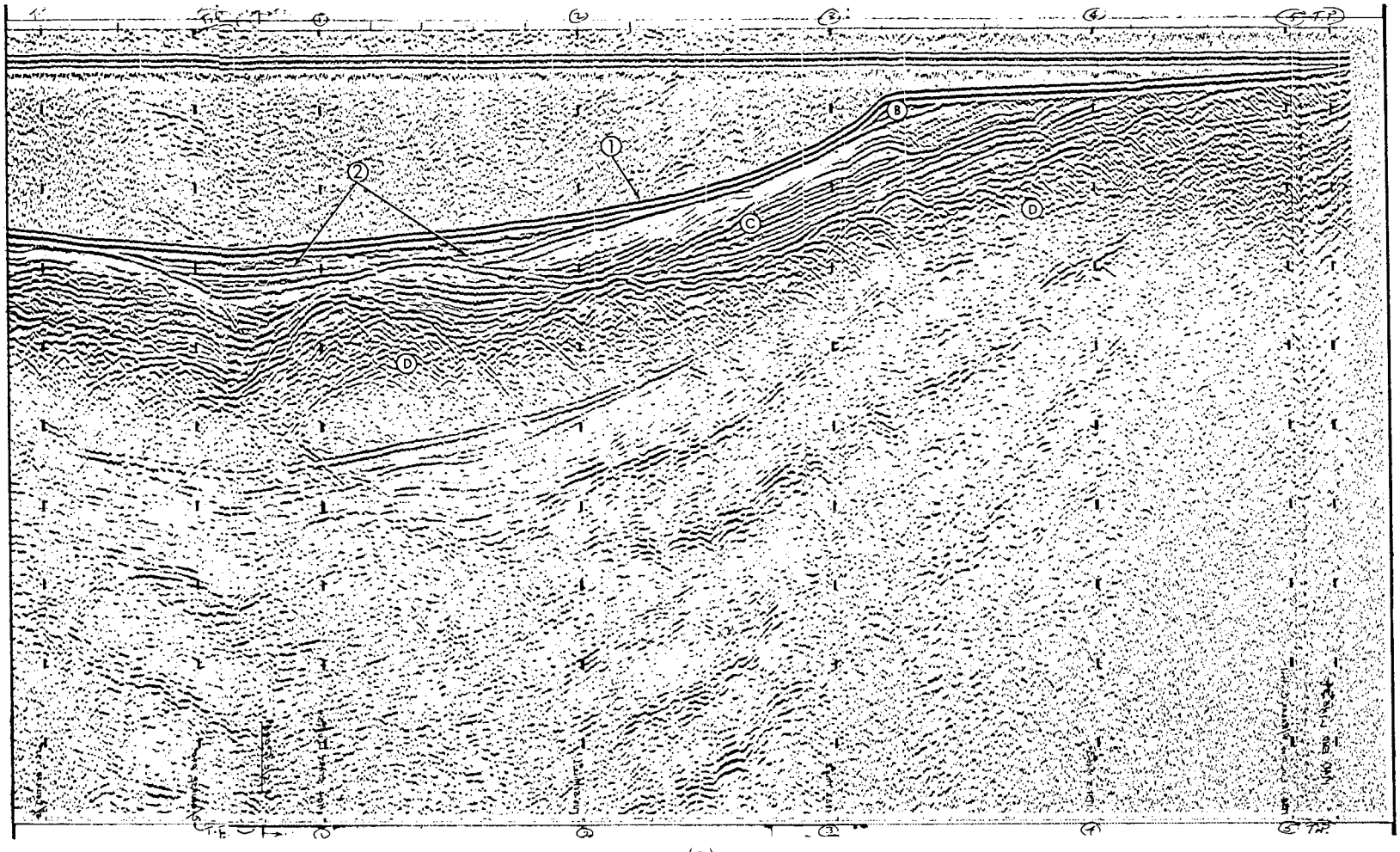

(a)

FIG. 47a. Reconnaissance Survey Profile 34 Showing Seafloor (1), Unconformity Between Unit X and Unit C, in Which Unit X Is Typically a Fan Deposit in the Area of Study Along This Side of the Island (2); Unit B; Unit C; and Unit D.

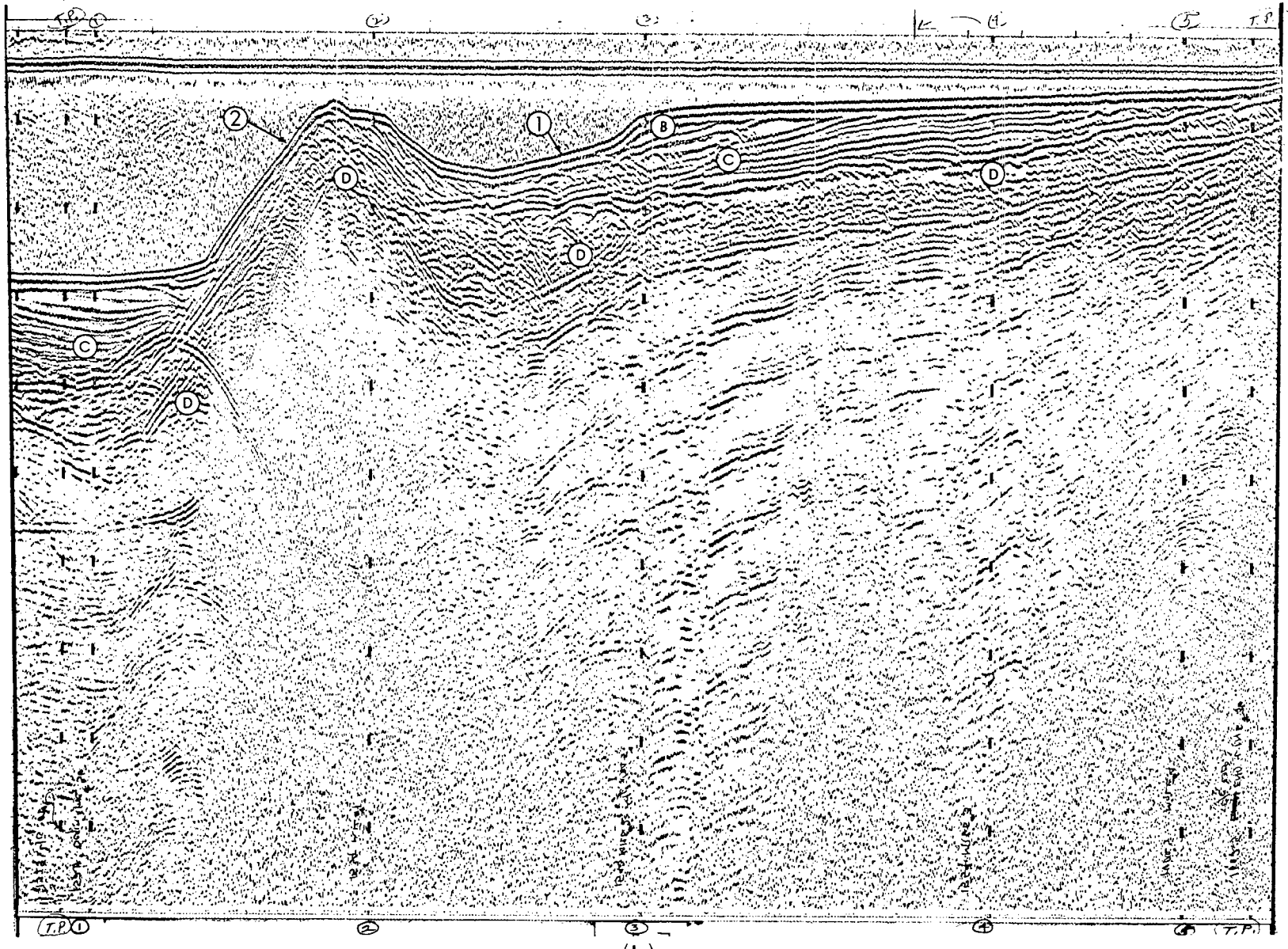

FIG. 47b. Reconnaissance Survey Profile 36 Showing Seafloor (1), Units B, C, and D, as Well as the Elongated Volcanic High With a Probable Fault Offset at the Crest (2).

The structural ridge about 8 kilometers off Mail Point is assumed to have diverted earlier canyon-derived sediment southwesterly to the San Nicolas Basin. Subsequent fill to the north of this high, and possibly structural change, has allowed a more recent southerly transport from the canyon (Fig. 15 and 20; Fig. 45, Cross-Section A-A′).

SEDIMENT ANALYSES

An aerial distribution of the phi-mean size of surface sediments taken from bottom samples and the tops of cores (Fig. 44 and 48; also Appendix C) permits a supplementary analysis of sediment transport trends and variations.

The general distribution of the finer sediments (6 to 8 phi) to the north and south of the Emery Seaknoll-San Clemente Island northeast-trending bathymetric and structural high is shown in Fig. 48. The finer sediments occupy much of the lower areas. A marked coarser-sediment "saddle" separates the major 6-to-8 phi-mean areas. Toward the basin and the finer-sediment zones, fingerlike projections off the escarpment are noted. These projections are believed to represent the general direction of sediment transport. This belief is based on the interpretation of turbidity-current and sand-flow origin for much of these sediment deposits and the diameter of detrital sediments normally decreasing with increased depth and distance from shore or source (e.g., Ref. 46 and 47).

The very fine (greater than 8 phi) sediment zone on the escarpment off the northeast side of the island probably resulted from a predominance of hemipelagic deposition. Seismic profiles in this area indicate a relatively uniform slope marked by only a few shallow depressions. The slope is therefore protected from disturbances along main sediment-transport channels. It is also conceivable that this part of the slope has not reached the point of instability required for slope failure (Ref. 48).

The postulated sediment transport along the direction of Elevation Profiles I and K to the intersection of Profiles I, J, and K is suggested by the southeastward projection of the 6-to-8 phi-mean zone in this area. The trend of the fine sediment northeastward along Profile J to the depression between the Emery Seaknoll and the Southern Plateau is interrupted in one area by coarser sediments projecting off the Southern Plateau. Recent sediment flows off the Southern Plateau are postulated to account for this interruption.

The fine (6 to 8 phi) sediments deposited at the western end of the Southern Plateau are believed to be primarily hemipelagic in origin. A trend toward coarser sediment off the west and north sides of this plateau presumably results from the mixing of pelagic and flow-type sediments that culminate in the trough represented by Profile L. A similar trend is noted off the sides of the Emery Seaknoll.

Although the isopleths off the southern end of the island are based on few data, the presence of finer sediments in the area shown suggests relatively inactive sediment transport (stable slopes). Hemipelagic deposition, more gentle bathymetric slopes, and possibly a change in water-current velocity by shoreward refraction around this end of the island are the controlling factors for deposition in this area. The high percentage of clay- and silt-sized material in the samples of this area support this argument.

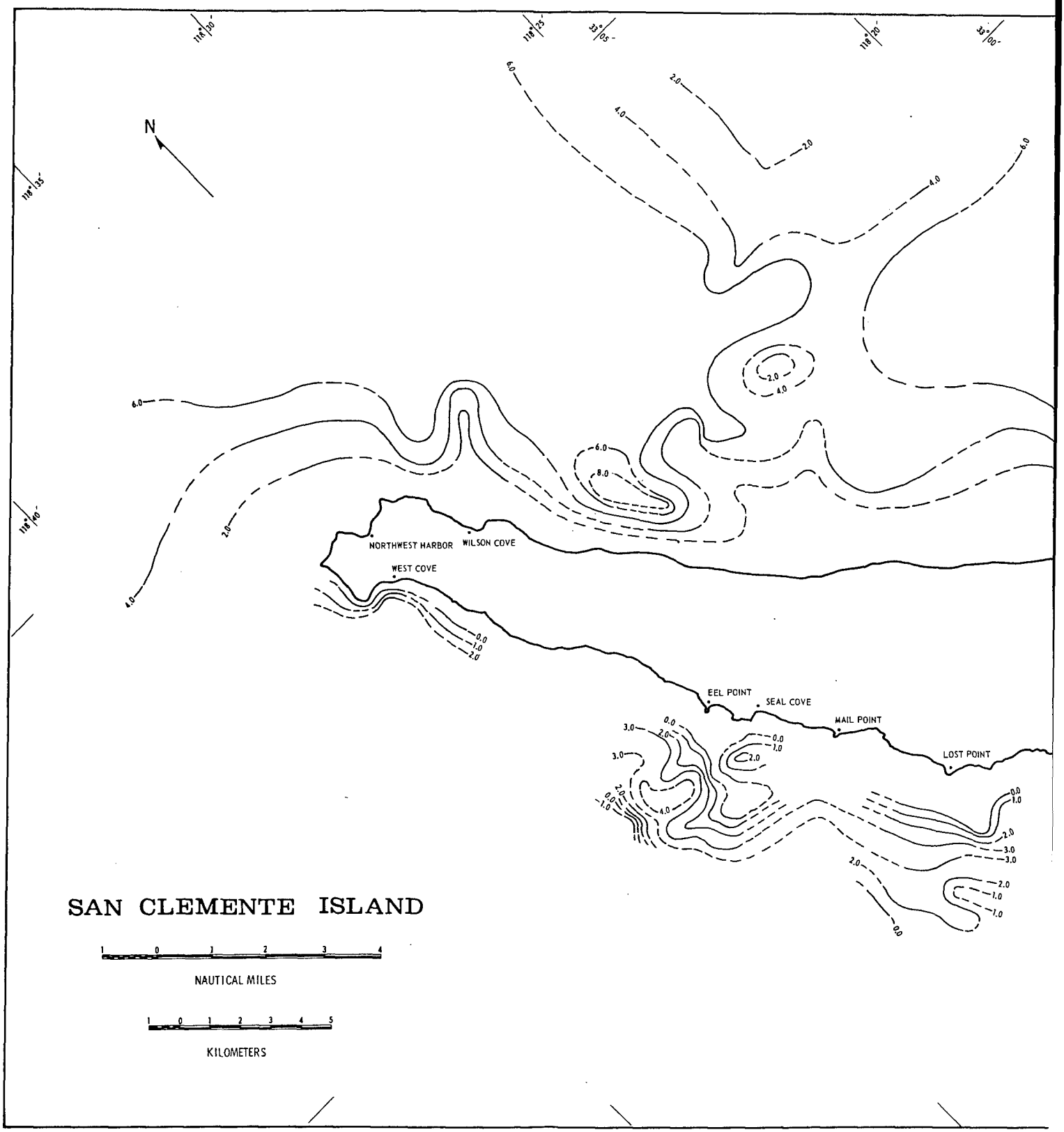

FIG. 48. Phi-Mean Distribution Map Based on Uppermost Section of Cores (East and South Sides of Islan Snapper Samples (West Side of Island) From Detailed Survey Leading to This Report.

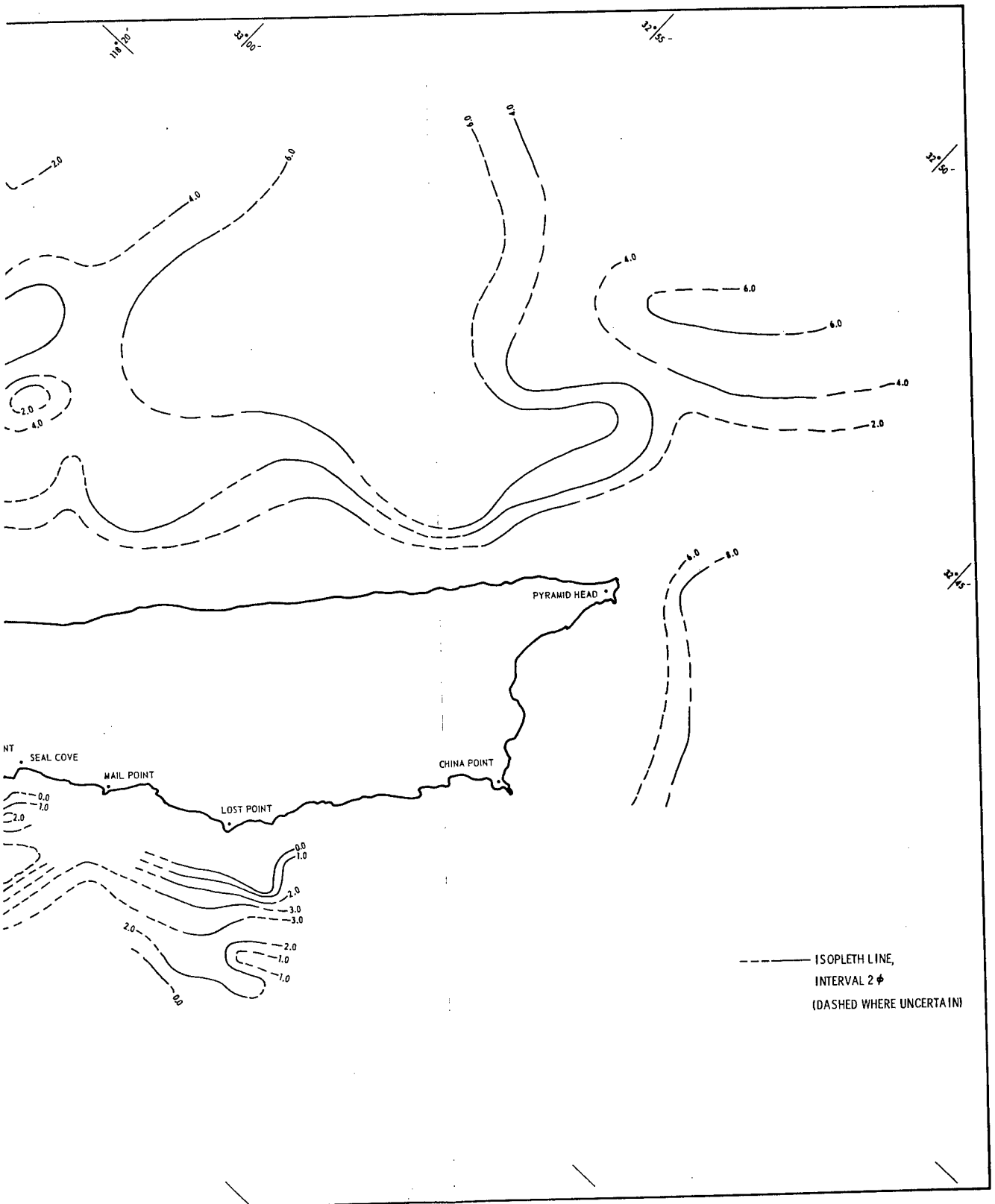

ɔst Section of Cores (East and South Sides of Island) From Earlier Surveys and Bottom
ɹrvey Leading to This Report.

2

Analysis of the detailed-survey bottom samples (see Part 1, Fig. 5) indicates the following:

1. At present, Eel Ridge Canyon is a relatively inactive route of transported sediment. The isopleths of this area suggest that southeasterly flowing and longshore water currents are transporting the coarser sediment toward Eel Ridge, while the finer sediments are carried out over the canyon to settle in its depths (as shown by the 3-to-5 phi-mean isopleths).

2. The configuration of the isopleths immediately to the south of Eel Ridge Canyon conforms to a generally seaward sediment transport off the sides of the bathymetric ridge in this area, as well as to the major gully incising the wave-cut terrace off Seal Cove.

3. Relict, residual, or both types of sediment (Ref. 46) may be present from the middle to the outer part of the wave-cut terrace. Figure 48 shows a zone of relatively coarse sediments that interrupts the general seaward trend of progressively finer sediments across the terrace; however, a heavy concentration of biogenous material possibly accounts for this phenomenon. Only a few terrace samples are available for study. Nevertheless, analyses of the samples reveal a grain-size distribution that suggests the presence of residual or relict-type sediment. Figure 49a-c shows a tendency for an increase in terrigenous material at the outer part of the terrace. This is countered by an increase in biogenous content (mostly Foraminifera) and a corresponding increase of grain size toward the center of the terrace (Fig. 49b, 50). However, the increase in phi-mean grain size toward the outer part is associated with a trend toward a pure sand-size material with less biogenous content. The tendency for a higher silt content in the middle of the terrace corresponds to an increase of terrigenous silt. The increase of sand-size material at Q10 results partially from the presence of very scattered and well-rounded, frosted quartz grains (eolian?). The presence of this type of sediment only at the middle of the terrace suggests that it is probably residual, particularly since there has been a major truncation of Miocene sediments with some outcrops present across part of the terrace.

4. The coarser sediments noted immediately off the terrace probably result from erosion by sediment transport along gullies cut normal to the outer part of the terrace.

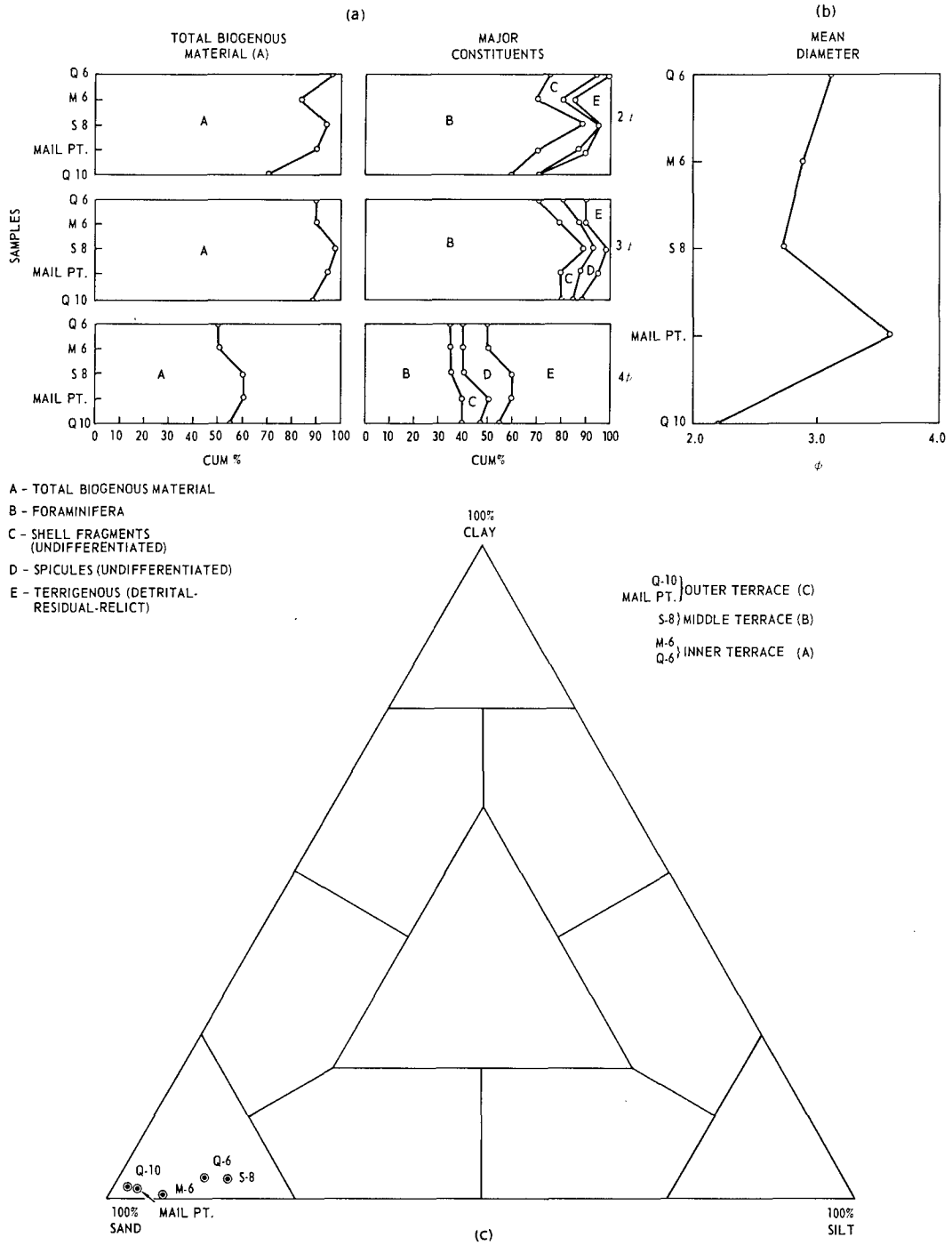

FIG. 49. Trends of Certain Sediment Parameters From the Wave-Cut Terrace Samples off Mail and Lost Points. Trends may be noted for (a), (b), and (c) in a general seaward direction.

(a) Cumulative Percent of Sample Clastic Content.

(b) Phi-Mean Diameter Graph.

(c) Ternary Diagram of Sediment Types.

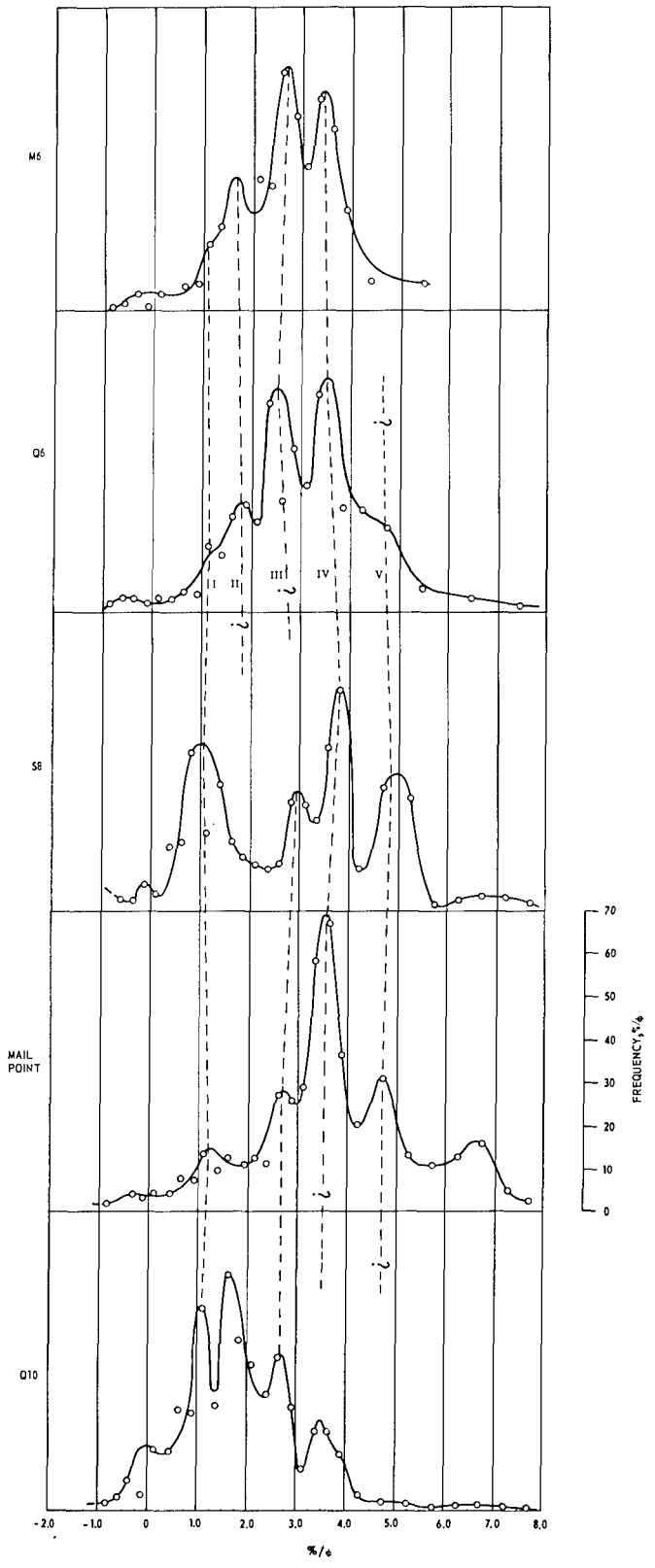

FIG. 50. Polymodal Distribution Curves of the Wave-Cut Terrace Samples off Mail and Lost Points (Ref. 16). The modes are identified by Roman numerals. The curves have not been adjusted to be symmetrical and are approximately normal.

CONCLUSIONS

Certain geologic features and the structure of the San Clemente Island block have been resolved with continuous acoustic reflection profiles augmented by seafloor samples. The more important of these relationships are summarized below.

1. Bathymetry, as interpreted from the seismic profiles, differs from that shown by charts such as U. S. Coast and Geodetic Survey 5111 because of a better definition of structural trends shown by elongated highs and depressions that often have linear outlines along the seafloor.

2. A sequence of five sediment and rock units has been identified, ranging from Middle Miocene to Recent. These are referred to as Units A, B, C, D, and X. Unit A is a sediment cover of Recent and possibly also Late Pleistocene age. Unit B represents a post-Miocene, probably Pliocene-Pleistocene, accumulation of debris derived mainly from island canyons. Microfossils from submarine limestone outcrops indicate a Middle Miocene age for Unit C. Unit D is the offshore equivalent of the Miocene volcanic rocks exposed on the island. The fifth unit (X) is, except for fan and apron deposits off the west side of the island, considered a post-orogenic deposit off the island block and is primarily an equivalent to Units A and B.

3. In most areas, the offshore fault-strike pattern is related to that on the island. The main exception is the San Clemente fault zone, delineated along the east side of the island only by the San Clemente Escarpment.

4. The structural pattern of the island block appears to conform to the wrench-fault system hypothesized by Moody and Hill (Ref. 29) but modified by a general north-south tensile fracturing. The latter feature may be related to (a) pure lateral extension; (b) upward bowing of the island block; (c) a shear-couple effect; or (d) a combination of these properties. The combination is thought to be the inclusive cause for all those faults believed to be of a tensional nature. There are alternate possibilities, for which a few faults may be explained by either shear or tension.

5. The San Clemente fault zone shows properties of lateral (wrench) faulting, and is considered to be the primary right-lateral wrench fault for the studied area, based on the model for wrench faulting proposed in this study.

6. Anomalous trends in isopach maps of the sedimentary units and structure contour maps on some units tend to substantiate the offshore pattern of faulting. This faulting, along with the effects of erosion, is reponsible for a major unconformity between Units B and C. Some evidence suggests a hiatus between Units C and D.

7. In general, faulting appears to have affected both Units C and D. Two faults are shown to have affected Unit B, but other evidence indicates that incompetency within Unit B may be responsible for the lack of fault evidence on the profiles.

8. The San Clemente Rift Valley to the southeast of the island is postulated to have resulted from "cross-strike separation" related to right-lateral movement along the gradual curvature of the San Clemente fault in the general region of the Rift Valley.

9. A canyon off Eel Point is believed to be caused mainly by pivotal faulting that is not evident on the island. The canyon represents a transition zone for different structural trends north and south of the canyon. Visual surveys and sediment data suggest that this canyon is not presently involved with sediment transport by turbidity currents. (See Part 1.)

10. A major offshore terrace that surrounds the island, and is prominent along the west side, is postulated to have been cut during Late Pleistocene-Holocene time as a consequence of the glacio-eustatic lowering of the sea level. This terrace, about 120 meters below sea level along the west side and about 90 meters below sea level along the east side, shows a tilt of the island block by Recent tectonism. Local faulting has affected the level of the terrace, along with a combination of northeasterly upward tilting and northwestward downward tilting. The net tilt to the west is probably associated with upward bowing of the island block in response to lateral compression under a shear couple encompassing the island block.

11. The strong trend of inferred tensional faulting suggests that some rotational type of stress-strain mechanism, such as a shear couple, is responsible for this tensional nature of the fault pattern.

12. The lack of strong primary folding of the island block implies a lack of the large component of compression normal to a primary shear fracture.

13. A steep magnetic gradient off the San Clemente Escarpment is probably the consequence of a combined effect of (a) the margin of the mass of volcanic flows; (b) a deep basic mass related to a large positive anomaly off West Cove; and (c) major faulting.

14. Statistical analyses of earthquake epicenters in the northern Continental Borderland show that (a) seismic activity is relatively low in the general region of study, increasing toward the mainland; (b) there is a tendency for a period of momentary quiescence in the studied area; and (c) there is evidence along part of the San Clemente fault zone for the association of recent fault activity with the epicenters of this area. The last analysis suggests that the area from the Rift Valley to the Emery Seaknoll is presently adjusting to local stress inequalities related to movement along the San Clemente fault.

15. A major lithostructural division, based upon that proposed by Moore (Ref. 11), differentiates pre-orogenic (Units C and D) from post-orogenic (Unit X) lithologies. The post-orogenic sediments are believed to have followed certain major transportation channels by means of turbidity currents, sand flows, and slides, and to have been deposited in basin lows

developed by faulting and folding. Fans and aprons of post-orogenic sediments have developed in some slope areas, particularly off the west side of the island.

16. Aerial distribution of the phi-mean size of seafloor sediments suggests certain directions of sediment transport from the island block and other bathymetric highs of the study area. These directions of transport and subsequent sediment deposition are essentially controlled by the structural nature of the island block and adjacent depressed areas.

17. Relict, residual, or both types of sediment may be present at the middle and outer part of the wave-cut terrace along the west side of the island.

RECOMMENDATIONS

Several recommendations have been made in Part 1 of this report relative to the feasibility of tunneling in the detailed survey area. The following are based on the reconnaissance survey and the findings of Ref. 4 and 49.

1. It is strongly recommended that no attempt be made to use the eastern side of the island for tunneling contrary to the ideal geomorphic nature of the escarpment. Extensive faulting, slumps, and slides are known to exist or to have occurred in this area. These features, when considered with other peculiarities of the island volcanic rocks, such as brecciation zones (including fault-zone gouges); a high degree of randomly oriented jointing; near-vertical jointing in shear zones, possibly up to several hundred feet in width; and flow parting in some of the flows, tend to conflict with any desirable degree of engineering safety.

2. As stated for the detailed survey in Part 1, it is considered that faulting can hardly be avoided in any attempt to tunnel in the studied area. The area between Mail and China Points appears to be the most favorable for tunneling in a generally seaward direction (southwesterly) to parallel the major faults.

3. The area off the southern end of the island affords a good opportunity to follow a thick sequence of Unit C. However, extensive faulting and folding of these sedimentary rocks exist, and may make this area less desirable for straight-line tunneling. As a probable consequence, a highly variable salt-water inflow could occur during tunneling.

4. The major volcanic rock outcrops seaward of the wave-cut terrace along the west side of the island are best outlined in Fig. 35b and 47b. If the tunneling is to follow massive structures of dense volcanic rock, it is recommended that a detailed survey of the four major bathymetric volcanic-rock outcrops be made to establish geomechanic features and the degree of surficial sediment cover.

5. It is recommended that Unit B be avoided in any tunneling attempt.

6. Finally, highly detailed offshore seismic profiling, visual studies, and test-core holes (Ref. 50) should be made for any selected tunnel-site area to ascertain the rock structure and physical properties that will be encountered in tunneling.

Appendix A

DEPTH AND THICKNESS DATA FOR THE RECONNAISSANCE SURVEY AREA

Station No.	Water depth, m	Corrected thickness of Unit B, m	Corrected thickness of Unit X, m	Corrected thickness of Unit C, m	Depth to Unit D, m
			LINE 27A		
CROSSING	83.1	.0	.0	.0	83.1
BEGIN LINE 27A	84.5	.0	.0	91.3	175.8
1/10	81.2	.0	.0	136.9	218.2
2/10	78.3	.0	.0	182.6	260.9
3/10	75.4	.0	.0	187.2	262.5
4/10	66.6	.0	.0	173.5	240.1
5/10	65.2	.0	.0	.0	65.2
6/10	65.2	.0	.0	111.8	177.0
7/10	68.1	.0	.0	75.3	143.4
8/10	71.0	.0	.0	98.1	169.1
9/10	71.0	.0	.0	143.8	214.8
END LINE 27A	72.5	.0	.0	219.1	291.6
			LINE 27		
END LINE 27	84.5	.0	.0	.0	84.5
1/3	93.3	.0	.0	41.1	134.4
2/3	100.6	.0	.0	157.5	258.1
MILE 3	105.3	.0	.0	273.9	379.2
1/5	108.2	.0	.0	303.6	411.8
2/5	109.7	.0	.0	408.5	518.2
3/5	112.6	38.9	.0	470.2	621.7
4/5	200.2	20.5	.0	447.3	668.1
MILE 2	262.4	.0	.0	442.8	705.2
1/5	310.1	.0	.0	429.1	739.2
2/5	333.8	.0	.0	447.3	781.2
3/5	360.5	.0	.0	438.2	798.7
4/5	381.4	.0	.0	447.3	838.7

MILE 1	393.4	.0	.0	451.9	845.3
1/5	402.2	.0	.0	442.8	845.0
2/5	416.8	.0	.0	447.3	864.1
3/5	446.4	.0	.0	438.2	884.6
4/5	476.7	.0	.0	433.6	910.3
BEGIN LINE 27	509.0	.0	.0	392.6	901.6

LINE 28

START LINE 28	65.2	.0	.0	95.9	161.0
1/5	75.4	.0	.0	159.8	235.2
2/5	83.1	.0	.0	294.4	377.5
3/5	84.5	.0	.0	397.1	481.7
4/5	87.5	.0	.0	447.3	534.8
MILE 1	90.4	.0	.0	502.1	592.5
1/5	96.2	.0	.0	547.8	644.0
2/5	102.1	.0	.0	543.2	645.3
3/5	105.3	.0	.0	547.8	653.1
4/5	109.7	55.3	.0	547.8	712.7
MILE 2	173.5	32.8	.0	497.6	703.8
1/5	220.9	.0	.0	547.8	768.7
2/5	262.4	.0	.0	529.5	791.9
3/5	295.1	.0	.0	529.5	824.6
4/5	339.7	.0	.0	515.8	855.5
MILE 3	384.3	.0	.0	506.7	891.0
1/5	416.8	.0	.0	502.1	918.9
2/5	446.4	.0	.0	511.2	957.6
3/5	467.6	.0	.0	524.9	992.5
4/5	494.0	.0	.0	524.9	1019.0
MILE 4	520.7	.0	.0	524.9	1045.6
END LINE 28	550.6	.0	.0	511.2	1061.8

LINE 29

END LINE 29	90.4	.0	.0	171.2	261.6
1/5	93.3	.0	.0	178.0	271.3
2/5	94.8	.0	.0	301.3	396.0
3/5	96.2	.0	.0	356.0	452.3
4/5	97.7	.0	.0	502.1	599.8
MILE 3	100.6	.0	.0	504.4	605.0
1/5	102.1	28.7	.0	515.8	646.6
2/5	114.1	57.4	.0	524.9	696.4
3/5	182.3	36.9	.0	511.2	730.4
4/5	236.0	.0	.0	534.1	770.0

MILE 2	286.3	.0	.0	524.9	811.2
1/5	330.9	.0	.0	497.6	828.5
2/5	369.7	.0	.0	502.1	871.8
3/5	405.1	.0	.0	493.0	898.1
4/5	428.8	.0	.0	474.7	903.6
MILE 1	458.8	.0	.0	470.2	928.9
1/5	494.0	.0	.0	474.7	968.8
2/5	526.6	.0	.0	488.4	1015.0
3/5	553.5	.0	.0	465.6	1019.1
4/5	583.1	.0	.0	461.0	1044.1
BEGIN LINE 29	606.8	.0	.0	447.3	1054.2
29 TO 28 (0)	613.0	.0	.0	442.8	1055.8
1/4	603.9	.0	.0	451.9	1055.8
2/4	595.1	.0	.0	456.5	1051.6
3/4	595.1	.0	.0	470.2	1065.3
T.P. TO 28	595.1	.0	.0	506.7	1101.8

LINE 29A

BEGIN LINE 29A	79.8	.0	.0	89.0	168.8
1/5	75.4	.0	.0	68.5	143.9
2/5	69.5	.0	.0	45.6	115.2
3/5	61.8	.0	.0	.0	61.8
4/5	55.9	.0	.0	.0	55.9
END LINE 29A	54.5	.0	.0	.0	54.5

LINE 30

START LINE 30	63.7	.0	.0	.0	63.7
1/4	66.6	.0	.0	.0	66.6
2/4	72.5	.0	.0	.0	72.5
3/4	75.4	.0	.0	.0	75.4
MILE 1	83.1	.0	.0	25.1	108.2
1/5	88.9	.0	.0	102.7	191.6
2/5	91.8	.0	.0	198.6	290.4
3/5	93.3	.0	.0	273.9	367.2
4/5	94.8	.0	.0	312.7	407.5
MILE 2	97.7	14.3	.0	360.6	472.6
1/5	102.1	45.1	.0	388.0	535.1
2/5	105.3	57.4	.0	388.0	550.6
3/5	146.9	55.3	.0	358.3	560.5
4/5	206.3	4.1	.0	378.9	589.3

MILE 3	236.0	.0	.0	401.7	637.7
1/5	261.0	.0	.0	417.7	678.6
2/5	283.0	.0	.0	465.6	748.6
3/5	318.9	.0	.0	447.3	766.2
4/5	345.5	.0	.0	483.9	829.4
MILE 4	372.6	.0	.0	447.3	819.9
1/5	402.2	.0	.0	497.6	899.8
2/5	434.7	.0	.0	479.3	914.0
3/5	517.8	.0	.0	420.0	937.7
4/5	532.7	.0	.0	493.0	1025.7
END LINE 30	553.5	.0	.0	543.2	1096.7

LINE 31

END LINE 31	93.3	.0	.0	41.1	134.4
1/5	94.8	.0	.0	43.4	138.1
2/5	96.2	.0	.0	27.4	123.6
3/5	84.5	.0	.0	.0	84.5
4/5	99.2	.0	.0	168.9	268.1
MILE 4	99.2	.0	.0	146.1	245.2
1/5	99.2	.0	.0	45.6	144.8
2/5	96.2	.0	.0	45.6	141.9
3/5	78.3	.0	.0	.0	78.3
4/5	75.4	.0	.0	.0	75.4
MILE 3	78.3	.0	.0	.0	78.3
1/5	93.3	.0	.0	45.6	139.0
2/5	99.2	.0	.0	41.1	140.2
3/5	93.3	.0	.0	.0	93.3
4/5	111.1	57.4	.0	77.6	246.1
MILE 2	129.0	69.6	.0	182.6	381.3
1/5	197.3	6.1	.0	362.9	566.4
2/5	236.0	.0	.0	461.0	697.0
3/5	280.1	.0	.0	502.1	782.2
4/5	342.6	.0	.0	524.9	867.6
MILE 1	387.6	.0	.0	561.5	949.0
1/5	405.1	.0	.0	529.5	934.7
2/5	424.1	.0	.0	477.0	901.1
3/5	446.4	.0	.0	465.6	912.0
4/5	467.6	.0	.0	493.0	960.5
END LINE 31	476.7	.0	.0	511.2	987.9
31 TO 30 (0)	520.7	.0	.0	552.3	1073.0
1/3	538.6	.0	.0	534.1	1072.6
2/3	562.3	.0	.0	556.9	1119.2
T.P. TO 30	580.2	.0	.0	584.3	1164.5

LINE 32

BEGIN LINE 32	94.8	.0	.0	43.4	138.1
1/5	99.2	.0	.0	45.6	144.8
2/5	105.3	.0	.0	59.3	164.6
3/5	109.7	.0	.0	143.8	253.5
4/5	112.6	6.1	.0	264.8	383.5
MILE 1	114.1	34.8	.0	244.2	393.1
1/5	115.5	63.5	.0	232.8	411.8
2/5	164.7	41.0	.0	251.1	456.7
3/5	209.2	.0	.0	251.1	460.3
4/5	253.7	.0	.0	205.4	459.1
MILE 2	280.1	.0	.0	187.2	467.2
1/5	313.0	.0	.0	182.6	495.6
2/5	333.8	.0	.0	173.5	507.3
3/5	351.8	.0	.0	123.2	475.0
4/5	364.9	.0	.0	102.7	467.6
MILE 3	363.5	.0	.0	82.2	445.6
1/3	350.3	.0	.0	79.9	430.2
2/3	379.9	.0	.0	79.9	459.8
END LINE 32	394.9	.0	.0	79.9	474.8

LINE 33

BEGIN LINE 33	362.0	.0	19.1	123.2	504.3
1/5	336.8	.0	.0	123.2	460.0
2/5	300.9	.0	.0	86.7	387.7
3/5	261.0	.0	.0	79.9	340.9
4/5	233.0	.0	.0	100.4	333.5
MILE 1	216.5	.0	.0	125.5	342.1
1/5	204.8	.0	.0	143.8	348.6
2/5	188.5	.0	.0	168.9	357.4
3/5	173.5	45.1	.0	187.2	405.7
4/5	155.7	49.2	.0	232.8	437.6
MILE 2	124.7	79.9	.0	178.0	382.6
1/5	119.9	69.6	.0	219.1	408.7
2/5	115.5	36.9	.0	239.6	392.0
3/5	112.6	.0	.0	239.6	352.3
4/5	109.7	.0	.0	130.1	239.8
MILE 3	102.1	.0	.0	95.9	197.9
1/4	97.7	.0	.0	34.2	131.9
2/4	83.1	.0	.0	.0	83.1
3/4	72.5	.0	.0	.0	72.5
MILE 4	57.4	.0	.0	.0	57.4
END LINE 33	48.6	.0	.0	.0	48.6

LINE 34

35 TO 34 (1/2)	399.3	.0	.0	278.4	677.7
BEGIN LINE 34	409.5	.0	69.3	178.0	656.8
MILE 1	402.2	.0	61.9	86.7	550.8
1/5	392.0	.0	54.5	91.3	537.7
2/5	381.4	.0	50.0	159.8	591.2
3/5	372.6	.0	50.0	196.3	618.9
4/5	360.5	.0	47.1	173.5	581.1
MILE 2	345.5	.0	26.4	182.6	554.5
1/5	328.0	.0	17.6	200.8	546.4
2/5	308.6	.0	.0	235.1	543.7
3/5	280.1	.0	.0	255.6	535.7
4/5	241.8	20.5	.0	223.7	486.0
MILE 3	201.7	45.1	.0	189.4	436.2
1/5	129.0	86.0	.0	210.0	425.0
2/5	115.5	84.0	.0	187.2	386.7
3/5	111.1	38.9	.0	198.6	348.6
4/5	108.2	.0	.0	200.8	309.1
MILE 4	105.3	.0	.0	136.9	242.2
1/5	102.1	.0	.0	95.9	197.9
2/5	94.8	.0	.0	84.4	179.2
3/5	91.8	.0	.0	43.4	135.2
4/5	87.5	.0	.0	27.4	114.8
MILE 5	83.1	.0	.0	.0	83.1
END LINE 34	75.4	.0	.0	.0	75.4
34 TO 33 (1/2)	81.2	.0	.0	.0	81.2

LINE 35

BEGIN LINE 35	66.6	.0	.0	.0	66.6
1/3	78.3	.0	.0	18.3	96.6
2/3	83.1	.0	.0	45.6	128.7
MILE 1	87.5	.0	.0	95.9	183.3
1/5	93.3	.0	.0	155.2	248.5
2/5	97.7	.0	.0	171.2	268.9
3/5	102.1	.0	.0	187.2	289.2
4/5	106.8	.0	.0	226.0	332.7
MILE 2	109.7	.0	.0	221.4	331.1
1/5	114.1	49.2	.0	273.9	437.1
2/5	121.4	79.9	.0	273.9	475.1
3/5	164.7	53.3	.0	283.0	501.0
4/5	200.2	43.0	.0	148.4	391.6
MILE 3	179.3	.0	.0	.0	179.3
1/10	152.8	.0	.0	.0	152.8
1/5	164.7	.0	.0	.0	164.7
2/5	261.0	.0	.0	.0	261.0
3/5	289.2	.0	50.0	95.9	435.1
4/5	313.0	.0	56.0	118.7	487.6
MILE 4	333.8	.0	58.9	127.8	520.6
END LINE 35	360.5	.0	56.0	114.1	530.6

LINE 36

BEGIN LINE 36	416.8	.0	58.9	159.8	635.5
1/5	409.5	.0	54.5	63.9	527.9
2/5	387.6	.0	.0	.0	387.6
3/5	246.3	.0	.0	.0	246.3
4/5	127.6	.0	.0	.0	127.6
MILE 2	134.9	.0	.0	.0	134.9
1/5	209.2	.0	.0	.0	209.2
2/5	230.1	.0	.0	82.2	312.3
3/5	213.6	14.3	.0	114.1	342.1
4/5	190.0	14.3	.0	114.1	318.5
MILE 3	134.9	81.9	.0	136.9	353.8
1/5	122.8	65.5	.0	127.8	316.2
2/5	117.0	38.9	.0	143.8	299.7
3/5	114.1	.0	.0	168.9	283.0
4/5	111.1	.0	.0	150.6	261.8
MILE 4	108.2	.0	.0	143.8	252.0
1/5	105.3	.0	.0	136.9	242.2
2/5	100.6	.0	.0	132.4	233.0
3/5	97.7	.0	.0	102.7	200.4
4/5	93.3	.0	.0	63.9	157.2
MILE 5	90.4	.0	.0	45.6	136.0
END LINE 36	81.2	.0	.0	.0	81.2

LINE 39

40 to 39 (1/2)	66.6	.0	.0	.0	66.6
BEGIN LINE 39	50.1	.0	.0	.0	50.1
1/5	53.0	.0	.0	.0	53.0
2/5	63.7	.0	.0	.0	63.7
3/5	76.9	.0	.0	.0	76.9
4/5	90.4	.0	.0	.0	90.4
MILE 1	97.7	.0	.0	34.2	131.9
1/5	100.6	.0	.0	63.9	164.5
2/5	105.3	.0	.0	91.3	196.6
3/5	108.2	.0	.0	132.4	240.6
4/5	109.7	.0	.0	130.1	239.8
MILE 2	114.1	32.8	.0	109.6	256.4
1/5	122.8	63.5	.0	84.4	270.8
2/5	144.0	77.8	.0	59.3	281.1
3/5	223.9	8.2	.0	59.3	291.4
4/5	262.4	.0	.0	54.8	317.2
1/10	274.2	.0	.0	.0	274.2
MILE 3	238.9	.0	.0	.0	238.9
1/5	182.3	.0	.0	.0	182.3
2/5	132.0	.0	.0	.0	132.0
3/5	201.7	.0	.0	.0	201.7
4/5	320.3	.0	.0	.0	320.3
MILE 4	396.4	.0	.0	77.6	474.0
END LINE 39	402.2	.0	32.3	132.4	566.9
39 TO 36 (1/2)	406.6	.0	45.6	219.1	671.3

LINE 40

41 TO 40 (1/2)	654.6	.0	.0	319.5	974.1
BEGIN LINE 40	617.4	.0	45.6	305.8	968.8
1/5	595.1	.0	47.1	474.7	1116.9
2/5	565.2	.0	47.1	520.4	1132.7
3/5	535.7	.0	44.1	479.3	1059.1
4/5	513.4	.0	45.6	488.4	1047.4
MILE 2	484.0	.0	66.3	593.4	1143.7
1/5	491.1	.0	44.1	661.9	1197.1
2/5	469.4	.0	51.5	570.6	1091.5
3/5	439.1	.0	57.4	493.0	989.5
4/5	416.8	.0	58.9	342.4	818.1
MILE 3	394.9	.0	54.5	246.5	695.9
1/5	364.9	.0	57.4	127.8	550.2
2/5	342.6	.0	50.0	.0	392.6
3/5	305.7	.0	.0	.0	305.7
4/5	261.0	.0	.0	.0	261.0
MILE 4	201.7	18.4	.0	73.0	293.2
1/5	130.5	73.7	.0	84.4	288.7
2/5	121.4	38.9	.0	102.7	263.0
3/5	115.5	.0	.0	109.6	225.1
4/5	108.2	.0	.0	86.7	194.9
MILE 5	105.3	.0	.0	68.5	173.8
1/5	102.1	.0	.0	50.2	152.3
2/5	99.2	.0	.0	32.0	131.1
3/5	90.4	.0	.0	.0	90.4
4/5	69.5	.0	.0	.0	69.5
MILE 6	72.5	.0	.0	.0	72.5
END LINE 40	63.7	.0	.0	.0	63.7

LINE 41

41 TO 42 (1/2)	68.1	.0	.0	.0	68.1
BEGIN LINE 41	53.0	.0	.0	.0	53.0
1/5	57.4	.0	.0	.0	57.4
2/5	68.1	.0	.0	.0	68.1
3/5	72.5	.0	.0	.0	72.5
4/5	84.5	.0	.0	.0	84.5
MILE 2	96.2	.0	.0	47.9	144.2
1/5	100.6	.0	.0	109.6	210.2
2/5	105.3	.0	.0	136.9	242.2
3/5	109.7	.0	.0	152.9	262.6
4/5	112.6	24.6	.0	155.2	292.4
MILE 3	115.5	53.3	.0	152.9	321.7
1/5	130.5	75.8	.0	150.6	356.9
2/5	209.2	.0	.0	182.6	391.8
3/5	271.3	.0	.0	121.0	392.3
4/5	307.1	.0	.0	77.6	384.7

MILE 4	345.5	.0	.0	.0	345.5
1/5	390.5	.0	.0	.0	390.5
2/5	421.2	.0	24.9	.0	446.1
3/5	443.5	.0	53.0	105.0	601.4
4/5	464.6	.0	58.9	269.3	792.9
MILE 5	482.5	.0	56.0	360.6	899.1
1/5	502.8	.0	56.0	420.0	978.7
2/5	520.7	.0	53.0	442.8	1016.5
3/5	543.0	.0	42.6	493.0	1078.6
4/5	565.2	.0	26.4	529.5	1121.2
MILE 6	583.1	.0	17.6	356.0	956.7
1/3	602.5	.0	1.5	214.5	818.5
2/3	624.7	.0	.0	182.6	807.3
END LINE 41	642.6	.0	.0	200.8	843.4

LINE 42

43 to 42 (0)	580.2	.0	.0	.0	580.2
1/4	587.5	.0	.0	.0	587.5
2/4	602.5	.0	13.2	.0	615.6
3/5	617.4	.0	27.9	82.2	727.5
T.P. TO 42	603.9	.0	47.1	301.3	952.3
BEGIN LINE 42	568.2	.0	70.8	479.3	1118.2
1/5	550.6	.0	85.7	392.6	1028.9
2/5	526.6	.0	103.6	264.8	894.9
3/5	502.8	.0	100.6	54.8	658.2
4/5	470.8	.0	11.7	.0	482.5
MILE 2	424.1	.0	.0	.0	424.1
1/5	381.4	.0	.0	.0	381.4
2/5	335.3	.0	.0	34.2	369.5
3/5	290.7	.0	.0	91.3	382.0
4/5	247.8	28.7	.0	91.3	367.8
MILE 3	204.8	43.0	.0	107.3	355.1
1/5	134.9	106.5	.0	109.6	351.0
2/5	122.8	106.5	.0	105.0	334.3
3/5	119.9	102.4	.0	45.6	268.0
4/5	114.1	65.5	.0	73.0	252.7
MILE 4	111.1	32.8	.0	91.3	235.2
1/5	108.2	.0	.0	86.7	194.9
2/5	102.1	.0	.0	50.2	152.3
3/5	90.4	.0	.0	.0	90.4
4/5	78.3	.0	.0	.0	78.3
MILE 5	66.6	.0	.0	.0	66.6
END LINE 42	63.7	.0	.0	.0	63.7

LINE 43

43 TO 44·(1/2)	60.3	.0	.0	.0	60.3
BEGIN LINE 43	51.5	.0	.0	.0	51.5
1/5	63.7	.0	.0	.0	63.7
2/5	69.5	.0	.0	.0	69.5
3/5	83.1	.0	.0	.0	83.1
4/5	99.2	.0	.0	77.6	176.8
MILE 2	109.7	51.2	.0	73.0	233.9
1/5	117.0	96.3	.0	57.1	270.3
2/5	134.9	108.6	.0	61.6	305.1
3/5	187.1	98.3	.0	38.8	324.2
4/5	246.3	71.7	.0	22.8	340.9
MILE 3	283.0	.0	.0	79.9	362.9
1/5	310.1	.0	.0	.0	310.1
2/5	335.3	.0	.0	.0	335.3
3/5	364.9	.0	.0	.0	364.9
4/5	387.6	.0	.0	.0	387.6
MILE 4	405.1	.0	.0	.0	405.1
1/5	450.0	.0	41.2	.0	491.2
2/5	470.8	.0	79.7	.0	550.5
3/5	491.1	.0	76.7	155.2	723.1
4/5	510.5	.0	69.3	182.6	762.4
MILE 5	532.7	.0	44.1	95.9	672.7
END LINE 43	550.6	.0	20.5	59.3	630.5

LINE 44

45 TO 44 (0)	461.7	.0	23.5	100.4	585.6
1/2	451.5	.0	54.5	68.5	574.4
T.P. TO 44	476.7	.0	58.9	22.8	558.4
BEGIN LINE 44	491.1	.0	47.1	18.3	556.5
1/5	491.1	.0	44.1	.0	535.2
2/5	479.6	.0	44.1	.0	523.7
3/5	491.1	.0	26.4	.0	517.5
4/5	479.6	.0	26.4	.0	506.0
MILE 2	470.8	.0	17.6	.0	488.4
1/5	461.7	.0	.0	.0	461.7
2/5	439.1	.0	.0	.0	439.1
3/5	419.7	.0	.0	.0	419.7
4/5	394.9	.0	.0	68.5	463.4
MILE 3	372.6	.0	.0	91.3	463.9
1/5	345.5	.0	.0	121.0	466.5
2/5	330.9	.0	.0	132.4	463.3
3/5	278.6	.0	.0	178.0	456.7
4/5	231.6	26.6	.0	187.2	445.4

MILE 4	167.6	65.5	.0	173.5	406.6
1/4	117.0	61.4	.0	175.7	354.2
2/4	105.3	8.2	.0	139.2	252.7
3/4	93.3	.0	.0	63.9	157.2
END LINE 44	78.3	.0	.0	.0	78.3

LINE 45

46 TO 45 (0)	63.7	.0	.0	.0	63.7
1/2	33.5	.0	.0	.0	33.5
T.P. TO 45	57.4	.0	.0	.0	57.4
BEGIN LINE 45	50.1	.0	.0	.0	50.1
1/5	68.1	.0	.0	.0	68.1
2/5	84.5	.0	.0	.0	84.5
3/5	93.3	.0	.0	.0	93.3
4/5	109.7	.0	.0	38.8	148.5
MILE 2	134.9	49.2	.0	59.3	243.4
1/5	213.6	.0	.0	175.7	389.4
2/5	269.9	.0	.0	180.3	450.2
3/5	298.0	.0	.0	182.6	480.6
4/5	308.6	.0	.0	178.0	486.6
MILE 3	317.4	.0	.0	175.7	493.1
1/5	348.8	.0	17.6	123.2	489.7
2/5	362.0	.0	57.4	63.9	483.3
3/5	378.5	.0	56.0	63.9	498.3
4/5	390.5	.0	61.9	59.3	511.7
MILE 4	402.2	.0	58.9	57.1	518.2
1/4	416.8	.0	44.1	79.9	540.8
2/4	428.8	.0	35.3	98.1	562.2
3/4	443.5	.0	23.5	105.0	571.9
END LINE 45	461.7	.0	8.8	111.8	582.3

LINE 46

46 TO 47 (1/2)	499.9	.0	.0	168.9	668.8
BEGIN LINE 46	461.7	.0	.0	148.4	610.1
1/5	440.5	.0	.0	168.9	609.4
2/5	424.1	.0	.0	159.8	583.9
3/5	405.1	.0	.0	166.6	571.8
4/5	390.5	.0	.0	166.6	557.1
MILE 2	372.6	.0	.0	159.8	532.4
1/5	351.8	.0	.0	146.1	497.8
2/5	330.9	.0	.0	132.4	463.3
3/5	348.8	.0	.0	82.2	431.0
4/5	342.6	.0	.0	68.5	411.1

MILE 3	315.9	.0	.0	86.7	402.7
1/5	313.0	.0	.0	79.9	392.9
2/5	295.1	.0	.0	73.0	368.1
3/5	298.0	.0	.0	57.1	355.1
4/5	286.3	.0	.0	41.1	327.4
MILE 4	256.6	.0	.0	63.9	320.5
1/4	209.2	.0	.0	68.5	277.7
2/4	134.9	.0	.0	136.9	271.8
3/4	105.3	.0	.0	148.4	253.6
END OF LINE 46	83.1	.0	.0	91.3	174.4

LINE 47

48 TO 47 (0)	54.5	.0	.0	.0	54.5
1/2	53.0	.0	.0	.0	53.0
T.P. TO 47	48.6	.0	.0	.0	48.6
BEGIN LINE 47	48.6	.0	.0	.0	48.6
1/5	60.3	.0	.0	.0	60.3
2/5	71.0	.0	.0	.0	71.0
3/5	83.1	.0	.0	.0	83.1
4/5	93.3	.0	.0	29.7	123.0
MILE 2	100.6	.0	.0	52.5	153.1
1/5	105.3	.0	.0	79.9	185.2
2/5	109.7	8.2	.0	257.9	375.8
3/5	114.1	34.8	.0	289.9	438.7
4/5	117.0	59.4	.0	292.1	468.5
MILE 3	121.4	79.9	.0	296.7	498.0
1/5	146.9	61.4	.0	164.3	372.7
2/5	194.4	4.1	.0	178.0	376.5
3/5	223.9	.0	.0	148.4	372.2
4/5	247.8	.0	.0	134.7	382.5
MILE 4	283.0	.0	.0	114.1	397.1
1/5	310.1	.0	.0	141.5	451.6
2/5	342.6	.0	.0	171.2	513.8
3/5	372.6	.0	.0	182.6	555.2
4/5	399.3	.0	.0	164.3	563.6
MILE 5	428.8	.0	.0	175.7	604.6
1/3	455.9	.0	.0	203.1	659.0
2/3	485.5	.0	.0	191.7	677.2
END LINE 47	514.9	.0	8.8	178.0	701.7

LINE 48

49 TO 48 (0)	758.6	.0	.0	365.2	1123.8
1/4	761.6	.0	33.8	34.2	829.6
2/4	755.7	.0	.0	18.3	774.0
3/4	669.2	.0	.0	114.1	783.4
T.P. TO 48	624.7	.0	.0	159.8	784.5
BEGIN LINE 48	535.7	.0	.0	159.8	695.4
1/5	505.8	.0	.0	91.3	597.0
2/5	464.6	.0	.0	121.0	585.6
3/5	439.1	.0	.0	125.5	564.6
4/5	402.2	.0	.0	148.4	550.6
MILE 2	375.5	.0	.0	166.6	542.1
1/5	335.3	.0	.0	171.2	506.5
2/5	300.9	.0	.0	178.0	479.0
3/5	268.4	.0	.0	205.4	473.8
4/5	227.2	16.4	.0	239.6	483.2
MILE 3	176.4	45.1	.0	319.5	541.0
1/5	127.6	84.0	.0	442.8	654.3
2/5	115.5	51.2	.0	337.8	504.5
3/5	112.6	.0	.0	285.3	397.9
4/5	108.2	.0	.0	166.6	274.8
MILE 4	105.3	.0	.0	68.5	173.8
1/5	99.2	.0	.0	20.5	119.7
2/5	93.3	.0	.0	.0	93.3
3/5	84.5	.0	.0	.0	84.5
4/5	75.4	.0	.0	.0	75.4
END LINE 48	63.7	.0	.0	.0	63.7

LINE 49

50 TO 49 (0)	57.4	.0	.0	.0	57.4
1/2	54.5	.0	.0	.0	54.5
T.P. TO 49	54.5	.0	.0	.0	54.5
BEGIN LINE 49	54.5	.0	.0	.0	54.5
1/5	66.6	.0	.0	.0	66.6
2/5	76.9	.0	.0	.0	76.9
3/5	84.5	.0	.0	.0	84.5
4/5	87.5	.0	.0	.0	87.5
MILE 2	99.2	.0	.0	45.6	144.8
1/5	105.3	.0	.0	125.5	230.8
2/5	111.1	.0	.0	264.8	375.9
3/5	117.0	8.2	.0	292.1	417.3
4/5	122.8	63.5	.0	255.6	442.0

MILE 3	158.6	73.7	.0	303.6	535.9
1/5	231.6	34.8	.0	372.0	638.4
2/5	295.1	4.1	.0	547.8	846.9
3/5	350.3	.0	.0	673.3	1023.6
4/5	405.1	.0	.0	725.8	1130.9
MILE 4	458.8	.0	.0	620.8	1079.6
1/4	517.8	.0	.0	575.2	1092.9
2/4	577.3	.0	.0	575.2	1152.4
3/4	639.7	.0	.0	547.8	1187.4
END LINE 49	699.1	.0	.0	456.5	1155.6

LINE 50

51 TO 50 (0)	809.7	.0	.0	718.9	1528.6
1/4	906.3	.0	14.7	639.1	1560.0
2/4	909.2	.0	44.1	588.8	1542.1
3/4	900.4	.0	73.8	534.1	1508.2
T.P. TO 50	898.9	.0	81.2	524.9	1505.1
BEGIN LINE 50	849.8	.0	35.3	545.5	1430.5
1/5	820.2	.0	.0	566.0	1386.2
2/5	737.8	.0	.0	579.7	1317.5
3/5	654.6	.0	.0	593.4	1248.0
4/5	583.1	.0	.0	566.0	1149.1
MILE 2	514.9	.0	.0	534.1	1048.9
1/5	455.9	.0	.0	511.2	967.1
2/5	405.1	.0	.0	474.7	879.9
3/5	345.5	.0	.0	451.9	797.4
4/5	292.2	.0	.0	465.6	757.8
MILE 3	238.9	20.5	.0	342.4	601.7
1/5	149.8	57.4	.0	232.8	440.0
2/5	117.0	.0	.0	232.8	349.8
3/5	111.1	.0	.0	150.6	261.8
4/5	105.3	.0	.0	114.1	219.4
MILE 4	96.2	.0	.0	59.3	155.6
1/4	93.3	.0	.0	27.4	120.7
2/4	87.5	.0	.0	27.4	114.8
3/4	79.8	.0	.0	.0	79.8
END LINE 50	66.6	.0	.0	.0	66.6

LINE 51

BEGIN LINE 51	54.5	.0	.0	.0	54.5
1/3	68.1	.0	.0	.0	68.1
2/3	78.3	.0	.0	22.8	101.1
MILE 2	84.5	.0	.0	45.6	130.2
1/5	93.3	.0	.0	68.5	161.8
2/5	97.7	.0	.0	136.9	234.6
3/5	100.6	.0	.0	257.9	358.5
4/5	105.3	.0	.0	260.2	365.5
MILE 3	108.2	.0	.0	164.3	272.5
1/5	111.1	.0	.0	219.1	330.2
2/5	124.7	63.5	.0	253.3	441.5
3/5	188.5	36.9	.0	333.2	558.6
4/5	238.9	26.6	.0	426.8	692.3
MILE 4	283.0	.0	.0	547.8	830.8
1/5	342.6	.0	.0	616.2	958.9
2/5	393.4	.0	.0	698.4	1091.8
3/5	437.6	.0	.0	698.4	1136.0
4/5	491.1	.0	.0	707.5	1198.6
MILE 5	565.2	.0	.0	730.3	1295.6
1/2	639.7	.0	.0	776.0	1415.7
END LINE 51	731.7	.0	.0	771.4	1503.1

LINE 52

BEGIN LINE 52	761.6	.0	.0	543.2	1304.8
1/5	705.0	.0	.0	378.9	1083.9
2/5	639.7	.0	.0	273.9	913.5
3/5	574.3	.0	.0	191.7	766.1
4/5	505.8	.0	.0	136.9	642.7
MILE 2	446.4	.0	.0	68.5	514.9
1/5	381.4	.0	.0	.0	381.4
2/5	333.8	.0	.0	.0	333.8
3/5	280.1	.0	.0	.0	280.1
4/5	227.2	12.3	.0	118.7	358.2
MILE 3	137.8	73.7	.0	130.1	341.7
1/5	119.9	14.3	.0	166.6	300.9
2/5	114.1	.0	.0	123.2	237.3
3/5	109.7	.0	.0	73.0	182.7
4/5	100.6	.0	.0	36.5	137.1
MILE 4	90.4	.0	.0	.0	90.4
1/5	79.8	.0	.0	.0	79.8
2/5	75.4	.0	.0	.0	75.4
3/5	83.1	.0	.0	.0	83.1
4/5	78.3	.0	.0	63.9	142.2

MILE 5	72.5	.0	.0	50.2	122.7
END LINE 52	66.6	.0	.0	36.5	103.1
52 TO 51 (0)	60.3	.0	.0	.0	60.3
1/3	68.1	.0	.0	11.4	79.5
2/3	65.2	.0	.0	.0	65.2
T.P. TO 51	65.2	.0	.0	.0	65.2

LINE 53

BEGIN LINE 53	66.6	.0	.0	.0	66.6
1/5	75.4	.0	.0	.0	75.4
2/5	78.3	.0	.0	.0	78.3
3/5	99.2	.0	.0	43.4	142.5
4/5	106.8	.0	.0	91.3	198.0
MILE 2	112.6	.0	.0	159.8	272.4
1/5	117.0	8.2	.0	223.7	348.9
2/5	136.4	47.1	.0	139.2	322.7
3/5	194.4	41.0	.0	159.8	395.1
4/5	241.8	10.2	.0	166.6	418.7
MILE 3	278.6	.0	.0	223.7	502.3
1/5	315.9	.0	.0	178.0	493.9
2/5	357.6	.0	.0	159.8	517.4
3/5	402.2	.0	.0	136.9	539.2
4/5	443.5	.0	.0	118.7	562.1
MILE 4	479.6	.0	.0	155.2	634.8
1/2	529.8	.0	.0	260.2	790.0
END LINE 53	592.2	.0	.0	255.6	847.8
53 TO 52 (0)	654.6	.0	.0	319.5	974.1
1/2	705.0	.0	.0	401.7	1106.7
T.P. TO 52	772.8	.0	.0	502.1	1274.9

LINE 54

BEGIN LINE 54	599.5	.0	.0	114.1	713.6
1/5	552.1	.0	.0	123.2	675.3
2/5	514.9	.0	.0	91.3	606.1
3/5	491.1	.0	.0	159.8	650.9
4/5	455.9	.0	.0	123.2	579.1
MILE 2	408.0	.0	.0	150.6	558.6
1/5	360.5	.0	.0	191.7	552.3
2/5	313.0	.0	.0	168.9	481.9
3/5	262.4	.0	.0	146.1	408.5
4/5	223.9	14.3	.0	143.8	382.0

MILE 3	185.6	32.8	.0	123.2	341.6
1/5	127.6	77.8	.0	100.4	305.8
2/5	119.9	30.7	.0	125.5	276.2
3/5	114.1	8.2	.0	136.9	259.2
4/5	108.2	.0	.0	114.1	222.3
MILE 4	100.6	.0	.0	136.9	237.6
1/2	96.2	.0	.0	86.7	183.0
54 TO 53 (0)	90.4	.0	.0	.0	90.4
1/2	78.3	.0	.0	.0	78.3
T.P. TO 53	72.5	.0	.0	.0	72.5

LINE 55

BEGIN LINE 55	97.7	.0	.0	.0	97.7
1/5	106.8	.0	.0	41.1	147.8
2/5	109.7	.0	.0	50.2	159.9
3/5	114.1	.0	.0	100.4	214.5
4/5	119.9	32.8	.0	100.4	253.1
MILE 2	129.0	63.5	.0	98.1	290.7
1/5	179.3	41.0	.0	68.5	288.8
2/5	215.1	4.1	.0	100.4	319.6
3/5	247.8	.0	.0	123.2	371.1
4/5	283.0	.0	.0	114.1	397.1
MILE 3	318.9	.0	.0	150.6	469.5
1/5	360.5	.0	.0	155.2	515.7
2/5	408.0	.0	.0	127.8	535.8
3/5	446.4	.0	.0	150.6	597.0
4/5	482.5	.0	.0	86.7	569.3
MILE 4	523.6	.0	.0	100.4	624.1
END LINE 55	574.3	.0	.0	105.0	679.3
55 TO 54 (0)	642.6	.0	.0	155.2	797.8
1/2	633.8	.0	.0	123.2	757.1
T.P. TO 54	632.4	.0	.0	79.9	712.2

LINE 56

BEGIN LINE 56	618.9	.0	.0	109.6	728.4
1/5	559.4	.0	.0	109.6	668.9
2/5	513.4	.0	.0	118.7	632.1
3/5	470.8	.0	.0	100.4	571.2
4/5	434.7	.0	.0	91.3	526.0

MILE 2	408.0	.0	.0	114.1	522.1
1/5	381.4	.0	.0	155.2	536.6
2/5	342.6	.0	.0	136.9	479.6
3/5	310.1	.0	.0	132.4	442.4
4/5	283.0	.0	.0	123.2	406.3
MILE 3	262.4	.0	.0	136.9	399.4
1/5	241.8	.0	.0	136.9	378.8
2/5	218.0	.0	.0	136.9	354.9
3/5	194.4	14.3	.0	189.4	398.2
4/5	134.9	65.5	.0	155.2	355.6
MILE 4	122.8	43.0	.0	166.6	332.5
END LINE 56	117.0	.0	.0	77.6	194.6
56 TO 55 (0)	103.8	.0	.0	29.7	133.5
1/2	94.8	.0	.0	.0	94.8
T.P. TO 55	97.7	.0	.0	.0	97.7

LINE 57 EAST

MILE 7	126.1	.0	.0	.0	126.1
1/5	121.4	.0	.0	.0	121.4
2/5	121.4	22.5	.0	43.4	187.3
3/5	121.4	51.2	.0	132.4	305.0
4/5	122.8	69.6	.0	150.6	343.1
MILE 8	129.0	81.9	.0	159.8	370.7

LINE 57 WEST

BEGIN LINE 57	136.4	129.0	.0	107.3	372.7
1/5	144.0	110.6	.0	82.2	336.7
2/5	173.5	81.9	.0	91.3	346.7
3/5	223.9	45.1	.0	109.6	378.5
4/5	256.6	36.9	.0	159.8	453.2
MILE 1	262.4	14.3	.0	203.1	479.9
1/5	265.5	.0	.0	232.8	498.3
2/5	271.3	.0	.0	214.5	485.9
3/5	275.7	.0	.0	219.1	494.8
4/5	278.6	.0	.0	246.5	525.1
MILE 2	289.2	.0	.0	241.9	531.2
1/5	313.0	.0	.0	219.1	532.1
2/5	338.2	.0	.0	223.7	561.9
3/5	359.1	.0	.0	191.7	550.8
4/5	387.6	.0	.0	196.3	583.9

MILE 3	416.8	.0	.0	159.8	576.6
1/3	450.0	.0	.0	136.9	586.9
2/3	514.9	.0	.0	86.7	601.6
END LINE 57	553.5	.0	.0	77.6	631.1
57 TO 56 (0)	620.3	.0	.0	59.3	679.7
1/2	614.5	.0	.0	73.0	687.5
T.P. TO 56	635.3	.0	.0	82.2	717.4

Station No.	Water depth, m	Corrected thickness of Unit X, m	Depth to pre-orogenic layer, m
	LINE 57		
MILE 5	783.3	.0	783.3
1/4	952.6	.0	952.6
2/4	1104.3	.0	1104.3
3/4	1156.1	44.1	1200.2
MILE 4	1185.7	73.8	1259.5
1/4	1215.3	73.8	1289.1
2/4	1230.2	81.2	1311.5
3/4	1230.2	96.1	1326.4
MILE 3	1237.6	66.3	1303.9
1/4	1237.6	73.8	1311.3
2/4	1245.2	96.1	1341.3
3/4	1252.5	126.1	1378.7
MILE 2	1252.5	171.5	1424.0
1/4	1245.2	186.7	1431.9
1/2	1245.2	209.6	1454.9
3/4	1245.2	217.3	1462.5
MILE 1	1252.5	217.3	1469.8
1/4	1237.6	234.1	1471.6
2/4	1237.6	243.2	1480.8
3/4	1237.6	271.3	1508.8
END 57	1237.6	290.5	1528.0

LINE 58

MILE 0	305.3	.0	305.3
1/4	405.8	.0	405.8
2/4	615.9	.0	615.9
3/4	826.5	.0	826.5
MILE 1	988.8	.0	988.8
1/4	1153.2	.0	1153.2
2/4	1178.4	96.1	1274.5
3/4	1193.3	88.7	1282.0
MILE 2	1193.3	81.2	1274.6
1/4	1200.7	58.9	1259.6
2/4	1208.0	81.2	1289.2
3/4	1222.9	103.6	1326.6
MILE 3	1237.6	141.2	1378.8
1/4	1245.2	194.4	1439.6
2/4	1245.2	300.2	1545.4
3/4	1245.2	310.1	1555.3
MILE 4	1237.6	320.0	1557.6
1/4	1237.6	320.0	1557.6
2/4	1237.6	310.1	1547.6
3/4	1237.6	290.5	1528.0
END 58	1237.6	280.8	1518.4
58 TO 57 (0)	1230.2	280.8	1511.1
1/2	1237.6	261.8	1499.4
T.P. TO 57	1237.6	280.8	1518.4

LINE 1

1/4	315.7	.0	315.7
2/4	354.2	.0	354.2
3/4	461.1	.0	461.1
MILE 5	591.3	.0	591.3
1/4	730.0	.0	730.0
2/4	934.7	.0	934.7
3/4	1050.9	.0	1050.9
MILE 4	1119.2	73.8	1193.0
1/4	1141.5	300.2	1441.7
2/4	1171.1	171.5	1342.6
3/4	1178.4	126.1	1304.5
MILE 3	1193.3	96.1	1289.5
1/4	1200.7	96.1	1296.8
2/4	1208.0	111.1	1319.1
3/4	1222.9	126.1	1349.1

MILE 2	1237.6	156.3	1393.9
1/4	1237.6	217.3	1454.9
2/4	1237.6	280.8	1518.4
3/4	1230.2	340.2	1570.5
MILE 1	1230.2	340.2	1570.5
1/4	1230.2	340.2	1570.5
2/4	1230.2	330.1	1560.3
3/4	1230.2	320.0	1550.3
BEGIN LINE 1	1230.2	320.0	1550.3

LINE 2

MILE 1	483.5	.0	483.5
1/4	632.0	.0	632.0
2/4	837.1	.0	837.1
3/4	1017.0	.0	1017.0
MILE 2	1074.7	133.7	1208.3
1/4	1111.6	320.0	1431.6
2/4	1133.9	576.5	1710.3
3/4	1163.4	436.1	1599.5
MILE 3	1178.4	290.5	1468.8
1/4	1193.3	194.4	1387.7
2/4	1208.0	126.1	1334.1
3/4	1222.9	118.6	1341.6
MILE 4	1230.2	148.8	1379.0
1/3	1230.2	186.7	1417.0
2/3	1230.2	217.3	1447.6
MILE 5	1227.3	265.6	1492.9
1/4	1227.3	304.1	1531.5
2/4	1227.3	294.3	1521.7
3/4	1227.3	294.3	1521.7
END LINE 2	1227.3	304.1	1531.5

LINE 3

BEGIN 3 (LINE)	63.4	.0	63.4
1/3	154.2	.0	154.2
2/3	247.4	.0	247.4
MILE 4	354.2	.0	354.2
1/4	487.9	.0	487.9
2/4	617.4	.0	617.4
3/4	746.4	.0	746.4

MILE 3	897.7	.0	897.7
1/4	1059.7	36.7	1096.5
2/4	1104.3	234.1	1338.3
3/4	1133.9	458.5	1592.3
MILE 2	1163.4	481.3	1644.7
1/4	1178.4	458.5	1636.9
2/4	1185.7	414.1	1599.8
3/4	1193.3	350.5	1543.8
MILE 1	1200.7	252.5	1453.1
1/4	1215.3	186.7	1402.0
2/4	1222.9	118.6	1341.6
3/4	1222.9	96.1	1319.1
END LINE 3	1222.9	103.6	1326.6
3 TO 4 (0)	1215.3	96.1	1311.4
1/3	1215.3	73.8	1289.1
2/3	1208.0	103.6	1311.6
T. P. TO 4	1208.0	194.4	1402.3

LINE 4

5 TO 4 (0)	43.9	.0	43.9
1/3	75.1	.0	75.1
2/3	84.3	.0	84.3
T.P. TO 4	85.8	.0	85.8
BEGIN 4	99.0	.0	99.0
1/2	284.8	.0	284.8
MILE 1	468.5	.0	468.5
1/4	638.2	.0	638.2
2/4	795.4	.0	795.4
3/4	964.6	.0	964.6
MILE 2	1087.8	.0	1087.8
1/4	1129.5	145.7	1275.2
2/4	1150.3	379.7	1530.0
3/4	1168.2	525.7	1693.8
MILE 3	1174.0	492.8	1666.8
1/4	1179.9	425.0	1604.9
2/4	1185.7	352.5	1538.2
3/4	1193.3	290.5	1483.8
MILE 4	1199.2	248.7	1447.9
1/2	1205.1	234.1	1439.1
END LINE 4	1209.4	218.8	1428.3

LINE 5

END LINE 5	82.9	.0	82.9
1/4	94.6	.0	94.6
2/4	161.5	.0	161.5
3/4	241.5	.0	241.5
MILE 5	293.6	.0	293.6
1/4	383.9	.0	383.9
2/4	588.4	.0	588.4
3/4	756.7	.0	756.7
MILE 4	946.7	.0	946.7
1/4	1150.3	.0	1150.3
2/4	1151.7	123.1	1274.9
3/4	1159.0	356.7	1515.7
MILE 3	1163.4	481.3	1644.7
1/4	1168.2	269.4	1437.5
2/4	1171.1	127.6	1298.7
3/4	1175.5	.0	1175.5
MILE 2	1102.8	.0	1102.8
1/4	1052.4	.0	1052.4
2/4	1067.4	.0	1067.4
3/4	1101.3	.0	1101.3
MILE 1	1111.6	.0	1111.6
1/4	1114.8	.0	1114.8
2/4	1147.3	29.4	1176.7
3/4	1126.5	35.3	1161.8
START LINE 5	1052.4	.0	1052.4
5 TO 6 (0)	969.0	.0	969.0
1/3	999.1	.0	999.1
2/3	986.6	.0	986.6
T.P. TO LINE 6	971.9	.0	971.9

LINE 6

BEGIN LINE 6	91.9	.0	91.9
1/3	182.3	.0	182.3
2/3	232.7	.0	232.7
MILE 1	354.2	.0	354.2
1/4	416.5	.0	416.5
2/4	569.0	.0	569.0
3/4	755.2	.0	755.2
MILE 2	879.8	.0	879.8
1/4	1102.8	.0	1102.8
2/4	1157.6	75.3	1232.8
3/4	1162.0	254.3	1416.3

MILE 3	1166.7	230.4	1397.1
1/4	1166.7	183.7	1350.4
2/4	1160.5	114.1	1274.6
3/4	1144.4	58.9	1203.3
MILE 4	1105.7	56.0	1161.7
1/4	1061.2	.0	1061.2
2/4	1019.9	.0	1019.9
3/4	1007.9	.0	1007.9
MILE 5	1004.9	.0	1004.9
1/4	1012.3	24.9	1037.2
2/4	1018.4	24.9	1043.4
3/4	1007.9	.0	1007.9
END LINE 6	1012.3	.0	1012.3

LINE 7

1/4	91.6	.0	91.6
END LINE 7	99.0	.0	99.0
1/3	158.6	.0	158.6
2/3	320.1	.0	320.1
MILE 4	374.7	.0	374.7
1/4	498.1	.0	498.1
2/4	600.1	.0	600.1
3/4	793.9	.0	793.9
MILE 3	957.0	.0	957.0
1/4	1091.1	.0	1091.1
2/4	1178.4	66.3	1244.7
3/4	1178.4	226.8	1405.2
MILE 2	1172.5	142.7	1315.3
1/4	1163.4	81.2	1244.6
2/4	1136.8	41.2	1177.9
3/4	1105.7	.0	1105.7
MILE 1	1064.4	.0	1064.4
1/4	1028.7	.0	1028.7
2/4	1007.9	.0	1007.9
3/4	996.2	.0	996.2
BEGIN LINE 7	996.2	23.5	1019.6
1/2	967.6	.0	967.6

LINE 8

9 TO 8 (0)	93.1	.0	93.1
1/2	78.5	.0	78.5
T.P. TO LINE 8	81.4	.0	81.4
BEGIN LINE 8	161.5	.0	161.5
1/3	241.5	.0	241.5
2/3	332.2	.0	332.2
MILE 1	410.6	.0	410.6
1/4	510.2	.0	510.2
2/4	706.2	.0	706.2
3/4	851.7	.0	851.7
MILE 2	1017.0	.0	1017.0
1/4	1128.0	.0	1128.0
2/4	1162.0	76.7	1238.7
3/4	1171.1	163.9	1335.0
MILE 3	1172.5	27.9	1200.4
1/4	1099.9	.0	1099.9
2/4	1040.7	.0	1040.7
3/4	1012.3	.0	1012.3
MILE 4	1007.9	.0	1007.9
1/3	996.2	.0	996.2
2/3	993.2	.0	993.2
END LINE 8	990.3	.0	990.3

LINE 9

END LINE 9	124.2	.0	124.2
1/3	255.1	.0	255.1
2/3	348.3	.0	348.3
MILE 4	431.1	.0	431.1
1/4	510.2	.0	510.2
2/4	691.6	.0	691.6
3/4	820.6	.0	820.6
MILE 3	1009.3	.0	1009.3
1/4	1126.5	.0	1126.5
2/4	1150.3	154.8	1305.1
3/4	1163.4	163.9	1327.3
MILE 2	1171.1	73.8	1244.8
1/4	1168.2	14.7	1182.8
2/4	1156.1	.0	1156.1
3/4	1144.4	.0	1144.4
MILE 1	1135.3	.0	1135.3
1/4	1126.5	.0	1126.5
2/4	1123.6	.0	1123.6
3/4	1076.1	.0	1076.1

BEGIN LINE 9	1043.6	.0	1043.6
9 TO 10 (0)	1045.1	.0	1045.1
1/2	1064.4	.0	1064.4
9 TO 10 (1)	1055.3	.0	1055.3
1/2	1094.0	.0	1094.0
T.P. TO 10	1119.2	47.1	1166.3

LINE 10

11 TO 10 (0)	179.4	.0	179.4
1/3	134.8	.0	134.8
2/3	105.2	.0	105.2
T.P. TO LINE 10	93.1	.0	93.1
BEGIN LINE 10	90.2	.0	90.2
1/4	134.8	.0	134.8
2/4	261.0	14.7	275.6
3/4	335.1	29.4	364.5
MILE 1	412.1	.0	412.1
1/4	459.7	.0	459.7
2/4	608.8	.0	608.8
3/4	744.9	.0	744.9
MILE 2	909.4	.0	909.4
1/4	1073.2	.0	1073.2
2/4	1094.0	157.8	1251.9
3/4	1116.3	99.1	1215.4
MILE 3	1138.2	47.1	1185.3
1/4	1156.1	51.5	1207.6
2/4	1145.9	60.4	1206.3
3/4	1147.3	53.0	1200.3
MILE 4	1145.9	54.5	1200.3
1/3	1143.0	51.5	1194.5
2/3	1138.2	47.1	1185.3
END LINE 10	1130.9	44.1	1175.0

LINE 11

END LINE 11	302.4	.0	302.4
1/2	404.3	70.8	475.1
MILE 4	471.4	26.4	497.8
1/4	549.6	38.2	587.8
2/4	620.3	.0	620.3
3/4	752.3	.0	752.3

MILE 3	854.6	.0	854.6
1/4	1022.8	29.4	1052.2
2/4	1025.7	93.1	1118.9
3/4	1030.1	.0	1030.1
MILE 2	1059.7	.0	1059.7
1/4	1071.8	.0	1071.8
2/4	1102.8	8.8	1111.6
3/4	1141.5	61.9	1203.4
MILE 1	1148.8	81.2	1230.0
1/4	1141.5	61.9	1203.4
2/4	1138.2	50.0	1188.3
3/4	1138.2	58.9	1197.2
MILE 0	1135.3	44.1	1179.4
1/4	1129.5	17.6	1147.1
2/4 BEGIN LINE 11	1116.3	.0	1116.3

LINE 12

13 TO 12 (0)	189.6	.0	189.6
1/3	179.4	.0	179.4
2/3	188.1	.0	188.1
T. P. TO 12	216.4	.0	216.4
BEGIN LINE 12	323.0	48.5	371.6
1/2	446.1	78.2	524.3
MILE 1	543.7	41.2	584.9
1/4	591.3	.0	591.3
2/4	707.7	.0	707.7
3/4	857.5	.0	857.5
MILE 2	1012.3	.0	1012.3
1/4	1019.9	32.3	1052.2
2/4	1027.2	.0	1027.2
3/4	1033.1	.0	1033.1
MILE 3	1055.3	.0	1055.3
1/4	1086.4	.0	1086.4
2/4	1141.5	.0	1141.5
3/4	1144.4	94.6	1239.1
MILE 4	1144.4	85.7	1230.1
1/2	1144.4	79.7	1224.1
END LINE 12	1138.2	70.8	1209.0

LINE 13

END LINE 13	302.4	42.6	345.0
MILE 4	450.5	48.5	499.0
1/4	552.5	20.5	573.0
2/4	642.6	.0	642.6
3/4	749.3	.0	749.3
MILE 3	897.7	.0	897.7
1/4	982.2	32.3	1014.5
2/4	996.2	.0	996.2
3/4	1012.3	.0	1012.3
MILE 2	1040.7	.0	1040.7
1/4	1084.9	17.6	1102.5
2/4	1126.5	209.6	1336.2
3/4	1147.3	194.4	1341.7
MILE 1	1147.3	195.9	1343.2
1/4	1150.3	179.1	1329.4
2/4	1151.7	162.4	1314.1
3/4	1150.3	145.7	1296.0
MILE 0	1145.9	132.2	1278.0
BEGIN LINE 13	1144.4	118.6	1263.0
13 TO 14 (0)	1147.3	112.6	1260.0
1/2	1156.1	136.7	1292.8
T.P. TO 14	1162.0	150.3	1312.2

LINE 14

15 TO 14 (0)	78.5	.0	78.5
1/4	78.5	.0	78.5
2/4	82.9	.0	82.9
3/4	101.9	.0	101.9
T.P. TO 14	119.8	.0	119.8
BEGIN LINE 14	231.3	.0	231.3
1/3	354.2	.0	354.2
2/3	475.8	35.3	511.0
MILE 1	579.2	35.3	614.5
1/4	666.4	45.6	711.9
2/4	742.0	.0	742.0
3/4	801.2	20.5	821.8
MILE 2	830.9	11.7	842.6
1/4	840.0	.0	840.0
2/4	979.3	.0	979.3
3/4	1067.4	44.1	1111.5
MILE 3	1071.8	24.9	1096.7
1/4	1105.7	29.4	1135.1
2/4	1141.5	133.7	1275.2
3/4	1150.3	139.7	1290.0

MILE 4	1156.1	145.7	1301.9
1/3	1159.0	166.9	1326.0
2/3	1162.0	173.0	1335.0
END LINE 14	1163.4	162.4	1325.8

LINE 15

END LINE 15	139.2	.0	139.2
1/2	296.5	.0	296.5
MILE 4	415.0	.0	415.0
1/4	556.9	.0	556.9
2/4	675.1	54.5	729.6
3/4	765.8	11.7	777.5
MILE 3	798.3	.0	798.3
1/4	825.0	94.6	919.6
2/4	822.1	.0	822.1
3/4	905.1	.0	905.1
MILE 2	955.5	41.2	996.7
1/4	1007.9	29.4	1037.2
2/4	1064.4	23.5	1087.9
3/4	1135.3	29.4	1164.7
MILE 1	1159.0	115.6	1274.7
1/4	1153.2	225.0	1378.2
2/4	1159.0	228.6	1387.7
3/4	1168.2	232.2	1400.4
BEGIN LINE 15	1172.5	214.2	1386.8
T.P. TO 15	1182.8	182.2	1364.9
1/2	1191.9	160.9	1352.8
16 TO 15 (0)	1191.9	115.6	1307.5

LINE 16

1/2	75.1	.0	75.1
T.P. TO 16	75.1	.0	75.1
BEGIN LINE 16	170.3	.0	170.3
1/2	314.2	.0	314.2
MILE 1	464.1	.0	464.1
1/4	564.6	67.8	632.4
3/8	614.4	97.6	712.1
2/4	641.1	5.9	647.0
3/4	614.4	.0	614.4

MILE 2	731.4	.0	731.4
1/4	866.7	8.8	875.5
3/8	893.4	58.9	952.3
2/4	893.4	5.9	899.2
3/4	902.1	.0	902.1
MILE 3	985.1	23.5	1008.6
1/8	985.1	23.5	1008.6
1/4	996.2	.0	996.2
2/4	1028.7	.0	1028.7
3/4	1116.3	.0	1116.3
MILE 4	1156.1	.0	1156.1
1/3	1174.0	.0	1174.0
2/3	1188.6	56.0	1244.6
END LINE 16	1187.2	126.1	1313.3

LINE 17

END LINE 17	212.0	.0	212.0
MILE 5	449.0	.0	449.0
1/4	511.7	82.7	594.4
2/4	539.3	108.1	647.4
3/4	523.4	.0	523.4
mile 4	505.4	.0	505.4
1/4	632.0	.0	632.0
2/4	810.0	.0	810.0
3/4	914.2	5.9	920.0
7/8	920.0	58.9	978.9
MILE 3	914.2	.0	914.2
1/4	893.4	.0	893.4
2/4	946.7	.0	946.7
3/4	1022.8	.0	1022.8
MILE 2	1073.2	.0	1073.2
1/4	1171.1	.0	1171.1
2/4	1200.7	53.0	1253.7
3/4	1212.4	97.6	1310.0
MILE 1	1230.2	112.6	1342.9
1/4	1245.2	106.6	1351.8
2/4	1252.5	84.2	1336.7
3/4	1256.9	94.6	1351.5
BEGIN LINE 17	1265.7	112.6	1378.3
1/2	1265.7	124.6	1390.3

LINE 18

19 TO 18 (0)	90.2	.0	90.2
1/4	81.4	.0	81.4
2/4	96.0	.0	96.0
3/4	94.6	.0	94.6
T.P. TO 18	99.0	.0	99.0
BEGIN LINE 18	216.4	.0	216.4
1/2	400.0	.0	400.0
MILE 1	558.7	.0	558.7
1/4	614.4	67.8	682.3
2/4	573.4	.0	573.4
3/4	605.9	.0	605.9
MILE 2	701.8	60.4	762.2
1/4	792.5	23.5	815.9
2/4	881.3	38.2	919.5
3/4	912.4	70.8	983.2
MILE 3	908.0	.0	908.0
1/4	890.4	.0	890.4
2/4	967.6	.0	967.6
3/4	1067.4	.0	1067.4
MILE 4	1156.1	.0	1156.1
1/4	1191.9	.0	1191.9
2/4	1227.3	.0	1227.3
5/8	1245.2	14.7	1259.9
3/4	1252.5	11.7	1264.2
MILE 5	1227.3	.0	1227.3
1/3	1227.3	.0	1227.3
2/3	1245.2	.0	1245.2
END LINE 18	1259.8	23.5	1283.3

LINE 19

BEGIN LINE 19	207.6	.0	207.6
MILE 4	394.1	.0	394.1
1/4	520.5	.0	520.5
2/4	605.9	17.6	623.5
5/8	623.2	50.0	673.3
3/4	623.2	.0	623.2
MILE 3	681.0	.0	681.0
1/4	762.9	.0	762.9
2/4	835.2	10.3	845.5
3/4	869.6	26.4	896.0
MILE 2	896.3	23.5	919.7
1/4	943.8	23.5	967.3
3/8	954.0	24.9	979.0
2/4	957.0	.0	957.0
3/4	976.3	.0	976.3

MILE 1	1010.8	.0	1010.8
1/4	1002.0	.0	1002.0
2/4	1025.7	.0	1025.7
3/4	1052.4	.0	1052.4
END LINE 19	1099.9	.0	1099.9
1/2 TURN	1120.7	14.7	1135.3
19 TO 20 (0)	1096.9	.0	1096.9
1/2	1040.7	.0	1040.7
T.P. TO 20	999.1	.0	999.1

LINE 20

1/2	93.1	.0	93.1
T.P. TO 20	122.7	.0	122.7
BEGIN LINE 20	191.1	.0	191.1
1/3	299.5	.0	299.5
2/3	395.6	.0	395.6
MILE 1	529.2	.0	529.2
1/4	623.2	88.7	711.9
2/4	632.0	.0	632.0
3/4	713.9	.0	713.9
MILE 2	801.2	.0	801.2
1/4	894.8	.0	894.8
2/4	949.6	32.3	982.0
3/4	976.3	61.9	1038.2
MILE 3	983.6	35.3	1018.9
1/4	940.9	.0	940.9
2/4	940.9	.0	940.9
3/4	957.0	.0	957.0
MILE 4	949.6	.0	949.6
1/2	946.7	.0	946.7
END LINE 20	954.0	.0	954.0

LINE 21

BEGIN LINE 21	91.6	.0	91.6
1/2	161.5	.0	161.5
MILE 4	336.6	.0	336.6
1/4	477.2	.0	477.2
2/4	605.9	.0	605.9
3/4	721.2	5.9	727.0
7/8	718.3	14.7	732.9

MILE 3	752.3	.0	752.3
1/4	822.1	.0	822.1
2/4	912.4	.0	912.4
3/4	946.7	41.2	987.9
MILE 2	982.2	106.6	1088.8
1/4	988.0	91.7	1079.7
2/4	925.9	.0	925.9
3/4	914.2	.0	914.2
MILE 1	914.2	.0	914.2
1/4	937.6	.0	937.6
2/4	925.9	.0	925.9
3/4	939.4	.0	939.4
END LINE 21	949.6	11.7	961.4
21 TO 22 (0)	958.4	32.3	990.7
1/2	949.6	33.8	983.4
T.P. TO 22	937.6	.0	937.6

LINE 22

23 TO 22 (0)	97.5	.0	97.5
1/2	90.2	.0	90.2
T.P. TO 22	201.3	.0	201.3
BEGIN LINE 22	278.5	.0	278.5
1/2	391.2	.0	391.2
MILE 1	566.0	.0	566.0
1/4	697.4	.0	697.4
2/4	801.2	.0	801.2
3/4	840.0	79.7	919.7
MILE 2	887.5	76.7	964.2
1/4	923.0	70.8	993.8
2/4	927.3	111.1	1038.5
3/4	937.6	191.3	1128.9
MILE 3	946.7	160.9	1107.6
1/4	957.0	44.1	1001.1
2/4	961.3	.0	961.3
3/4	973.4	.0	973.4
MILE 4	958.4	.0	958.4
1/2	957.0	.0	957.0
END LINE 22	934.7	.0	934.7

LINE 23

END LINE 23	101.9	.0	101.9
1/2	116.9	.0	116.9
MILE 4.5	219.3	.0	219.3
1/3	303.9	.0	303.9
2/3	383.9	.0	383.9
MILE 4	498.1	.0	498.1
1/4	615.9	.0	615.9
2/4	697.4	.0	697.4
3/4	739.1	.0	739.1
MILE 3	816.2	.0	816.2
1/4	851.7	.0	851.7
2/4	884.2	.0	884.2
3/4	910.9	.0	910.9
MILE 2	925.9	56.0	981.8
1/4	940.9	148.8	1089.6
2/4	964.6	173.0	1137.6
3/4	967.6	185.2	1152.8
MILE 1	973.4	163.9	1137.3
1/4	982.2	73.8	1055.9
2/4	982.2	35.3	1017.4
3/4	897.7	.0	897.7
BEGIN LINE 23	882.8	.0	882.8
23 TO 24 (0)	872.5	.0	872.5
1/3	860.5	.0	860.5
2/3	851.7	.0	851.7
T.P. TO 24	842.9	.0	842.9

LINE 24

25 TO 24 (0)	335.1	.0	335.1
1/3	315.7	.0	315.7
2/3	283.4	.0	283.4
T.P. TO 24	261.0	.0	261.0
BEGIN LINE 24	268.3	.0	268.3
1/4	357.1	.0	357.1
2/4	478.7	.0	478.7
3/4	532.2	.0	532.2
MILE 1	651.4	.0	651.4
1/8	756.7	.0	756.7
1/4	765.8	.0	765.8
2/4	819.1	.0	819.1
3/4	868.1	58.9	927.0
MILE 2	884.2	5.9	890.1
1/4	920.0	.0	920.0
2/4	957.0	44.1	1001.1
3/4	971.9	118.6	1090.6

MILE 3	982.2	170.0	1152.2
1/4	999.1	97.6	1096.7
2/4	967.6	.0	967.6
3/4	899.2	.0	899.2
MILE 4	878.4	.0	878.4
1/2	860.5	.0	860.5
END LINE 24	845.8	.0	845.8

LINE 25

END LINE 25	300.9	.0	300.9
1/2	395.6	.0	395.6
MILE 4	588.4	.0	588.4
1/4	819.1	.0	819.1
3/8	890.4	.0	890.4
2/4	845.8	.0	845.8
3/4	860.5	.0	860.5
MILE 3	920.0	58.9	978.9
1/4	928.8	50.0	978.8
2/4	958.4	35.3	993.7
3/4	1002.0	17.6	1019.6
MILE 2	1022.8	64.9	1087.7
1/4	1022.8	133.7	1156.5
2/4	1027.2	171.5	1198.7
3/4	1030.1	156.3	1186.5
MILE 1	1022.8	.0	1022.8
1/4	897.7	.0	897.7
2/4	845.8	.0	845.8
3/4	840.0	.0	840.0
BEGIN LINE 25	827.9	.0	827.9
25 TO 26 (0)	830.9	.0	830.9
1/4	857.5	.0	857.5
2/4	881.3	.0	881.3
3/4	923.0	.0	923.0
T.P. TO 26	952.6	.0	952.6

LINE 26

BEGIN LINE 26	600.1	.0	600.1
1/2	649.9	.0	649.9
MILE 1	804.2	.0	804.2
1/5	946.7	.0	946.7
2/5	1194.8	.0	1194.8
3/5	1015.5	.0	1015.5
4/5	952.6	.0	952.6
7/8	958.4	64.9	1023.3
MILE 3	946.7	47.1	993.8
1/4	937.6	.0	937.6
2/4	937.6	.0	937.6
3/4	1002.0	.0	1002.0
MILE 4	1055.3	85.7	1141.0
1/4	1058.3	112.6	1170.9
2/4	1061.2	88.7	1149.9
3/4	1061.2	50.0	1111.2
MILE 5	1061.2	14.7	1075.8
1/3	1037.5	.0	1037.5
2/3	1002.0	.0	1002.0
END LINE 26	973.4	.0	973.4

Appendix B

WATER SOUND-VELOCITY DATA

Water-column sound-velocity corrections (Fig. 51a-b) were made for the reconnaissance-survey profile data, using a composite of three stations along the east side of the island for the profiles in this area and a single station located off Sea Cove for the profiles along the west side (Fig. 5). Depth intervals of 20 meters were programmed into the computer for this correction. Extrapolation of the curves was made for depths below that covered by the sound-velocity survey.

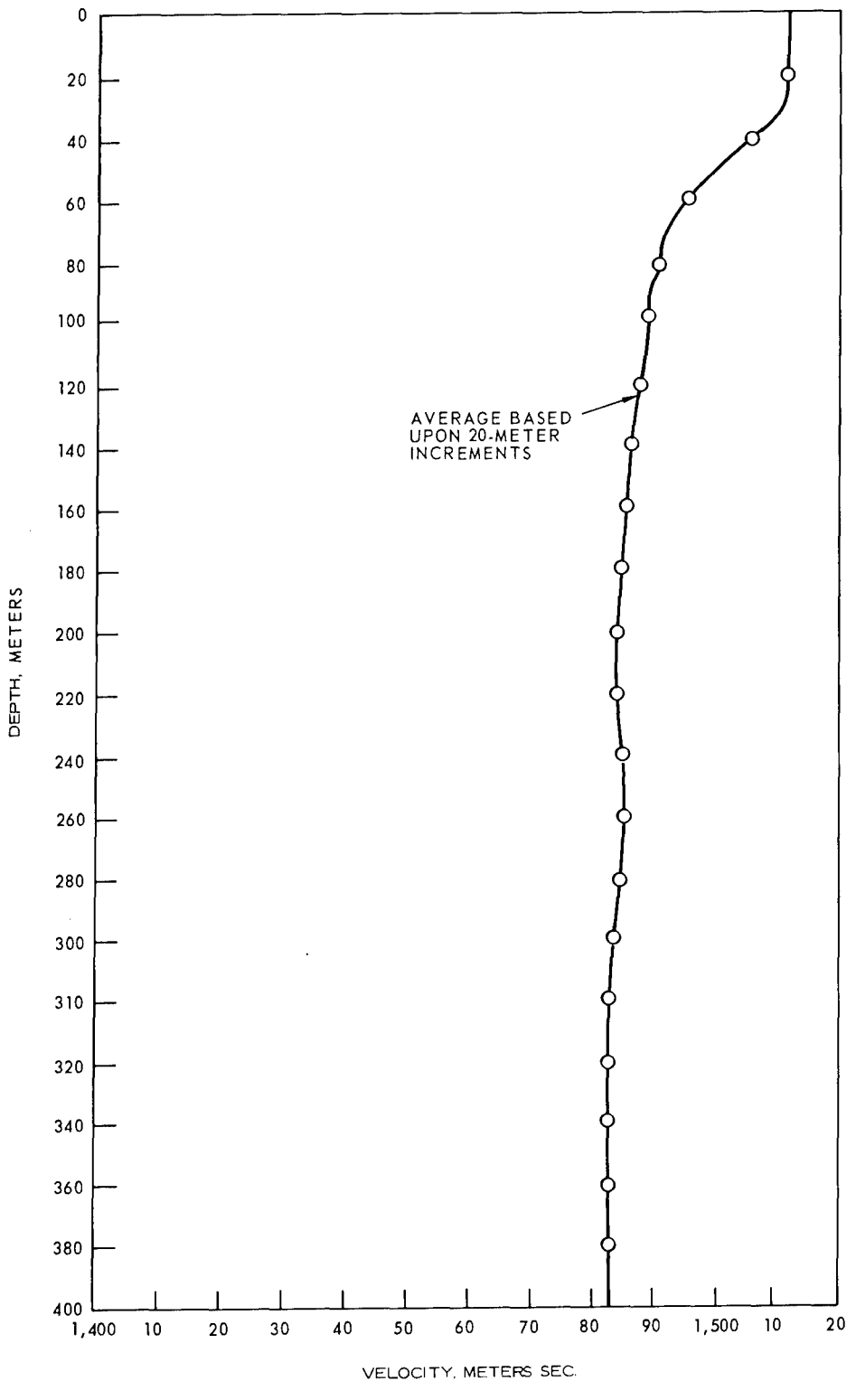

FIG. 51a. Water Column Sound-Velocity Curves Based on SVPT Stations; Composite of Three Stations Along East Side of Island.

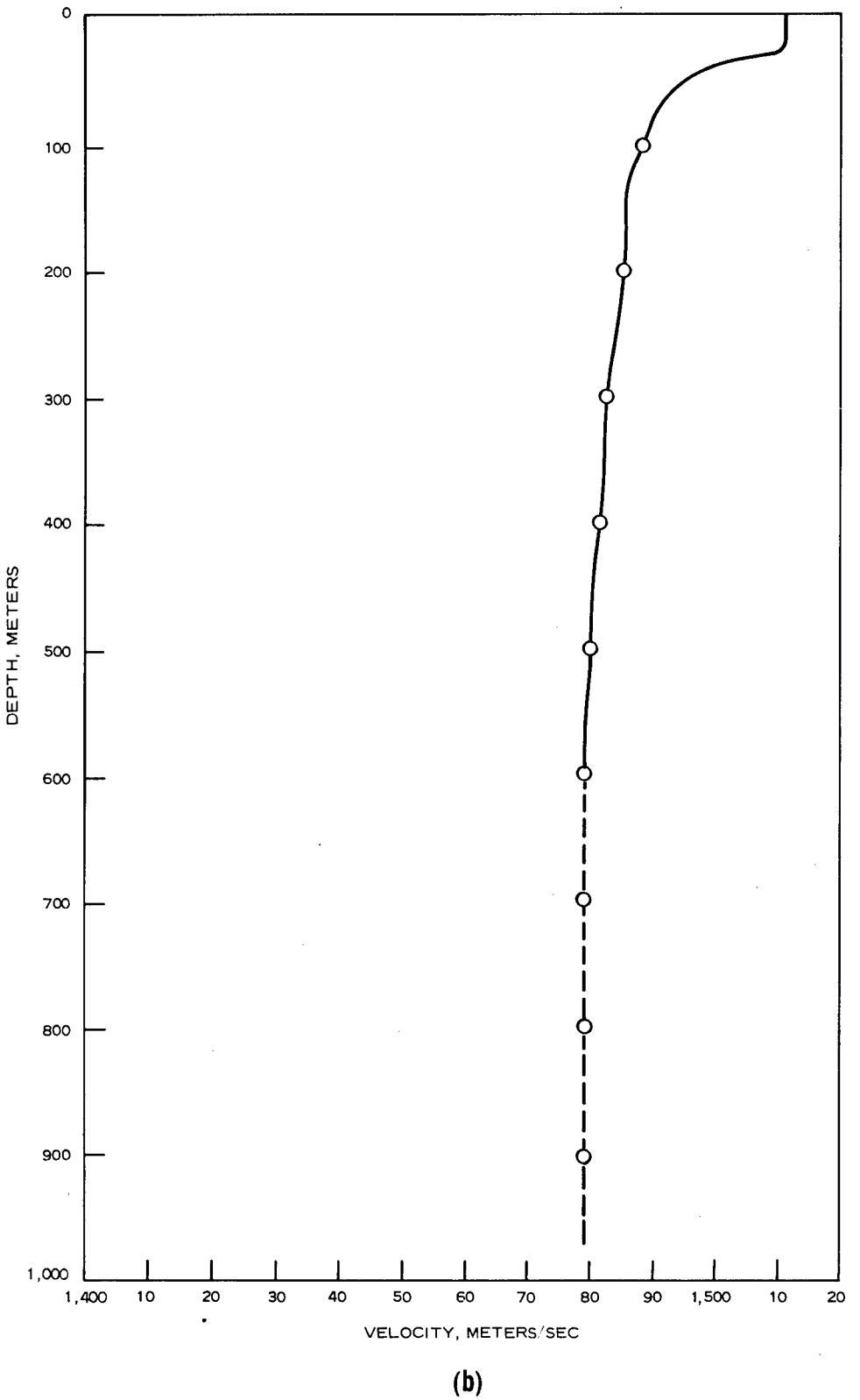

FIG. 51b. Water Column Sound-Velocity Curves Based on SVPT Stations; Single Station off West Side of Island (Fig. 4).

Appendix C

DEPTH AND POSITION DATA FOR CORES AND BOTTOM SAMPLES

No.	Depth, m	Position		Phi mean
		North	West	
DSSP Sample				
1	1,134.0	32°58.6′	118°28.5′	6.88
5	960.0	33°00.7	25.7	6.63
8	252.0	03.4	34.9	2.92
9	95.0	32°48.2	20.1	8.10
10	1,198.0	33°03.2	28.3	7.08
11	969.0	00.4	25.8	4.73
12	1,077.0	32°59.7	25.4	7.83
16	1,244.0	33°06.4	35.6	7.05
17	247.0	04.2	39.0	4.06
18	1,218.0	05.5	33.5	7.66
30	1,181.0	32°51.5	16.2	6.29
31	223.0	46.5	22.5	7.70
32	997.0	49.8	16.4	4.26
33	613.0	51.3	21.4	3.75
34	915.0	52.6	19.2	3.10
35	1,134.0	54.9	22.2	7.61
36	658.0	53.8	24.0	1.89
37	860.0	56.0	26.6	4.77
38	521.0	58.4	30.2	8.35
39	219.0	58.4	31.0	8.08
40	860.0	33°01.3	31.7	3.64
41	302.0	02.2	33.2	5.08
42	995.0	32°58.5	23.0	5.96
Gaal 1966 Sample (Ref. 7)				
AHF8319	1,227.8	33°05.6′	118°34.2′	7.61
AHF8320	1,260.4	32°55.5	20.3	7.81
AHF8419	728.0	33°02.0	23.5	1.92
AHF8420	785.0	02.2	23.8	2.19
AHF8421	530.2	02.2	31.7	2.33
AHF8689	999.4	32°50.8	17.9	3.97
AHF8690	781.5	51.7	22.0	6.28
AHF8691	1,150.9	58.7	26.4	1.82
NOTS-6	1,157.0	33°05.5	27.5	7.14
NOTS-7	505.4	02.4	32.9	7.02

No.	Depth, m	Position		Phi mean
		North	West	
Gaal 1966 Sample (Ref. 7)				
NOTS-8	1,101.3	32°57.7′	118°28.4′	6.16
NOTS-9	757.9	51.0	20.3	4.47
NOTS-15	1,045.8	55.6	16.1	4.26
NCEL-4	1,258.6	56.2	20.0	7.83
SCUBA Sample				
8	45	32°54.2′	117°32.7′	...
9	30	54.7	32.9	...
10	35	54.2	32.4	0.14
15	40	50.0	29.6	1.15
33	30	59.6	35.3	0.69
36	20	33°00.6	35.9	3.01
39	20	01.2	36.6	0.44
Snapper Sample				
B4	80	32°55.5′	117°33.9′	3.07
B8	230	55.1	34.7	3.92
B12	230	54.8	35.6	-1.68
D5	130	55.1	33.8	2.98
D7	250	54.8	34.3	2.84
D10	340	54.6	34.9	...
F5	70	54.7	33.6	1.65
F7	140	54.5	34.1	3.97
F12	355	54.1	35.1	2.61
H6	105	54.1	33.7	-0.51
H10	290	53.8	34.4	1.71
J4	80	54.1	32.9	2.05
J9	280	53.6	33.9	-0.17
J12	345	53.3	34.6	2.87
Mail Pt.	100	52.5	32.4	3.61
L13	315	50.4	33.1	0.97
M6	95	50.9	31.5	2.88
M10	120	50.5	32.2	...
O4	70	50.9	30.8	0.60
O8	105	50.4	31.6	3.45
O12	275	50.0	32.4	2.14
Q6	95	50.3	30.9	3.11
Q10	120	49.8	31.8	2.15
Q13	255	49.4	32.5	1.50
S4	75	50.1	30.3	-0.07
S8	105	49.7	31.1	2.71
S12	250	49.3	32.0	2.87
Dome	125	48.1	31.4	1.57

Appendix D

METHODS OF SEDIMENT ANALYSES

The analyses of the top increment of cores taken along the east side of the island are from Ref. 7 and an unpublished report by the United States Naval Oceanographic Office, San Diego, California. Since the size analyses made in different laboratories are not entirely comparable, the results from these cores are conservatively (i.e., broadly) interpreted.

The grain-size distribution of the detailed-survey samples were made by standard laboratory techniques in the sedimentology laboratory at the University of Southern California. Hydrometer analysis was used for the silts and clays (Ref. 50), and sieve analysis for the coarse fraction (greater than 62 microns). Percentage estimates of the coarse-fraction constituents were made under the binocular microscope.

REFERENCES

1. U. S. Geological Survey. A Geological Sketch of San Clemente Island, by W. S. T. Smith. Washington, D. C., U. S. G. S., 1898. (18th Annual Report, Part 2, pp. 459 - 596.)

2. ———— . Geologic Reconnaissance of San Clemente Island, California, by F. H. Olmsted. Washington, D. C., U S. G. S., 1958. (U. S. G. S. Bulletin 1071-B, pp. 55 - 68.)

3. Mitchell, E. D., Jr., and F. H. Lipps. "Fossil Collecting on San Clemente Island." Pacific Discovery, 1965, Vol. 18, No. 3, pp. 2 - 8.

4. Naval Weapons Center, China Lake. Engineering Geology of Central San Clemente Island, by R. M. Merifield and D. L. Lamar. China Lake, Calif., NUWC, 1967. (NWC TP 4469.)

5. Shepard, F. P., and K. O. Emery. Submarine Topography off the California Coast: Canyons and Tectonic Interpretation. Geological Society of America Special Paper 31, 1941.

6. Emery, K. O. The Sea Off Southern California. New York, Wiley, 1960.

7. Gaal, R. A. P. Marine Geology of the Santa Catalina Basin Area. Doctoral Dissertation, University of Southern California, 1966.

8. U. S. Oceanographic Office. Oceanographic Data Report, San Clemente Island Area, October to December 1966, by R. K. Oser and others. Washington, D. C., U. S. O. O., 1967.

9. Naval Ordnance Test Station. Condensed San Clemente Island Survey Handbook, by E. L. Crowe and others. China Lake, Calif., NOTS, 1955. (NAVORD 3369, NOTS 948.)

10. Krause, D. C. "Tectonics, Bathymetry, and Geomagnetism of the Southern Continental Borderland West of Baja California, Mexico." Geological Society of America Bulletin, 1965, Vol. 76, pp. 617 - 50.

11. Moore, D. G. Structure, Litho-orogenic Units and Postorogenic Basin Fill by Reflection Profiling. Doctoral Dissertation, University of Groningen (Netherlands), 1966, pp. 1 - 151.

12. Bradley, W. C. Submarine Abrasion and Wave-cut Platform. Geological Society of America Bulletin, 1958, Vol. 69, pp. 967 - 74.

13. Curray, J. R. "Transgressions and Regressions," in Papers in Marine Geology, Shepard Commemorative Volume, edited by R. L. Miller. New York, Macmillan, 1964, pp. 175 - 203.

14. ———— . "Late Quaternary History, Continental Shelves of the United States," in Quaternary of the United States, edited by H. E. Wright and D. G. Frey. Princeton, N. J., Princeton University Press, 1965.

15. Shepard, F. P. Submarine Geology, 2nd ed. New York, Harper, 1963. 557 p.

16. Curray, J. R. "Sediment and History of Holocene Transgressions, Continental Shelf, Northwest Gulf of Mexico," in Recent Sediments, Northwest Gulf of Mexico, edited by F. P. Shepard and others. Tulsa, Oklahoma, American Association of Petroleum Geologists, 1960, pp. 221 - 266.

17. Curray, J. R. Late Quaternary Sea Level; a Discussion, Geological Society of America Bulletin, Vol. 72(11), 1961, pp. 1707 - 1712.

18. Shepard, F. P. "Thirty-Five Thousand Years of Sea Level," in Essays in Marine Geology in Honor of K. O. Emery, edited by Thomas Clements. Los Angeles, University of Southern California Press, 1963.

19. Shepard, F. P., and H. E. Seuss. "Rate of Post-Glacial Rise of Sea Level," Science, Vol. 123, 1956, pp. 1082 - 1083.

20. Van Andel, Tj. H., and P. L. Sachs. "Sedimentation in the Gulf of Paria During the Holocene Transgression; a Subsurface Acoustic Reflection Study," Journal of Marine Research, Vol. 22, No. 1, 1964, pp. 30 - 50.

21. Emery, K. O. "Shallow Submerged Marine Terrace of Southern California," Geological Society of America Bulletin, Vol. 69, 1958, pp. 39 - 60.

22. Menard, H. W. "Deep-Sea Channels, Topography, and Sedimentation," American Association of Petroleum Geologists Bulletin, Vol. 39, 1955, pp. 236 - 255.

23. Hafner, W. "Stress Distributions and Faulting," Geological Society of America Bulletin, Vol. 62, 1951, pp. 373 - 398.

24. Anderson, E. M. The Dynamics of Faulting, 2nd ed. Edinburgh and London, Oliver and Boyd, 1951.

25. Harrison, J. C., and others. "Bouguer Gravity Anomalies and Magnetic Anomalies off the Coast of Southern California," Journal of Geophysical Research, Vol. 71, No.20, 1966, pp. 4921 - 4941.

26. Beloussov, V. V. Basic Problems in Geotectonics. New York, McGraw-Hill, 1962.

27. McKinstry, H. E. "Shears of the Second Order," American Journal of Science, Vol. 251, 1953, pp. 401 - 414.

28. Chinnery, M. A. "Secondary Faulting; I. Theoretical Aspects; II. Geological Aspects," Canadian Journal of Earth Sciences, Vol. 3, 1966, pp. 163 - 174(I), pp. 175 - 190(II).

29. Moody, J. D., and M. J. Hill. "Wrench-Fault Tectonics," Geological Society of America Bulletin, Vol. 67, No. 9, 1956, pp. 1207 - 1246.

30. Allen, C. R., and others. "Agua Blanca Fault--A Major Transverse Structure of Northern Baja California, Mexico," Geological Society of America Bulletin, Vol. 71, 1960, pp. 457 - 482.

31. Cotton, C. A. "Geomechanics of New Zealand Mountain Building," New Zealand Journal of Science and Technology, Section B, Vol. 38, 1956, pp. 187 - 200.

32. ———— . "An Example of Transcurrent-Drift Tectonics," New Zealand Journal of Science and Technology, Section B, Vol. 38, 1957, pp. 939 - 942.

33. Kingma, J. T. "Possible Origin of Piercement Structures, Unconformities, and Secondary Basins in the Eastern Geosyncline, New Zealand," New Zealand Journal of Geology and Geophysics, Vol. 1, 1958, pp. 269 - 274.

34. Moody, J. D. "Wrench-Fault Tectonics," Mines Magazine, Vol. 52, No. 5, 1962, pp. 22 - 26.

35. St. Amand, P. "Circum-Pacific Orogeny," Dominican Observatory, Vol. XX, No. 2, 1958, pp. 403 - 411.

36. Shor, G. G., Jr., and R. W. Raitt. "Seismic Studies in the Southern California Continental Borderland," Congreso Geologico Internacional, Mexico Session IX, Vol. 2, 1956, pp. 243 - 259.

37. Lensen, G. J. "A Method of Graben and Horst Formation," Journal of Geology, Vol. 66, No. 5, 1958, pp. 579 - 587.

38. Harrison, J. C., and R. E. von Huene. "The Surface-Ship Gravity Meter as a Tool for Exploring the Geologic Structure of Continental Shelves," Ocean Science and Ocean Engineering, Vol. 1, 1965, pp. 414 - 431.

39. Nettleton, L. I. "Regionals, Residuals, and Structures," Geophysics, Vol. 19, No. 1, 1954, pp. 1 - 22.

40. Von Huene, Roland, and J. B. Ridlon. Offshore Gravity Anomalies in the Santa Barbara Channel, California. Journal of Geophysical Research, Vol. 71, No. 2, 15 January 1966, pp. 457 - 463.

41. Richter, C. F. Elementary Seismology. San Francisco, W. H. Freeman, 1958.

42. Allen, C. R., and others. "Relationship Between Seismicity and Geologic Structure in the Southern California Region, " Seismological Society of America Bulletin, Vol. 55, No. 4, 1965, pp. 753 - 797.

43. Wood, H. O. "Earthquakes in Southern California With Earthquake Relations," Seismological Society of America, Vol. 37, No. 3, 1947, pp. 107 - 157, 217 - 258.

44. Clement, T., and K. O. Emery. "Seismic Activity and Topography of the Sea Floor off Southern California," Seismological Society of America Bulletin, Vol. 37, 1947, pp. 307 - 313.

45. Hamilton, E. L. "Marine Geology of Abyssal Plains in the Gulf of Alaska," Journal of Geophysical Research, Vol. 72, No. 16, 1967, pp. 4189 - 4213.

46. Emery, K. O. "Continental Shelf Sediments of Southern California," Geological Society of America Bulletin, Vol. 63, 1952, pp. 1105 - 1108.

47. Byrne, John V., and others. "Textural Trends of Recent Sediment From River to Abyssal Plain off Oregon (Abstract)," American Association of Petroleum Geologists Bulletin, Vol. 50, 1966, pp. 645 - 646.

48. Moore, D. G. "Submarine Slumps," Journal of Sedimentary Petrology, Vol. 13, No. 3, 1961, pp. 343 - 357.

49. Naval Weapons Center. Geologic Evaluation of San Clemente Island as a Location for a Rock Site I Installation, by C. F. Austin. China Lake, Calif., NWC, 1968. (NWC TP 4161.)

50. Krumbein, W. C., and F. J. Pettijohn. Manual of Sedimentary Petrography. New York, D. Appleton-Century, 1938.

INITIAL DISTRIBUTION

11 Chief of Naval Material
- MAT-00
- MAT-01B
- MAT-02B
- MAT-03
- MAT-03L
- MAT-032A
- MAT-03262 (Cdr. G. H. Jayne)
- MAT-033
- PM-8
- PM-11
- NSP-001

6 Naval Air Systems Command
- NAIR-03C
- NAIR-03E
- NAIR-103
- NAIR-350
- NAIR-370
- NAIR-604

7 Naval Ordnance Systems Command
- NORD-00
- NORD-03A
- NORD-05
- NORD-05121
- NORD-052
- NORD-054
- NORD-9132

2 Naval Facilities Engineering Command
- AFEC-032
- AFEC-0321

1 Naval Ship Systems Command (NSHP 205)

4 Office of Naval Research
- Chief Scientist, Dr. Sidney Reed
- Code 104
- Code 416, John Heacock
- Code 466

3 Anti-Submarine Warfare Systems Project Office
- ASW-13
- ASW-14
- ASW-20

1 Atlantic Undersea Test and Evaluation Center, West Palm Beach (Capt. LeRoy Jackson)
1 National Oceanographic Data Center
1 Naval Academy, Annapolis (Technical Library)
1 Naval Air Development Center, Johnsville
4 Naval Civil Engineering Laboratory, Port Hueneme
    Technical Library (1)
    H. Herrmann
    M. Kironaka
    T. Kretschmer
1 Naval Electronics Laboratory Center, San Diego
1 Naval Mine Defense Laboratory, Panama City
1 Naval Ordnance Laboratory, White Oak (H. A. Perry)
1 Naval Personnel Research and Development Laboratory
3 Naval Postgraduate School, Monterey
    Library, Technical Reports Section
    Department of Business Administration and Economics, F. C. Horton
    Department of Meteorology and Oceanography
1 Naval Research Laboratory
2 Naval Ship Research and Development Center
    Annapolis Division
    Carderock Division
2 Naval Torpedo Station, Keyport
    Quality Evaluation Laboratory, Technical Library
    Director, Research and Engineering
1 Naval Underwater Weapons Research and Engineering Station, Newport
5 Naval Weapons Center, China Lake
    Code 50
    Code 502
    Code 503 (C. Austin)
    Code 751
    Code 753
1 Naval Weapons Center Corona Laboratories
1 Naval Weapons Services Office (Code DM)
2 Navy Underwater Sound Laboratory, Fort Trumbull (1)
    Code 912.3, W. Whitaker (1)
1 Oceanographer of the Navy
1 Office of Naval Research Branch Office, Chicago (LCdr. R. G. Gantt)
1 Office of Naval Research Branch Office, Pasadena
1 Chief of Engineers (Bruce Hall)
1 Army Coastal Engineering Research Center (J. Caldwell)
1 Director of Defense Research and Engineering (Dr. J. Foster)
3 Advanced Research Projects Agency
    C. Akaid
    R. Black
    Dr. S. Ruby
20 Defense Documentation Center (TISIA-1)

UNCLASSIFIED
Security Classification

DOCUMENT CONTROL DATA - R & D

(Security classification of title, body of abstract and indexing annotation must be entered when the overall report is classified)

1. ORIGINATING ACTIVITY *(Corporate author)*
Naval Undersea Research and Development Center
San Diego, Calif. 92132

2a. REPORT SECURITY CLASSIFICATION
UNCLASSIFIED

2b. GROUP

3. REPORT TITLE
SAN CLEMENTE ISLAND ROCKSITE PROJECT: OFFSHORE GEOLOGY; PART 2. RECONNAISSANCE SURVEY AROUND THE ISLAND

4. DESCRIPTIVE NOTES *(Type of report and inclusive dates)*
Survey report

5. AUTHOR(S) *(First name, middle initial, last name)*
J. B. Ridlon

6. REPORT DATE	7a. TOTAL NO. OF PAGES	7b. NO. OF REFS
August 1969	132	50

8a. CONTRACT OR GRANT NO.

b. PROJECT NO. This study was supported by Independent Exploratory Development, Director of

c. Laboratory Programs Task Assignment Z-F008-98-01.

d.

9a. ORIGINATOR'S REPORT NUMBER(S)
NUC TP 156

9b. OTHER REPORT NO(S) *(Any other numbers that may be assigned this report)*

10. DISTRIBUTION STATEMENT This document is subject to special export controls and each transmittal to foreign governments or foreign nationals may be made only with the prior approval of the Naval Undersea Research and Development Center.

11. SUPPLEMENTARY NOTES Part 2 of NWC TP 4442: San Clemente Island Rocksite Project; Offshore Geology, Part 1, by J.B.Ridlon. China Lake, Calif., NWC, 1968.

12. SPONSORING MILITARY ACTIVITY
Naval Ordnance Systems Command
Washington, D. C. 20360

13. ABSTRACT

Interpretations from a nearshore geophysical and geological survey off San Clemente Island, Calif., are presented. Bathymetry around the island block is shown to differ from that of published charts. Extensive offshore faulting relates partially to that which occurs on the island. Differentiation of a major pre-orogenic surface from the post-orogenic sedimentation is shown. A steep magnetic gradient off the east side is considered the consequence of (1) volcanic flow, (2) a possible deep basic mass related to a large positive anomaly off the northwest side of the island, and (3) major faulting. Anomalous magnetic trends also reflect some of the major structural and outcrop trends. Earthquake epicenter analyses suggest less seismic activity than the adjacent land area, a tendency to quiescence at present, and an association of recent fault activity with recent epicenters. The post-orogenic sediments, believed to have followed certain major transportation channels from the island block by means of turbidity currents, sand flows, and slides, have been deposited in basin lows developed by faulting and folding.

14. KEY WORDS	LINK A		LINK B		LINK C	
	ROLE	WT	ROLE	WT	ROLE	WT
Geophysical surveys						
Geological surveys						
Ocean bottom						
Seismic reflection						
Underwater excavation						
San Clemente Island, Calif.						
Project Rocksite						

ABSTRACT CARD

Naval Undersea Research and Development Center
San Clemente Island Rocksite Project: Offshore Geology; Part 2. Reconnaissance Survey Around the Island, by J.B.Ridlon. San Diego, Calif., NUC, August 1969. 132 pp. (NUC TP 156), UNCLASSIFIED.

ABSTRACT. Interpretations from a nearshore geophysical and geological survey off San Clemente Island, Calif., are presented. Bathymetry around the island block is shown to differ from that of published charts. Extensive offshore faulting relates partially to that which occurs on the island. Differentiation of a major pre-orogenic surface from the post-orogenic sedimentation is shown. A steep

(Over)
1 card, 4 copies

Naval Undersea Research and Development Center
San Clemente Island Rocksite Project: Offshore Geology; Part 2. Reconnaissance Survey Around the Island, by J.B.Ridlon. San Diego, Calif., NUC, August 1969. 132 pp. (NUC TP 156), UNCLASSIFIED.

ABSTRACT. Interpretations from a nearshore geophysical and geological survey off San Clemente Island, Calif., are presented. Bathymetry around the island block is shown to differ from that of published charts. Extensive offshore faulting relates partially to that which occurs on the island. Differentiation of a major pre-orogenic surface from the post-orogenic sedimentation is shown. A steep

(Over)
1 card, 4 copies

Naval Undersea Research and Development Center
San Clemente Island Rocksite Project: Offshore Geology; Part 2. Reconnaissance Survey Around the Island, by J.B.Ridlon. San Diego, Calif., NUC, August 1969. 132 pp. (NUC TP 156), UNCLASSIFIED.

ABSTRACT. Interpretations from a nearshore geophysical and geological survey off San Clemente Island, Calif., are presented. Bathymetry around the island block is shown to differ from that of published charts. Extensive offshore faulting relates partially to that which occurs on the island. Differentiation of a major pre-orogenic surface from the post-orogenic sedimentation is shown. A steep

(Over)
1 card, 4 copies

Naval Undersea Research and Development Center
San Clemente Island Rocksite Project: Offshore Geology; Part 2. Reconnaissance Survey Around the Island, by J.B.Ridlon. San Diego, Calif., NUC, August 1969. 132 pp. (NUC TP 156), UNCLASSIFIED.

ABSTRACT. Interpretations from a nearshore geophysical and geological survey off San Clemente Island, Calif., are presented. Bathymetry around the island block is shown to differ from that of published charts. Extensive offshore faulting relates partially to that which occurs on the island. Differentiation of a major pre-orogenic surface from the post-orogenic sedimentation is shown. A steep

(Over)
1 card, 4 copies

magnetic gradient off the east side is considered the consequence of (1) volcanic flow, (2) a possible deep basic mass related to a large positive anomaly off the northwest side of the island, and (3) major faulting. Anomalous magnetic trends also reflect some of the major structural and outcrop trends. Earthquake epicenter analyses suggest less seismic activity than the adjacent land area, a tendency to quiescence at present, and an association of recent fault activity with recent epicenters. The post-orogenic sediments, believed to have followed certain major transportation channels from the island block by means of turbidity currents, sand flows, and slides, have been deposited in basin lows developed by faulting and folding.

NUC TP 156

magnetic gradient off the east side is considered the consequence of (1) volcanic flow, (2) a possible deep basic mass related to a large positive anomaly off the northwest side of the island, and (3) major faulting. Anomalous magnetic trends also reflect some of the major structural and outcrop trends. Earthquake epicenter analyses suggest less seismic activity than the adjacent land area, a tendency to quiescence at present, and an association of recent fault activity with recent epicenters. The post-orogenic sediments, believed to have followed certain major transportation channels from the island block by means of turbidity currents, sand flows, and slides, have been deposited in basin lows developed by faulting and folding.

NUC TP 156

magnetic gradient off the east side is considered the consequence of (1) volcanic flow, (2) a possible deep basic mass related to a large positive anomaly off the northwest side of the island, and (3) major faulting. Anomalous magnetic trends also reflect some of the major structural and outcrop trends. Earthquake epicenter analyses suggest less seismic activity than the adjacent land area, a tendency to quiescence at present, and an association of recent fault activity with recent epicenters. The post-orogenic sediments, believed to have followed certain major transportation channels from the island block by means of turbidity currents, sand flows, and slides, have been deposited in basin lows developed by faulting and folding.

NUC TP 156

magnetic gradient off the east side is considered the consequence of (1) volcanic flow, (2) a possible deep basic mass related to a large positive anomaly off the northwest side of the island, and (3) major faulting. Anomalous magnetic trends also reflect some of the major structural and outcrop trends. Earthquake epicenter analyses suggest less seismic activity than the adjacent land area, a tendency to quiescence at present, and an association of recent fault activity with recent epicenters. The post-orogenic sediments, believed to have followed certain major transportation channels from the island block by means of turbidity currents, sand flows, and slides, have been deposited in basin lows developed by faulting and folding.

1 Department of the Interior (Dr. T. F. Bates, Science Advisor)
1 Atomic Energy Commission (Dr. S. G. English, Assistant Manager for R&D)
1 Central Intelligence Agency (Dr. F. Spilhaus, Jr.)
1 Coast and Geodetic Survey (Office of Oceanography)
1 Coast and Geodetic Survey, Rockville, Md. (ESSA, Engineering Division)
3 Geological Survey
    Marine Geology Unit
    Dr. V. E. McKelvey
    Dr. E. Roedder
1 Geological Survey, Denver (Howard Waldron)
8 Geological Survey, Menlo Park
    Dr. D. McCulloch
    Dr. H. Olsen
    Dr. G. Rusnak
    Dr. D. W. Scholl
    P. G. Smith
    P. Snavely
    J. C. Vedder
    Dr. R. von Huene
1 California Division of Mines, San Francisco (Dr. I. Campbell)
1 State Department of Water Resources, Sacramento (Raymond C. Richter)
1 Applied Physics Laboratory, University of Washington, Seattle
1 Benthos, Inc., North Falmouth, Mass.
2 The Boeing Company, Seattle
    Dr. W. A. Roberts
    H. M. Segal
1 The Rand Corporation, Santa Monica (Technical Library)
1 University of California, Berkeley (Biology Department Library)
1 University of California at Los Angeles (Department of Geology)
1 University of California, San Diego, Scripps Institution of Oceanography, La Jolla (W. Gayman)
3 University of California, San Diego, Scripps Institution of Oceanography, Marine Physical Laboratory
    Dr. J. R. Curray
    Dr. H. W. Menard
    Dr. F. P. Shepard
2 The University of Michigan, Ann Arbor (Department of Meteorology and Oceanography)
    Dr. J. L. Hough
    Dr. A. C. Wiin-Nielsen
2 The University of Southern California, Los Angeles
    Dr. D. S. Gorsline
    Geology Department
1 University of Washington, Seattle (Department of Oceanography)
1 Woods Hole Oceanographic Institution, Woods Hole, Mass. (Technical Library)

Center Distribution

01
05
131 (2)
133
201 (G. Wilkins)
251
2512 (T. Cooke, F. Fehl)
2531 (B. D. Jones, Jr.)
4011
40112 (Y. Igarashi)
504 (E. C. Buffington, Dr. E. L. Hamilton, Dr. D. G. Moore)